Triple-decker assemblies based on strapped di-porphyrins

Muteb Hashim Alshammari

School of Chemistry

University of East Anglia, Norwich, United Kingdom

June 2024

Abstract

Over the last few decades, remarkable attention has been focused on the study of multidecker sandwich type complexes. Porphyrins and/or phthalocyanines (Pcs) are heterocycle-containing macrocycle compounds that can be used as building blocks to form multidecker complexes. These complexes have potential applications in imaging technology and information storage. Owing to their unique properties in material science, mixed porphyrins and /or phthalocyanines were investigated by our group to synthesise triple decker complexes. As a result, a number of complexes have been prepared by our group. The ultimate goal of this study was to extend the strategy to threaded systems (catenanes and rotaxanes). Our model system is designed to demonstrate this strategy by synthesizing the triple decker complex based on the clipping strategy followed by removal of metals.

Initially, the current work focused on the synthesis of *trans* porphyrins as key building blocks for our model system. Their synthesis proved challenging due to the formation of scrambled products, but within the project's later stages we solved this by employing removable blocking bromide substituents. As the *cis* porphyrin was obtained as a side product from *trans* porphyrin reactions, it was used in this thesis. A triple decker (TD) complex from a *cis* 5,10-double bridged porphyrin was designed and synthesised using a clipping strategy. The triple decker complex from *trans* 5,15-double bridged porphyrin was synthesised via an uncontrolled strategy due to the poor solubility of *trans* porphyrin dyad intermediate that was initially targeted. These novel TDs have been successfully characterized using spectroscopic tools including NMR, MALDI-tof MS, UV and unambiguously through X-ray crystallography. Treatment of the TD with TFA resulted in the removal of both the metals and the sandwiched Pc, as expected for this particular Pc.

Acknowledgements

First and foremost, I would like to thank my supervisor, Prof. Andrew Cammidge, for giving me the opportunity to carry out the research described in this thesis. It has been an honour to be part of his research group. I would like to express my deepest gratitude for all the support, advice, confidence, and freedom he has given me to pursue research without any objection. I have learned so much from him and could not have imagined a better mentor. For this, I cannot thank him enough.

I would also like to express my appreciation to Dr. Isabelle Fernandes for her help, advice, and constant support and encouragement. She always made time for discussions whenever I asked, which made a significant difference in my work. I also thank Dr. David Hughes for providing the X-Ray crystallography service.

Additionally, I would like to thank all my previous and current colleagues and friends with whom I have shared Lab 3.10 for their support during my PhD. A special thanks to my friends from other labs, 3.17 and 3.08, with whom I have shared great memories. Thanks are extended to everyone in the chemistry school, especially those who work on the third floor.

I am deeply thankful to my lovely parents, brothers, and sisters for their help and support while I have been so far away. I would also like to thank my beloved family, my wife Sultanah and my daughters Leen and Tala, in particular. I really appreciate my wife for her understanding and love during the past years. Without my family and their never-ending love, this research would not have been possible.

I would like to thank Northern Borders University for providing me with a full scholarship to complete my studies in the United Kingdom. I also extend my gratitude to the Saudi Arabia Cultural Bureau in London for their support during my PhD.

List of abbreviation

Ac	Acetate
AcOH	Acetic acid
acac	Acetylacetonate
AMT	Active Metal Template
Ar	Argon
br	Broad
δ	Chemical shift
^{o}C	Celsius
CuAAC	Copper(I) catalysed azide-alkyne cycloaddition
CBPQT4^{+}	Cyclobis (paraquat-*p*-phenylene)
DABCO	1,4-diazabicyclo [2.2.2] octane
DIPEA	Diisopropylethylamine
DMF	Dimethylformamide
dpp	2,9-diphenyl-1,10-phenanthroline
DDQ	2,3- Dichloro-5,6-dicyano-1,4-benzoquinone
DMSO	Dimethyl sulfoxide
DNA	Deoxyribonucleic acid
d	Doublet
dd	Doublets of doublets
dt	Doublet of triplets
eq	Equivalent
g	Gram
h	Hours

Hz	Hertz
J	Coupling value
Ln	Lanthanide
MIMs	Mechanically interlocked molecules
MIMAs	Mechanically Interlocked Molecular Architectures
MALDI-tof MS	Matrix-assisted laser desorption/ionization (time of flight)
M	Multiplet
Mmol	Millimol
mg	Milligrams
MeOH	Methanol
M	Metal
min	Minutes
mL	Millilitres
*m*TPP	*meso*-tetraphenylporphyrin
NaBArF	Sodium tetrakis[3,5-bis(trifluoromethyl)phenyl]borate
NMR	Nuclear Magnetic Resonance
nm	nanometers
PMT	Passive Metal Template
ppm	Parts per million
Por	Porphyrin
Pc	Phthalocyanine
rt	Room temperature
RCM	Ring-closing metathesis
s	Singlet

SWCNTs	Single-Walled Carbon Nanotubes
TCB	1,2,4-trichlorobenzene
TBAF	Butylammonium fluoride
t	Triplet
TLC	Thin Layer Chromatography
TFA	Trifluoroacetic acid
TPP	Tetraphenylporphyrin

Table of Contents

Introduction

1.1 Supramolecular Chemistry

The fabrication of minuscule structures carries great importance in modern science and technology. Although physical methods for miniaturization have limitations, a chemical strategy known as the 'bottom-up'[1] approach provides a solution. This approach involves constructing architectural formations starting at the atomic scale, utilizing synthetic chemistry to manipulate chemical constituents.[2] These constituents come together to form complex structures that are specifically designed to perform specific tasks, in accordance with the field of supramolecular chemistry.

Supramolecular chemistry, also referred as “chemistry beyond the molecule”, is a field focused on the study of reversible interactions between molecules. Unlike molecular chemistry, which deals with covalent bonds of atoms, supramolecular chemistry explores the interactions and associations between molecules through intermolecular forces to make larger, organized structures.[3] There is a wide range of strengths among these forces, ranging from the weaker and reversible non-covalent interactions to the strong covalent bonds. Supramolecular interactions include hydrophobic effects, electrostatic interactions, van der Waals forces, and metal coordination. Consequently, supramolecular chemistry stands as an interdisciplinary field, examining the chemical, physical, and biological characteristics of complex chemical entities. Moreover, supramolecular chemistry’s inception dates back to Emil Fischer's depiction of the molecular recognition in enzymes, describing a 'lock and key' fit between molecules.[4]

Jean-Marie Lehn's pioneering work played a fundamental role in shaping the field, particularly in the development of 'host-guest' assemblies, where a host molecule selectively binds to a specific guest. This contribution earned Lehn the Nobel Prize in Chemistry in 1987

alongside Donald J. Cram and Charles J. Pedersen, recognizing their innovations in structure-specific interactions.[3,5,6]

Supramolecular chemistry can be broadly categorized into 'self-assembly' and 'host-guest chemistry,' both involving the aggregation of molecules guided by non-covalent forces. In self-assembly, molecules have the ability to come together and make complex structures such as the well-known double helix structure of DNA. In this case, the intertwining of two strands is driven by molecular recognition, which is facilitated by hydrogen bonds and aromatic stacking interactions.[7] In host-guest chemistry a larger molecule, known as the host, has the ability to encapsulate a smaller 'guest' molecule forming a supermolecule via non-covalent interactions within a specific binding site. The binding site possesses the required dimensions, shape, and features to adequately accommodate and attach a guest molecule through non-covalent interactions.[8]

The scope of supramolecular chemistry has been expanded significantly in modern times. The field has expanded beyond basic host-guest systems and now includes a wide range of systems, such as molecular machines, devices, and mechanically interlocked molecular architectures. More recently, in 2016, significant advancements in this area were recognised with the Nobel Prize in Chemistry, honouring the achievements of Jean-Pierre Sauvage,[9] Fraser Stoddart,[10] and Ben Feringa.[11] They were recognised for their groundbreaking work in the development and creation of molecular machines. The remarkable achievements of Sauvage and Stoddart involved the creation of prototypes for molecular nano-machines. These machines were constructed using interlocked molecules, which they referred to as 'the mechanical bond.' This recognition signifies a pivotal moment in supramolecular chemistry, highlighting its progression from the basic understanding of molecular interactions to the design and construction of functional molecular machines. Also, it underscores the profound

impact of manipulating molecules at such a precise scale, offering potential avenues in data storage and processing,[12] catalysis,[8] biomaterials,[13] and drug delivery.[14]

1.1.1 Mechanically Interlocked Molecules (MIMs)

The concept of the mechanical bond has brought a significant shift in chemical sciences, through introducing a novel entanglement between molecular entities in space.[15] This bond forms the basis of mechanically interlocked molecules (MIMs), involving entwining multiple molecular components through noncovalent mechanical bonds, preventing separation without disrupting chemical bonds between atoms.[10] Naturally, the nature of these "bonds" enables a substantial movement within the system, serving as a unique tool to establish a contact between covalent structures, meanwhile preserving stability akin to the weakest covalent bond without altering their fundamental structure. Mechanically Interlocked Molecular Architectures (MIMAs) exemplify this entanglement through the depicting of large molecular architectures linked not by traditional covalent bonds but by their topology. These selected MIMAs exhibit structural diversity like rotaxanes, catenanes, knots, and Borromean rings, which showcase entangled molecular fragments held together by these mechanical bonds (Figure 1). In this section, the objective is not to exhaustively review this field but rather to offer definitions and discuss a curated selection of historically and significantly relevant examples of MIMAs, including rotaxanes and catenanes.

Rotaxane catenane knot Borromean rings

Figure 1: Schematic depictions of diverse mechanically interlocked molecules. Adapted from reference.[10,16]

1.1.2 Rotaxanes and Catenanes

Rotaxanes and catenanes are two fundamental structures within the realm of mechanically interlocked molecules (MIMs). The term ‘catenane’ originates from the Latin ‘catena,’ meaning ‘chain’, while a rotaxane derives its name from the Latin *rota* for "wheel" and *axis* for "axle". These compounds are characterized by their assembly of two or more interlocked structures. Basically, starting with just two simple molecular components like a macrocycle and an axle molecule, it is feasible to create a supramolecular structure known as pseudorotaxane, wherein the macrocycle threads onto the axle molecule (Figure 2). Subsequently, two pathways can be followed. Firstly, a rotaxane is formed by capping the axle with two bulky groups, often referred to as stoppers.[17] These stoppers secure the macrocycle around the axle, forming a distinctive molecular architecture and preventing unwanted disassembly of the structure (Figure 2). Secondly, catenanes can be assembled via a clipping reaction.[18] The interlocking mechanism within catenated structures forms a bond that renders separating the rings impossible without breaking a chemical bond and opening one of the macrocycles (Figure 2). The simplest form of a rotaxane is a [2]rotaxane, where the rotaxane's ring could potentially encircle several threads or a single thread that could hold multiple rings. On the other hand, the simplest form of a catenane involves two rings, exemplified by [2]catenane, but it could contain various rings linked in different manners.

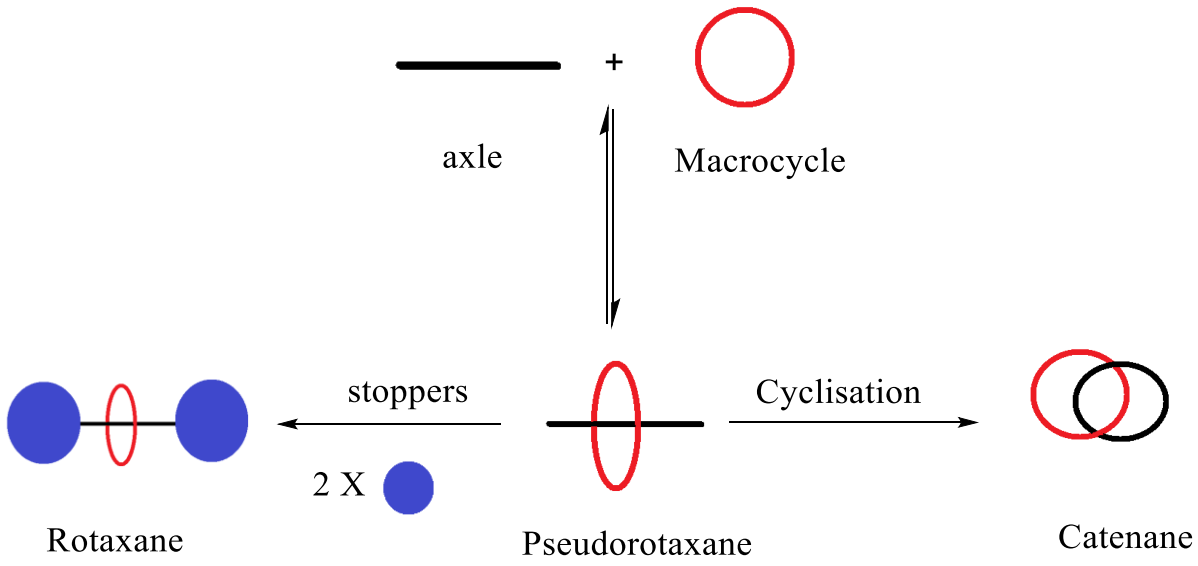

Figure 2: Illustration depicting two components—a macrocycle and an axle —that can combine to create a pseudorotaxane, followed by the creation of a catenane and rotaxane.

1.1.2.1 Synthesis Strategies Toward Catenanes and Rotaxanes

The discovery of mechanically interlocked molecules can be traced back to 1960 with the work of researchers such as Frisch and Wasserman who reported the first synthesis of catenane (Figure 3 (1.1)).[19] Later, in 1967, I. T. Harrison and S. Harrison demonstrated the first synthesis of rotaxane utilizing a solid-supported thread.[20] These syntheses were based on random interlocking before forming covalent bonds. The yields of these statistical methods were very low (~ 0.0001%). Intriguingly, in 1964, G. Schill and co-workers reported the first systematic directed synthesis of a catenane by introducing a method based on the use of covalent bonds as a template for crafting the desired interlocked architecture.[21] The same group also reported the synthesis of a rotaxane using a covalent bond template, constructing a bis-macrocycle with functionalized chains extending from either side. The introduction of bulky end groups and subsequent cleavage of the orienting covalent bonds yielded the free rotaxane (Figure 3 (1.2)).[22] Despite these early advancements, such synthetic endeavours encountered challenges such as low yields and complex procedures.

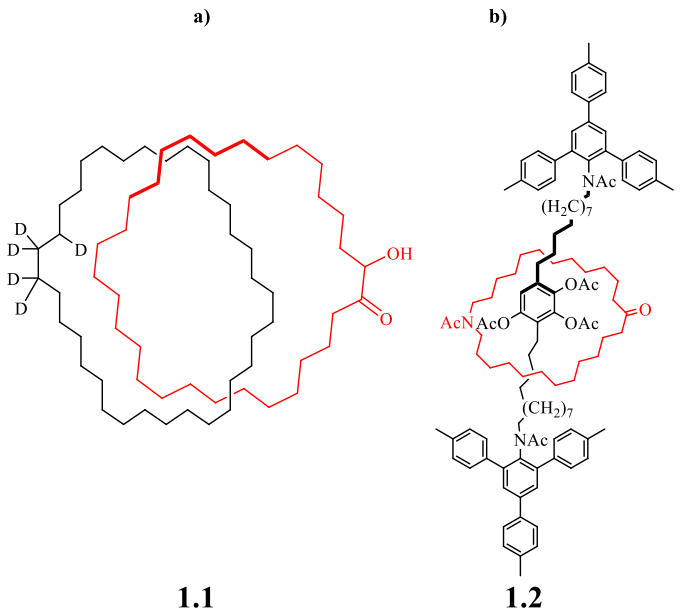

Figure 3: The earlier examples of synthetic mechanically interlocked molecules: a) The Wasserman catenane. (**1.1**). b) Rotaxane developed by Schill and coworkers (**1.2**).

Over time, diverse synthetic strategies have been developed to create interlocked structures. A significant breakthrough occurred with the introduction of metal template synthesis for entwined and interlocked structures, pioneered by Sauvage *et al.* in 1983.[23] The author used a copper(I) ion to organize the formation of a [2]catenane through two different strategies. Strategy A required the formation of homoleptic copper (I) bis-phenanthroline complex **1.5** in an orthogonal orientation in the first step. This was followed by a Williamson ether double macrocyclization producing **1.6** intermediate**.** Subsequentially removal of copper from **1.6** afforded the interlocked [2]catenane **1.7** in 27% overall yield (Scheme 1i). Strategy B, known as a "threading followed by stoppering" approach, involved the formation of a heteroleptic pseudorotaxane intermediate **1.9** and resulted in the production of the same [2]catenane **1.7** after Williamson ether macrocyclization reaction, with an overall yield of 42% (Scheme 1i). Later, the same group was able to improve the [2]catenane yield from 42% to 92% by utilizing ring-closing metathesis (Scheme 1ii).[24] Therefore, this method showed a significant improvement over other methods that required 6 to 20 steps.

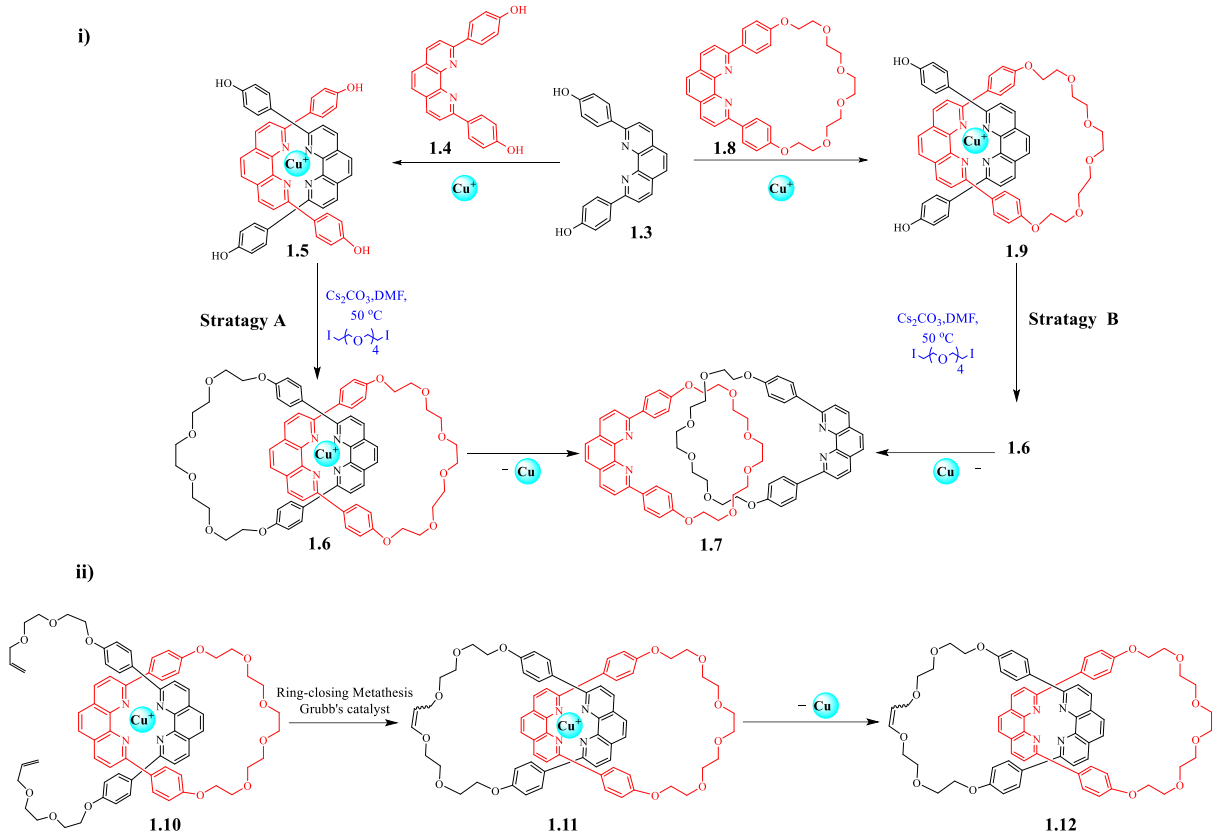

Scheme 1: Synthesis of [2]catenane through a passive metal template strategy.

Gibson and co-workers found that for the synthesis of a rotaxane, the passive metal template approach is highly beneficial. For example, they successfully synthesised a rotaxane by taking advantage of copper (I) ions which were tetrahedrally coordinated with two dpp moieties, furnishing a pseudorotaxane **1.13**. Subsequently, terminating the phenolic groups with bulky triarylmethyl groups via Williamson ether reaction, followed by demetallation utilizing cyanide, afforded the desired rotaxane **1.14** in 42% overall yield (Scheme 2).[25]

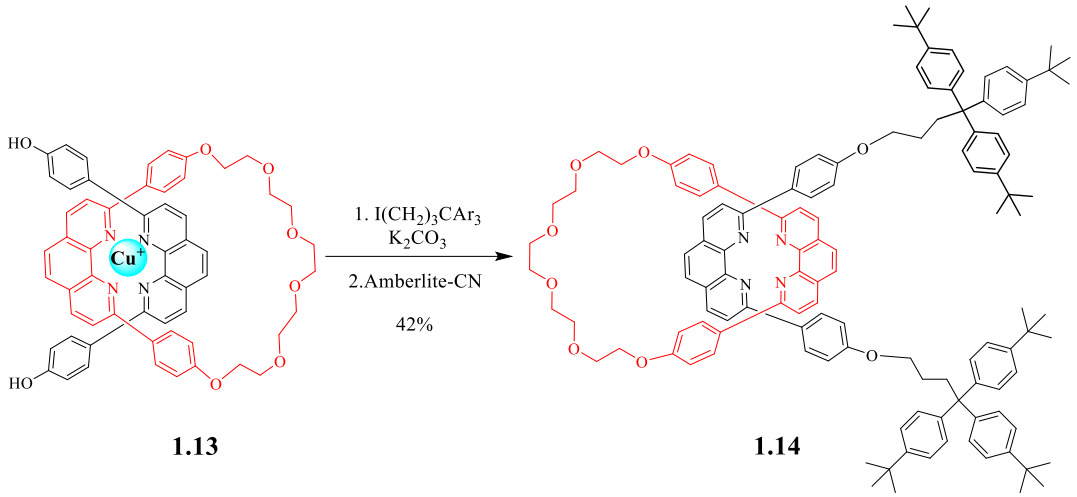

1.13 **1.14**

Scheme 2: Synthesis of [2]rotaxane (**1.14**) through a passive metal template strategy.

As has been shown in the previous example, the role of metal ions is to act as a passive metal template (PMT) for organising the components for mechanically interlocked molecule assembly. On the other hand, in 2006, Leigh and co-workers developed the metal template approach to introduce an active metal template (AMT) that uses the metal ion not only as a template but also as a catalyst at the same time for forming the mechanical bond.[26] In this approach, only the macrocycle requires a permanent coordination site. Basically, the metal guides the fragments into place and catalyzes their reaction, forming the desired interlocked product. The initial example of this approach was the synthesis of [2] rotaxane utilizing a copper(I) catalysed azide-alkyne cycloaddition (CuAAC) (Figure 4a). This method was used as well to prepare a [2]catenane interlocked system by the same group (Figure 4 b).[27]

Additionally, other methods based on the non-covalent interactions between the macrocycle and the axle have been extensively employed to create catenanes and rotaxanes. For instance, Stoddart discovered a useful method for making rotaxanes by using a charged template, initially designed for catenanes.[28] This approach was applied to create the rotaxane, where strong attractions between specific components led to the formation of a threaded structure known as cyclobis (paraquat-*p*-phenylene) ($CBPQT^{4+}$) (Figure 4 c).[29]

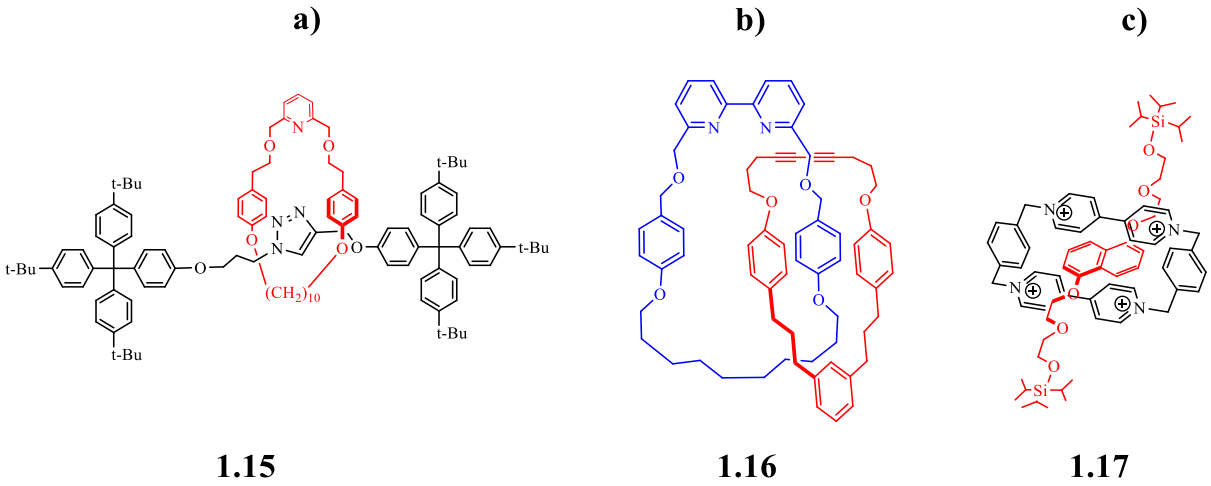

1.15 **1.16** **1.17**

Figure 4: Examples of rotaxane (**1.15**) and catenane (**1.16**) prepared using active metal template strategy with one instance of rotaxane (**1.17**) constructed through non-covalent interactions.

Following these ground-breaking discoveries, more researchers started investigating deeply in this field, coming up with innovative methods to create rotaxanes and catenanes. Their overall objective was to explore the characteristics of these structures and find ways to utilise them in constructing molecular machines. Although this introduction does not cover the topic in detail, there are numerous focused review articles that explore this rapidly growing field of research.[12,15,16,30–34]

1.2 Porphyrin

Porphyrins are heterocyclic macrocycle compounds which have four pyrrole rings fused together at α-carbons by methine bridges. They are deeply coloured and normally fluorescent, having bright purple pigmentation. Biologically, they are key to the biochemically processes encompassing energy capture and utilization. Representative examples of these biological important molecules are the chlorophyll **1.18** and heme **1.19** (Figure 5). Both contain tetra-pyrrolic units, referred to as chlorins and porphyrins respectively.[35,36]

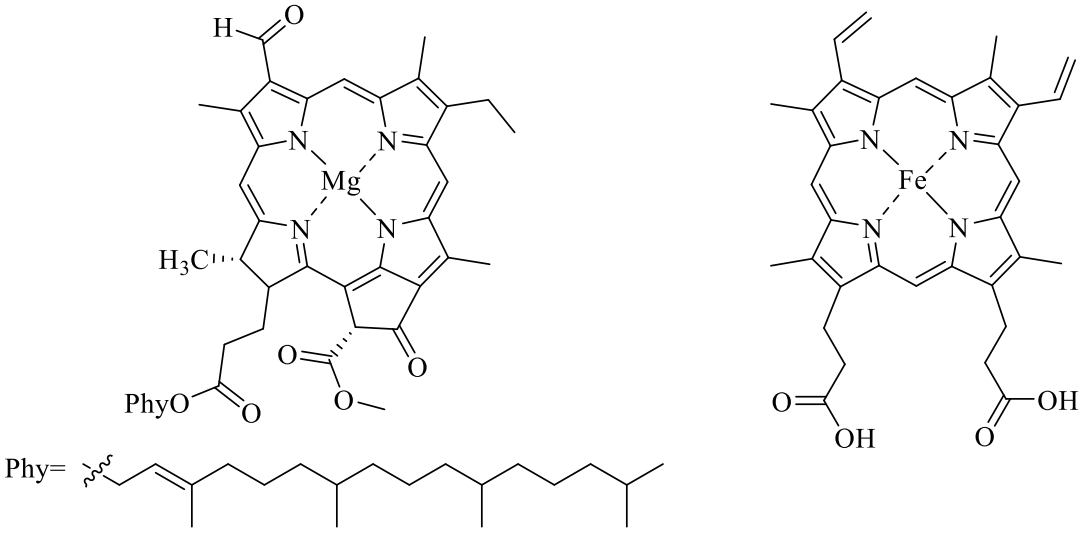

1.18 **1.19**

Figure 5: Structures of natural occurring tetra-pyrrolic molecules, chlorophyll **1.18** and heme **1.19**.

Historically, the porphyrin can be traced back to 1840s from the work of researchers such as Scherer and Mulder. Scherer treated dried and powdered blood with sulfuric acid, leading to the extraction of iron from the precipitates. He found that the red colour of blood was not attributed to the iron in the complexes. Similarly, in Mulder's study, he discussed an iron-free purple-red fluid and called it iron-free haematin. In the later years, researchers such as Thudichum, Schultz, MacMunn, and Hoppe-Seyler studied different derivatives of Por in various studies. The term porphyrin was first brought into limelight by Church during a study on Turaco feathers. In 1883, Soret discussed the key spectroscopic character of porphyrins, i.e. the strong absorption band around 400 nm, also referred to now as the Soret band.[37]

1.2.1 Porphyrin Structure

At the beginning of 20th-century, Kuster was the first to suggest structures of the cyclic tetrapyrroles.[38] Moreover, subsequent research works affirmed that the *trans* NH-

tautomer is the most stabilized structural form.[39] In the porphyrins, four pyrrole rings are fused together at their α-carbons via methine bridges, thus having 20-carbon-based macrocycles with four nitrogens at the center encircling two protons or metal cation as shown in (Figure 6).[37,40]

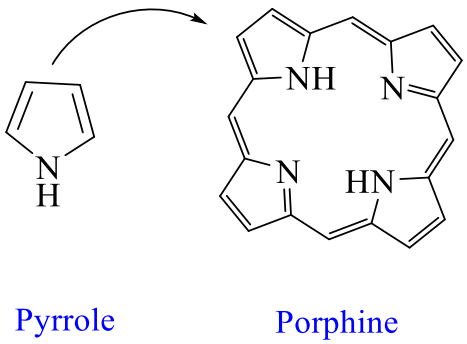

Figure 6: The structure of pyrrole (left) and tetrapyrrole (right).

Porphyrins possess a π system comprising 22 π electrons, with 18 of these electrons contributing to a highly conjugated environment within the porphyrin macrocycle. It adheres to Hückel's rule of aromaticity [4n+2] where n=4, and porphyrins emerge as stable aromatic systems.[41] Hollingsworth's work has delineated six distinct delocalized pathways in porphyrins, each involving 18π electrons (Figure 7).[42]

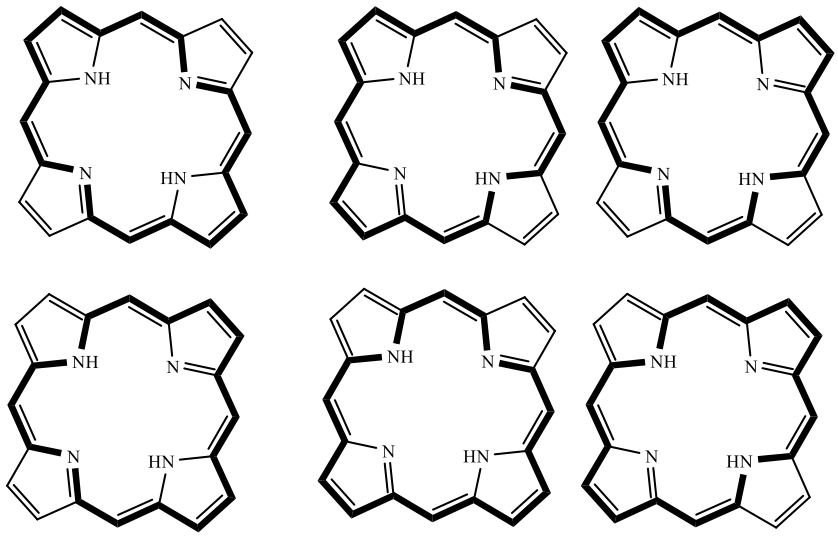

Figure 7: Various delocalised 18π electron pathways for porphyrin.

All porphyrin derivatives share a similar basic architecture with high symmetry structure. The IUPAC numbering and naming of a porphyrin structure is given in (Figure 8). Substitution is limited to methine carbons (also called *meso*-carbons), at positions, 5, 10, 15, 20, and pyrrolic carbons (also called β-carbons), at positions 2, 3, 7, 8, 12, 13, 17, 18.[39,43] The two central nitrogen atoms can either bond two protons or form a di-anion by losing two protons. This di-anion is the key to metalation of free-base porphyrins resulting in formation of porphyrin's metal complexes, often referred to as 'metalloporphyrins' as shown in (Figure 9).[44]

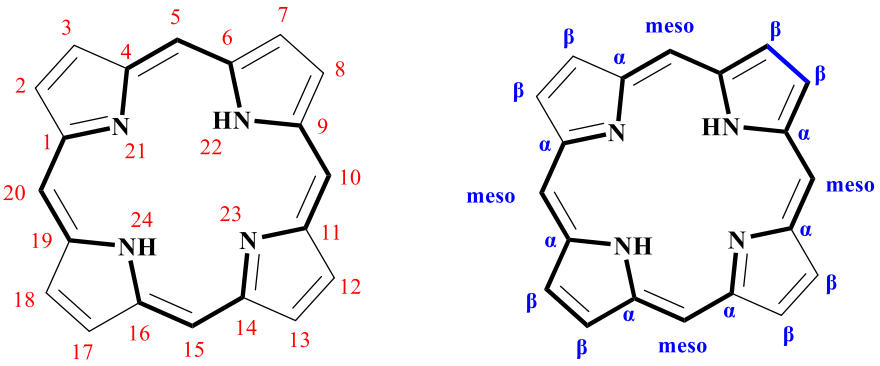

Figure 8: The IUPAC numbering and naming of porphyrin structure.

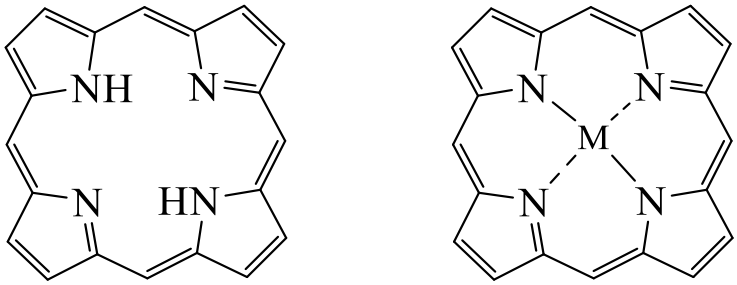

Figure 9*:* The free base porphine and metalloporphyrin structure.

1.2.2 Porphyrins' UV-Vis Spectroscopy

The high conjugation of porphyrin structures enables them to absorb in the visible and near UV. Porphyrins display a fascinating and distinctive visible spectrum because of two

distinct types of bands. The first band is called the Soret or B band which is typically observed between 380 and 450 nm based on whether the porphyrin is (β) or *meso*-substituted. It represents a strong transition from the ground state S_0 to the second singlet excited state S_2. The other bands, known as the Q bands, represent weaker transitions from the ground state S_0 to the first singlet excited state S_1, in the range between 500-750 nm. The number of these bands can depend on whether the porphyrins contain metal or not. Typically, metal-free porphyrin has four Q bands between 500-750 nm while in metalloporphyrin two Q bands are observed due to the increased symmetry of the molecule.

The absorption spectrum of porphyrins has been well-explained by the Gouterman four-orbital model, which emphasises the significance of charge localization on electronic spectroscopic properties.[45] The Soret and Q bands arise from π–π* transitions in the porphyrin systems according to the Gouterman four-orbital model. This model includes four orbitals: two π orbitals a_{1u} (HOMO) and a_{2u} (HOMO-1), and two π* orbitals e_{gx} (LUMO) and e_{gy} (LUMO +1) (Figure 10a,b). By changing the peripheral substituents on the porphyrin ring or the metal centre, it is possible to affect the energies of these transitions, which in turn causes a change in the spectral properties of the porphyrin.

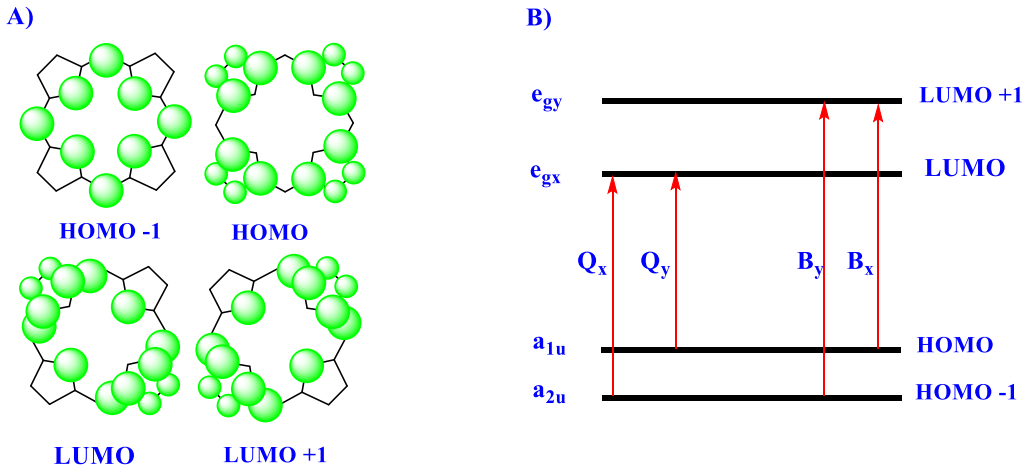

Figure 10: a) Gouterman four orbital model and b) the transitions between energy levels.

1.2.3 Synthesis of Porphyrin

Many β-porphyrins can be conveniently extracted from natural sources, such as protoporphyrin IX. However, *meso*-porphyrins don't occur naturally, and they have to be synthesized from basic units, such as pyrroles. The basic mechanism involves the electrophilic substitution of pyrrole units at positions 2 and 5.[39] Generally, a porphyrin with identical substituents at four *meso*-positions can be synthesized via the condensation of pyrrole and aldehyde units.[46] However, when mixed-aldehydes (different aldehyde species) are employed in this condensation reaction, the outcome is a mixture of porphyrins with a variety of different substitution patterns.[47] Numerous methods have been developed over the past hundred years for constructing porphyrin-based macromolecules, as given below.

Rothemund Synthesis

This method, pioneered in 1935 by Rothemund, was based on the condensation of pyrroles with aldehydes in sealed tubes.[48] In his subsequent efforts, he was able to obtain several porphyrins, such as *meso*-tetraphenylporphyrin (TPP, **1.22**), by condensing pyrrole **1.20** and benzaldehyde **1.21** in pyridine in a sealed vessel at 155 °C for around two days (Scheme 3).[49] However, this method produces **1.22** in very low yield (9%) with the main side product being *meso*-substituted chlorin **1.23**. Calvin and co-workers addressed this issue by adding zinc acetate to the reaction mixture, which not only decreased the amount of chlorin **1.23** obtained but also increased the yield of porphyrin.[50]

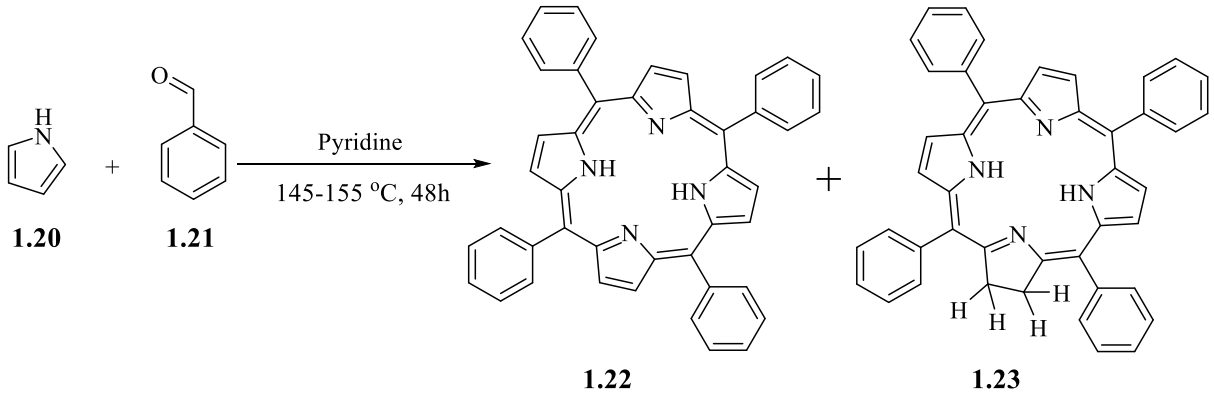

Scheme 3: The synthesis of *meso* TPP as per Rothemund synthesis.

Adler Synthesis

The Rothemund synthesis was further refined in 1967 by Adler and Longo.[51] In this method, pyrrole was reacted with benzaldehyde in refluxing propionic acid for 30 minutes under open air conditions (Scheme 4). The yield of TPP **1.22** was improved by this method and obtained in ~20%.

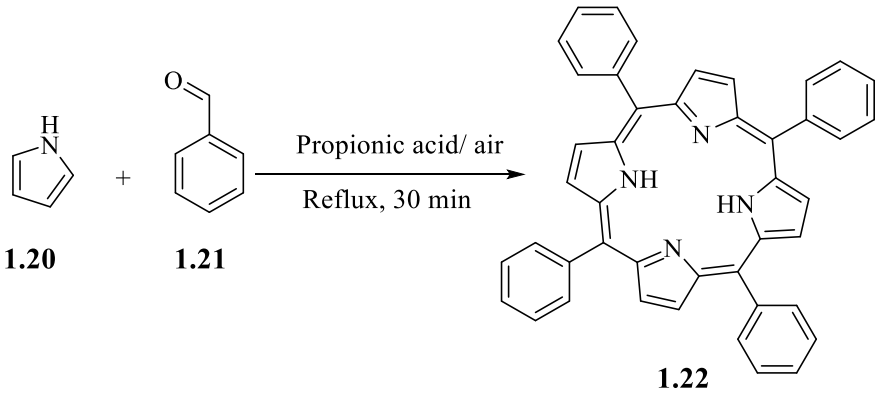

Scheme 4: The synthesis of *meso* TPP as improved by Adler.[51]

Although this method offers improvements over the Rothemund method, such as higher yields and faster reaction rates, it still has some challenges. The conditions remain relatively harsh which complicated the inclusion of aldehydes with sensitive groups and the purification process due to the formation of tar. Despite these issues, this method is effective and still used extensively for synthesizing symmetrical porphyrins.

Lindsey Synthesis

In 1987, Lindsey developed a new method for synthesizing symmetric porphyrins.[46,52] This method was an improvement on previous two methods and utilized acid as a catalyst ($BF_3 \cdot Et_2O$ or TFA) for carrying out TPP **1.22** synthesis reaction in milder conditions. Under such reaction conditions, aldehydes sensitive to high temperature could also be used affording product in a good yield, as high as 30-40%, were obtained. 2,3-Dichloro-5,6-dicyanobenzoquinone (DDQ) or *p*-chloranil was required for oxidizing the initially obtained porphyrinogen **1.24** into porphyrin (Scheme 5). This method is very useful for the synthesis of highly symmetrical porphyrins utilizing only one aldehyde.

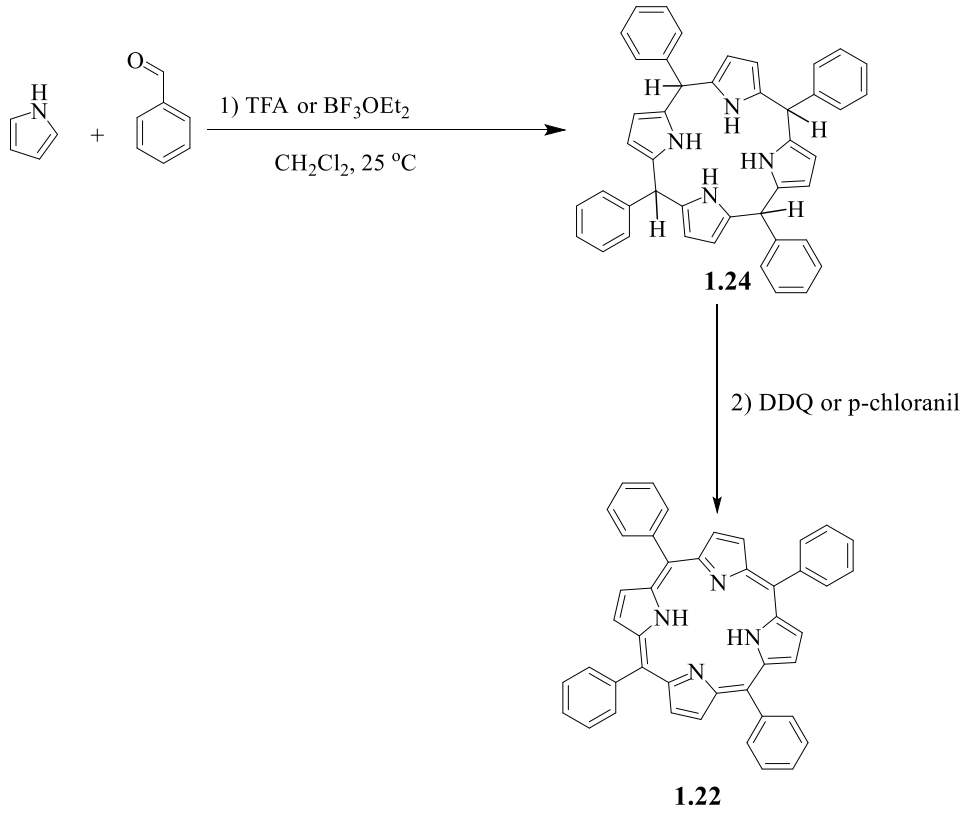

Scheme 5: The synthesis of *meso* TPP **1.22** as per improved Lindsey synthesis.

The Synthesis of Unsymmetrical Porphyrins

In order to obtain porphyrins bearing various *meso* substituents, a different method was required. In 1975, Little and coworkers presented a method which is often referred to as a mixed-aldehyde.[53] It was a derivation of Adler's synthesis and involves two different aldehydes (A and B) reacting with pyrrole resulting in various porphyrin products (*e.g.*, A_4, A_3B, AABB, ABAB, AB_3 and B_4). The yield of the desired porphyrin is dependent on its isolation as well as the ratio and reactivity of the aldehydes. Typically, this method is used to obtain A_3B unsymmetrical porphyrins with an initial aldehyde ratio of 3:1. as shown in (scheme 6).

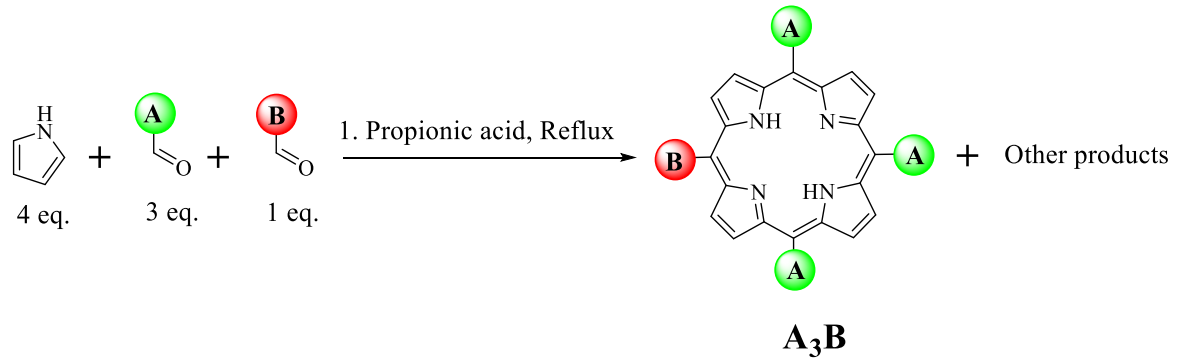

Scheme 6: The synthesis of a non-symmetrical porphyrin as per Little's method.

However, this method is not efficiently used to form pure *trans*-A_2B_2-porphyrins because of the formation of six different porphyrins/isomers which have been proved to be difficult to separate and result in very low yield of the desired product as shown in (Scheme 7).[51] Additionally, in many cases it is not possible to separate the *cis* and *trans* isomers.[54]

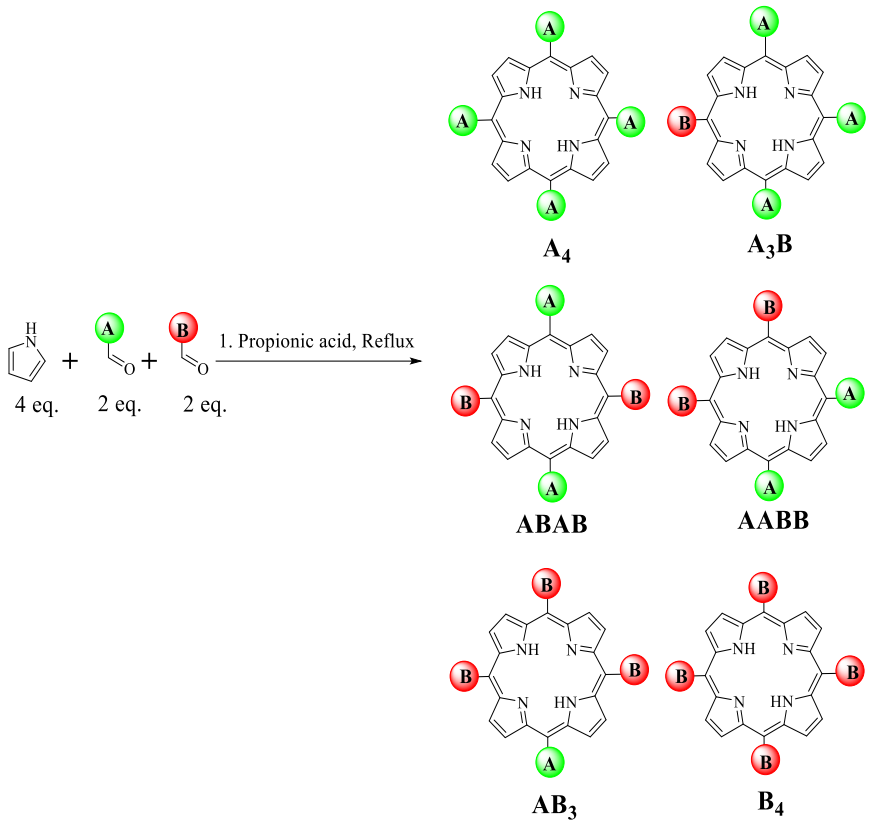

Scheme 7: The synthesis of complex mixture of porphyrins from the condensation of mixed aldehydes with pyrrole.

The Synthesis of Porphyrins from Dipyrromethanes

Porphyrins with two different *meso* substituents, particularly *trans* porphyrins ABAB are more conveniently synthesized using MacDonald-type 2+2 condensations.[55] This protocol involves two steps in which, initially, a dipyrromethene **1.26** intermediate is synthesized through the condensation of pyrrole **1.20** with aldehyde **1.25**. Then, this intermediate is reacted with a second aldehyde **1.27** to produce a *trans* porphyrin **1.28** (Scheme 8).[47]

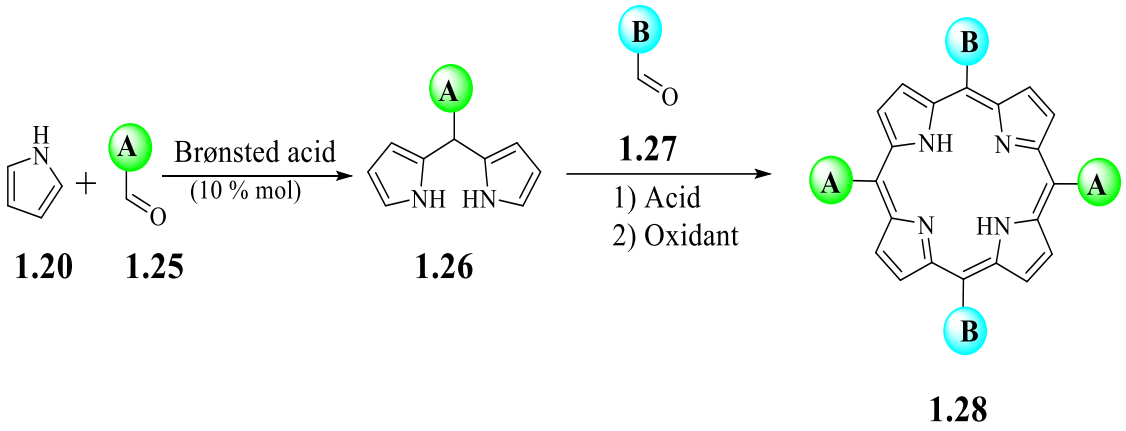

Scheme 8: Synthesis of dipyrromethane **1.26** followed by its condensation with a second aldehyde for the preparation of a *trans* porphyrin ABAB.

In the first step, a dipyrromethane **1.26**, also referred to as dipyrrin,[56] consisting of two pyrrole units fused together by a methylene bridge, can be obtained through a condensation reaction of pyrrole **1.20** with aldehyde **1.25** in the presence of Brønsted acid catalyst, such as TFA.[57] However, the main disadvantage of synthesizing dipyrromethane is the formation of polymers and oligomers from which it was often found to be very hard to isolate the desired product. Therefore, in 1994, Lindsey put forward an improved form of the one-flask classical synthesis (Scheme 8). Thus, a large excess (40-fold) of pyrrole was used in the absence of solvent and in the presence of a catalyst such as trifluoroacetic acid or $BF_3 \cdot Et_2O$ in order to avoid the formation of by-products. The suppression of byproducts led to a considerable improvement (~50-75%) in the yield of desired 5-dipyrranes (dipyrromethanes, DPMs), which were purified using flash column chromatography.[58]

The second step involves the condensation of the dipyrromethane with an aldehyde, again, in acidic conditions. This method, however, often results not only in the targeted *trans* A_2B_2-porphyrin but also in a wide statistical distribution of porphyrin products, equal to that of a mixed aldehyde condensation. This is because of the reversible nature of the reaction which

leads to a phenomenon known as scrambling (Scheme 9).[59] This happens under acidic conditions, causing rearrangement and recombination of pyrromethane oligomers, producing a broad mixture of porphyrins which are difficult to separate.

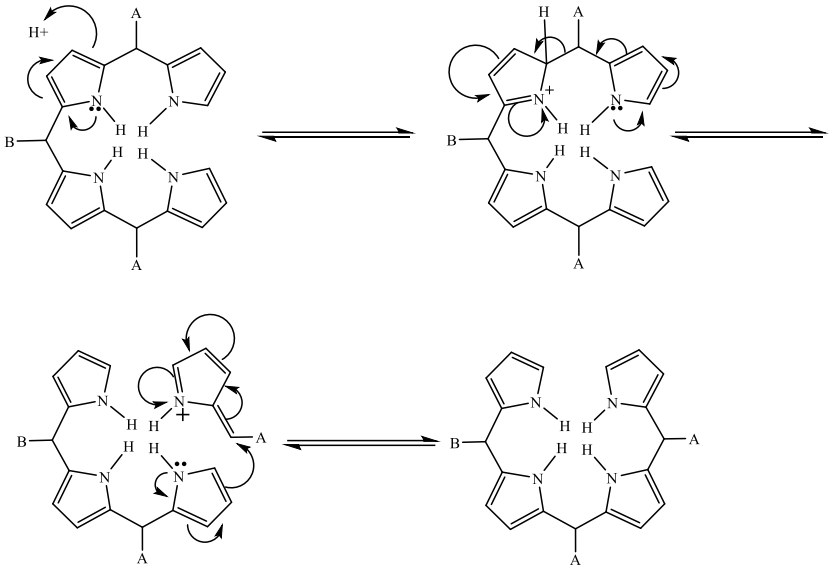

Scheme 9: Illustration of a typical scrambling process.

Therefore, Lindsey *et al* optimized the reaction conditions for the 2+2 condensation of a dipyrromethane and an aldehyde.[59] They found that the use of sterically hindered DPMs (A= mesityl **1.29**) or electron-withdrawing substituents (A= pentafluorophenyl **1.32**) exhibit less susceptibility to scrambling (10 mM in CH_2Cl_2 containing 17.8 mM TFA for 1 h followed by DDQ oxidation). Under similar conditions the use of unhindered DPMs resulted in scrambling with low yield of the desired *trans* porphyrin (Scheme 10).

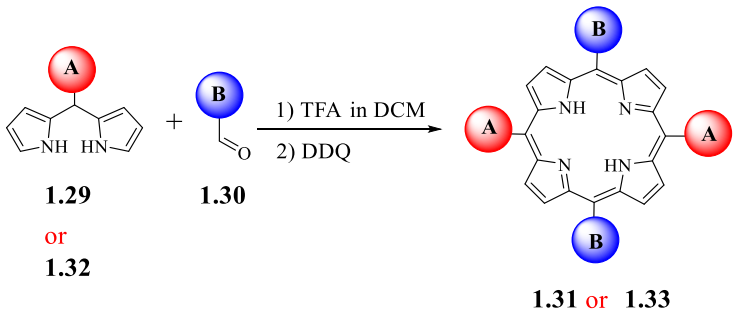

Scheme 10: Synthesis of a *trans* porphyrin from a DPM and an aldehyde.

Later, in 2000, Lindsey introduced a new protocol in order to synthesize *trans*-A_2B_2-porphyrins from either hindered or unhindered DPMs.[60] This protocol exploited a stepwise synthesis which commenced with the synthesis of a dipyrromethane **1.34** and its subsequent monoacylation followed by reduction to dipyrromethane-carbinol **1.37**. Finally, self-condensation produces porphyrins. Here dipyrromethane is synthesized in the same way as described previously (see scheme 8).[58] This dipyrromethane is treated with EtMgBr followed by pyridyl thioester **1.35** to obtain 1-acyldipyrromethane **1.36** which can then be easily reduced with excess $NaBH_4$ in THF/MeOH to form carbinol **1.37**. Finally, a self-condensation of carbinol **1.37** results in the formation of *trans* porphyrin **1.38** without scrambling (Scheme 11).

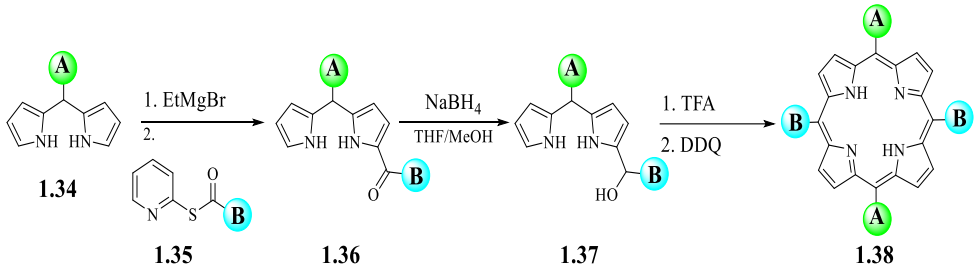

Scheme 11: Synthesis of monoacyl dipyrromethane **1.36** and the pathway leading to *trans*-A_2B_2-porphyrins.

Alternatively, a novel and environmentally friendly method towards formation of *trans* porphyrin was reported by Gryko and co-workers.[61] Their method is based on previous achievement of synthesizing tetrapyrrane (bilane (**1.41**)), in high yield in aqueous media under acid catalysis, which was used as intermediate to form corrole precursor.[62] Later, they found that the tetrapyrrane can be used as a key intermediate to obtain a variety of *trans*-A_2B_2-and A_2BC-porphyrins. The condensation of DPMs and aldehydes in a mixture of MeOH/water or EtOH/water under HCl-catalysis produced a tetrapyrrane intermediate which was oxidized with *p*-chloranil or DDQ to afford *trans* porphyrins

without scrambling in (9-25%) yields (Scheme 12). Recently, Kar and co-workers developed a method of synthesizing *trans*-A_2B_2-porphyrins in aqueous media.[63,64] This is also a two-step protocol where the tetrapyrrane is formed in the first step from the condensation of DPMs and aldehydes in MeOH/H_2O mixture in the presence of HCl. The second step involves refluxing the first intermediate in DMF, followed by stirring in air at room temperature, resulting in the formation of *trans* porphyrins with no detectable scrambling (Scheme 12) in a reasonable (~10-40%) yield.

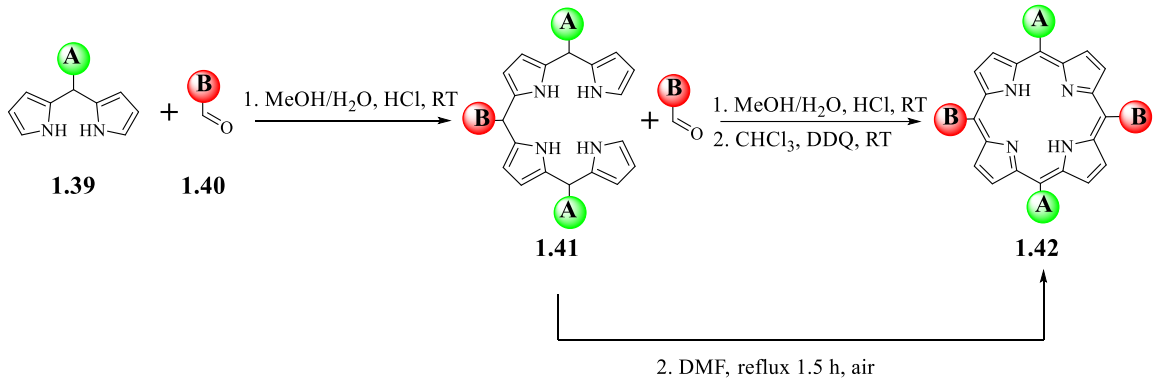

Scheme 12: Synthesis of *trans*-A_2B_2-porphyrin in aqueous media according to Kar and co-workers.

1.3 Phthalocyanine

Phthalocyanine **1.43**, also referred to as pigment blue or H_2Pc, was first discovered by Braun in 1907.[65] It is based on a tetra-isoindole structure interlinked via nitrogen atoms. In the 1930s, its structure was first investigated by Linstead and co-workers, who later developed different type of phthalocyanine metal complex as shown in (Figure 11).[39] The two central hydrogen atoms of **1.43** can be replaced by nearly all metallic ions of the periodic table to form metal complexes. These complexes find extensive applications in several commercial areas such as dyes, organic solar cells and catalysis.

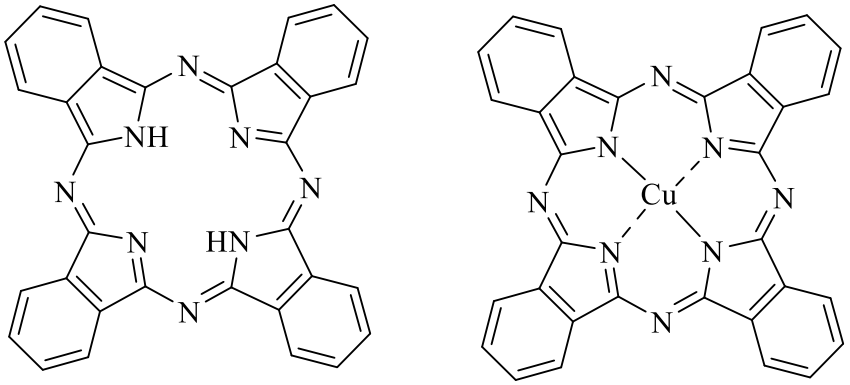

1.43 **1.44**

Figure 11: Phthalocyanine (left), metallated phthalocyanine (right).

Similar to porphyrins, phthalocyanines can be formed by several methods. These methods are generally based on the cyclotetramerization of small molecules. For example, phthalic acid derivatives, numerous ortho-substituted benzenes (*e.g.*, *o*-cyanobenzamide), and phthalimide derivatives, as shown in figure 12. In all of the syntheses involving these molecules, except phthalimides, a metal salt is required under elevated temperatures.

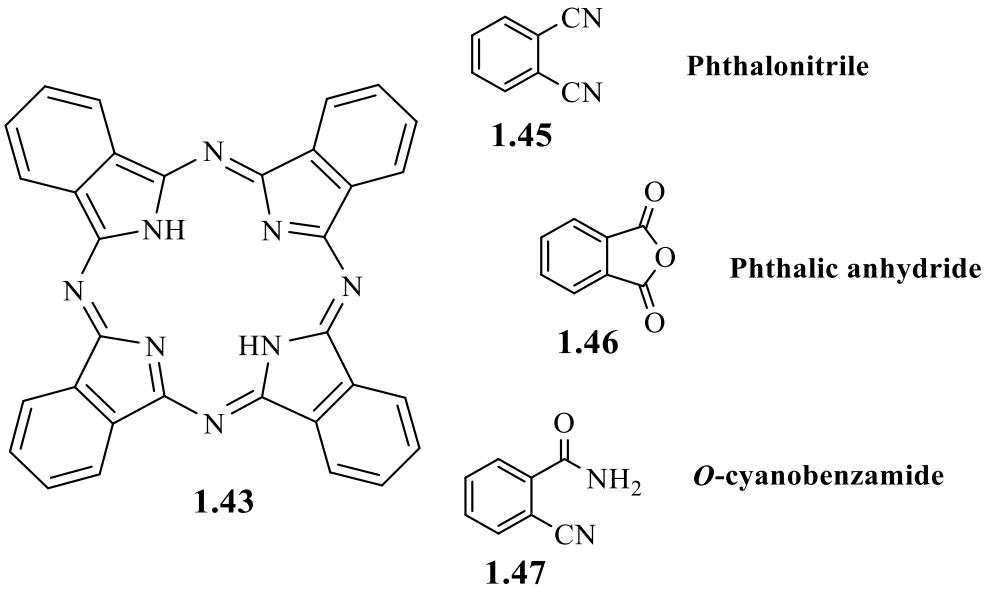

Figure 12: Examples of small molecules that undergo cyclotetramerization to form H_2Pc **1.43**.

1.4 Porphyrin-based rotaxanes

Previously, we presented the basic concepts of supramolecular chemistry, mechanical interlocked molecules particularly (Catenanes and Rotaxanes), porphyrins and phthalocyanines, along with their synthesis. Herein, we aim to present some examples of porphyrin-containing rotaxane structures in which porphyrins can be incorporated as essential subunits attached to macrocycles or employed as stoppers.

Due to the attractive properties of porphyrins in electron and energy transfer processes (See 1.2), remarkable attention has been focused on the study of incorporating porphyrin into mechanically interlocked molecules. This incorporation has led to the discovery of new groups of compounds, extending beyond models related to photosynthesis to include diverse fields like molecular machinery.[66]

1.4.1 Porphyrins as stoppers

There are several ways to use porphyrin units for incorporation in a rotaxane structure. One of the ways is using porphyrins as stoppers at the end of the axle molecule because their large size can prevent the dissociation of a macrocycle from the thread. Additionally, they can be either symmetrical or unsymmetrical stoppers and can be connected to the axle through either axial coordination [67,68] or covalent substitution on one of the *meso* positions.[69,70]

Sauvage reported one of the first example of porphyrin stoppered rotaxanes in 1992.[71] He has taken advantage of "threading followed by stoppering" approach and reported the synthesis of a rotaxane that bears two different porphyrin units as chemical stoppers. The synthesis began with the formation of a pseudorotaxane intermediate **1.50** via the reaction of a pre-synthesized macrocycle **1.48** and gold porphyrin **1.49**. This assembly was facilitated through the coordination of a copper(I) centre, which played a crucial role in the template-

directed assembly process. The Cu(I)-complexed product [2]rotaxane **1.53** was then formed by treating **1.50** with (3,3′-diethyl-4,4′-dimethyl-2,2′-dipyrryl)-methane **1.51** and 3,4-di-tert-butylbenzaldehyde **1.52** in dichloromethane, using trifluoroacetic acid as a catalyst. An oxidation step, using chloranil, followed by a metalation step with zinc acetate resulted in the formation of **1.53** in 19% overall yield. The process was then completed by eliminating the copper(I) centre, which was achieved with the use of KCN.[66] This resulted in a free rotaxane **1.54** as shown in scheme 13.

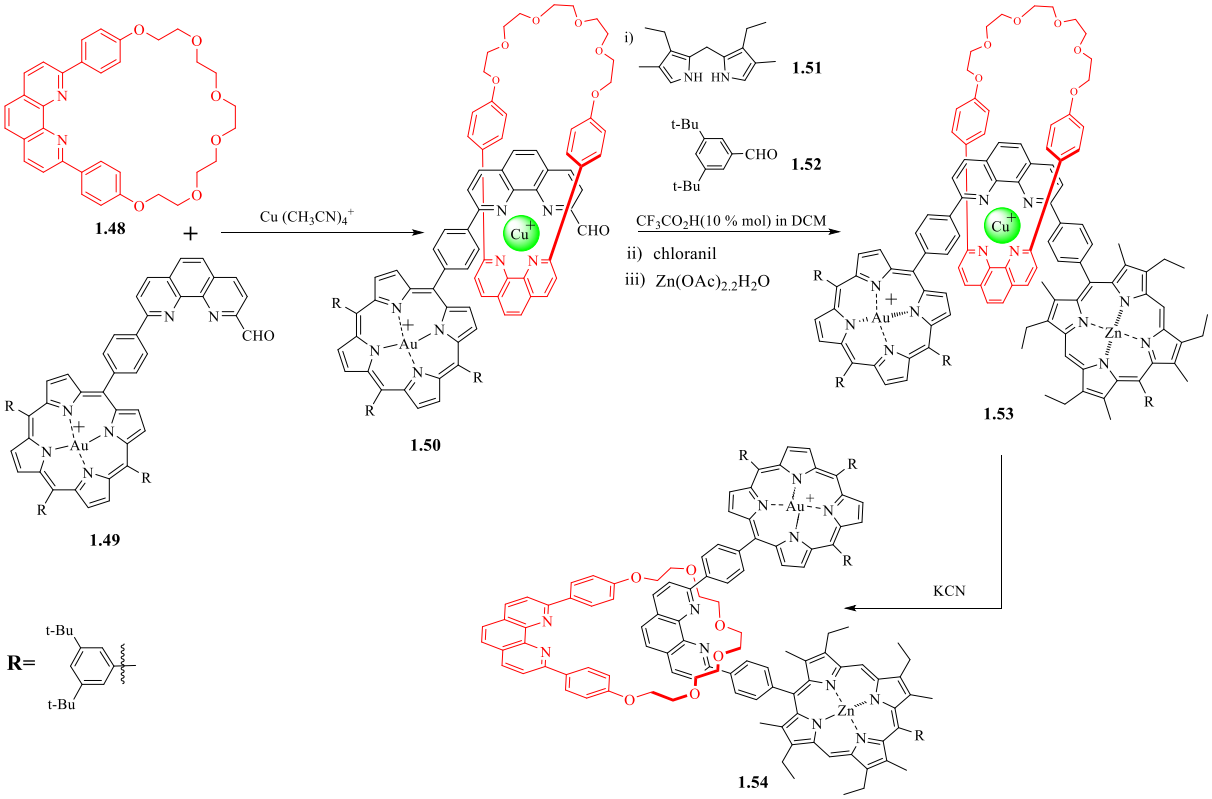

Scheme 13: Synthesis of [2]rotaxane **1.54** using two porphyrins as stoppers.

Previously, we highlighted that the active metal template protocol is widely used in the synthesis of rotaxanes and has been also shown to be useful in the synthesis of rotaxanes containing conjugated porphyrins. Interestingly, Anderson *et al.*, reported a facile formation of a [2]rotaxane **1.57** consisting of a butadiyne linked to porphyrins as stoppers in 61% overall yield.[72] Their method extends not just in using porphyrins as stoppers but also in creation of

more complex designs such as catenanes. Initially, a [2]rotaxane **1.57** was achieved by stirring porphyrin **1.55** with phenanthroline macrocycle **1.56**, copper(I) iodide, iodine and potassium carbonate in a mixture of (1: 1) toluene and THF for 5 days at 60 °C. Additionally, they were able to transform [2]rotaxane **1.57** into a [4]catenane **1.61** using the obtained rotaxane **1.57** as an intermediate. Thus **1.57** was deprotected using TBAF to obtain porphyrin [2]rotaxane **1.58** that contains two terminal alkynes. The use of hexapyridyl template **1.59** was necessary to pre-organise the rotaxane units via coordination to the axial sites of the zinc metalloporphyrin centres with subsequent palladium-catalysed Glaser-coupling between their alkyne extremities, efficiently giving the higher-order catenane **1.61** in 89% overall yield after the removing of the template with DABCO. This is an excellent example showing how the synthesis of rotaxane can lead to further developments in the catenane chemistry (Scheme 14).

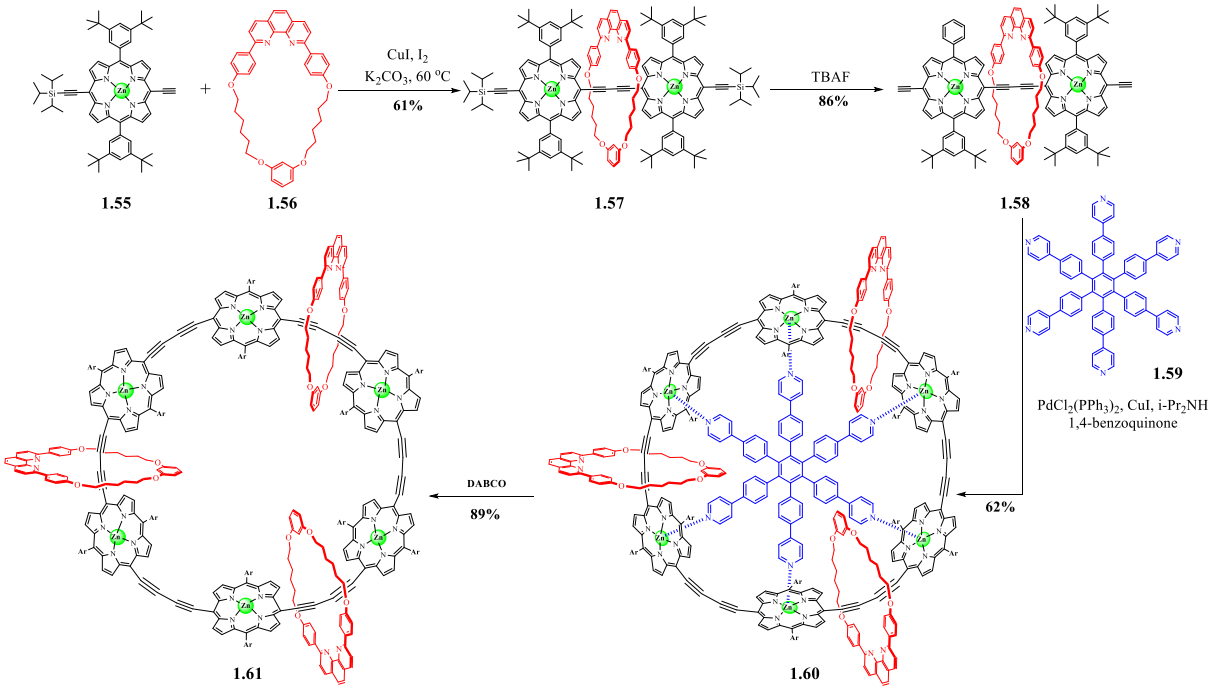

Scheme 14: Anderson's synthesis of [4]catenane from an active metal templated [2]rotaxane.[72]

1.4.2 Porphyrins as Part of a Macrocycle

Previously, we have seen several examples of porphyrins serving as stoppers and now some recent examples of porphyrins as macrocycles are described. The shift towards incorporating porphyrins within macrocyclic components has significantly advanced the field of porphyrin-containing rotaxanes, bringing about novel structural and functional properties. These macrocycles act as host systems, capable of integrating either a single porphyrin unit or multiple units into their structure. In the case of single strapped porphyrins (See next section), a specific molecular linker is joined to two opposite corners of the porphyrin molecule, leading to form a hollow structure that can function as the macrocycle of a rotaxane assembly. Furthermore, the assembly can be complexed by joining multiple porphyrins with two or more linkers, leading to the formation of molecular containers.[73] Such molecular containers can also be extended to cyclic dimers having metalloporphyrins connected covalently with two linkers. These linkers can be conformationally flexible or rigid and they determine the conformational characteristics of the molecule. Based on these conformations, the binding cavity can host different types of guest molecules resulting in mechanically interlocked molecules as will be discussed in the following section.

1.4.2.1 Examples of rotaxanes incorporating porphyrins in the macrocycle

The synthesis of such strapped porphyrins and their integration into mechanically interlocked architectures has been widely described.[68,74–77] In one study, Weiss e*t al*., described the synthesis of [2]rotaxane **1.65** that contained a strapped zinc porphyrin-phenanthroline **1.62** as a macrocycle utilizing a "tandem active metal template" approach. A second metal ion, zinc (II), was introduced into the porphyrin ring alongside the phenanthroline-bound copper, which plays a crucial role in the Huisgen 1,3-dipolar

cycloaddition reaction, a vital step for assembling the final rotaxane **1.65**.[78] In this example, zinc porphyrin macrocycle **1.62** was treated with $Cu(MeCN)_4PF_6$, producing the zinc-copper complex *in situ*. Subsequently, treatment with azide **1.63** and alkyne **1.64**, bearing bulky stoppers, in the presence of diisopropylethylamine (DIPEA) resulted in the formation of a mixture of rotaxanes containing copper, zinc, or both. Sequential removal of the copper and zinc using ethylenediaminetetraacetic acid (EDTA) and trifluoroacetic acid (TFA) yielded the metal-free rotaxane **1.65** (Scheme 15).

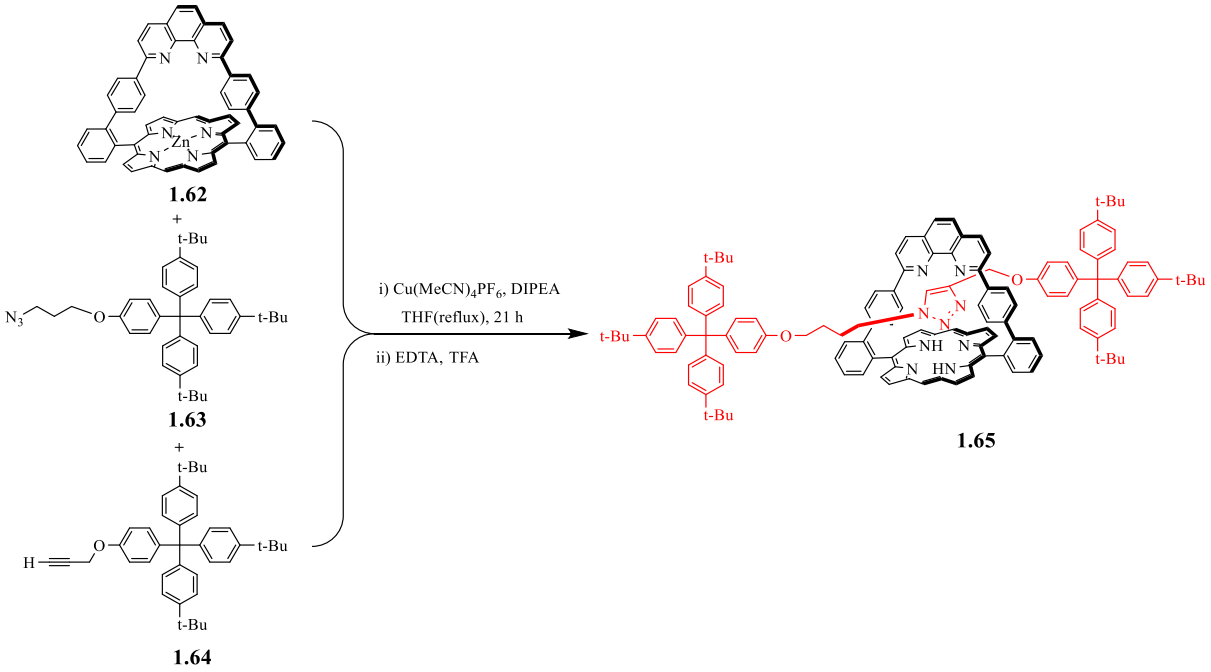

Scheme 15: Synthesis of [2]rotaxane **1.65** using strapped porphyrin macrocycle **1.62**.

Recently, the group of E. M. Pérez described rotaxane-type mechanically interlocking carbon nanotubes (MINTs) that contain two metalloporphyrin units and SWCNT based on non-covalent interactions within **1.76**.[79] This was performed using a cyclic porphyrin dimer **1.74** as a macrocycle and the SWCNT **1.75** as a thread. Their method, based on a clipping strategy, initially required the formation of U-shape molecule **1.74**. This was formed from multistep synthesis starting from the reaction of 2,4,6-trimethylphenyldipyrromethane **1.66** with benzaldehyde **1.67** under Lindsey conditions, resulting in the formation of protected porphyrin

1.68. Deprotection of porphyrin **1.68** using TBAF gave key intermediate **1.69**. The *o*-alkylation reaction was then applied to selectively form mono-alkylated porphyrin **1.71** which subsequently reacted again under Williamson ether reaction conditions in the presence of 1,6-dibromohexane **1.72** to obtain the U-shaped intermediate **1.73** in 67% overall yield. The use of the hexamethylene as a spacer was necessary to provide flexibility to template the macrocyclization around SWCNTs via ring-closing metathesis (RCM) of the terminal alkenes affording the desired MINTs **1.76** (Scheme 16). The characterization of MINTs confirmed the mechanical interlocking of the porphyrin rings with the SWCNTs via various spectroscopic and analytical techniques like UV-vis-NIR absorption and fluorescence.

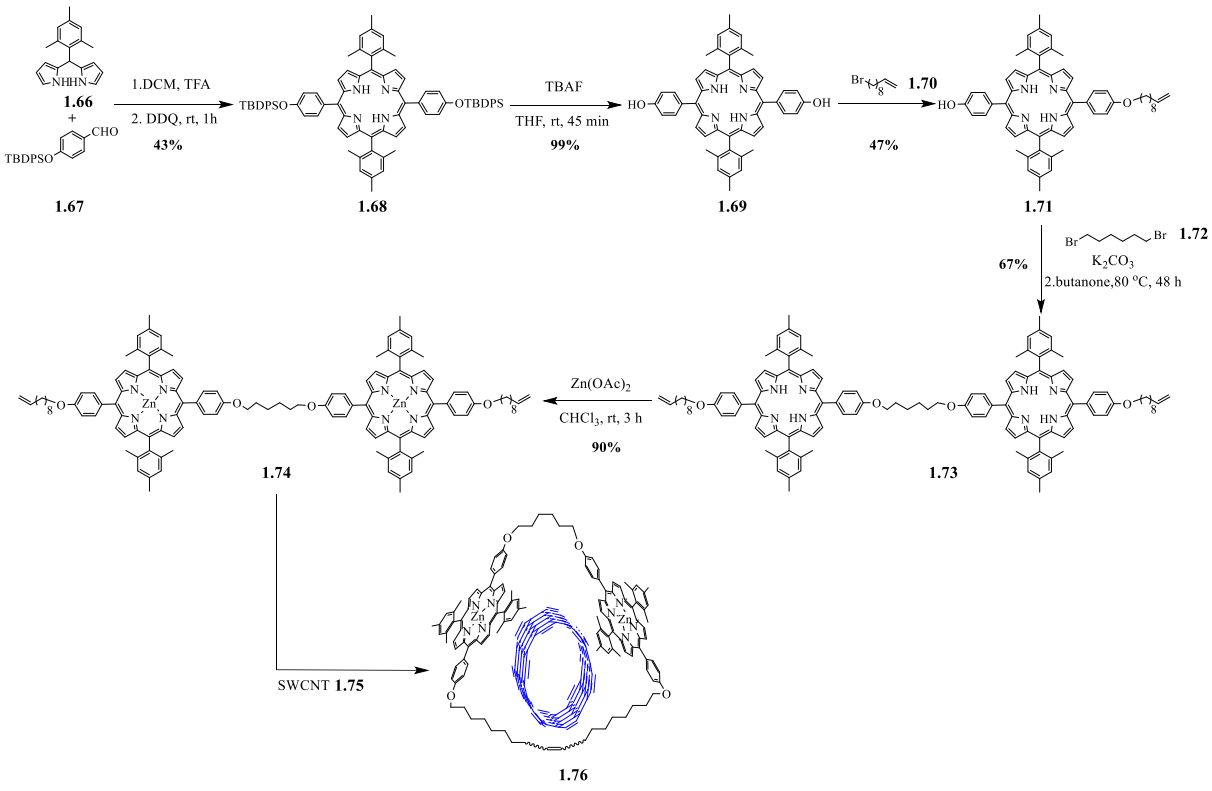

Scheme 16: The Synthesis of Mechanically Interlocked Carbon Nanotubes (MINTs) incorporating metalloporphyrin units **1.74** and SWCNTs.[79]

Building on the previously synthesized bis-porphyrin macrocycle **1.77** by Yashima and coworkers, the same group have recently used **1.77** to synthesize [2]rotaxane **1.79** based on π-

π stacking interactions.[80,81] This advancement uses a distinctive approach to encapsulate a derivative of naphthalene-diimide, bearing bulky stoppers at both ends (**1.78**) within the bis-porphyrin cavity. This process takes advantage of the distinctive characteristics of a double-stranded spiroborate helicate, utilizing its dynamic boron-oxygen (B−O) bond cleavage and reformation to incorporate **1.78**. The procedure is facilitated by heating a 1:1 mixture of **1.77** and **1.78** in CD_3CN with a significant excess of water at 80 °C for 92 h or extended to 1 week. This approach resulted in the formation of [2] rotaxane in a 68% yield for the shorter period and almost quantitative yield for the longer period. They found that the addition of water greatly increases the flexibility of the helicate, enabling its bis-porphyrin cavity to expand and close around the guest molecule. After encapsulation, the B−O bonds become dynamic and reform, securing the guest molecule within the macrocycle (Scheme 17). This procedure highlights the possibility of creating complex [2]rotaxane structures.

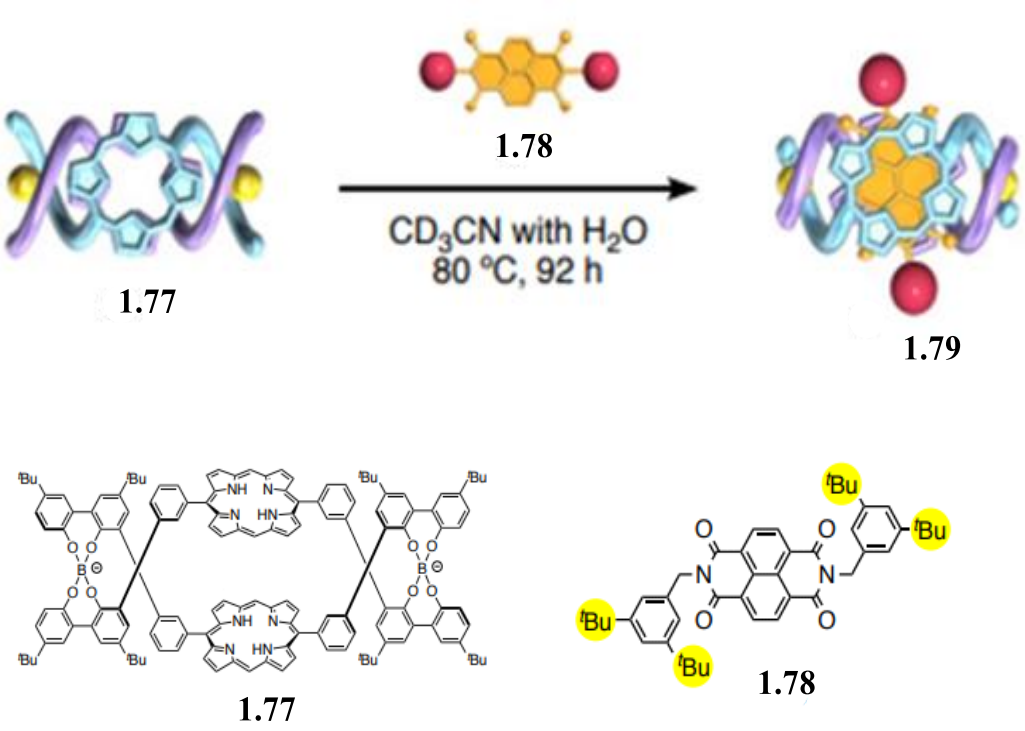

Scheme 17: The preparation of [2]rotaxane **1.79** via dynamic bis-porphyrin macrocycles **1.77** adapted from Yashima and coworkers.[81]

Very recently, in 2023, a [2]pseudorotaxane was reported by Heitz *et al.*[82] This study demonstrates an advanced method for building mechanically interlocked molecules (MIMs) through allosteric regulation mechanisms. The procedure includes the strategic assembly of a half-dumbbell component with a pyrazine coordination site **1.82** with a bis-Zn(II) porphyrin cage **1.80**, where the latter serves as a multisite ring. Initially, this cage **1.80** was previously reported by the same group, and it consists of two cofacial Zn (II) porphyrins linked by connectors that bear eight peripheral 1,2,3-triazoles.[83] The assembly of the [2]pseudorotaxane **1.83** was achieved in two steps. The initial step involves the use of AgOTf with cage **1.80** followed by anion metathesis with NaBArF in order to bind the Ag(I) ions to the 1,2,3-triazole sites located on the porphyrin connectors of the cage. This results in a significant conformational change from a flattened structure to an open one **1.81**. The [2]pseudorotaxane **1.83** was then formed through the reaction of cage **1.81** with a half-dumbbell **1.82** (Scheme 18).

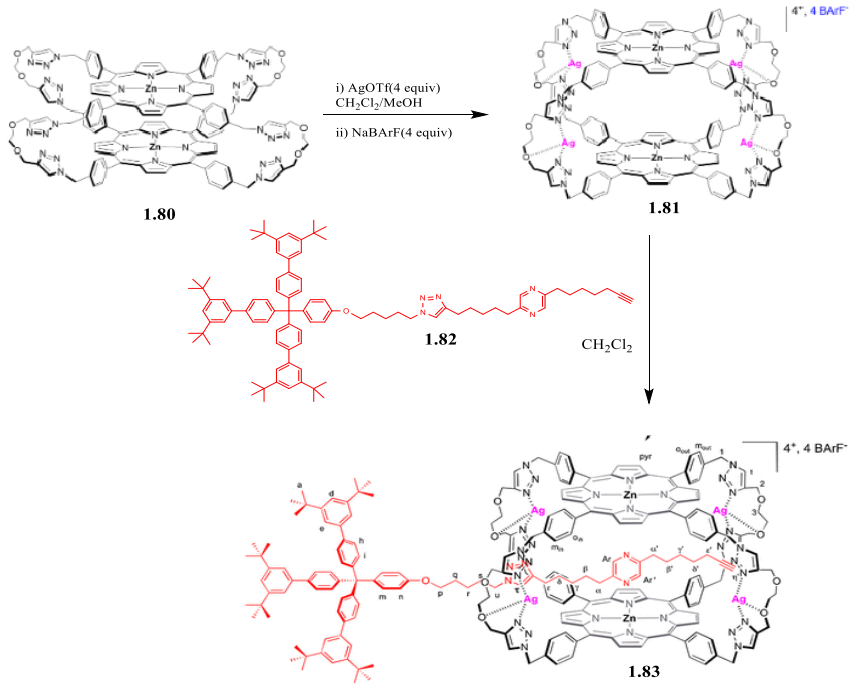

Scheme 18: The synthetic method of [2]pseudorotaxane **1.83** preparation developed by Heitz *et al.*[82]

As the examples above show, porphyrins are interesting due to their unique interactions and binding properties with different molecules, which justifies their integration into rotaxanes. This integration has led to significant advancements in the field of supramolecular chemistry. By strategically incorporating porphyrins as either pivotal components of the macrocycle or as chemical stoppers, new possibilities for the design and synthesis of mechanically interlocked molecules with unique properties has been established. This approach not only allows exploitation of porphyrins' remarkable electron and energy transfer capabilities but also extends the application of rotaxanes beyond traditional models, venturing into the development of molecular machinery and complex molecular systems. The detailed examples underscore porphyrins' versatility in enhancing the structural complexity and functional diversity of rotaxane assemblies, offering insights into the potential for further innovation in materials science and nanotechnology. This exploration of porphyrin-containing rotaxane structures highlights the compound's pivotal role in advancing supramolecular chemistry, suggesting an exciting future for their application in creating sophisticated molecular architectures. Therefore, we will investigate the formation of a new rotaxanes based on cyclic porphyrin dimers as a macrocycle, and phthalocyanine as a thread by our strategy, which will be discussed in the next chapter.

Results & Discussion

2.1 Previous study

In this section, we aim to cover some previous studies about the formation of triple decker complexes as an introduction to a recently developed strategy by our group that has been used in this work.

2.1.1 Triple Decker Complexes

In recent years, a considerable attention has been focused on the study of complexes of porphyrins and/or phthalocyanines with various metals especially lanthanides. The insertion of metal ions into the central cavity of these macrocycles can produce a variety of structural configurations like double- and triple- decker complexes. These complexes can be classified as homoleptic (same macrocycle type) or heteroleptic (different macrocycle types). They have unique structural, photophysical and electronic properties that make them highly intriguing for a range of applications, such as information storage, photovoltaics, and magnetic resonance.[84]

The synthesis of sandwich complexes with different porphyrins or phthalocyanines has been known since 1986. Interest in these compounds grew further in the 1990s, especially with the introduction of mixed phthalocyaninato and porphyrinato ligands.[85] Since then, several methods have been developed for the synthesis of porphyrin and phthalocyanine triple decker complexes. One of these methods was known as ‘‘one by one deck construction of triple decker’’ which required multistep reactions. The reaction of porphyrin **2.1** with $M(acac)_3$ in TCB generated (Por)M(acac) **2.2** which was then treated with phthalonitrile to give the desired double decker complex **2.3**. Its further reaction with (Por)M(acac) **2.2** gave heteroleptic triple decker complex **2.4** as shown in scheme19.[85]

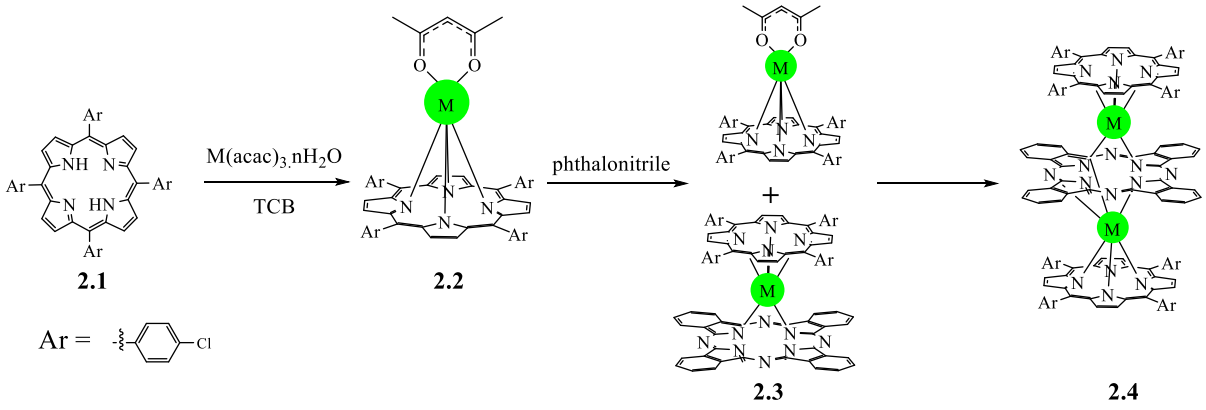

Scheme 19: Synthetic pathway for the formation of triple decker complex **2.4**.

Alternatively, Tsivadze *et al.,* proposed a new strategy known as a one-pot procedure to improve the yield of triple decker complexes. This was based on the reaction of tetra-*meso*-aryl-porphyrin **2.5** with 4,5-dicyanobenzo-15-crown-5 **2.6** and $La(acac)_3.nH_2O$ in the presence of DBU in refluxing octanol. Complex **2.8** was obtained in moderate yield 32 % after being separated from double decker complex **2.7**. Following the same protocol, a series of lanthanides (*e.g.*, Ce, Pr, Nd, Sm, Eu) were examined, yielding their corresponding triple complexes in 12-35%, as shown in scheme 20. Therefore, this protocol has proved its efficiency in the formation of triple decker complexes compared with the previous protocol.[86]

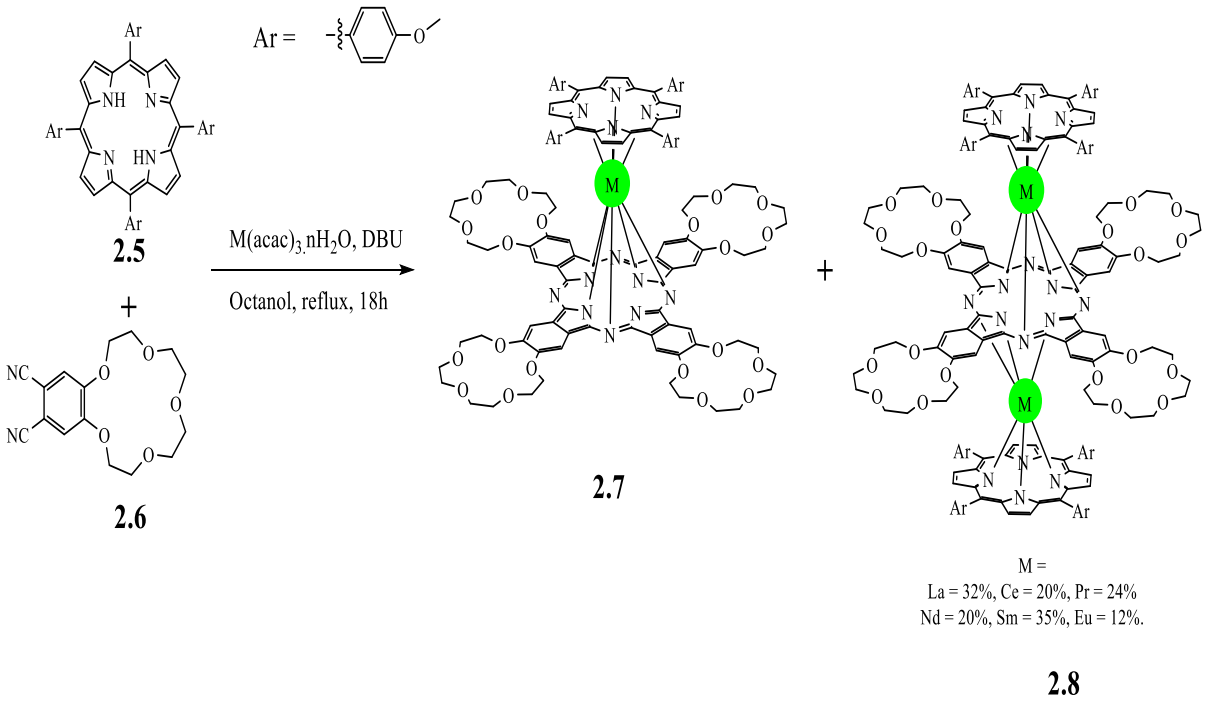

Scheme 20: The synthetic method of triple decker complex preparation developed by Tsivadze *et al.*

Recently, in 2020, our group documented an efficient strategy for accessing triple decker complexes in excellent yield. The protocol involved the synthesis of porphyrin dyad **2.9** which features two porphyrins linked by a decyl chain. Dyad **2.9** then efficiently captures phthalocyanine (Pc) and lanthanide ions to obtain the desired triple decker complex **2.10** in high yield 86%. Following the same protocol, a series of complexes with different lanthanide ions (*e.g.*, Pr, Nd, Sm, Eu) were synthesized. However, when the equivalents of lanthanide ions and phthalocyanine was increased, an open bis-triple decker complex **2.11** was obtained in 34% yield as shown in scheme 21.[87]

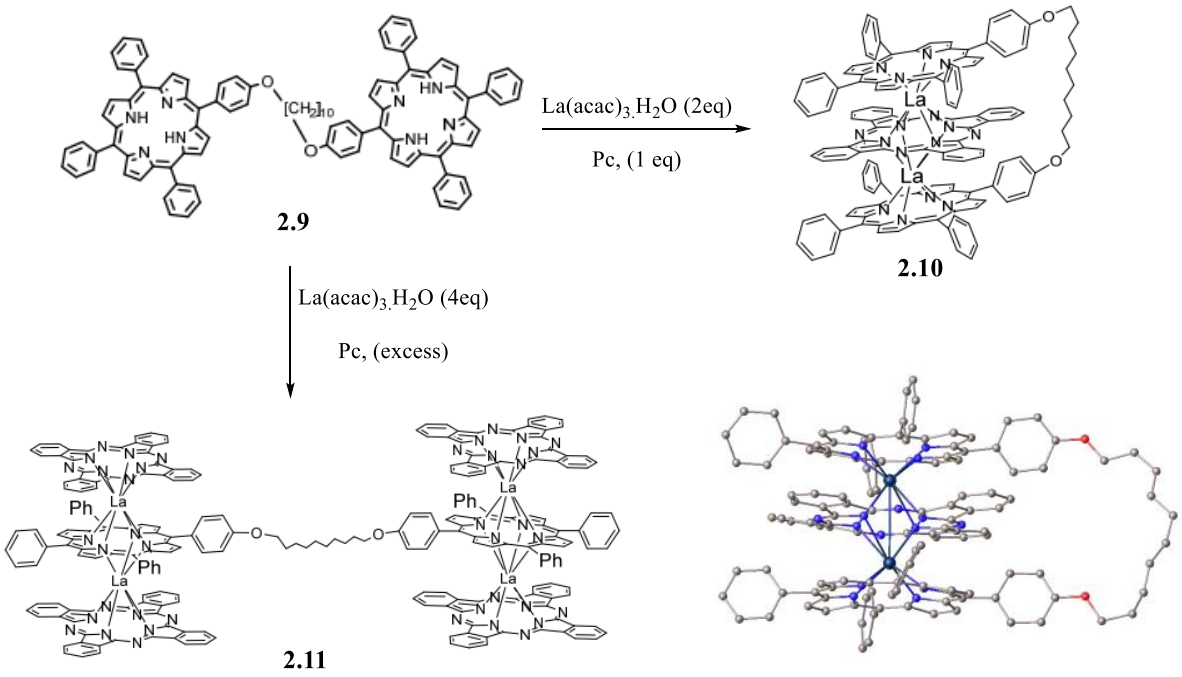

Scheme 21: Cammidge *et al.,* general method for preparing triple decker complexes **2.10** and **2.11** X-ray crystal structure of **2.10** demonstrating the precise alignment of the three macrocycles.

2.2 Present study

The ultimate aim of this project was to design and construct a new rotaxane structure that incorporates a unique assembly of cyclic porphyrin dimer and phthalocyanine motifs. This model will be established by an initial construction of a controlled triple-decker complex through employing our recently developed strategy as described earlier.[87] Once formed, the terminal alkene will be metathesized to entrap Pc within the cyclic porphyrin after the removal of metal ions (Scheme 22).

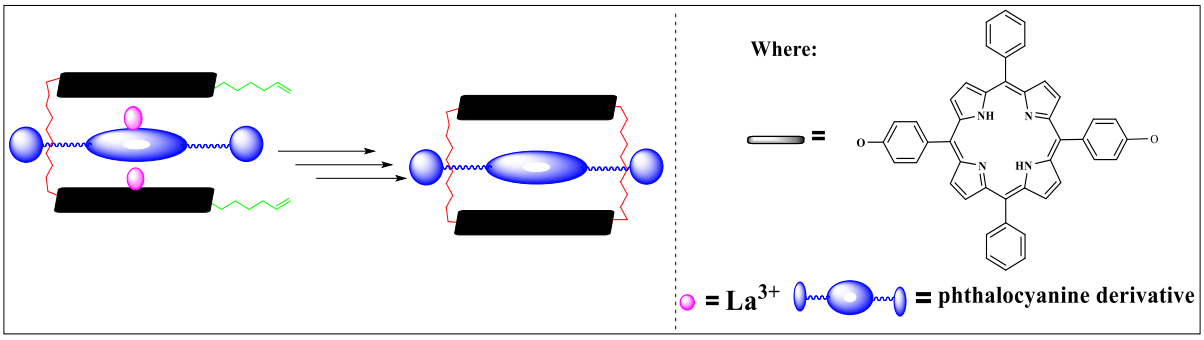

Scheme 22: Cartoon depiction of a rotaxane target.

2.2.1 Strategy

Scheme 23 shows the planned synthetic route for the preparation of our final target. Treating *trans*-5,15-bis(*p*-hydroxyphenyl)porphyrin **2.12** with 6-bromo-1-hexene using the Williamson reaction should afford porphyrin **2.13**. *O*-alkylation using two equivalents of mono-functionalized porphyrin **2.12** with one equivalent of 1,10 dibromodecane should result in the formation of porphyrin dyad intermediate **2.14**. This dyad will then act as a clipping precursor, facilitating the encapsulation of Pc with lanthanide metals serving as templates. Overall, this process should lead to the formation of a controlled triple-decker intermediate **2.15**.

A subsequent cyclization through a metathesis reaction, followed by C=C reduction reaction, aims to produce cyclic triple-decker complex **2.17**. The final step entails removing the bridging metal ions from complex **2.17**, to yield a unique, mechanically entrapped system **2.18**, thereby validating our experimental approach, and demonstrating the feasibility of our hypothesis. Unsubstituted Pc will not be retained in the structure of course.

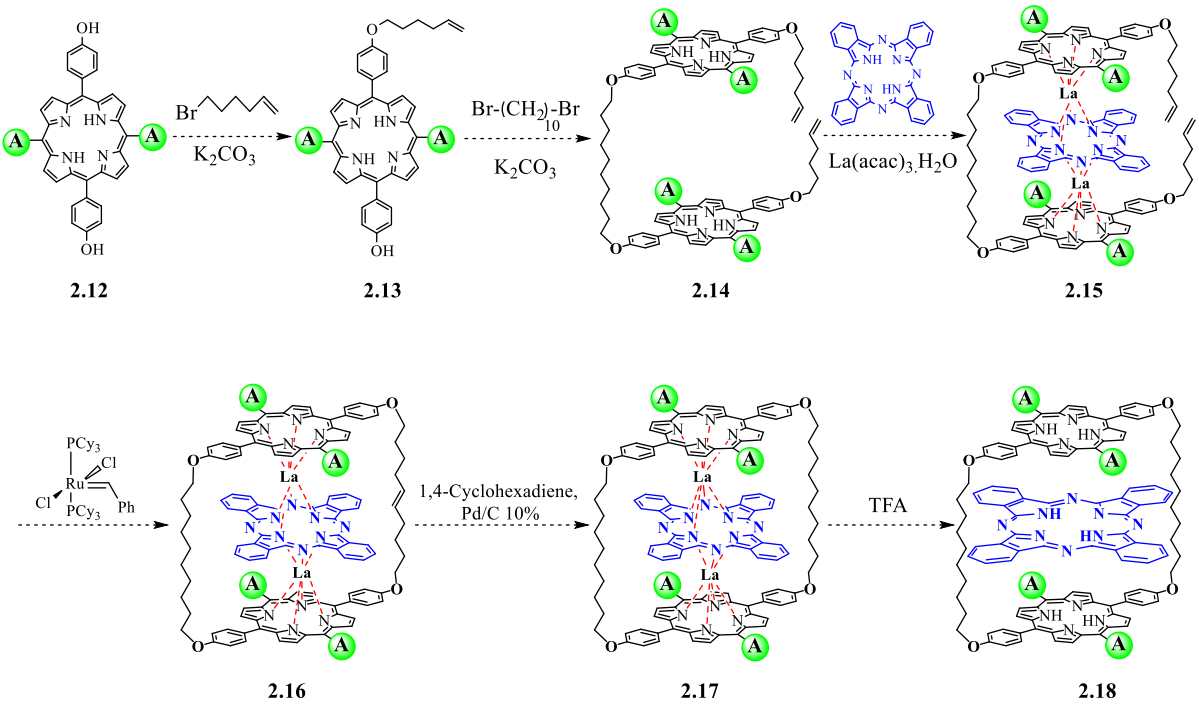

Scheme 23: Proposed synthetic route for entrapping Pc into the cyclic porphyrin *via* Cammidge's protocol. "**A**" represents aromatic phenyl substitution.

2.3 Synthesis of *trans* 5,15-bis(*p*-hydroxyphenyl)porphyrin 2.12a from 5-pentafluorophenyldipyrromethane

Title compound **2.12a** was the first *trans* porphyrin chosen as the building block for this project. As outlined in the introduction, dipyrromethanes that bear electron withdrawing groups (*e.g.*, fluorines) are found to be stable in the synthesis of *trans* porphyrins.[59,88] Therefore, pentafluorophenyldipyrromethane **2.20** was selected as a key starting material. This offers significant advantages in the synthesis and characterization of *trans* porphyrins. Indeed, it both prevents scrambling during the condensation reaction and simplifies the interpretation of the final target's ^{1}H-NMR spectrum by reducing the number of ^{1}H signals due the presence of F atoms. Furthermore, it would enable the investigation of the desired compound using ^{19}F-NMR spectroscopy.

Thus, our synthetic route involves the synthesis of pentafluorophenyldipyrromethane **2.20** which would be subsequently reacted with 4-hydroxybenzaldehyde **2.21** to afford *trans* porphyrin **2.12a** as shown in scheme 24.

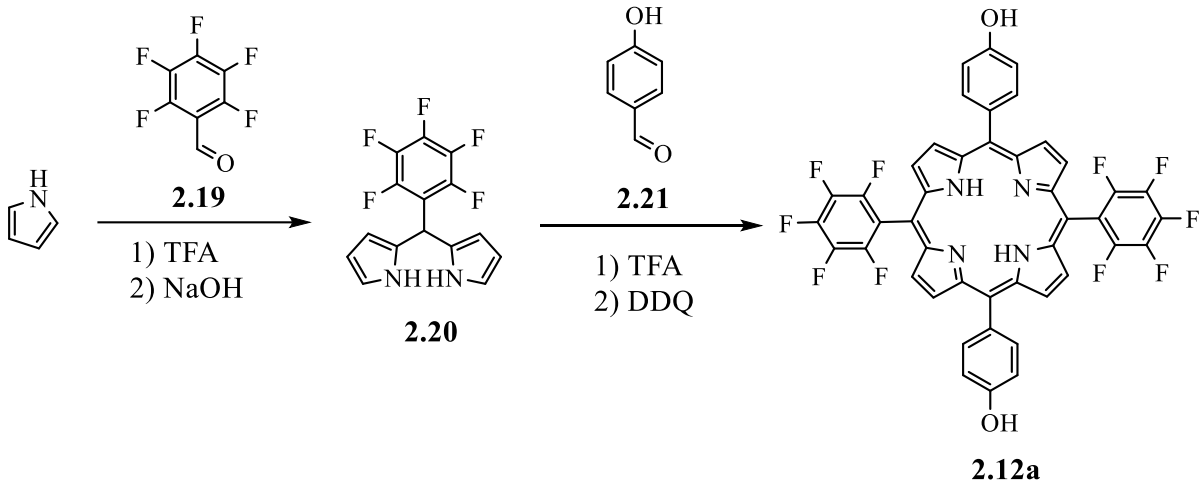

Scheme 24: Proposed synthetic route to *trans* porphyrin **2.12a**.

Following the Lindsey method,[59] DPM **2.20** was synthesised by stirring pentafluorobenzaldehyde **2.19** (1 equivalent) with freshly distilled pyrrole (25 equivalents) under inert gas conditions (Ar). The mixture was stirred at room temperature for 30 minutes. Then (0.1 eq) catalytic amount of TFA was added dropwise and the colour of the reaction changed to dark brown indicating pyrrole reaction. The reaction was monitored by thin-layer chromatography (TLC). The DPM was observed as a pink-stained spot upon exposure to bromine vapor after 5 minutes.

Generally, DPMs are known to be unstable compounds which gradually caused a darkening of the reaction mixture when exposed to air, light or high temperature. This behaviour is well-known for pyrrolic compounds and is associated with their polymerization. Therefore, the work up and purification needed to be done carefully. Thus, aqueous solution of NaOH was used to terminate the condensation and after stirring the mixture for 5 minutes ethyl

acetate was added. The organic layer was washed with water to eliminate inorganic materials and dried over Na_2SO_4. After the solvent was removed, a green oily material was obtained.

For the purification of DPM **2.20**, we wanted to avoid the use of column chromatography. Other techniques such as kugelrohr distillation or crystallization are often successful techniques to avoid the decomposition of DPMs. DPM **2.20** was obtained in an 18% yield as a white crystalline solid after slow recrystallization from ethanol. Characterisation by ^{1}H NMR spectroscopy confirmed the identity of the product obtained.

With DPM **2.20** in hand, the synthesis of *trans* porphyrin **2.12a** was attempted following a modified method by Lindsey (Scheme 25).[59]

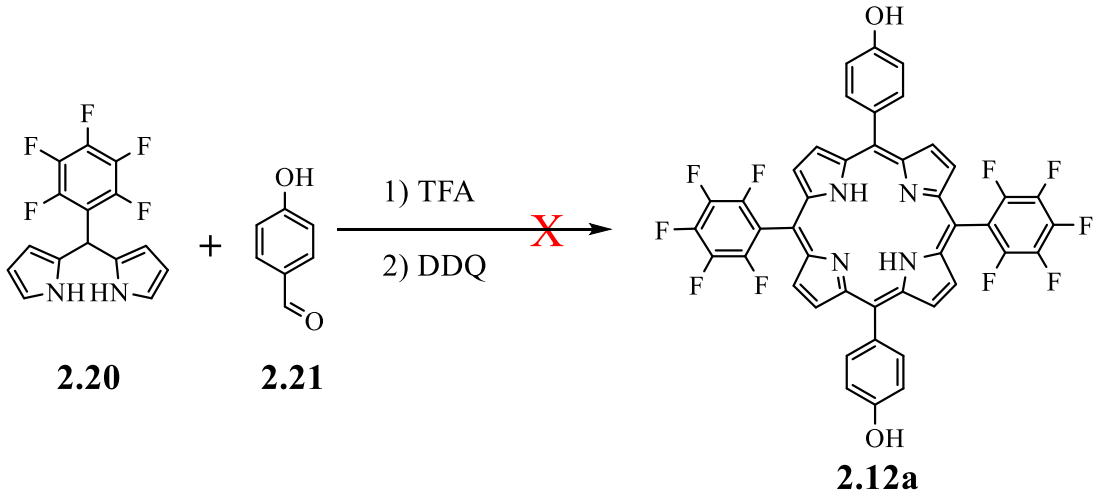

2.20 **2.21** **2.12a**

Scheme 25: Attempted synthesis of *trans* porphyrin **2.12a**.

DPM **2.20** and 4-hydroxybenzaldehyde **2.21** were stirred in dry DCM at room temperature under Ar for 20 min. A catalytic amount of trifluoroacetic acid (10 mol %) was added slowly to the reaction mixture and wrapped with aluminum foil, then the reaction mixture was stirred at room temperature. After 1 h, the reaction was oxidized using DDQ to convert porphyrinogen to porphyrin and stirred for a further 1h. A few drops of TEA were then

added to neutralize the mixture and the solvent was removed under reduced pressure to afford an insoluble black solid material. Consequently, alternative routes were investigated.

2.3.1 Alternative route towards *trans* porphyrin 2.12a

After failing in attempts to synthesize the desired *trans* porphyrin **2.12a** by a direct route, an alternative protocol was employed. This was designed to synthesize a (O-CH_3) protected *trans* porphyrin **2.23** from pentafluorophenyldipyrromethane **2.20** and *p*-methoxybenzaldehyde **2.22** under Lindsey's method,[59] followed by *O*-demethylation with BBr_3 would produce the desired *trans* porphyrin **2.12a** as shown in scheme 26. This synthetic route requires more steps, but it was expected to form the *O*-protected porphyrin **2.23** due to the lower reactivity of *p*-methoxybenzaldehyde **2.22** compared to the *p*-hydroxybenzaldehyde **2.21**.

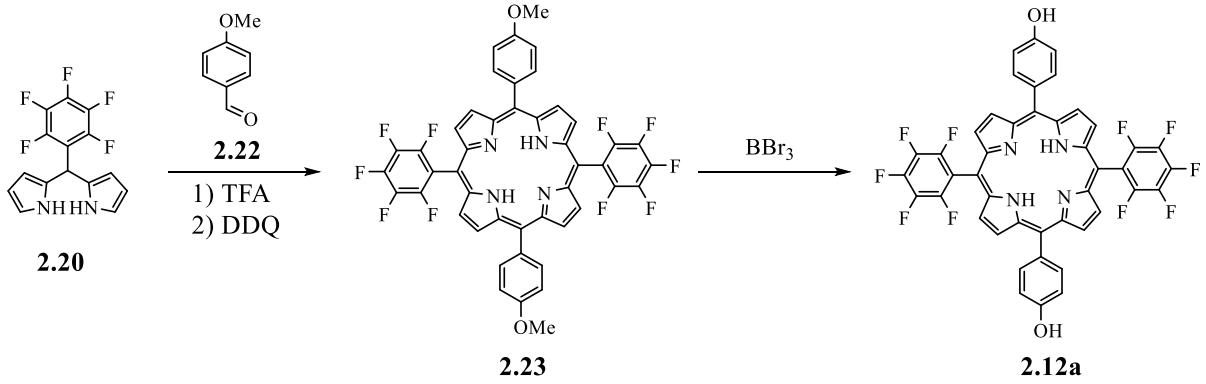

Scheme 26: Alternative synthetic route for *trans* porphyrin **2.12a** formation.

Trans-5,15-bis(*p*-methoxyphenyl)-10,20-bis(pentafluorophenyl)porphyrin **2.23** was synthesized through the condensation of pre-synthesised DPM **2.20** and *p*-methoxybenzaldehyde **2.22** in anhydrous dichloromethane, in the presence of a catalytic amount of TFA (10 mol %). The reaction mixture was stirred at room temperature. After 1 h, TLC indicated that the starting materials remained unreacted. Hence, excess of TFA was added and the mixture colour turned from yellow to dark indicating the dipyrromethane condensation.

After 20 h, the reaction was oxidized using DDQ for an additional 1 h. The completion of the reaction was further monitored by TLC which observed the formation of porphyrin **2.23** target molecule. It is worth noting that the prolongation of the reaction time and the use of excess TFA is crucial for formation of *trans*-porphyrin **2.23**. The resultant solid was purified on silica gel using Pet. Ether/DCM (1:1). The product was crystallized using DCM/MeOH to give porphyrin **2.23** as a purple solid in a 13% yield. Characterisation by ^{1}H NMR spectroscopy confirmed the identity of the product obtained.

The hydrolysis of *O*-protected *trans* porphyrin **2.23** was performed utilizing BBr_3 in dry DCM at -78 ^{o}C under N_2.[89,90] The reaction mixture was gradually warmed to room temperature and was further stirred for 24 h. Monitoring by TLC showed the starting material **2.23** was not completely consumed. Therefore, the addition of more BBr_3 was needed to complete the demethylation process and the mixture was left stirring overnight. After workup and crystallization, the desired product **2.12a** was obtained in an 83% yield. The compound was structurally characterized using ^{1}H-NMR spectroscopy, which confirmed the complete demethylation of the protected porphyrin by the absence of *O*-methyl groups at 4.04 ppm.

2.4 Is *trans* bis-10,20-pentafluorophenylporphyrin (2.12a) suitable for the formation of a triple decker complex?

As our strategy was based on the formation of a triple decker complexes, it was essential to answer the above question before moving to the next steps. Therefore, it was decided to test whether porphyrin **2.12a**, with its electron withdrawing fluorine groups, would be suitable for the construction of the triple decker complex.

To probe this, we decided to synthesize the 5,10,15,20-tetra-(pentafluorophenyl)porphyrin **2.24**, rather than use the precious unsymmetrical porphyrin,

which was subsequently reacted with phthalocyanine (Pc), in the presence of lanthanum metal ions as a test reaction for the formation of triple decker complex (Scheme 27).

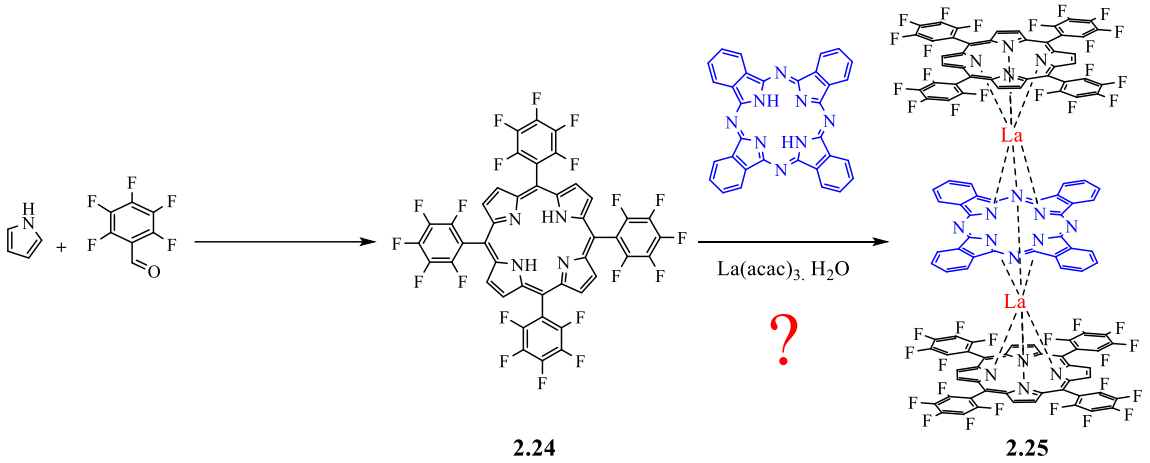

Scheme 27: Proposed synthetic route for **2.25.**

2.4.1 Synthesis of 5,10,15,20-tetra-(pentafluorophenyl)porphyrin

Following a modified procedure for the synthesis of tetrakis-pentafluorophenylporphyrin **2.24**,[91] a mixture of 2,3,4,5,6-pentafluorobenzaldehyde **2.19** and freshly distilled pyrrole was stirred in dry DCM for 20 min under N_2, followed by dropwise addition of TFA (10 mol %). After completion (5 h) DDQ was added, and the reaction mixture was further refluxed for 2 h. After work-up and short column chromatography, the desired porphyrin **2.24** was then collected in 20% overall yield (Scheme 28).

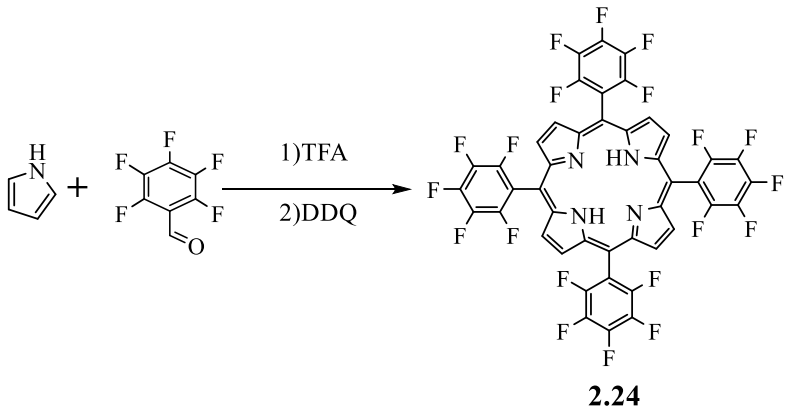

Scheme 28: Synthesis of **2.24**.

2.4.2 Synthesis of phthalocyanine

As phthalocyanine (Pc) was required for testing the formation of triple decker complex **2.25**, it was successfully synthesized following the general procedure reported by Galanin and Shaposhnikov (Scheme 29).[92]

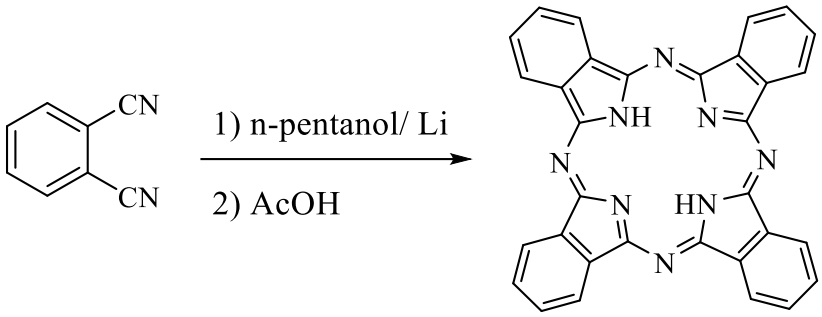

Scheme 29: Synthesis of phthalocyanine.

Phthalonitrile was dissolved in 1-pentanol and heated at 120 °C. An excess of lithium metal was added, and refluxing continued for a further 1 h. Acetic acid was added, and the mixture was refluxed for an additional 1 h. After cooling to room temperature, MeOH was added to precipitate the Pc which was collected as a blue solid in a 40% yield. The poor solubility of Pc made it impossible to confirm its structure by NMR spectroscopy; however, MALDI-tof MS successfully confirmed its formation see figure 13.

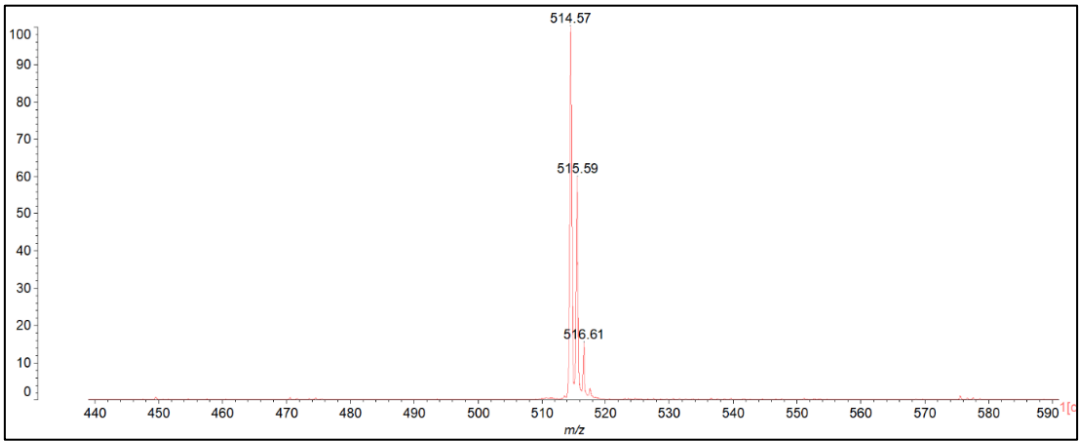

Figure 13: MALDI-tof MS confirms the formation of Pc.

2.4.3 Test reaction for the formation of triple decker complex based on 5,10,15,20-tetra-(pentafluorophenyl)porphyrin

With 5,10,15,20-tetra(pentafluorophenyl) porphyrin **2.24** and Pc in hand, it became possible to attempt the synthesis of triple decker complex **2.25** using a modified method typically employed by our group.[87] This standard protocol requires refluxing two equivalents of porphyrin **2.24** with two equivalents of lanthanum metal ions and one equivalent of phthalocyanine in 1-pentanol or 1-octanol (Scheme 30).

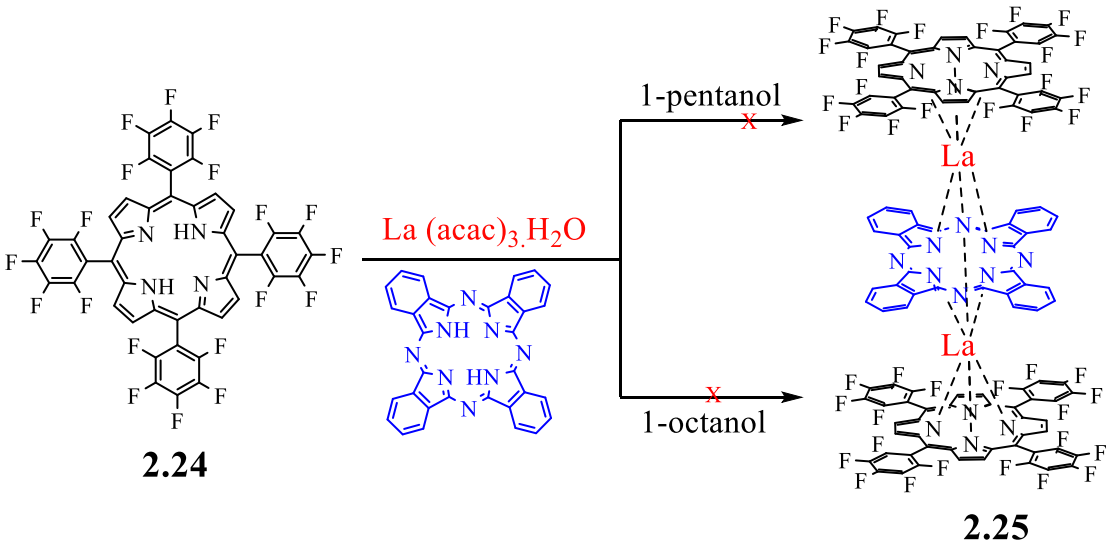

Scheme 30: Attempted synthesis of **2.25.**

The reaction was followed by TLC and after 12 h showed no new spot indicating no sign of triple decker **2.25** formation, and the mixture was left to reflux for a further 12 h. The MALDI-tof MS was also used to monitor the reaction, again this showed no sign of the desired product after this 24 h of refluxing. Moreover, when changing reaction conditions, including the ratio of reactants (*e.g.*, 3.5 eq. of **2.24** and 1.5 eq. of pc), solvents (*e.g.*, 1-pentanol, 1-octanol) and temperatures (*e.g.*, 175 ºC, 200 ºC) this reaction proved unsuccessful. Unfortunately, this failure indicated that the fluorine substituents prevented triple-decker

formation, due to either electronic or steric reasons. As a result, the pathway of using *trans*-10,20-pentafluorophenylporphyrin **2.12a** in this project was abandoned.

2.5 Testing the steric limits for the formation of *trans* porphyrin-A_2B_2 as a building block and in triple decker complexes

To design a new building block (*trans* porphyrin **2.12**) that can be straightforwardly obtained as well as suitable for the formation of triple decker (TD), it was suggested to use sterically hindered aryl substituents.[88] To test the steric limits it was decided to initially prepare three symmetrical porphyrins each bearing bulky groups at different positions, including mesityl, *t*-butylphenyl- and 3,5-dimethylphenyl-. Once formed, they were to be individually examined for their potential to construct the triple decker complex (Scheme 31).

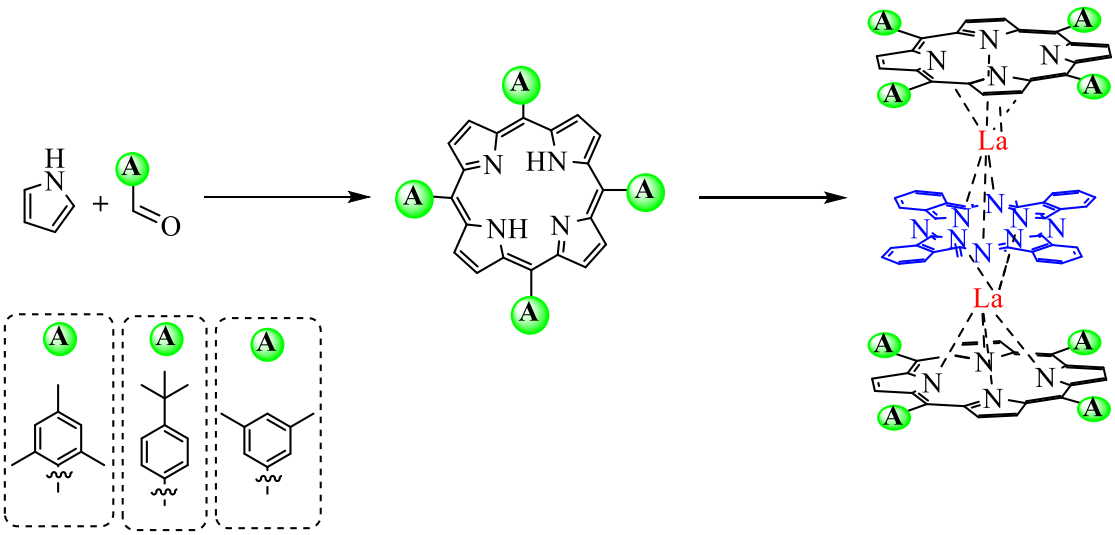

Scheme 31: General proposal of attempting the formation of triple decker complexes.

2.5.1 Synthesis of symmetrical sterically hindered porphyrins

As mentioned earlier, three aldehydes were chosen to be starting materials for synthesizing different sterically hindered porphyrins using Adler and Lindsey methods (Scheme 32).[51,93]

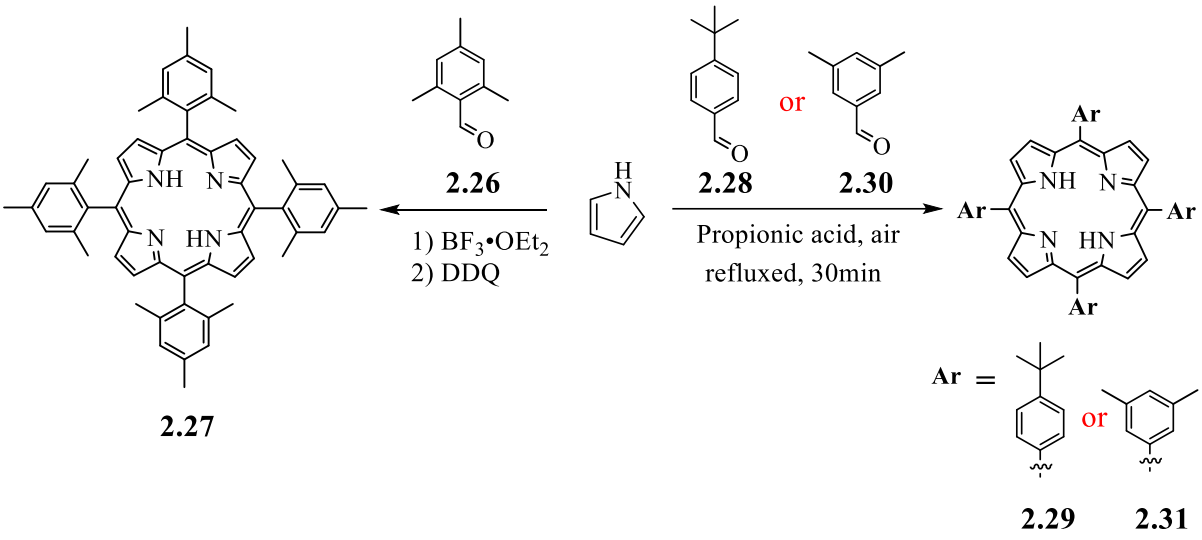

Scheme 32: General scheme of synthesising **2.27, 2.29** and **2.31.**

Mesityl porphyrin **2.27** was prepared using Lindsey's procedure.[93] Thus, mixture of mesitylaldehyde **2.26** and freshly distilled pyrrole were stirred in dry DCM for 20 min under N_2. Then, BF_3•OEt_2 was added slowly, and the reaction mixture was further stirred at room temperature for 3 h. DDQ was added, and the mixture was additionally refluxed for 2h. Work-up and a short flash chromatography gave **2.27** as purple crystals in a 11 % yield.

The *t*-butylphenylporphyrin **2.29** and 3,5-dimethylphenylporphyrin **2.31** were successfully synthesized under Adler's method.[51] Generally, the desired aldehyde was refluxed in propionic acid and subsequently freshly distilled pyrrole was added dropwise. The mixture was refluxed for 30 min then cooled down to room temperature. MeOH was added and the mixture was left in the fridge overnight. The precipitated porphyrin was collected after filtration and washed with methanol to yield the desired porphyrins as pure purple solids.

2.5.2 Attempted synthesis of triple decker complexes based on sterically hindered porphyrins

Having successfully synthesized the symmetrical porphyrins **2.27**, **2.29** and **2.31**, their suitability for the formation of triple decker complexes was tested. To evaluate this, each porphyrin was tested individually using the same reaction conditions as seen in scheme 33.

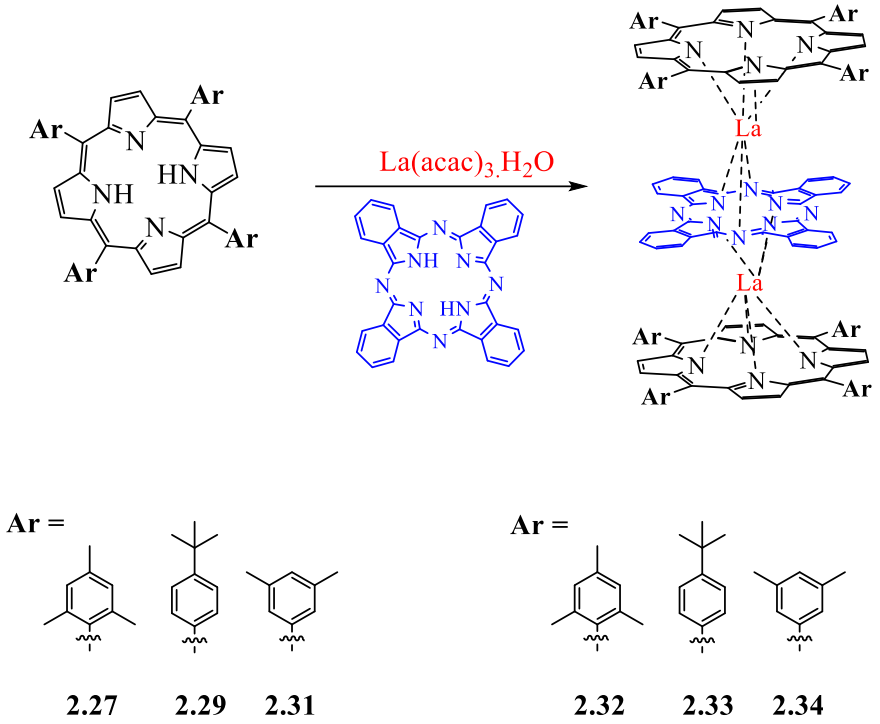

Scheme 33: General proposed synthetic route for **2.32, 2.33** and **2.34.**

The mesityl porphyrin **2.27** was tested following our group's standard method.[87] Two equivalents each of **2.27** and lanthanum metal, and one equivalent of Pc were refluxed in octanol for 12 h. TLC showed no sign of the formation of triple decker **2.32**. Even when the reaction was left refluxing for a further 12 h, there was no indication for its formation. This could be attributed to the steric factor, where the presence of methyl groups at the 2- and 6-ortho positions hinder formation of triple decker **2.32**. This hypothesis could be synthetically proved by attempting the formation of triple decker complexes **2.33** and **2.34** since the presence of the bulky groups are at meta and para positions.

Therefore, using the same aforementioned reaction conditions, porphyrin **2.29** with lanthanum metal ion in the presence of Pc was refluxed in octanol for 24 h. The formation of complex **2.33** was monitored by TLC, which showed a typically characteristic brown spot. The solvent was removed, and the resulting dark solid material subject to column chromatography. The desired triple decker **2.33** was collected as a brown solid after recrystallization from DCM: MeOH (1:1) in a 13% yield. The triple decker **2.34** was also successfully furnished in an 11% yield using the same reaction conditions. These results proved that the presence of bulky groups at meta and para positions has no effect on the formation of triple decker complex unlike at ortho position which prevents the formation of triple decker as seen in the earlier attempt. Unfortunately, however, the bulky ortho substituents are needed for easy synthesis of *trans* porphyrins.

2.5.2.1 ^{1}H-NMR characterization of triple decker complexes 2.33 and 2.34

Identification of the complexes **2.33** and **2.34** was confirmed by ^{1}H-NMR spectroscopy (Figure 15) as compared with the previously prepared triple-decker complex (Figure 14) reported by Tsivadze (under identical conditions) which is totally analysed.[94]

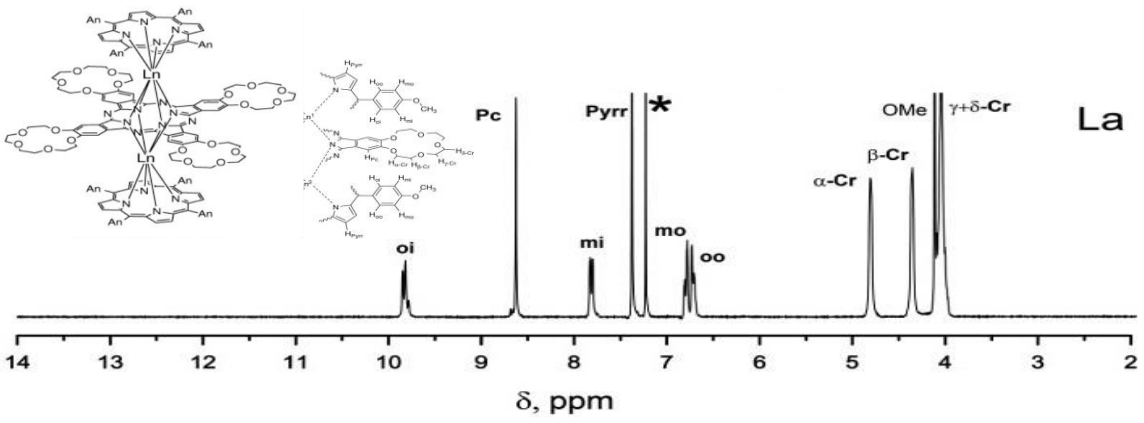

Figure 14: ^{1}H-NMR spectrum of triple decker complex by Tsivadze.[94]

Structurally, the TDs (**2.33** and **2.34**) showed a notable similarity to their complex but additional splitting of the Pc signals was expected due to the Pc not being functionalized in our case. Thus, the Pc signals in both spectra of **2.33** and **2.34** (Figure 15) show two similar splitting patterns. Additionally, the presence of a singlet peak for the porphyrin β protons in both spectra (Figure 14) suggests a symmetrical triple decker with Pc in the middle. On the other hand, differences arise in the signals attributed to inner and outer protons of the phenyl rings and the impacts of bulky substituents (*t*-butyl and 3,5-dimethyl) (Figure 15).

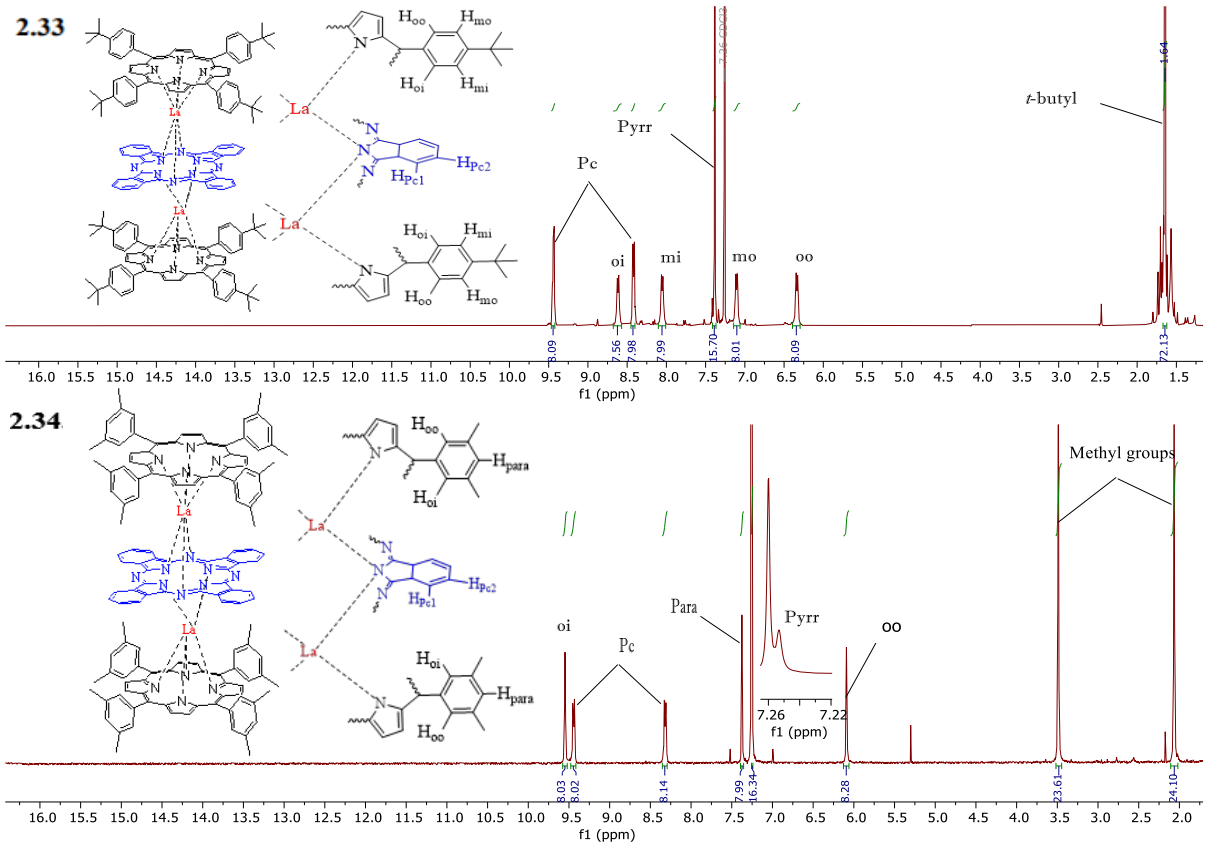

Figure 15: ^{1}H NMR spectra of triple decker complexes **2.33** and **2.34.**

Further evidence for the formation of complexes **2.33** and **2.34** was obtained through UV-Vis spectroscopy (Figure 16). The spectral profiles of **2.33** and **2.34** are consistent with each other and distinct from the absorption spectra of their starting materials. This difference suggests overlapping interactions between heteroleptic components mediated by lanthanum.

Also, this observation aligns with the anticipated spectral characteristics for similar structures, where a Pc is sandwiched between two porphyrins $[M_2(Pc)(Por)_2]$.[95]

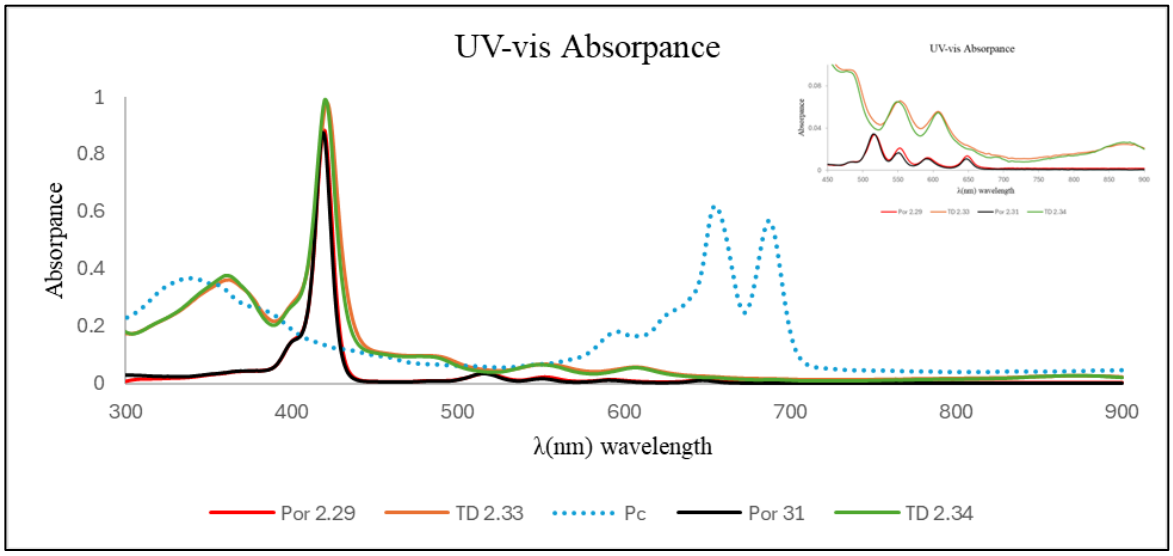

Figure 16: UV-Vis spectra of new triple deckers **2.33** and **2.34** with their starting materials.

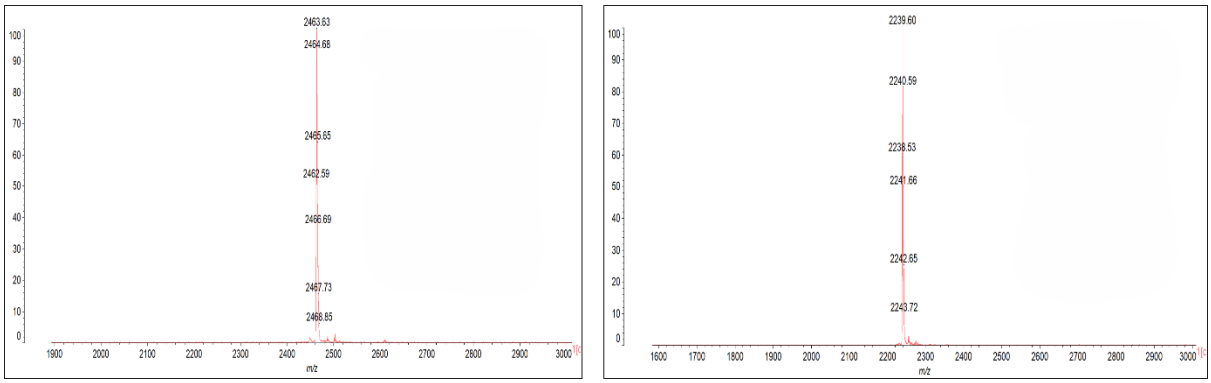

Figure 17: MALDI-tof MS confirms the formation of TD **2.33** (left) and TD **2.34** (right).

2.6 Attempted synthesis of *trans* 5,15-bis(*p*-hydroxyphenyl)porphyrin using sterically hindered DPMs

Previously, we successfully accomplished the synthesis of two different triple-decker complexes **2.33** and **2.34**. Now, our attention moved to the synthesis of *trans* porphyrin **2.12** with the same substituents to see if they could be prepared easily. We expected potential problems with scrambling but carried out a short investigation to be sure. The synthetic plan

involved the synthesis of dipyrromethane from 4-tert-butylbenzaldehyde **2.28** and 3,5-dimethylbenzaldehyde **2.30**, then investigating the synthesis of a protected *trans* porphyrin. This protected porphyrin is targeted to ease the purification and avoid any solubility problems of **2.12**, while its deprotection will afford the desired porphyrin (Scheme 34).

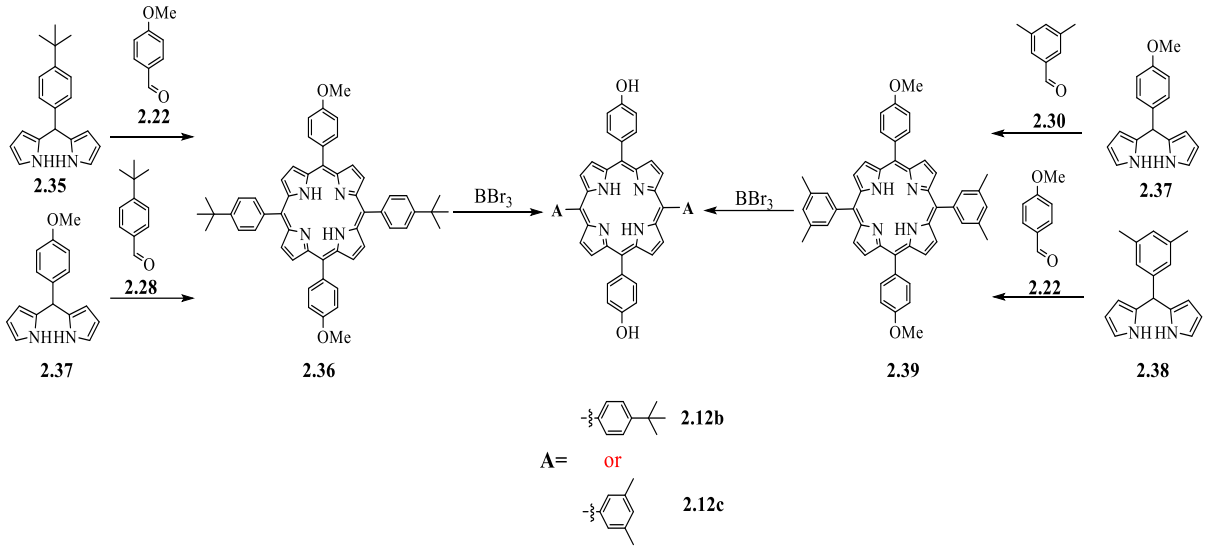

Scheme 34: A proposed synthesis of *trans* porphyrins **2.12b** and **2.12c.**

First Route:

The first route involved using 4-*tert*-butylbenzaldehyde **2.28** as a starting material to attempt the synthesis of 10,20-(di-4-*tert*-butylphenyl) porphyrin **2.36** (Scheme 35).

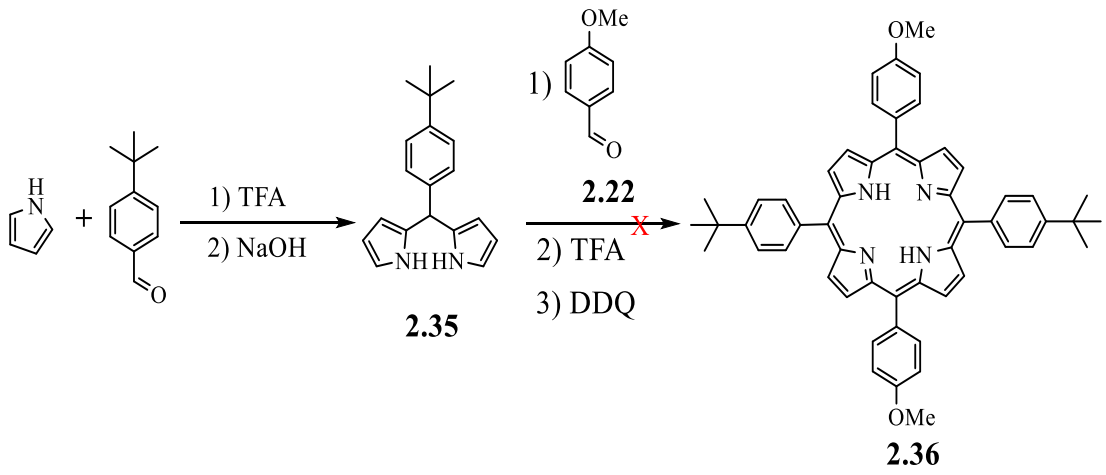

Scheme 35: Attempted synthesis of **2.36.**

Dipyrromethane **2.35** was successfully synthesized in a 45% yield using the Lindsey method.[59] Afterwards, two equivalents of DPM **2.35** with 4-methoxybenzaldehyde **2.22** were stirred in dry DCM under N_2 at room temperature for 20 minutes. Then, TFA was added dropwise, and the mixture was further stirred for 30 min. DDQ was added and the mixture continued stirring for a further 1 h. Unfortunately, TLC analysis of the reaction indicated the formation of scrambling products, making purification quite difficult.

Second Route:

The second route involved the synthesis of 4-methoxyphenyldipyrromethane **2.37**, followed by applying the aforementioned conditions as shown in (Scheme 36).

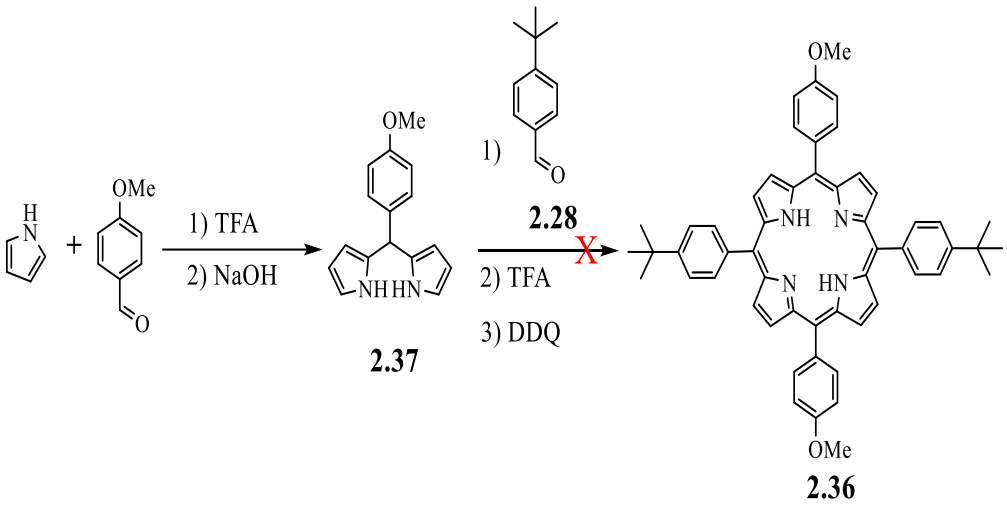

Scheme 36: Alternative pathway of *trans* porphyrin **2.36** formation.

Following the Lindsey method,[59] 4-methoxyphenyldipyrromethane **2.37** was successfully obtained in a 61 % yield as colourless crystals. Under N_2, the DPM **2.37** and the 4-*tert*-butylbenzaldehyde **2.28** were stirred in dry DCM at room temperature in the presence of TFA. The reaction mixture was stirred for 30 minutes and DDQ was added to the reaction. Again, the formation of scrambling during the reaction was detected as seen from the MALDI-tof MS shown in (Figure 18). Although the desired porphyrin **2.36** has formed, the purification

was not performed due to the formation of an inseparable mixture of *trans*/*cis* isomers. Therefore, this synthetic route is not appropriate for accessing our desired *trans* porphyrin.

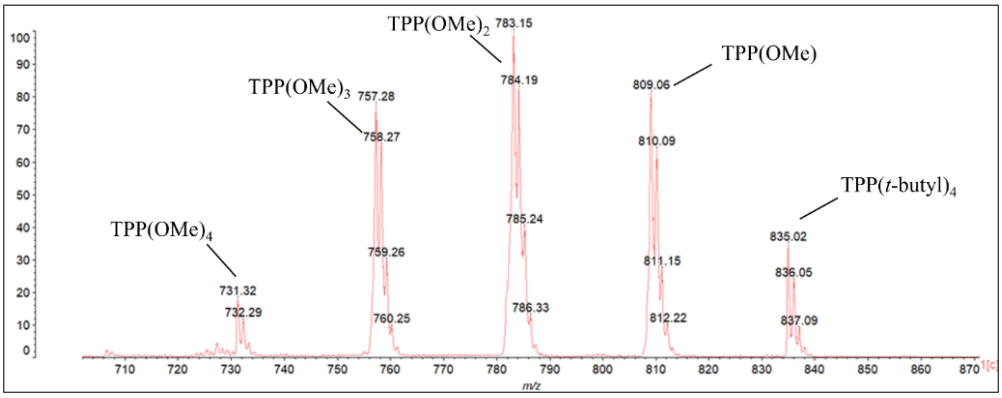

Figure 18: MALDI-tof MS obtained for the crude reaction of the formation of *trans*-porphyrins **2.36** from two routes.

Unfortunately, scrambling occurred even when 3,5-dimethylbenzaldehyde **2.30** was used as a starting material when the two previously described routes were applied. This suggests that the presence of bulky group at the meta positions in DPM **2.38** does not effectively prevent the formation of scrambling. Therefore, it became clear that these routes were not suitable for synthesizing the desired *trans*-porphyrin.

2.7 Synthesis of *trans* 5,15-bis-(*p*-hydroxyphenyl)porphyrin 2.12d from protected dipyrromethanes

Due to the lack of success in the formation of *trans*-porphyrins **2.12** without scrambling in our earlier attempts, we decided to focus on the simplest building block, the 5,15-bis-hydroxyphenyl-10,20-phenylporphyrin **(2.12d)** from an *o*-benzyl protected *trans* porphyrin followed by deprotection.

The first protected *trans*-porphyrin **2.42** was decorated with two benzyl groups at the *para* positions, which can be easily converted into phenol groups by a palladium-catalysed reaction if the synthesis is accomplished. Two routes were explored. The first route involved

the synthesis of DPM **2.41**, which was subsequently reacted with benzaldehyde. Meanwhile, the second route entailed the synthesis of 5-phenyldipyrromethane **2.43** which was then reacted with 4-benzyloxybenzaldehyde **2.40**. Finally, if scrambling was detected, an alternative approach involving a methoxy-protected porphyrin **2.44** was to be considered. This method involves the use of pre-synthesized DPM **2.37** with benzaldehyde, followed by demethylation using BBr_3 to yield the desired porphyrin **2.12d**, as illustrated in (Scheme 37). These routes were selected to assess their effectiveness in obtaining the desired *trans*-porphyrin product. While they may not necessarily prevent scrambling, they were designed to facilitate purification by improving solubility and simplifying the separation of the desired product from byproducts, helping us identify an optimal synthetic route.

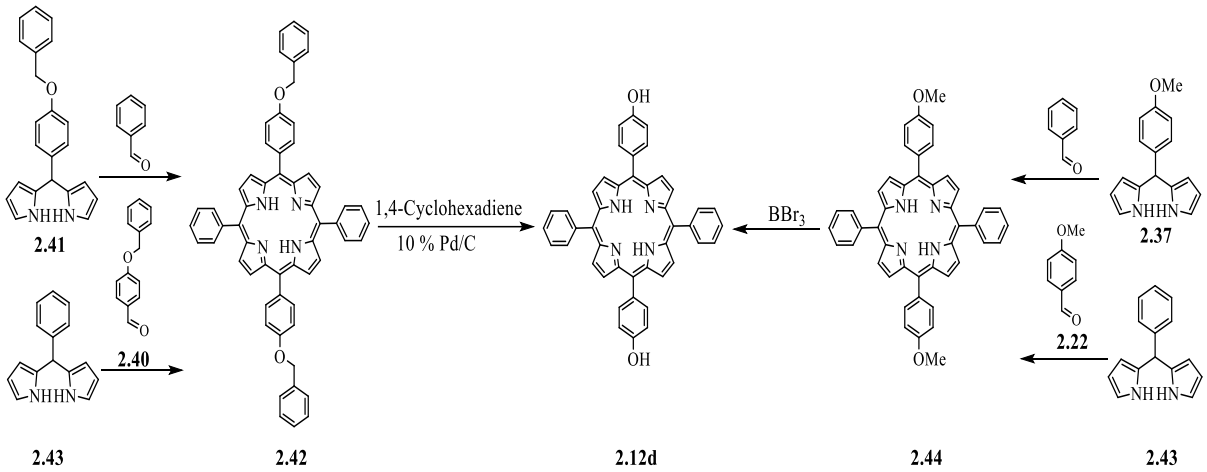

Scheme 37: Possible synthetic route for the synthesis of *trans*-porphyrin **2.12d**.

2.7.1 Synthesis of protected *trans* porphyrin 2.42

Initially, the synthesis of dipyrromethane **2.41** was successfully achieved following the procedure developed by Lindsey.[59] This particular DPM **2.41** had not been previously reported, whereas the *trans*-porphyrin **2.42** had been reported using a statistical method.[96] Two routes were examined for further reactions. In the initial attempt, 5-benzylephenyldipyrromethane **2.41** and benzaldehyde were dissolved in dry DCM, in the

presence of TFA as catalyst, followed by the addition of DDQ. Preliminary investigations by TLC analysis revealed scrambling. The second attempted reaction involved employing 5-phenyldipyrromethane **2.43** with 4-benzyloxybenzaldehyde **2.40** following the same reaction condition. TLC analysis also indicated scrambling. Further purification attempts by column chromatography or recrystallization were unsuccessful, making it impossible to isolate a pure *trans*-porphyrin **2.42**.

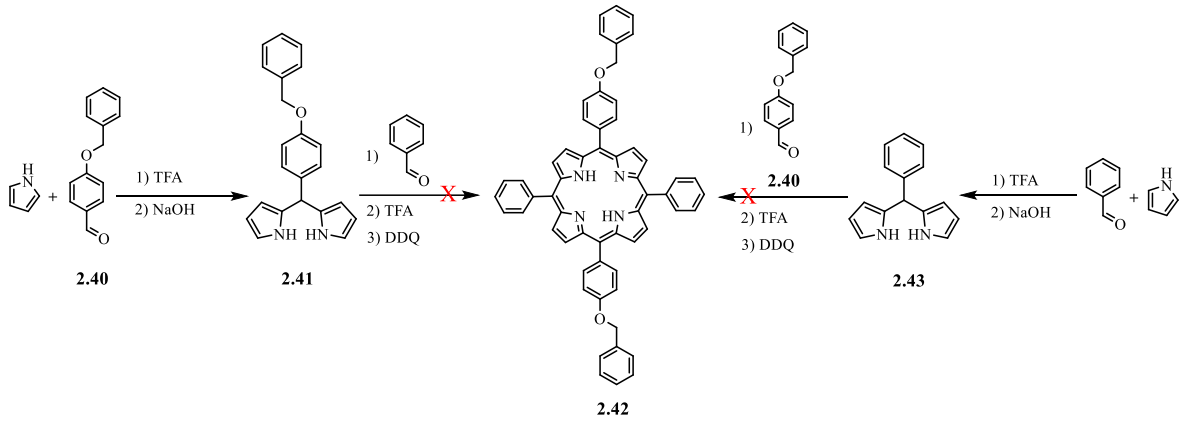

Scheme 38: Synthesis of protected *trans*-porphyrin **2.42**.

2.7.2 Synthesis of protected *trans* porphyrin 2.44

Due to the failure to obtain pure *trans*-porphyrin in previous attempts, the synthesis of methyl-protected porphyrin **2.44** was investigated (Scheme 39).

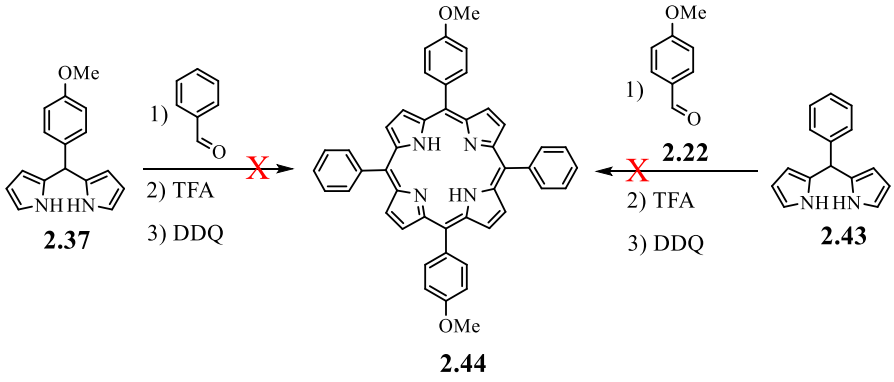

Scheme 39: Synthesis of protected *trans*-porphyrin **2.44**.

Initially, the pre-synthesised DPM **2.37** and benzaldehyde were dissolved in dry DCM in the presence of TFA followed by DDQ. After workup, the TLC analysis showed multiple porphyrins indicating scrambling. The pre-synthesised 5-phenyldipyrromethane **2.43** and 4-methoxybenzaldehyde **2.22** were also used as starting materials for the formation of *trans*-porphyrin **2.44**, and scrambling was again detected (Figure 19). As a result, it appeared that the formation of scrambling could not be avoided by these routes.

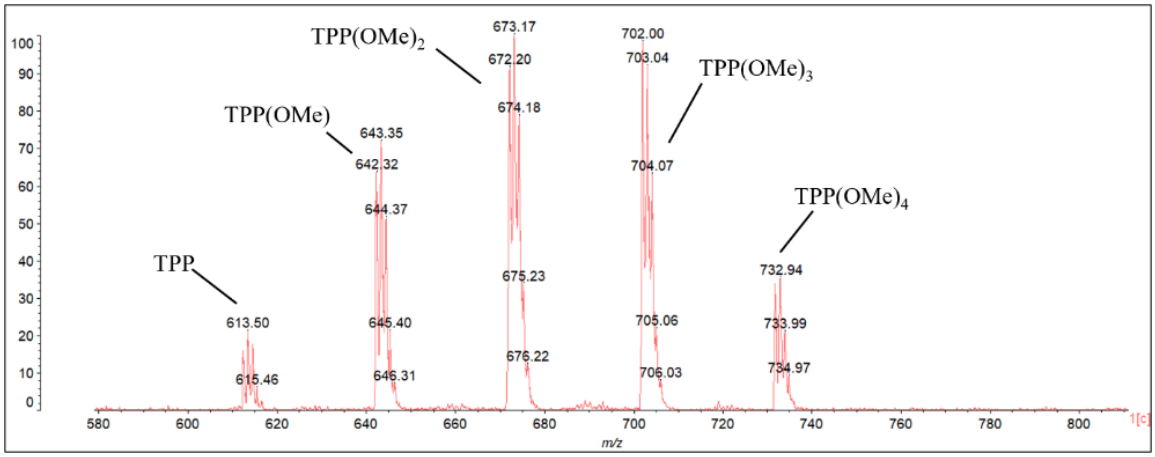

Figure 19: MALDI-tof MS obtained for the crude reaction of the formation of *trans*-porphyrins **2.44** from two routes.

2.7.2.1 Optimization to minimize scrambling in protected *trans*-porphyrin 2.44; synthesis and purification

Several methods were reported for the synthesis of *trans* porphyrins by the condensation of dipyrromethane and aldehyde utilizing different solvents and acids as described in the introduction section.[60,63,97] Therefore, it was decided to attempt minimizing the formation of scrambling during porphyrin reaction using different reaction conditions and purifying the desired porphyrin **2.44** if possible. TLC was used to monitor the formation of scrambling.

Lindsey reported that $BF_3 \cdot Et_2O$ or TFA can be used for the formation of *trans* porphyrin. Thus, both were tested at different temperatures and reaction times but neither of them provided the desired product without scrambling (entry: 1-5). When using DMSO as a solvent with inorganic chloride salts (open to air) or reflux in propionic acid, the scrambling was detected (entry: 6-7). Similarly, using HCl in methanol and water at room temperature for 1 h, resulted in the formation of scrambling (entry: 8). Consequently, scrambling was observed under all tested conditions, leading us to attempt the purification of the desired porphyrin.

Entry	Solvent	Catalyst	Time	Temp.	Result
1.	Dry DCM	TFA	1.5 h	R.T.	Scrambling
2.	Dry DCM	TFA	30 min	R.T.	Scrambling
3.	Dry DCM	TFA (3 eq)	10 min	R.T.	Scrambling
4.	Dry DCM	TFA	30 min	0 °C	Scrambling
5.	Dry DCM	$BF_3.Et_2O$	30 min	R.T.	Scrambling
6.	Propionic acid	…..	1 h	Reflux	Scrambling
7.	DMSO	NH_4Cl	24 h	90 °C	No reaction
8.	MeOH/Water (2:1)	HCl	60 min	R.T.	Scrambling

Table 1: Representation of various reaction conditions screened.

Purification was a challenge, due to the presence of undesired porphyrins with similar polarities. The TLC analysis showed reasonable separation of porphyrins using DCM: Pet. ether 3:1 as the eluent system and therefore the crude solid was subjected to column chromatography. The first fraction was collected using DCM: Pet ether 1:1 and it was identified as tetra-phenylporphyrin (TPP). Gradually increasing the DCM proportion allowed the separation of mono-methoxyphenylporphyrin (TPP(OMe)) as the second fraction and $TPP(OMe)_2$ as the third, which was the major product in most cases (entries 1-8). Crystallization from DCM:MeOH yielded a maximum of 12% $TPP(OMe)_2$ (entry 1), significantly higher than other conditions, which only ranged from 4-8% (entries 2-8). The purification of **2.44** was extremely challenging and tedious but its yield would be acceptable if

it was not a mixture of *trans/cis* isomers (entry: 1). Although the MALDI-tof MS spectrum showed the expected mass, and the TLC showed only one spot even by different solvent systems, the ^{1}H-NMR spectrum (Figure 20) showed no clear evidence of a pure *trans* isomer, and it is probably a mixture of *trans*/*cis* isomers. This was based on the observation of a double singlet for the (OCH_3) group at ~4.10 ppm, instead of a single singlet, as well as a variation in the pattern of β-pyrrolic protons at 8.88/8.83 ppm. Therefore, a decision was made to proceed to the next step with the hope of achieving high purity of *trans* porphyrin **2.12d** after hydrolysis.

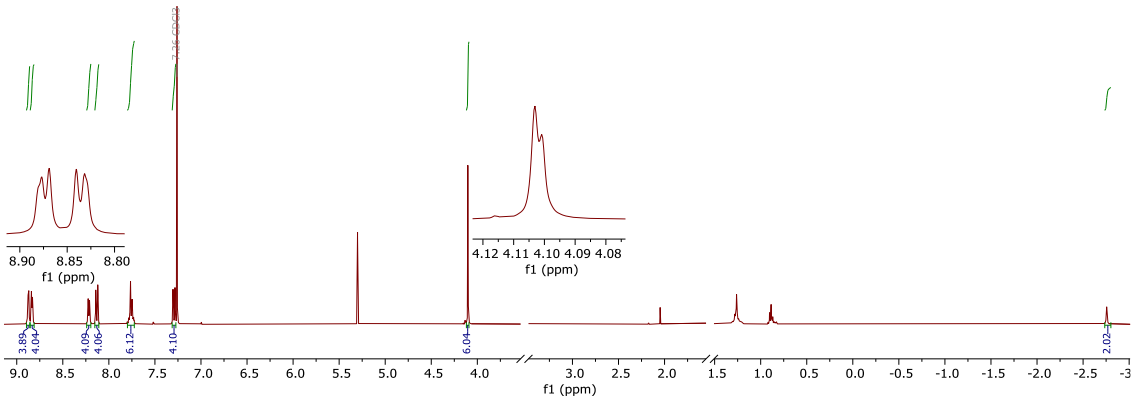

Figure 20: ^{1}H NMR spectra of **2.44** (*trans* + *cis*).

2.7.2.2 Deprotection of *trans* porphyrin 2.44

The demethylation of **2.44** to obtain **2.12d** was carried out at room temperature using BBr_3 (Scheme 40).

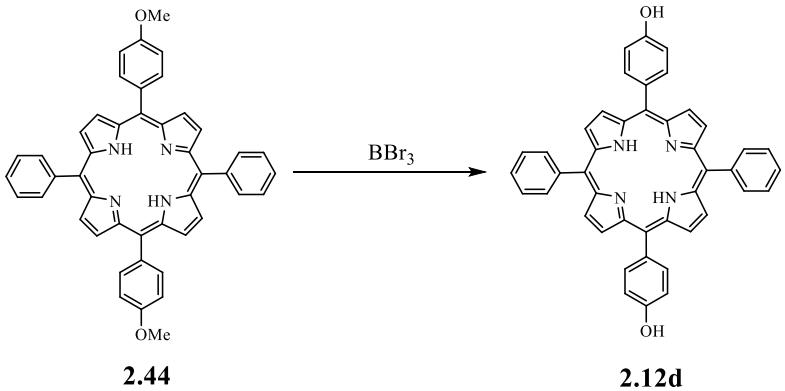

2.44 **2.12d**

Scheme 40: Deprotection of $TPP(OMe)_2$ using BBr_3 (*trans* isomer only shown).

The porphyrin **2.44** was dissolved in dry DCM and stirred under N_2. A solution of BBr_3 (1 M in DCM) was then added slowly to the mixture at -78 ^oC and the mixture turned to green colour and gradually warmed to room temperature and stirred. The progress of the reaction was monitored by TLC which showed, after 48 h, a strong spot on the baseline with different solvent systems indicating the formation of **2.12d** which was confirmed by MALDI-tof MS. However, when DCM: THF (99.5:0.5) were used as solvent system, TLC showed two distinct spots indicating it was a mixture of *trans* and *cis* isomers. Thus, after work-up, the solids were subjected to column chromatography using DCM:THF (99.5:0.5) as the eluent to collect the *trans* isomer ***trans*-2.12d** as first fraction (27%) and *cis* isomer ***cis*-2.12d** as second fraction (53%). It became clear that the major product was the *cis* isomer rather than the desired *trans* isomer. This was unexpected and the reason behind it unclear. However, this outcome aligns with previously reported findings from the direct synthesis of di(4-hydroxyphenyl)porphyrins, where the *cis*-isomer is also preferentially produced.[98]

The analysis of ^{1}H-NMR spectra showed the absence of the methoxy groups for both purified products. The ^{1}H-NMR spectra unambiguously distinguishes the *trans* isomer from the *cis* isomer because their different symmetry influences the splitting patterns of the *β*-pyrrolic protons (Figure 21).

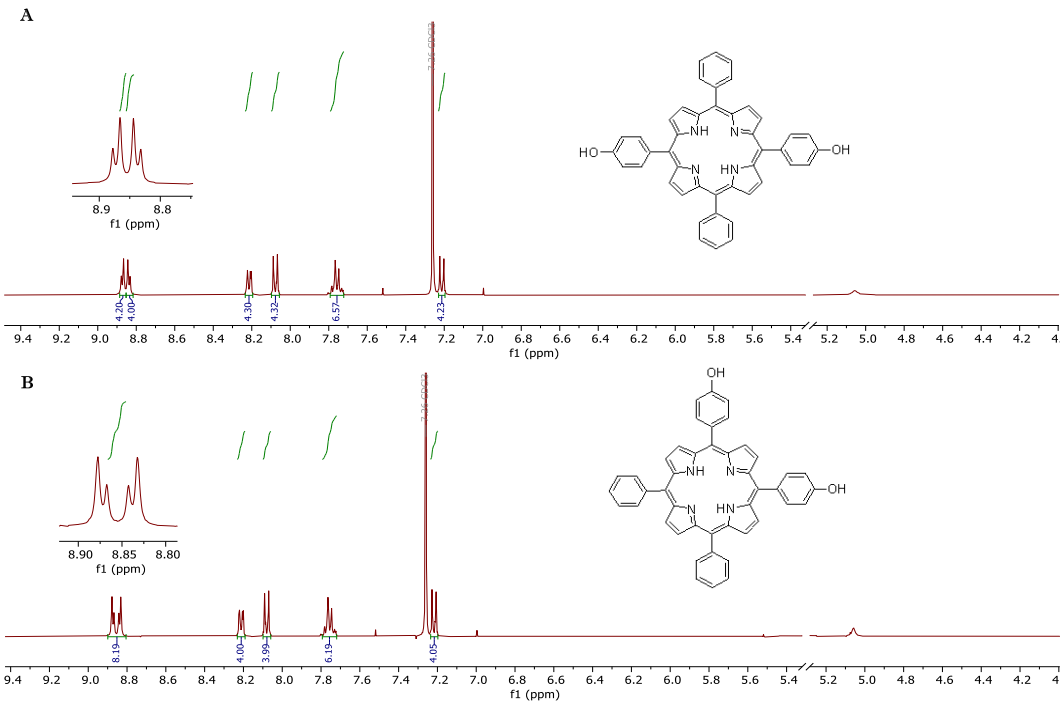

Figure 21: Aromatic region of **2.12d** *trans*-TPP(OH)$_2$ and *cis*-TPP(OH)$_2$.

2.8 Direct synthesis of *trans*-porphyrin 2.12d

As a result of the unsuccessful preparation of *trans* porphyrin **2.12d** in a reasonable yield using a 2+2 protocol, other synthetic strategies were explored. A mixed aldehyde Adler method was investigated to prepare the *trans* porphyrin **2.12d** (Scheme 41). Although this protocol is not optimal for preparing *trans* porphyrins in reasonable yield, the advantage of its simplicity was considered.

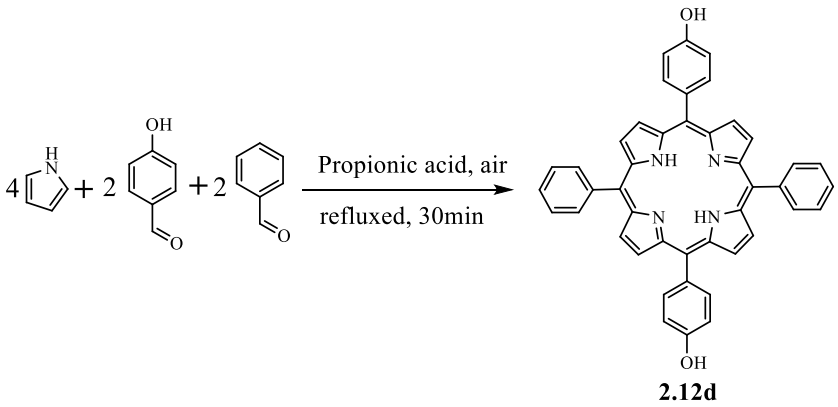

Scheme 41: Synthesis of *trans*-porphyrin **2.12d** from one step.

Two equivalents each of *p*-hydroxybenzaldehyde **2.21** and benzaldehyde were refluxed in propionic acid. Then four equivalents of freshly distilled pyrrole were added carefully, and the mixture continued refluxing for a further 1 hour. After cooling down, MeOH was added, and the mixture left in the fridge overnight for precipitation. The crude solid was collected by filtration and washed several times with MeOH. It has previously been shown that it was possible to separate the *trans* isomer from *cis* isomer by column chromatography. Thus, using the same method, **2.12d** was isolated but its yield was a very low 0.3%. This low yield is consistent with previously reported findings using the same method.[99] Thus, we suspended this route.

2.8.1 Alternative route towards *trans* porphyrin 2.12d

In order to increase the overall yield of **2.12d**, we decided to synthesize it in two steps. The first step involved the synthesis of protected porphyrin **2.44** using Adler method followed by a deprotection reaction to obtain the desired product (Scheme 42).

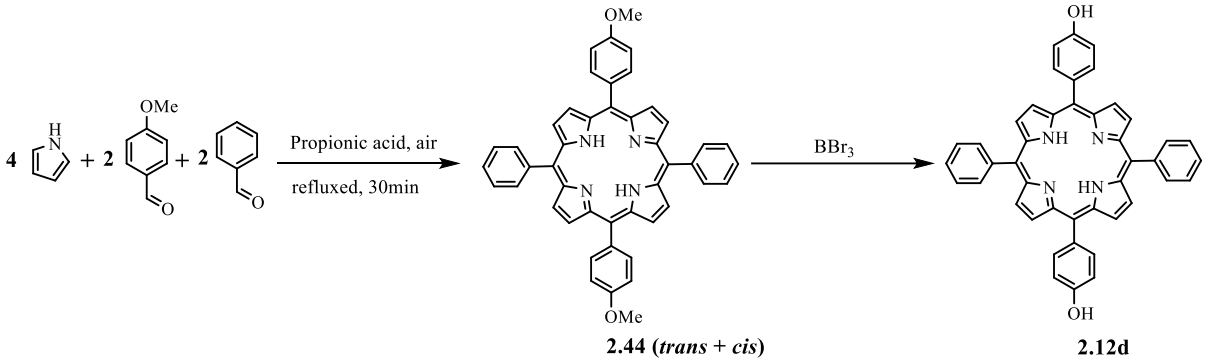

Scheme 42: Synthesis of *trans*-porphyrin **2.12d** in two steps.

First step:

The synthesis of **2.44** was achieved using the same reaction condition that was used in the previous attempt (Scheme 41). It was previously shown that it was difficult to separate the *trans* isomer from *cis* isomer by column chromatography, but the mixture of isomers could be

isolated. Therefore, using the same purification method, $TPP(OMe)_2$ **2.44-(*trans*+*cis*)** was isolated in a 5% yield. Although it was an isomeric mixture, its yield was acceptable.

Second step:

The *O*-demethylation of the isomeric mixture was again successfully achieved for obtaining the *trans* isomer as the first fraction (24%) and *cis* isomer as the second fraction (62%). Characterization by ^{1}H NMR again proved their identity as well as their purity. Despite the difficulty of obtaining porphyrin ***trans*-2.12d**, it was decided to continue using this route to recover enough material to complete the main project. Also, the obtained ***cis*-2.12d** can be a useful intermediate for future work.

2.9 A new strategy to synthesize *trans* porphyrin 2.12d

The challenges to synthesize *trans* porphyrin without scrambling did not quench our desire to keep looking for alternative pathways to obtain it. Therefore, in the project's later stages, we thought of using a dipyrromethane that bears steric blocking groups (*e.g.*, bromines) particularly at the 2- and 6-positions and then react it with an aldehyde, resulting in the formation of *trans*-porphyrins without scrambling. Upon formation, these blocking groups would need to be removed to obtain the desired porphyrin, and we recognised the challenge to identity a suitable group. Thus, we explored an alternative intermediate to examine the removable strategy before testing our hypothesis on the *trans* porphyrin **2.44**. The plan was to synthesize a ABBB porphyrin that bears bulky groups which can be easily synthesized from a statistical method and then investigate the removal of these groups. If successful, then the conditions will be used to synthesize the desired *trans* porphyrin. This plan was investigated by my colleague Sultanah Alhunayhin who collaborated with me on this subproject.

2.9.1 Synthesis of mono-hydroxyphenylporphyrin

The selected 3-hydroxy-2,4,6-tribromobenzaldehyde **2.45** was chosen as a cheap and useful starting material, and the corresponding 3:1 porphyrin was synthesised and isolated, albeit in low yield reflecting the lower reactivity of substituted **2.45**. Successful debromination was achieved using triethylsilane as a solvent in the presence of palladium chloride as a catalyst (Scheme 43).[100] It was found that the use of metalated porphyrin as a starting material was crucial to avoid any insertion of the palladium during the reduction reaction (See 2.9.2).

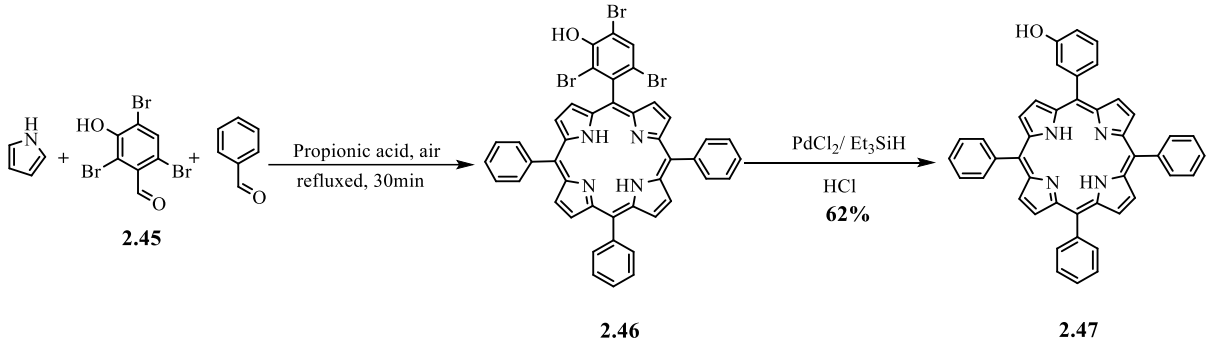

Scheme 43: Preparation of TPPOH **2.47** from the debromination of **2.46.**

2.9.2 Investigation of the synthesis of *trans* porphyrin and the removal of its blocking groups

To investigate our hypothesis for the preparation of intermediate *trans* porphyrins (including **2.44**), we again used 3-hydroxy-2,4,6-tribromobenzaldehyde **2.45** as the starting material. Its reaction of this aldehyde with pyrrole affords the desired dipyrromethane **2.48**, which then reacted smoothly with 4-methoxybenzaldehyde **2.22** using the Lindsey method, followed by the addition of zinc acetate, to produce a metalated *trans* porphyrin **2.49**. This can theoretically be used as an intermediate for two different *trans* porphyrins **2.50** and the desired **2.44** (routes A and B).

In route A, a direct reduction of intermediate **2.49** using $Et_3SiH/PdCl_2$ would result in a novel *trans* porphyrin **2.50**. In route B, the desired porphyrin **2.44** can be produced by initially treating **2.49** with triflic anhydride yielding a triflate product **2.51** followed by a reduction of both triflates and bromides. Therefore, we decided to examine both routes as illustrated in (Scheme 44).

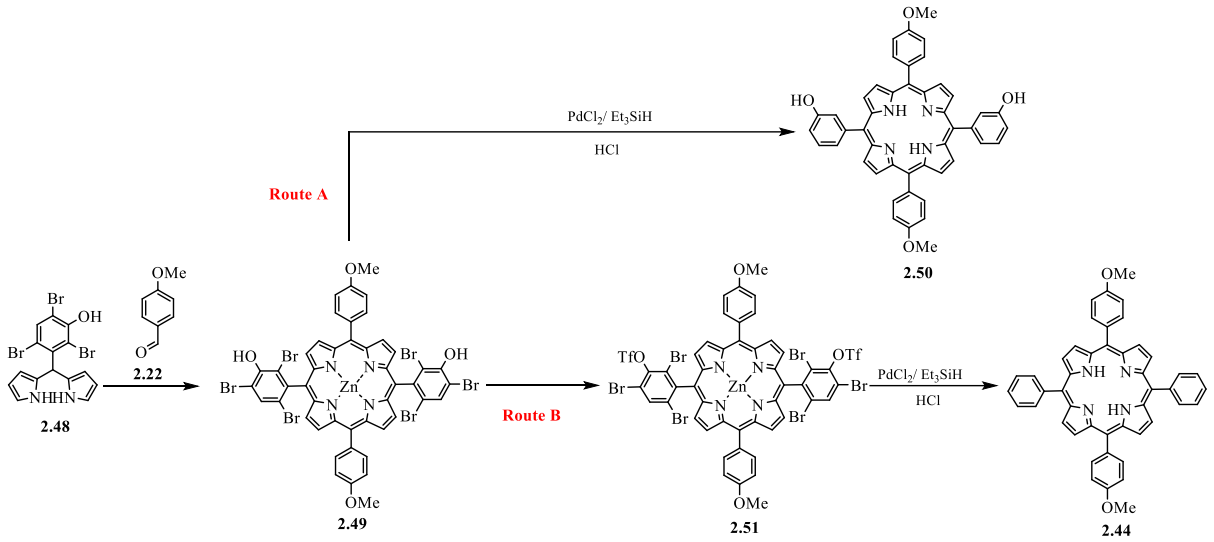

Scheme 44: General synthetic pathways for the synthesis of *trans* porphyrins **2.50** and **2.44.**

2.9.2.1 Synthesis of *trans* porphyrin 2.49

2,4,6-Tribromo-5-hydroxyDPM **2.48** was successfully synthesized in a 53% yield following the optimized method by Lindsey as described earlier. With this novel DPM in hand, the synthesis of *trans* disubstituted porphyrin **2.49** was achieved following Lindsey's protocol for porphyrin synthesis (Scheme 45).

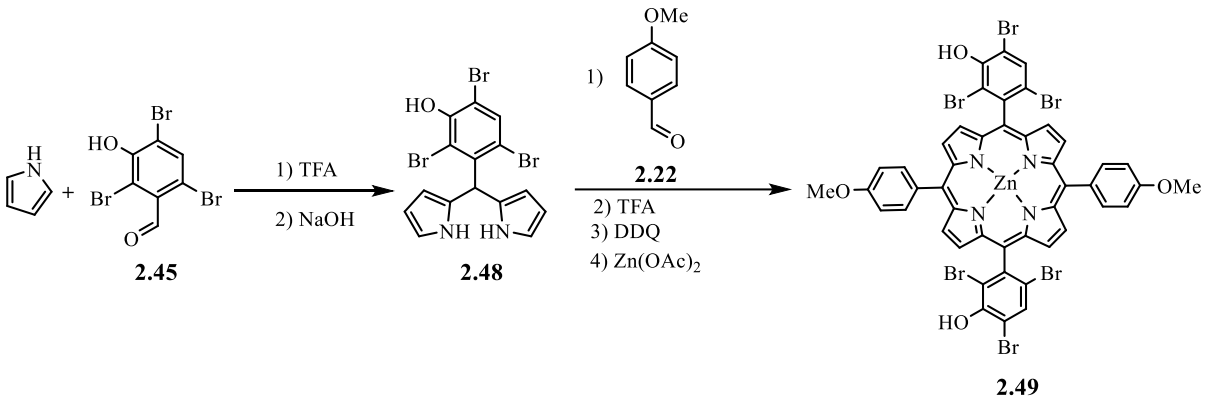

Scheme 45: Synthesis of *trans* Zn porphyrin **2.49.**

The DPM **2.48** and 4-methoxybenzaldehyde **2.22** (0.42 mM in dry DCM containing 1 mM TFA) were stirred at 0 ºC under N_2 for 1.5 h. DDQ was then added, and the reaction stirred for an additional 1 hour. Then, zinc acetate was added, and the mixture was stirred for 12 h. After solvent removal, the resulting solid material was subjected to short column chromatography using DCM/ethyl acetate (100:5) as the eluent. Pure porphyrin **2.49** was obtained as purple crystals in a 50 % yield, without any detectable scrambling. These conditions were found to be optimal, although different concentrations of TFA, temperatures, solvents, and time were tried, as summarized in table 2. Additionally, it is worth mentioning that although TLC showed two different spots, the ^{1}H-NMR and MALDI-tof MS interpretations confirmed that these spots were identical and identified as porphyrin atropisomers (Figure 22). This resulted from the presence of the hydroxy groups at meta-positions on the phenyl rings of porphyrins, and the restricted rotation of *meso*-aryls.

Entry	DPM (0.42 mMol)	Aldehyde (0.42 mMol)	Solvent/Acid	Reaction Condition	Temp. °C	Time	Oxidizing agent	Metal: Zinc acetate	yield %
1	0.2g	0.07g	Propionic Acid	Open to air	160	1 h	-	0.11 g	No precipitation
2	0.2g	0.07g	Propionic Acid	Open to air	160	1 h	-	-	No precipitation
3	0.2g	0.07g	Dry DCM/ TFA (0.76 mMol)	N_2	RT	1 h	DDQ	-	13
4	0.2g	0.07g	Dry DCM/ TFA (0.76 mMol)	N_2	RT	Overnight	DDQ	-	Scrambling
5	0.2g	0.07g	Dry DCM/ TFA (1 mMol)	N_2	0	1.5 h	DDQ	0.13 g	50

Table 2: Optimization of *trans* porphyrin **2.49** synthesis with different reaction condition.

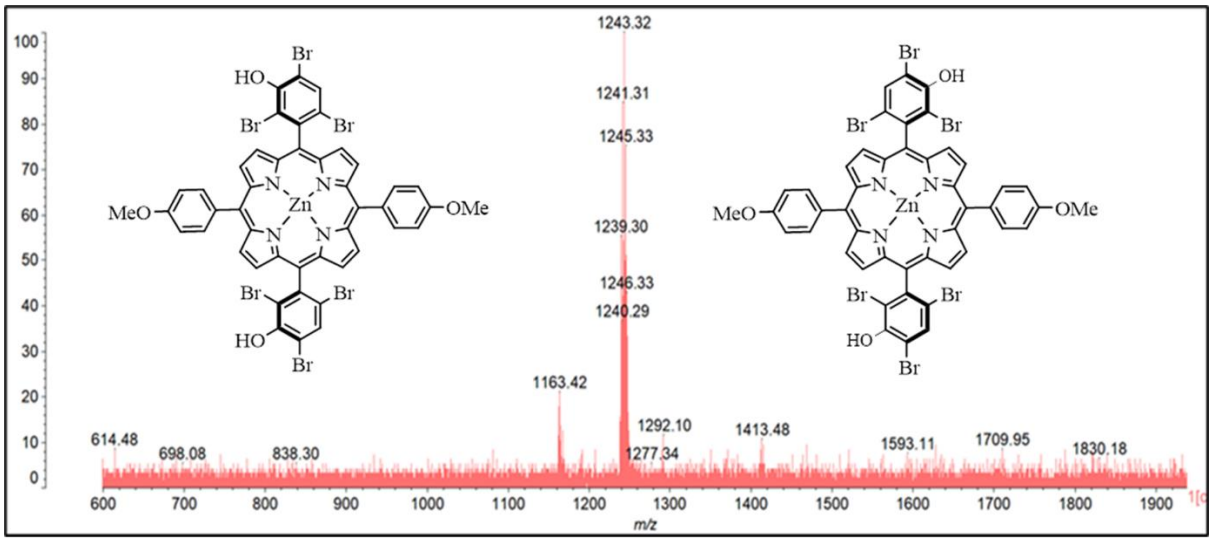

Figure 22: MALDI-tof MS of **2.49** and its two atropisomers.

2.9.2.2 Reductive debromination of zinc porphyrin 2.49 to form 2.50

The reduction of the aryl bromides was achieved using triethylsilane as a reactant and solvent, in presence of palladium chloride as catalyst (Scheme 46).[100]

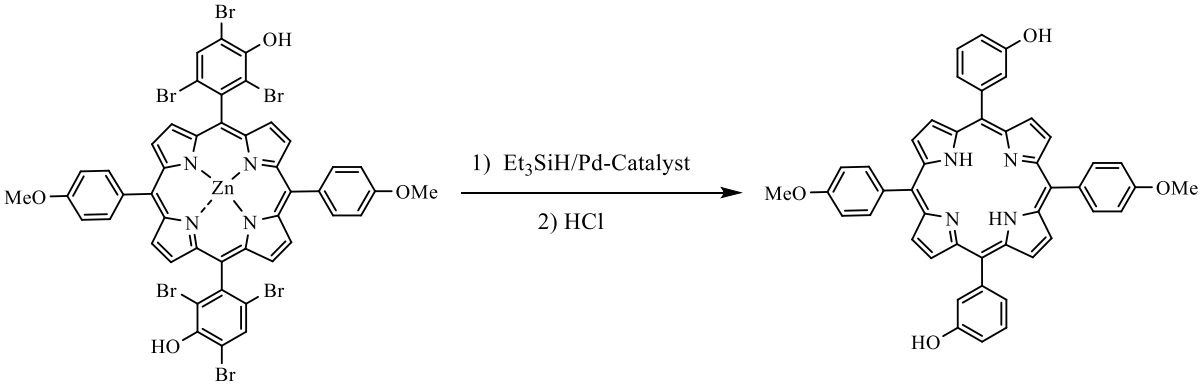

2.49 **2.50**

Scheme 46: Reduction of zn porphyrin **2.49**.

Therefore, **2.49** was dissolved in excess triethylsilane in the presence of $PdCl_2$ (5 mol %) as a catalyst. The mixture was heated at 120 °C in a sealed tube and monitored periodically by MALDI-tof MS. After 5 days, the full reduction was detected by MALDI-tof MS. The solvent was removed and the resulting green solid redissolved in DCM and HCl to remove any remaining zinc, thus releasing metal-free porphyrin **2.50**. The mixture was stirred at room temperature overnight. Water was added and the mixture extracted with DCM and a few drops of TEA, finally the solution was dried over $MgSO_4$. Purification by flash column chromatography using a mixture of DCM and ethyl acetate (100:0.5), the desired porphyrin **2.50** was collected in an 88% yield as a purple solid. Interestingly, the use of Pd/C instead of $PdCl_2$ was found to be useful and resulted in the full reduction of bromines (C-Br) with a 79% yield. The table below represents a series of experimental entries with different reaction conditions and corresponding results.[100,101] Porphyrin **2.50** was structurally characterised by ^{1}H-NMR and MALDI-tof MS (Figure 23).

Entry	**2.49**	Solvent	Catalyst	Temp. °C	Time	Yield%
1	30 mg	Et_3SiH	Et_3SiH/ $PdCl_2$	120	5 d	88
2	10 mg	Et_3SiH	Et_3SiH/ Pd/C	120	3 d	79
3	5 mg	TFA	Zn	80	2 h	No reaction
4	20 mg	Et_3SiH/TEA (1:1)	Et_3SiH/ $PdCl_2$	120	7 d	Not complete
5	20 mg	DMF	Formic acid/TEA $Pd(OAc)_2$/dppf	60	7 d	Not complete
6	5 mg	TFA	Zn	Rt	2 d	No reaction

Table 3: Optimization of *trans* porphyrin **2.50** synthesis with different reaction condition.

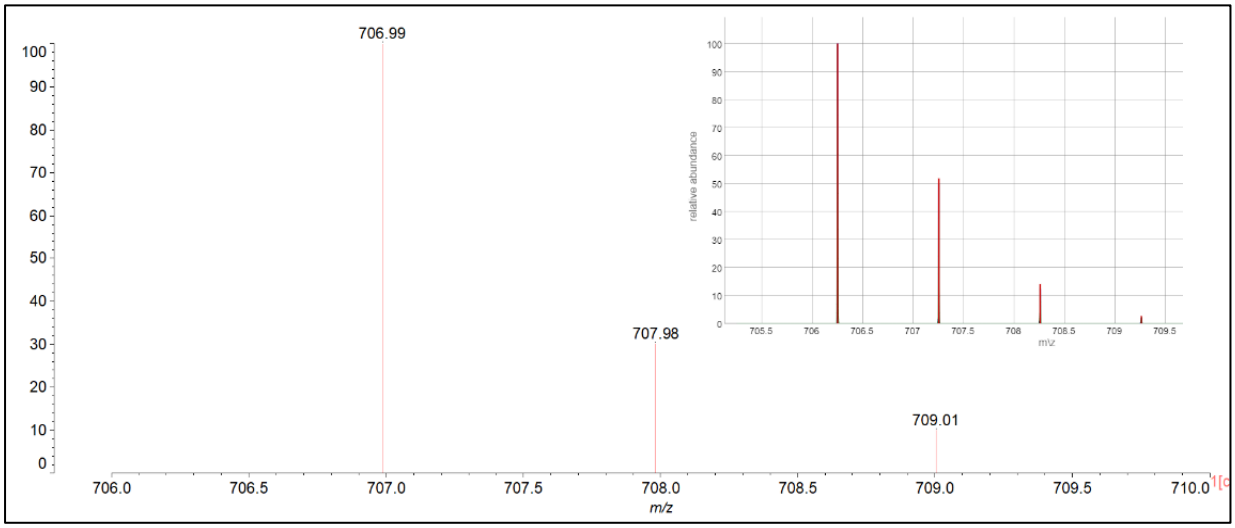

Figure 23: MALDI-tof MS of **2.50.**

2.9.2.3 Triflation of zinc porphyrin 2.49 to form compound 2.51

After the successful deprotection/reduction of **2.49** in the previous section, we attempted to synthesize **2.44** using a modified route. This required the synthesis of porphyrin triflate **2.51** which can be synthesized by reacting **2.49** with triflic anhydride in pyridine (Scheme 47).

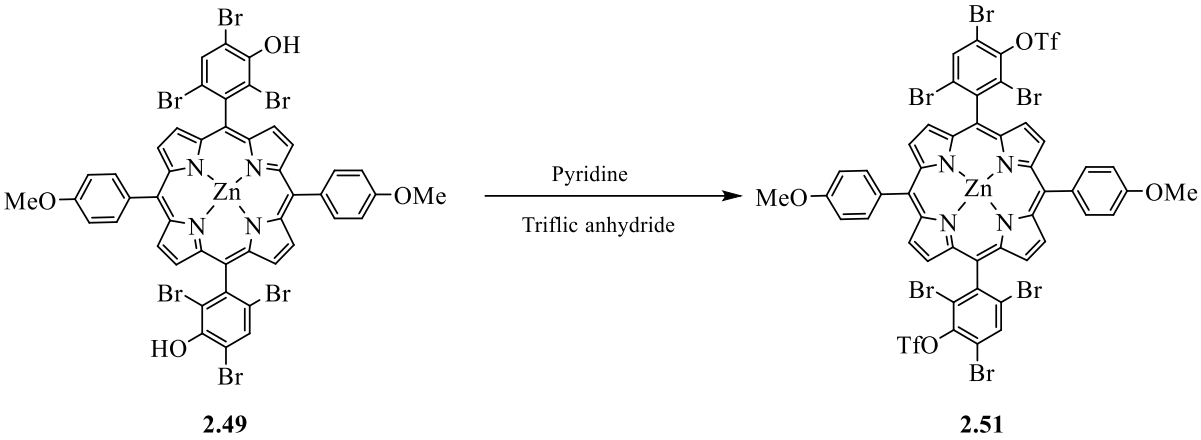

2.49 **2.51**

Scheme 47: Triflation of **2.49.**

The porphyrin triflate **2.51** was successfully achieved in an 81% yield. The reaction was performed by stirring **2.49** with pyridine in dry DCM, triflic anhydride was then added dropwise at 0 °C. The mixture was gradually warmed to room temperature and left stirring overnight. The reaction showed the full consumption of the starting material, where two spots on TLC indicated the formation of the desired porphyrin **2.51** as a major product with zn-free porphyrin in trace amounts as confirmed by ^{1}H-NMR spectroscopy. After workup, the crude product was redissolved in a mixture of DCM/MeOH in the presence of $Zn(OAc)_2$ to furnish zinc porphyrin **2.51**. Finally, the product was collected as a purple amorphous solid and its chemical structure was confirmed by ^{1}H-NMR spectroscopy.

2.9.2.4 Reduction of *trans*-porphyrin 2.51 to afford 2.44

The reduction of the bromide and triflate groups in **2.51** was investigated following the same optimized reduction procedures employed previously for **2.50** (Scheme 48).

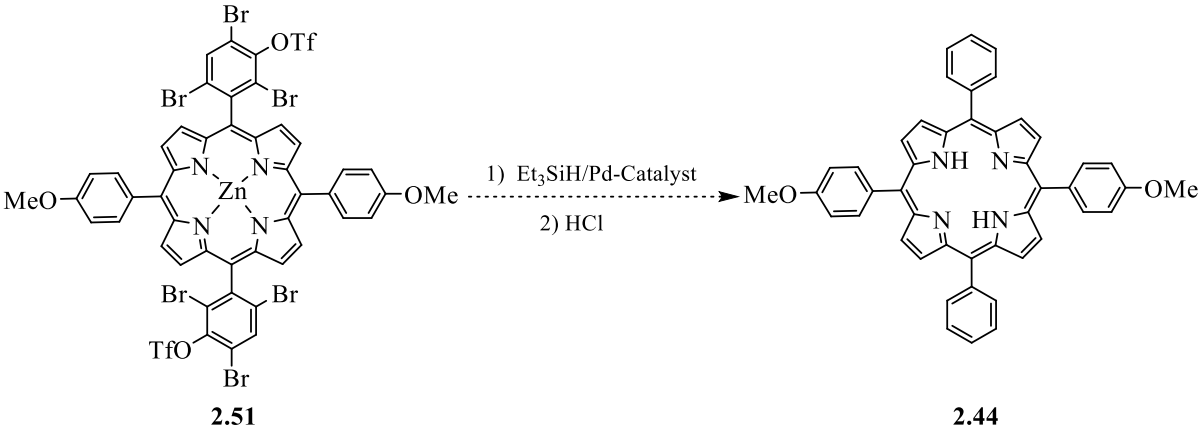

2.51 **2.44**

Scheme 48: Reduction of **2.51.**

2.51 was dissolved in excess triethylsilane with $PdCl_2$ (5 mol %) in a sealed tube and heated at 120 ºC. The progress of the reaction was monitored periodically by MALDI-tof MS. After 5 days, the reaction showed only the reduction of bromides whereas there was no sign of the reduction of triflates. This indicates the loss of bromine is faster than triflate which proves the effectiveness of these conditions in reducing bromides as seen previously. Prolongation of the reaction time to three weeks with the addition of $Et_3SiH/PdCl_2$ resulted in a full deprotection of bromides and some triflates as seen in MALDI-tof MS spectra (Figure 24), but overall, the reaction was not satisfactory.

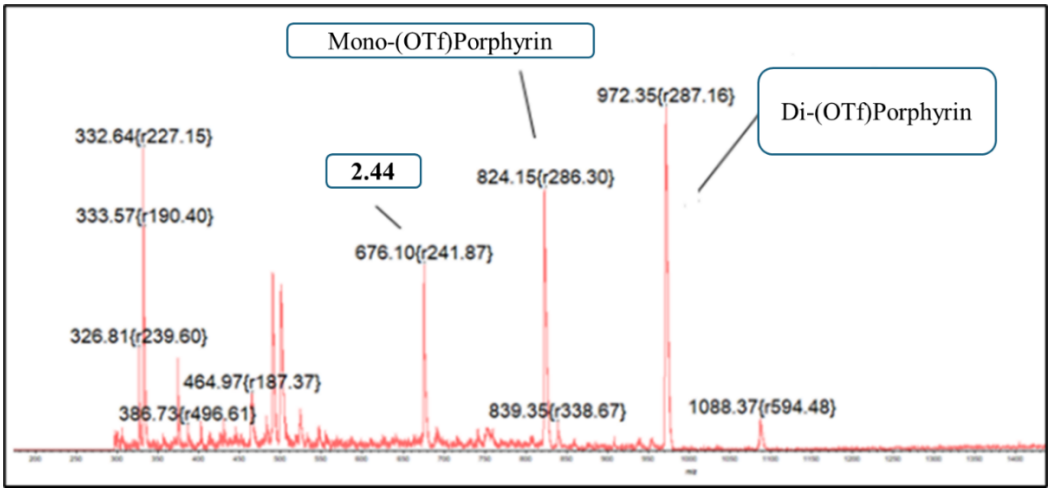

Figure 24: MALDI-tof MS for the deprotection of porphyrin **2.51** under $Et_3SiH/PdCl_2$ conditions.

Further palladium-based reduction conditions were investigated, by employing either Pd/C in Et_3SiH at 120 °C or $Pd(OAc)_2$/dppf in formic acid and TEA at 60 °C (see Table 4).[100,101] The reactions were monitored by MALDI-tof MS, but unfortunately, none of the conditions afforded full deprotection. Instead, the reactions became more complicated due to the hydrolysis of triflate (entry 2). As a result, these attempts indicated that there were problems in the simultaneous reduction of both triflates and bromides. This led us to re-consider alternative routes that require a sole reduction of bromide to produce **2.44**.

Entry	**2.51**	Solvent	Catalyst	Temp. °C	Time	Yield %
1	30 mg	Et_3SiH	Et_3SiH/ $PdCl_2$	120	+ 5 d	Not complete
2	20 mg	DMF	Formic acid/TEA $Pd(OAc)_2$/dppf	60	+ 5 d	Not complete
3	10 mg	Et_3SiH	Et_3SiH/ Pd	120	+ 5 d	Not complete

Table 4: Summary of an optimized deprotection reaction.

2.10 Alternative pathway to obtain 2.44

As an alternative route to obtain *trans* 5,15-dimethoxyphenylporphyrin **2.44** using our blocking strategy, 2,6-dibromobenzaldehyde **2.52** was selected as a starting material. This aldehyde is commercially available and has been used previously for the synthesis of *trans* porphyrins. However, it hasn't been tested by challenging electron-rich partners.[102] The general proposal for the synthesis of *trans* porphyrin **2.44** is shown in (Scheme 49).

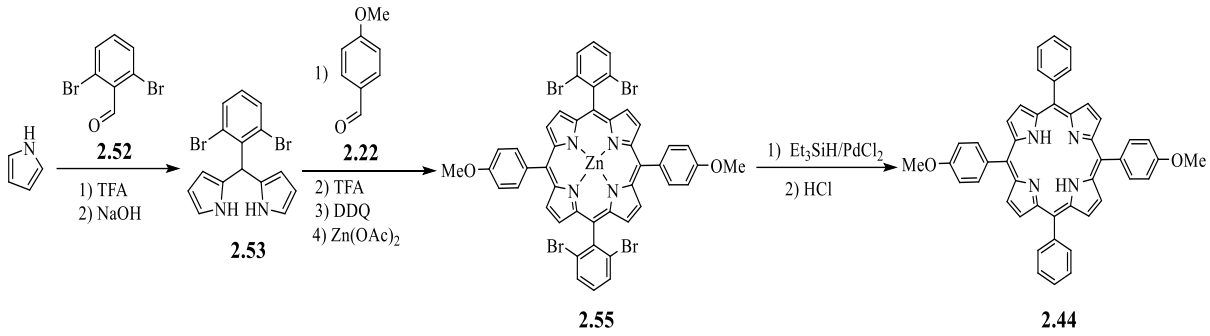

Scheme 49: General synthetic pathways for the synthesis of *trans* porphyrin **2.44.**

2.10.1 Synthesis of *trans* Zn porphyrin 2.55

Initially, (2,6-dibromophenyl)dipyrromethane **2.53** was successfully obtained in a 45% yield following the previously described protocol (Page 42).[59] With this in hand, the synthesis of *trans* porphyrin **2.55** was achieved using equimolar amounts of DPM **2.53** with 4-methoxybenzaldehyde **2.22** (1 mM in dry DCM containing 2 mM TFA) at 0 °C under N_2.

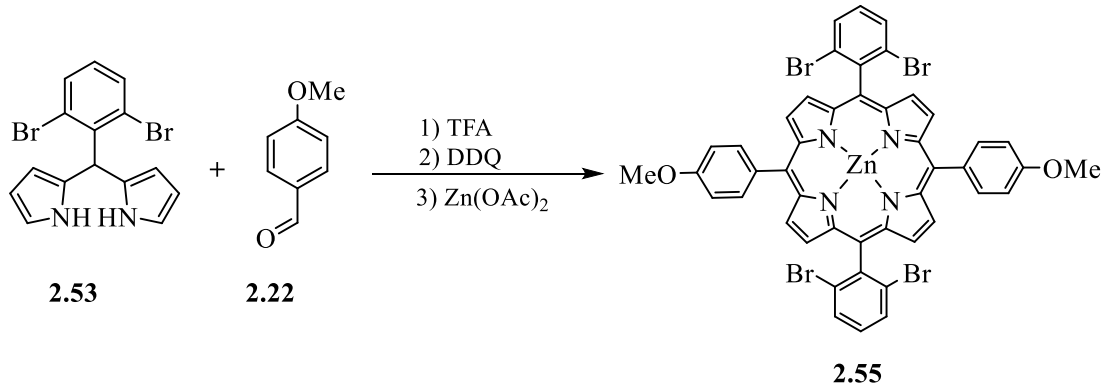

Scheme 50: Synthesis of zinc *trans*-5,15-*bis*-(2,6-dibromophenyl)-10,20-di(methoxyphenyl)porphyrin **2.55**.

The reaction mixture was monitored by TLC and MALDI-tof MS which showed complete formation of metal-free *trans* porphyrin **2.54** intermediate without any sign of scrambling in 1.5 h. This proves that the presence of bromine atoms at 2- and 6- positions inhibits the scrambling process. DDQ was then added followed by the addition of zinc acetate and the mixture stirred at room temperature overnight. After completion, the resulting solid

material was dry loaded onto column chromatography with hexane then DCM 100% as the eluent system. Although this solvent system showed good separation on TLC, only partial separation on the column was achieved. This is because the product crystallized within the column, impeding proper separation even when better solvents such as acetone, ethyl acetate, and methanol were used. However, when THF was used the material was collected. ^{1}H-NMR spectroscopy showed the desired product with a trace of metal-free porphyrin and other unknown side products. Recrystallization using different solvents (*e.g.*, DCM: MeOH, DCM: hexane, DCM: pet. ether) to obtain a pure sample was not successful.

Therefore, we decided to repeat the reaction and isolate the metal-free *trans* porphyrin **2.54** in the first step followed by the insertion of zinc acetate in the second step as outlined in scheme 51.

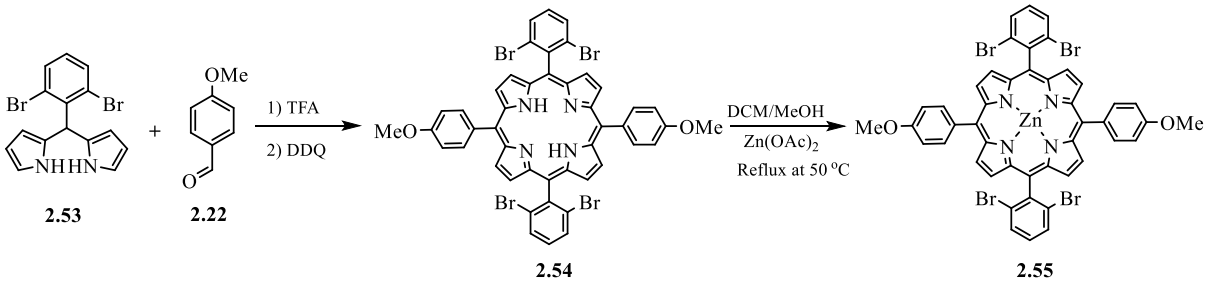

Scheme 51: Synthesis of zinc *trans*-5,15- *bis*-(2,6-dibromophenyl)-10,20-di(4-methoxyphenyl)porphyrin **2.55.**

Repeating the reaction conditions as described earlier, the metal-free *trans* porphyrin **2.54** was obtained in a 57% overall yield, and the zinc *trans* porphyrin **2.55** was smoothly achieved by refluxing the free porphyrin with zinc acetate in a mixture of DCM/MeOH overnight. The desired product was obtained as purple crystals in a 94% yield. The ^{1}H-NMR spectrum (Figure 25) proved the formation of zinc porphyrin. The absence of the characteristic peak at -2.55 ppm suggested the metal-containing porphyrin had been successful. The porphyrin β-protons were assigned as doublets 8.98 ppm and 8.73 ppm, respectively.

Moreover, the para-protons were assigned at 7.53 ppm as a triplet, integrating for two protons, while the ortho and meta-protons were observed as expected. The methoxy protons were observed at 4.09 ppm as a singlet as shown in (Figure 25).

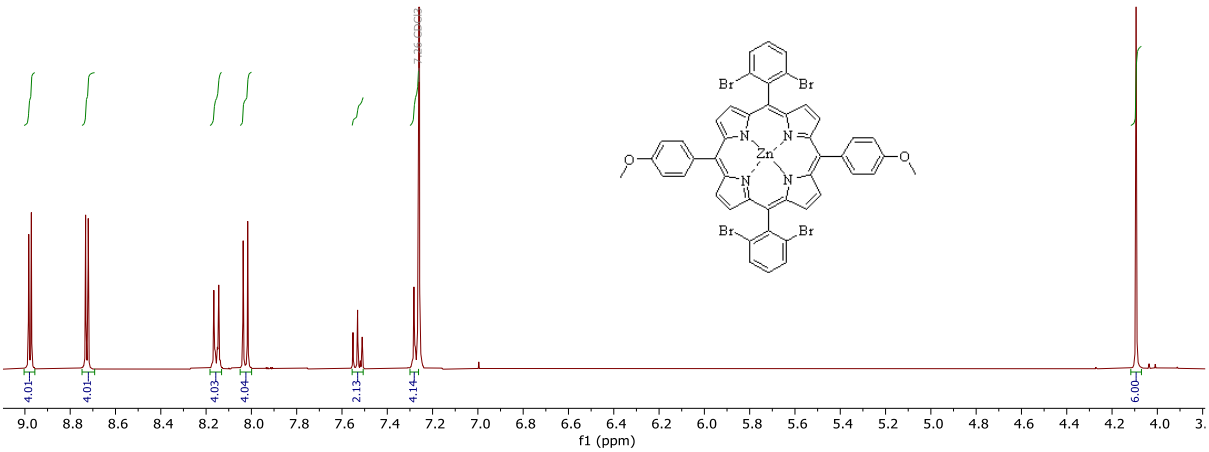

Figure 25: The ^{1}H-NMR spectrum of zinc *trans* porphyrin **2.55**.

The structure of the zinc porphyrin **2.55** was unambiguously confirmed by single crystal X-ray diffraction analysis (Figure 26).

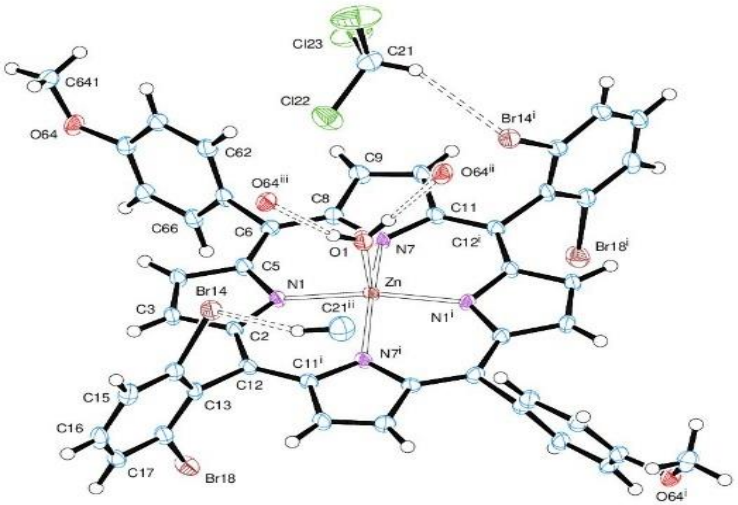

Figure 26: X-ray crystal structure of zinc porphyrin **2.55**.

2.10.2 Debromination of *trans* porphyrins 2.54 and 2.55

Following the successful synthesis of *trans* porphyrins **2.54** and **2.55**, it became feasible to attempt the synthesis of *trans*-5,15-di(methoxyphenyl)porphyrin **2.44** *via* debromination of either **2.54** or **2.55**. The initial attempt involved using metal-free porphyrin **2.54** as the starting material (Scheme 52). For this reaction, Pd/carbon was used as the catalyst instead of $PdCl_2$ to avoid palladium insertion, however, employing $PdCl_2$ was favoured for the reductive debromination of **2.55**.

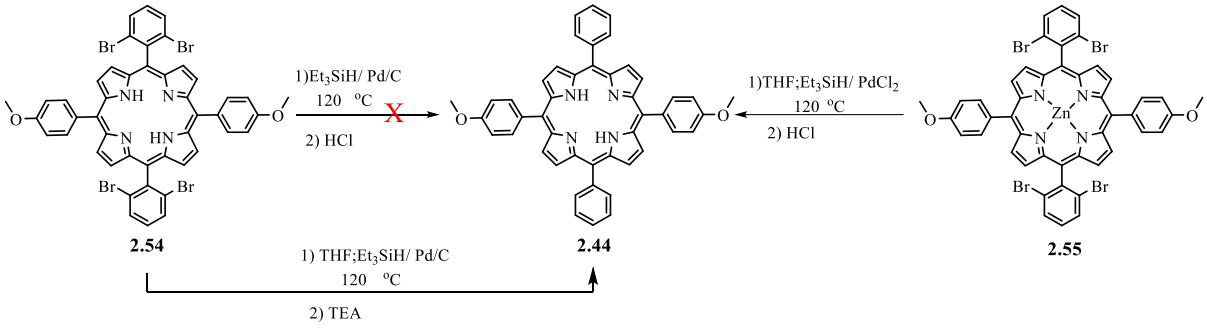

Scheme 52: Debromination of **2.54** and **2.55.**

Therefore, **2.54** was heated at 120 °C in Et_3SiH in the presence of Pd/C in a sealed tube. After two days, the reaction was monitored by MALDI-tof MS which showed the desired product **2.44,** alongside a mixture of side products and unreacted starting material **2.54**. Although Pd/C and triethylsilane were added to the reaction mixture and left for longer time at high temperature, the reaction was not complete. This is partly because the starting material was not completely soluble in triethylsilane which affected the debromination process of **2.54**.

To overcome this issue, the reaction was repeated in THF to increase the solubility of porphyrin **2.54**. After three days MALDI-tof MS showed the formation of **2.44** with two side products (where three and two bromines were reduced at (752.18 *m/z*) and (832.09 *m/z*)) without metal insertion as shown in (Figure 27). Thus, the reaction mixture was left for a further 48 h. After completion and work up, **2.44** was collected in a 60% yield.

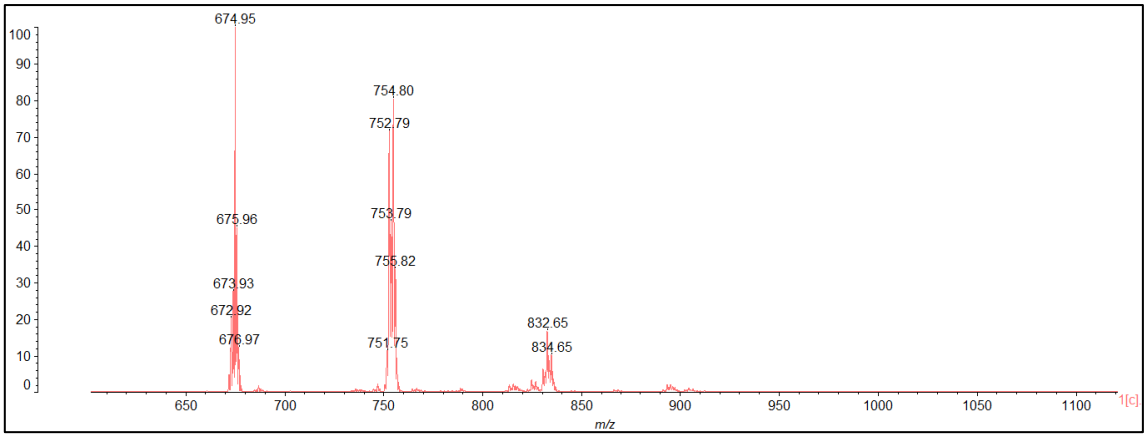

Figure 27: MALDI-tof MS obtained for the synthesis of porphyrin **2.44** under Pd conditions after three days.

Alternatively, the second attempt involved using **2.55** as a starting material for the formation of **2.44**. The porphyrin **2.44** and $PdCl_2$ were heated in a mixture of THF and triethylsilane in a sealed tube. After 5 days, the reaction showed complete consumption of the starting material and the formation of the desired product **2.44** was confirmed by MALDI-tof MS. Compound **2.44** was obtained in a 74% yield. As a result, both routes afforded the complete reduction of all bromides within 5 days with a slightly improved outcome for the second method.

Characterization by ^{1}H-NMR spectroscopy proved the successful reduction of the bromine groups. Additionally, the ^{1}H-NMR spectrum of **2.44** was compared with a previously recorded spectrum, reported for a mixture of **2.44** (***trans*** + ***cis***), which confirms the structural identification and purity of ***trans*-2.44** (Figure 28).

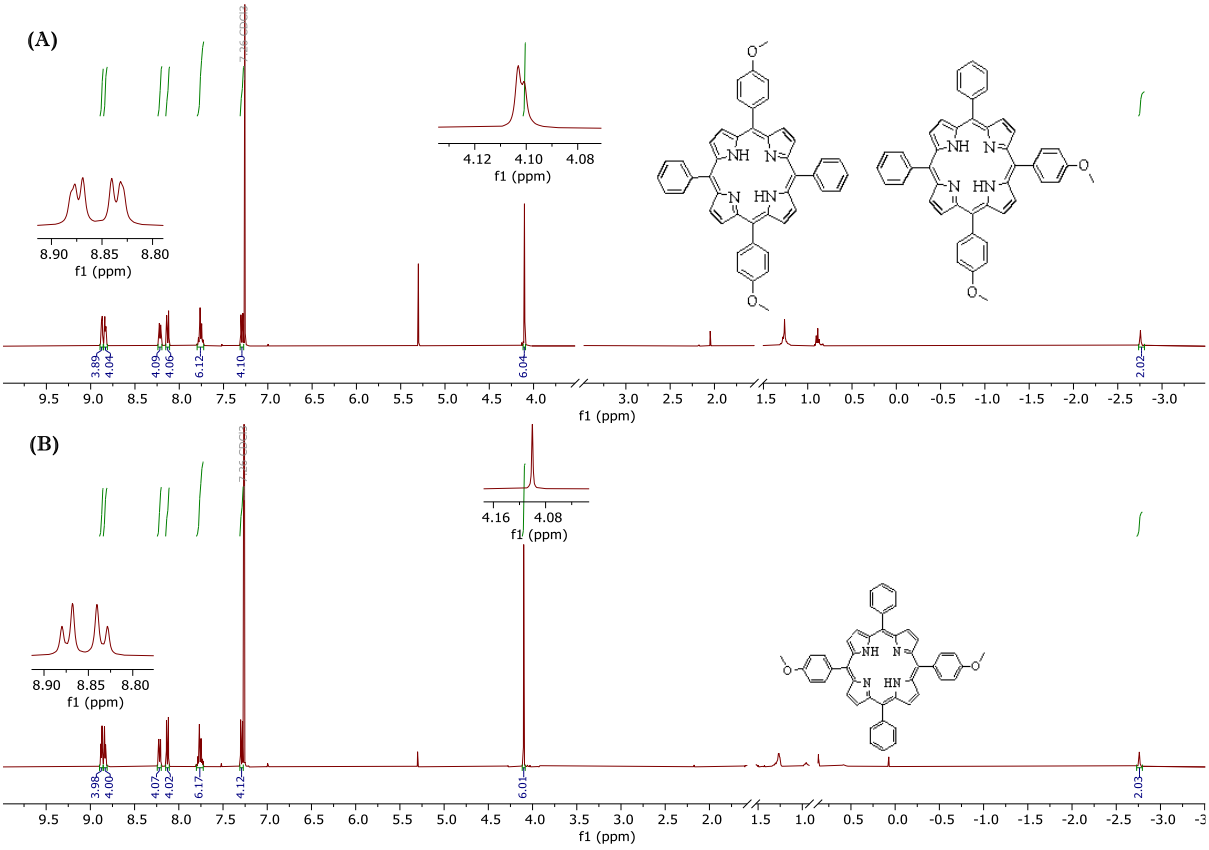

Figure 28: The ^{1}H-NMR spectra of a mixture of isomers *cis*/*trans*- (**A**) and pure *trans*-isomer **2.44** (**B**).

2.11 Utilizing *cis*-5,10-di(*p*-hydroxyphenyl)porphyrin (*cis*-2.12d)

At this stage of the project, even though our main target was to achieve the synthesis of a triple decker complex based on a *trans* porphyrin ***trans*-2.12d**, we decided to extend our efforts to use the *cis*-5,10-di-(*p*-hydroxyphenyl)porphyrin ***cis*-2.12d** due to its availability as pure crystals in high yield and its similarity to the *trans* structure ***trans*-2.12d**. Additionally, it enabled us to refine and optimize the triple-decker's synthetic route, before applying these conditions to the more valuable ***trans*-2.12d**.

Therefore, our target in this section was to synthesize a triple decker complex based on the use of ***cis*-2.12d**. To achieve this, the pre-synthesized ***cis*-2.12d** possesses two *p*-hydroxy groups and one of them will be functionalized with an *O*-hexenyl chain and the other one will

be functionalized for coupling porphyrins through a decyl chain resulting in dyad **2.57**. This will be then used to capture Pc in the presence of lanthanum ions forming the triple decker complex **2.58** as a key intermediate on route to **2.60**. This step will organise the molecules in the order of porphyrin-phthalocyanine-porphyrin which will be followed by the metathesis reaction to link the terminal alkene which then undergoes a reduction reaction to furnish the final target **2.60** (Scheme 53).

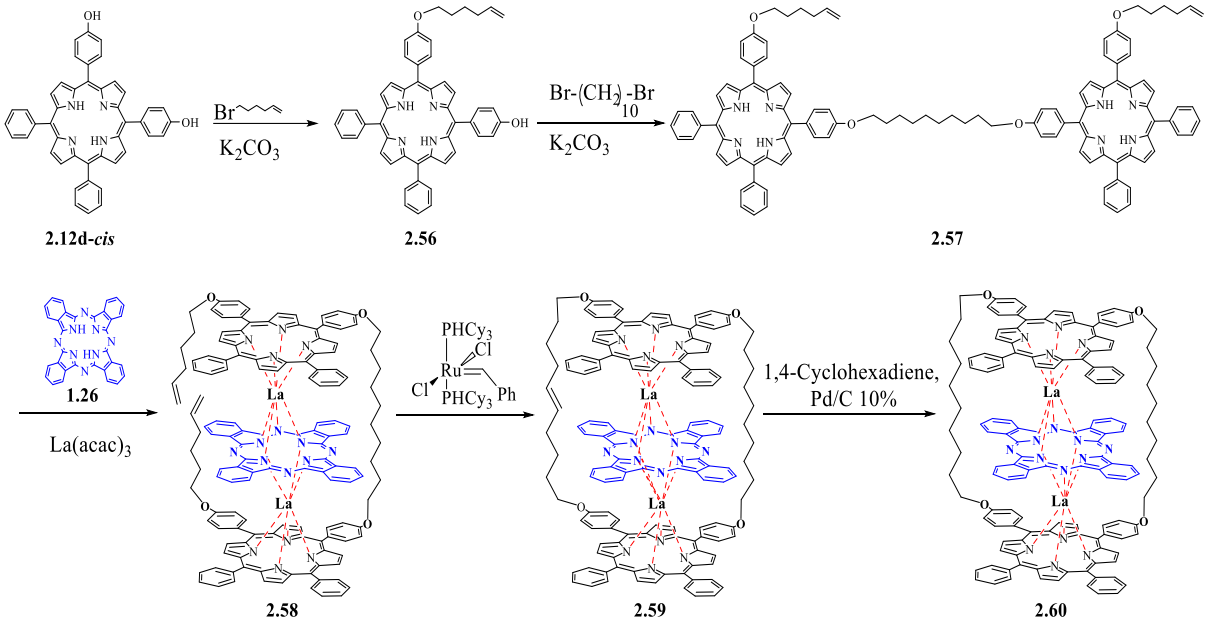

Scheme 53: Possible synthetic pathway for the synthesis of *cis*-triple decker complex **2.60**.

2.11.1 Functionalisation of porphyrin *cis*-2.12d

As mentioned earlier, the ***cis*-2.12d** was obtained as a side product from the *O*-demethylation reaction of **2.44**-(***trans*+*cis***). Thus, the first reaction in this sequence was the functionalisation of ***cis*-2.12d** to obtain **2.56**. This reaction can be achieved using an optimized method of a Williamson reaction with 6-bromo-1-hexene as shown in scheme 54.[103,104]

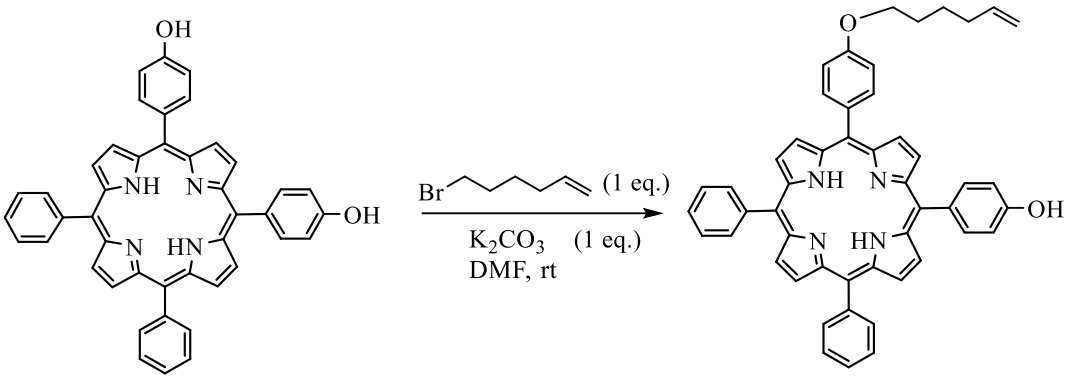

2.12d-*cis* **2.56**

Scheme 54: *O*-Alkylation of ***cis*-2.12d**.

One of the challenges encountered during this reaction was dealing with two phenol groups, where we aimed to maximize the yield of the mono-substituted product **2.56** while minimizing the formation of the unwanted di-*O*-hexenyl substituted product. To do so, the synthesis of mono-functionalized porphyrin **2.56** was successfully obtained in 11 % yield by treating **2.12d-*cis*** with one equivalent of 6-bromo-1-hexene in the presence of K_2CO_3 in dry DMF at room temperature. The reaction was monitored and, after 60 minutes, TLC showed the formation of the desired product **2.56** with unreacted starting material ***cis*-2.12d**.

Prolonging the reaction time was expected to produce a mixture of mono- and di-functionalized porphyrins. Therefore, the reaction mixture was quenched with water, extracted with DCM three times and dried over $MgSO_4$. The crude mixture was then easily purified by a short column chromatography using DCM as the eluent. The desired product **2.56** was collected as the second fraction while traces of dialkylated porphyrin were collected in first fraction. The unreacted starting material ***cis*-2.12d** was recovered as the major fraction from this reaction. However, the yield of **2.56** was required to be optimized.

2.11.1.2 Optimization of mono-functionalized porphyrin 2.56

The synthesis of compound **2.56** was successful but the yield was insufficient to provide enough material for the following steps. Therefore, we adjusted the reaction temperature, time,

and equivalents of 6-bromo-1-hexene. The initial attempts using dry DMF as solvent at room temperature improved the yield (Entry: 1-2) but the substitution of potassium carbonate with a stronger base, cesium carbonate did not. A moderate yield improvement was achieved when changing the solvent to acetone and conducting the reaction under reflux conditions for 48 hours (Entry: 4). However, a significant yield was observed by increasing both the base and reagent's equivalents, along with using more dilute concentration (Entry: 5, highlighted in grey). In these attempts we observed that room temperature and diluted concentrations of the reaction mixture were helpful to minimize the formation of the unwanted di-functionalized porphyrin. Table 5 summarise all optimization attempts of mono-functionalisation of compound ***cis*-2.12d** with 6-bromo-1-hexene.

Entry	**2.12d-(*cis*)**/ mMol	Base/ eq.	6-bromo-1-hexene /eq.	Solvent	Temp. °C	Time	Yield %
1	50 mg/0.077	K_2CO_3/(1eq)	(1eq)	DMF(5 mL)	RT	2 h	15
2	50 mg/0.077	K_2CO_3/(2eq)	(2eq)	DMF(5 mL)	RT	6 h	18
3	50 mg/0.077	Cs_2CO_3/(4eq)	(2eq)	DMF (5 mL)	RT	6 h	20
4	50 mg/0.077	K_2CO_3/(4eq)	(2eq)	Acetone (20 mL)	70	48 h	29
5	50 mg/0.077	K_2CO_3/(4eq)	(4eq)	DMF (15 mL)	RT	12 h	43
6	50 mg/0.077	K_2CO_3/(4eq)	(2eq)	DMF (10 mL)	RT	60 h	30

Table 5: Optimization of mono-functionalisation of ***cis*-2.12d** using 6-bromo-1-hexene.

2.11.2 Synthesis of porphyrin dyad 2.57

The porphyrin dyad **2.57** contains two porphyrin units connected *via* a flexible *n*-alkyl chain. Recently, our group found that a C_{10} chain was the suitable linker length for the formation of triple decker complexes from porphyrin dyads and phthalocyanine.[87] Consequently, the preparation of porphyrin dyad **2.57** was achieved by reacting two

equivalents of **2.56** with one equivalent of 1,10-dibromodecane in the presence of potassium carbonate (Scheme 55).

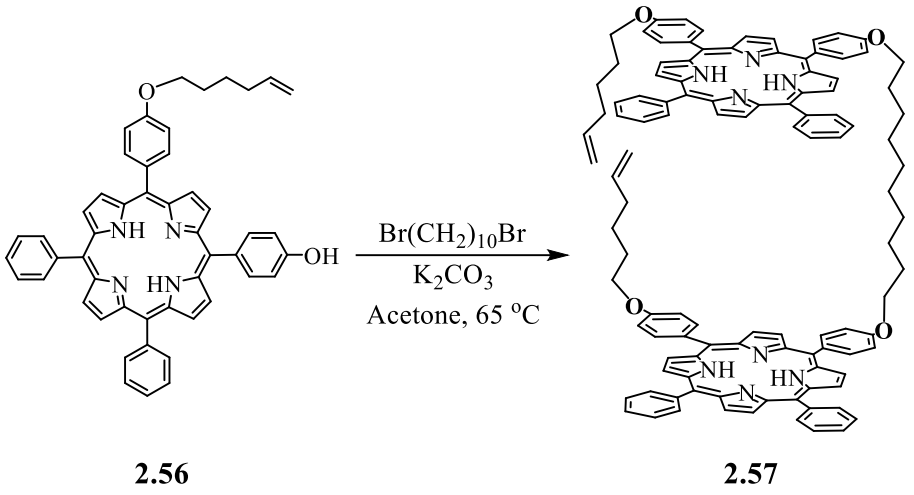

2.56 **2.57**

Scheme 55: Formation of porphyrin dyad **2.57**.

After 72 h, the progress of reaction was monitored by TLC which showed three spots corresponding to the starting material **2.56**, mono-(bromoalkoxyphenyl)porphyrin (TPPO$(CH_2)_{10}$Br) and porphyrin dyad **2.57**. The disappearance of the starting material was observed after 8 days with the appearance of mono-(bromoalkoxyphenyl)porphyrin (*m/z* 946.21) and dyad **2.57** (*m/z* 1595.12) by MALDI-tof MS. Therefore, a further small amount of starting material **2.56** was added in order to convert the remaining mono-bromoalkoxyphenylporphyrin to the desired product **2.57**. After completion, the reaction was quenched with water, extracted with DCM and dried over $MgSO_4$. The solvent was removed, and the resultant solid was crystallized using DCM:MeOH (1:1) to obtain the pure dyad **2.57** as purple crystals in 61 % yield. The structure of this intermediate **2.57** has been confirmed by ^{1}H-NMR spectroscopy (also recorded for the precursor under identical conditions in $CDCl_3$) (Figure 29).

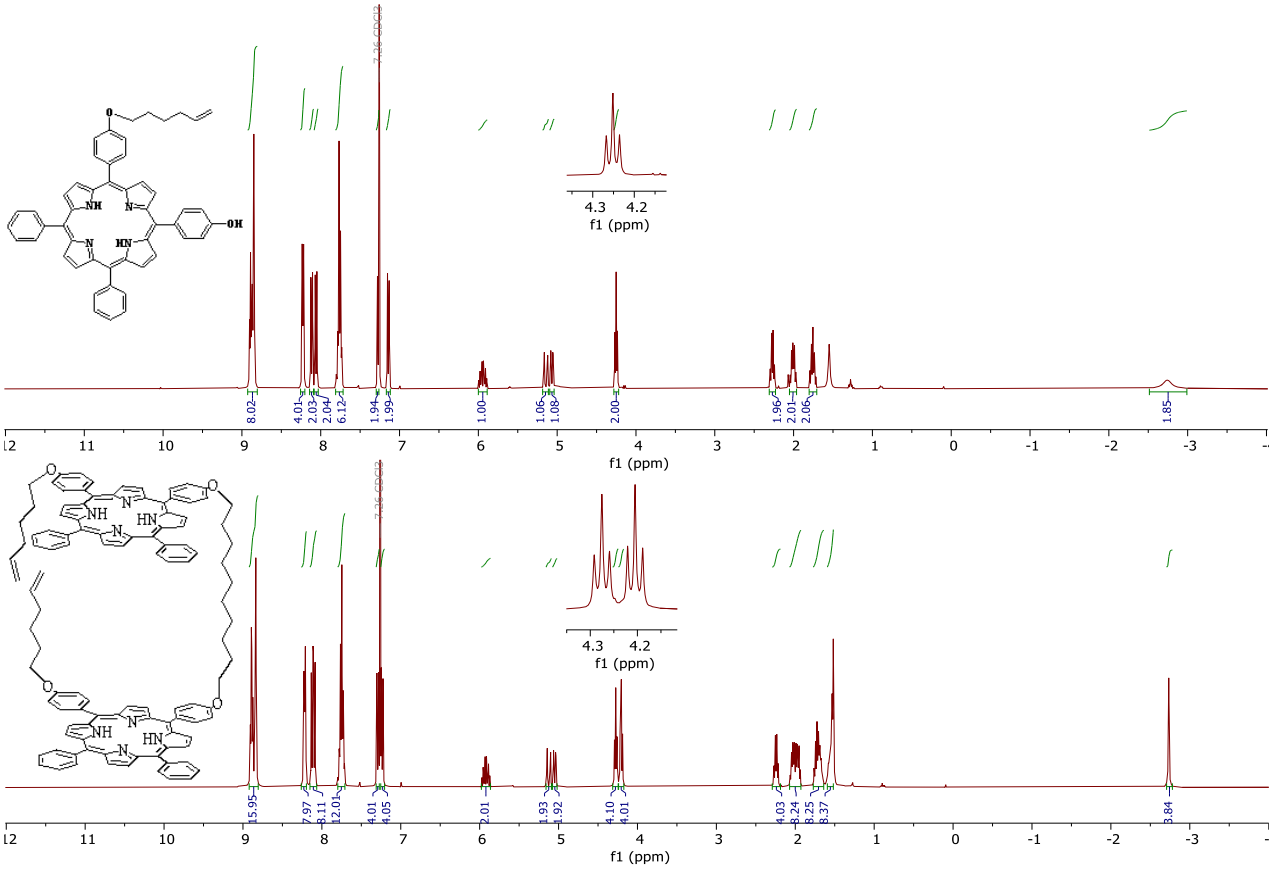

Figure 29: ^{1}H-NMR spectral comparison obtained for **2.56** and **2.57**.

2.11.3 Selective synthesis of triple decker complex 2.58

With the successful synthesis of porphyrin dyad **2.57** in good yield, the synthesis of triple decker **2.58** was attempted following a modified procedure by our group. This method will organise the formation of porphyrin-phthalocyanine-porphyrin in the presence of lanthanum metals. However, it was anticipated that the presence of hexenyl chain in both porphyrins in *cis* configuration may result in two isomers. **2.58** and ***trans*-2.58a**, of which only **2.58** can react in an intramolecular metathesis reaction (Scheme 56).

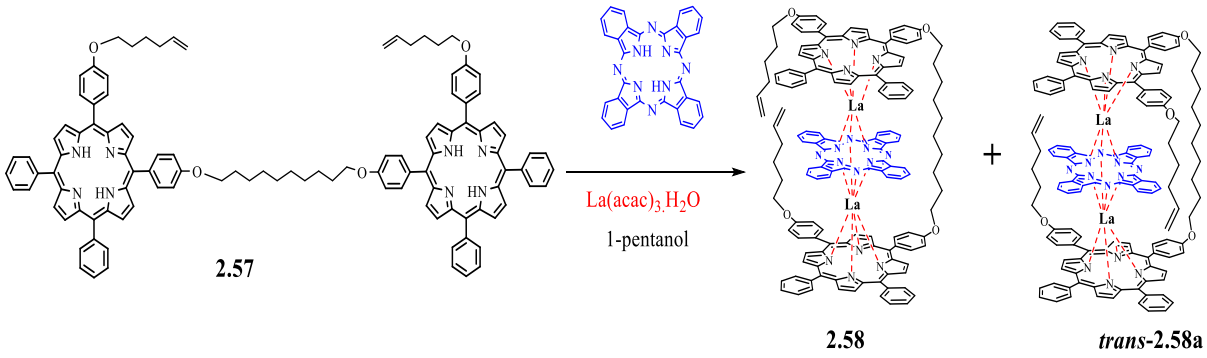

Scheme 56: Preparation of triple decker complex **2.58**.

One equivalent each of porphyrin dyad **2.57** and phthalocyanine were refluxed in pentanol under N_2 for 24 h, followed by the addition of two equivalents of lanthanum acac. After 2 hours, TLC showed two spots: one corresponding to the starting material **2.57** and the other to compound **2.58** (as a brown spot), with no indication of unwanted ***trans*-2.58a** formation. This was further confirmed by MALDI-tof MS spectroscopy. After a further 2 h the reaction mixture was cooled to room temperature and the solvent removed. The resulting solid was subjected to column chromatography using DCM:hexane (1:2) to collect the desired product **2.58**, as second fraction, and traces of the starting material **2.57** were collected as first fraction. After crystallization from DCM:MeOH, **2.58** was obtained as dark brown crystals in 62% yield.

The ^{1}H-NMR spectra confirmed the formation of the expected product **2.58** (Figure 30). The absence of the characteristic peak at -2.73 ppm proved that no metal-free porphyrin remained. The symmetrical Pc signals were shown at 8.3 ppm and 9.4 ppm as a result of the influence of nearby Lanthanum atoms. Also, more signals for the inner and outer protons were expected as they are chemically inequivalent. Additionally, the two signals of the two *O*-CH_2 appeared as triplets at 4.40 ppm and 4.60 ppm while the rest of the aliphatic chains were observed as expected. The ^{1}H-NMR spectrum indicates the presence of a single molecule, as there is no evidence of a mixture of isomers.

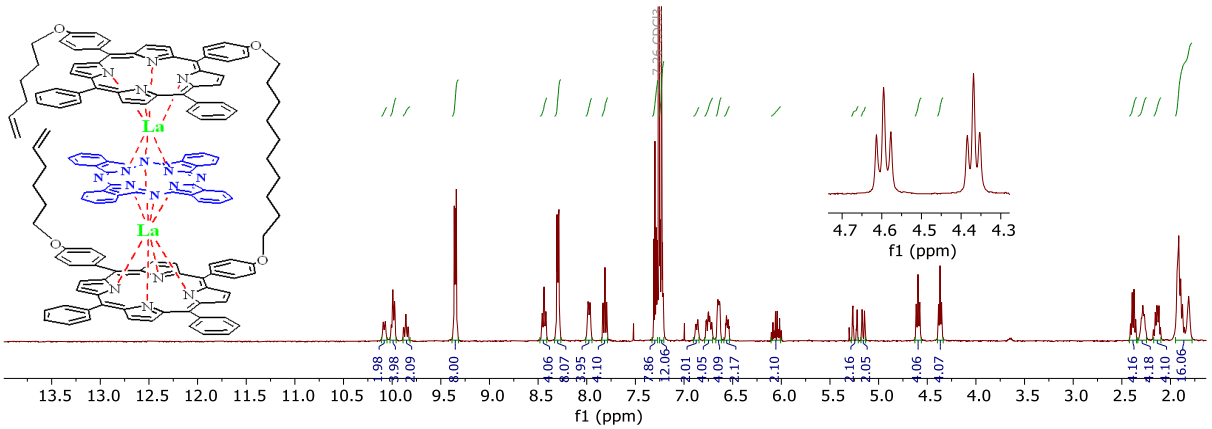

Figure 30: ^{1}H-NMR spectrum of **2.58**.

The MALDI-tof MS displayed an almost identical match to the theoretical isotope pattern corresponding to the desired product **2.58**. While this provides additional confirmation that the TD has been isolated, it does not help to distinguish if it a mixture or not at this stage (Figure 31).

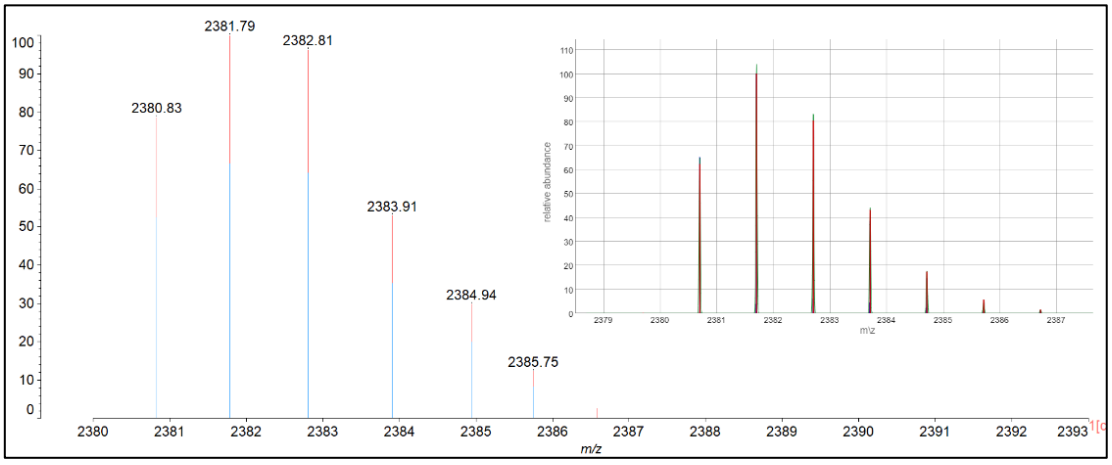

Figure 31: MALDI-tof MS of triple decker **2.58**.

Further evidence for the formation of triple decker complex **2.58** was obtained through UV-Vis spectroscopy (Figure 32). The spectral profile of **2.58** is different from the absorption spectra of its starting materials (dyad **2.57** and Pc**)** which shows a typical absorbance behaviour of TDs.

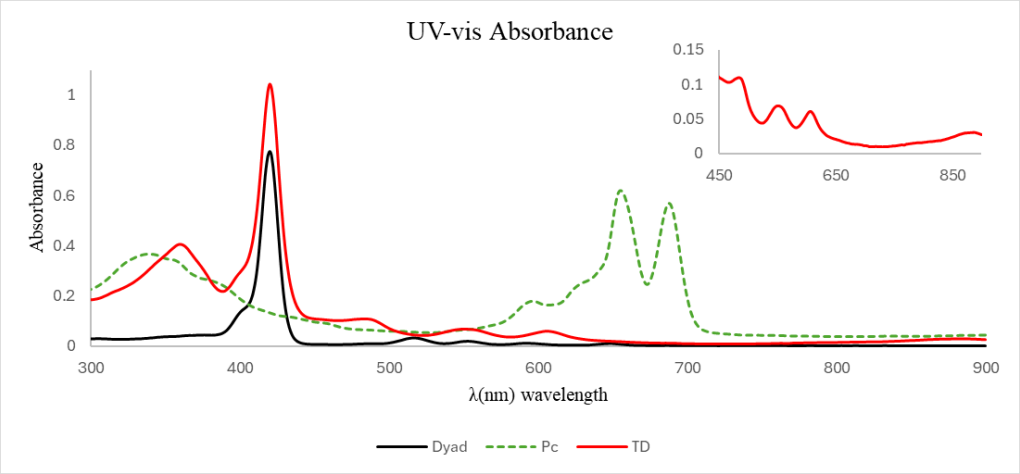

Figure 32: Uv-Vis of triple decker complex **2.58**.

2.11.4 Cyclisation of triple decker complex 2.58

After successfully preparing and isolating the controlled triple-decker complex **2.58** with a satisfactory yield, our next objective was to synthesize a cyclic (double-bridged) triple-decker complex **2.59**. This could be done by applying the olefin metathesis reaction which would covalently connect the two porphyrin units.[105] In a previous study by Cammidge's group (unpublished data) the successful formation of cyclic triple decker complex utilizing metathesis reaction has been demonstrated, using the 1st generation of Grubbs catalyst to cyclize four alkene chains for each porphyrin placed at the *para*-position of the *meso*-phenyl groups. The cyclisation process was easily achieved without any notable effect or disorder on the structure of triple decker complex.

In our case, only one alkene chain for each porphyrin needed to undergo metathesis. Therefore, we made an attempt to synthesize the cyclic TD **2.59** via olefin metathesis using Grubbs catalyst.[105] The catalyst was dissolved in dry DCM and then added to pre-dissolved TD **2.58** in dry DCM. The reaction is moisture and air sensitive and thus it was stirred under N_2 atmosphere for 24 h (Scheme 57).

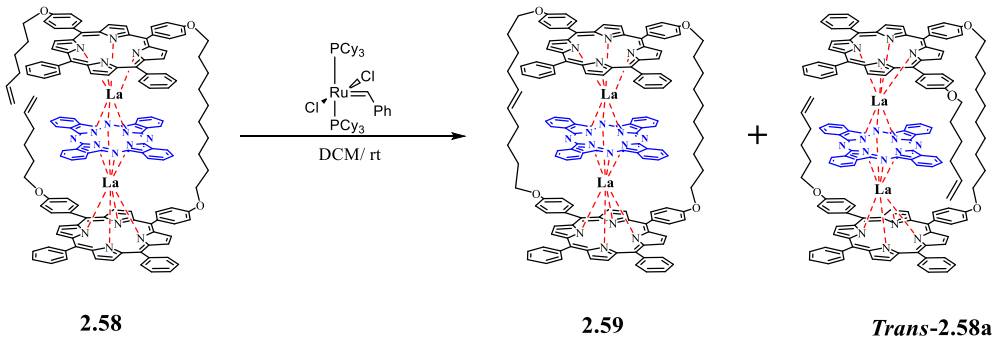

2.58 **2.59** ***Trans*-2.58a**

Scheme 57: Cyclisation of triple decker complex **2.58**.

[105]The metathesis process was monitored by TLC, which indicated only two spots, and MALDI-tof MS spectroscopy indicated formation of the cyclised TD **2.59** alongside the starting material **2.58**. This may be consistent with the hypothesis that the unreacted starting material was the isomer with the alkene chains separated from each other ***trans*-2.58a** (See 2.11.3). Therefore, the reaction was quenched in order to prevent the formation of any side product. The mixture was separated using DCM:hexane as the eluent to collect the desired product in the first fraction and unreacted starting material ***trans*-2.58a** was collected in the second fraction. Unfortunately, the yield of the desired product **2.59** was low (20%).

Analysis of the ^{1}H-NMR spectrum for **2.59** shows the absence of the characteristic peak at 5.51 ppm and 5.25 ppm (vinyl protons), indicating that there is no terminal alkene. Additionally, signals at 5.75 ppm and 6.10 ppm (each as broad multiplets, corresponding to two olefinic protons) indicated the formation of the new bridge. The presence of a double bond on the new linker likely leads to a mixture of *cis* and *trans* isomers around the alkene bonds, causing signal splitting in the aliphatic region. This can be fixed in the next step to increase the symmetry of the complex.

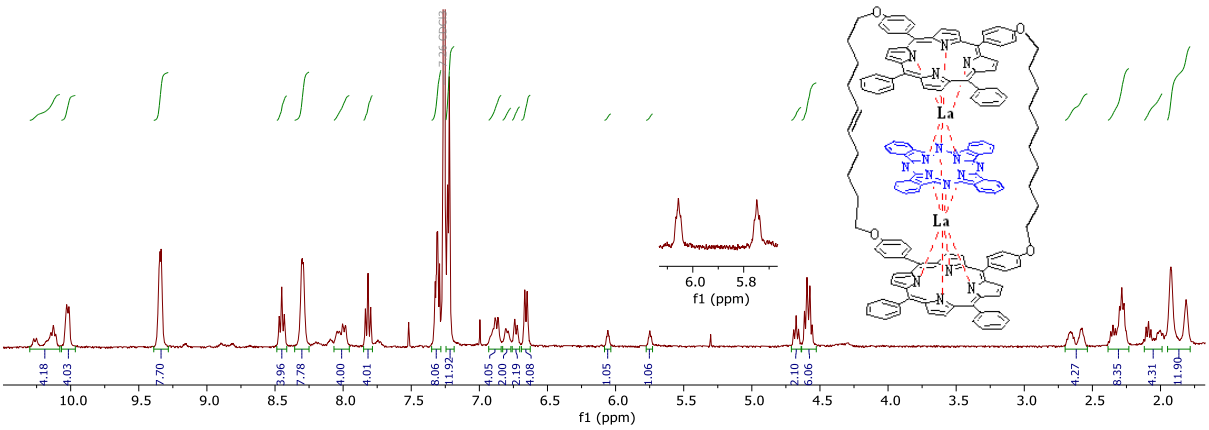

Figure 33: ^{1}H-NMR spectrum of **2.59**.

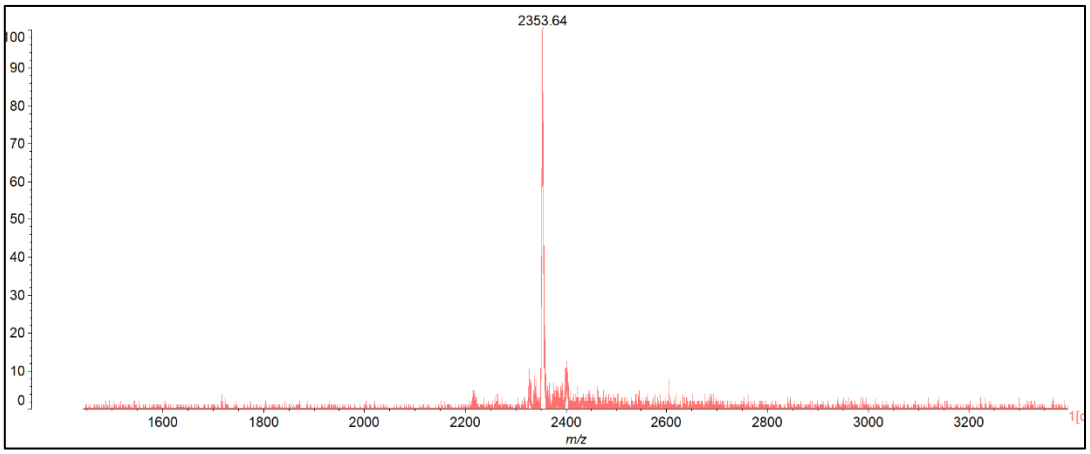

Figure34: MALDI-tof MS confirms the formation of TD **2.59**.

2.11.5 Hydrogenation of the C=C in triple decker complex 2.59

The alkene obtained after the metathesis reaction needed to be reduced in order to achieve the final target for this subproject. Despite the fact that there are several methods that can be applied to reduce the alkene, a method developed by Felix *et al.*[106] was chosen. This method was based on the use of 1,4-cyclohexadiene as a transfer hydrogenation reagent with palladium-carbon (Pd/C 10%) as catalyst. Therefore, the TD **2.59** was dissolved in a mixture of ethyl acetate and 1,4-cyclohexadiene in the presence of palladium-carbon (Pd/C 10%) as a catalyst. The use of ethyl acetate as co-solvent was necessary to increase the solubility of the **2.59** (Scheme 58).

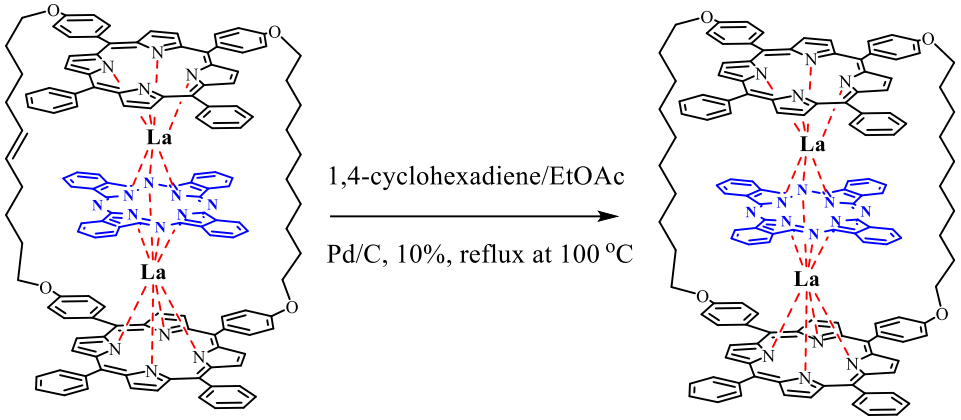

2.59 **2.60**

Scheme 58: Reduction of alkene bond to achieve TD **2.60**.

The reaction mixture was refluxed under argon and monitored by ^{1}H-NMR spectroscopy. The full reduction of the olefinic bond was observed in 6 h. The solvents were removed, and the resultant solid was redissolved in DCM and filtered to remove the catalyst. Recrystallization from DCM:MeOH gave the desired product **2.60** in a good yield (80%) as dark brown crystals.

The structure of **2.60** was confirmed by ^{1}H-NMR spectroscopy as shown in figure 35. The absence of the characteristic olefinic peaks at 5.75 ppm and 6.10 ppm indicates complete saturation of the double bond. Also, the new signal at 4.60 ppm as a typical triplet (J = 7.5) corresponds to alkoxy protons, which proves the symmetry of the complex alongside the characteristic aromatic signal splitting. Moreover, the porphyrin β protons appeared as a typical *cis* splitting as seen earlier (section **2.7.2.2** (Figure 21)).

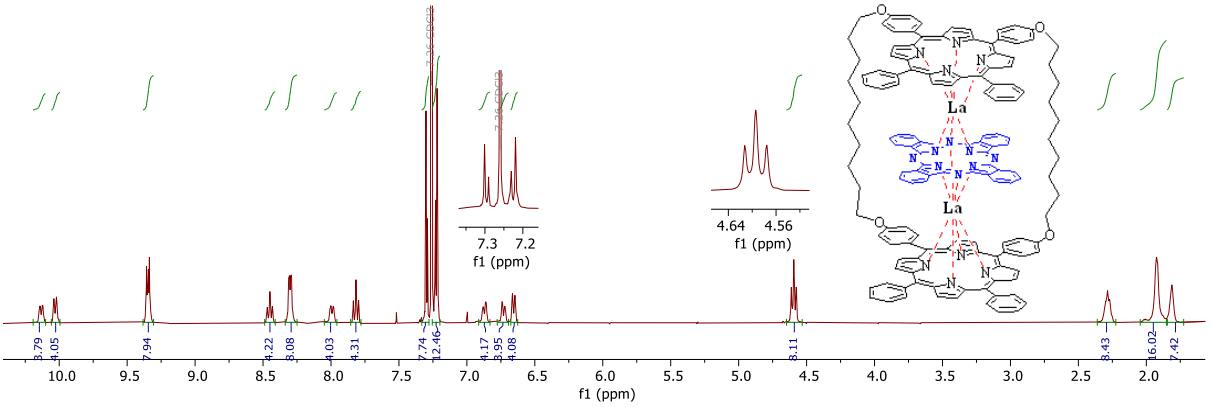

Figure 35: ^{1}H-NMR spectrum of **2.60**.

Additionally, the identity of compound **2.60** was further confirmed by the MADLI-tof mass spectrometry, which gave a cluster at *m/z* 2355.36. Final confirmation for the formation of triple decker complex **2.60** was obtained through X-ray crystallography (Figure 36). The crystallographic data clearly showed the expected sandwich-like structure, confirming the precise arrangement of the ligands and metal centres in the complex. Therefore, the combination of NMR, X-ray crystallography and MALDI-tof mass spectroscopy provides robust evidence for the structural integrity and composition of TD **2.60**.

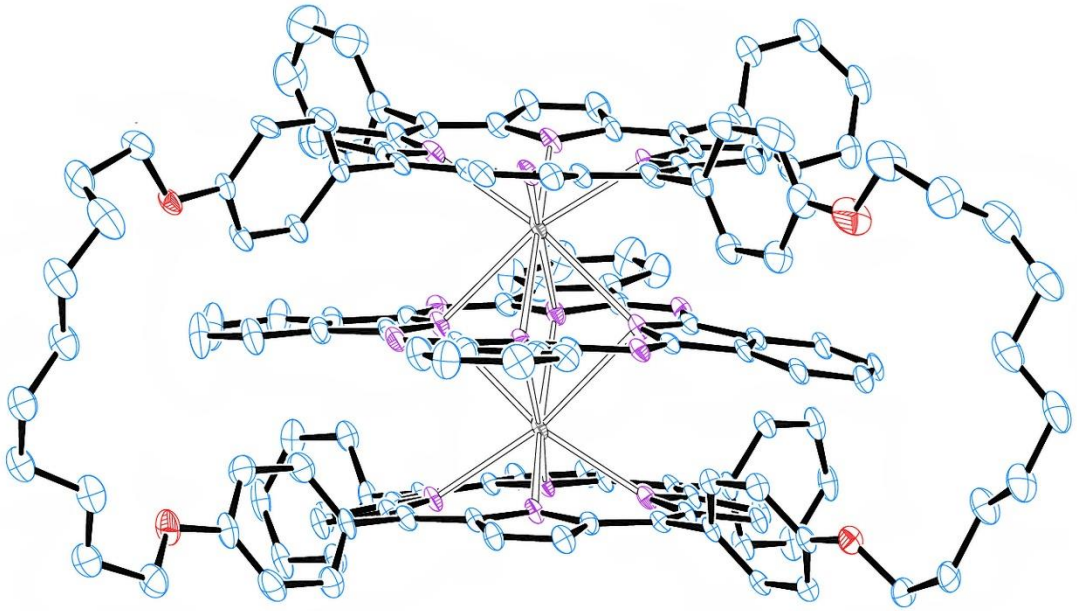

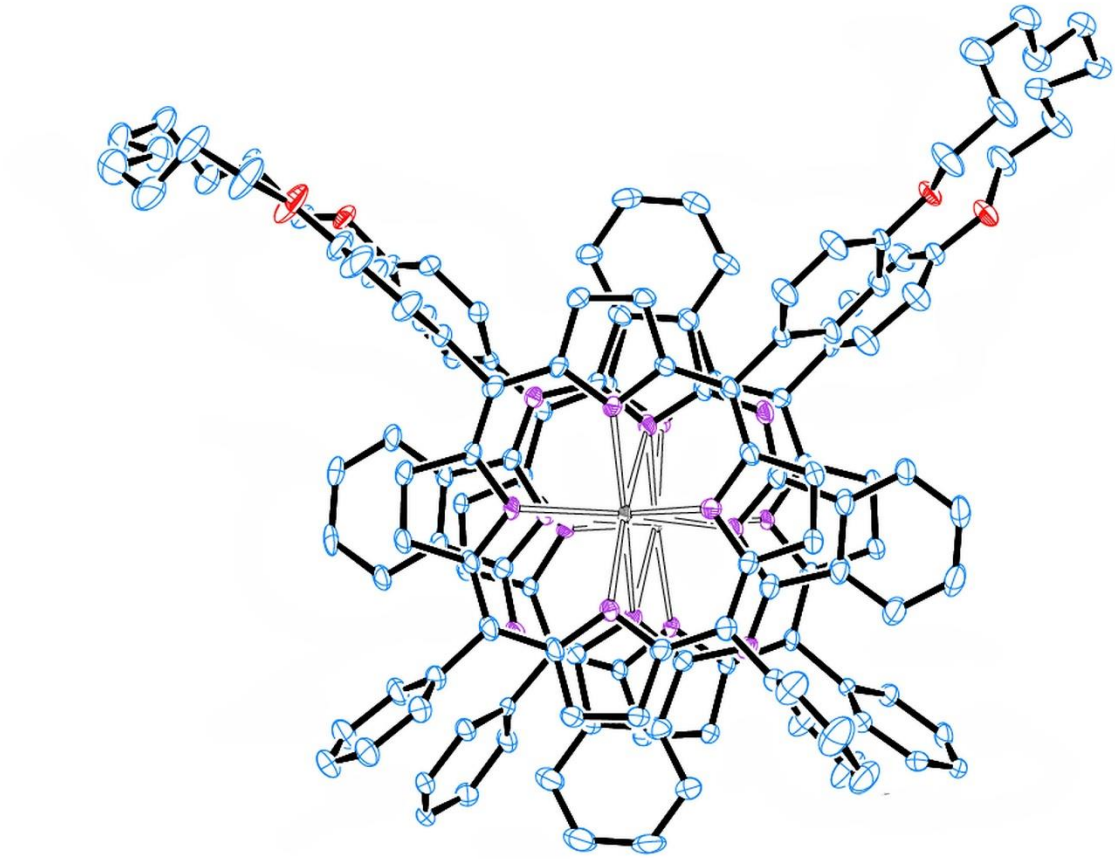

Figure 36: X-ray structure of triple decker complex **2.60.**

2.12 Utilizing *trans*-5,15-di-(*p*-hydroxyphenyl)porphyrin *trans*-2.12d

With the knowledge that we gained from the *cis* project it became feasible to investigate the formation of a triple decker complex based on the use of *trans*-porphyrin ***trans*-2.12d**. The scheme below summarizes the pathway to achieve our target as explained earlier (Scheme 59).

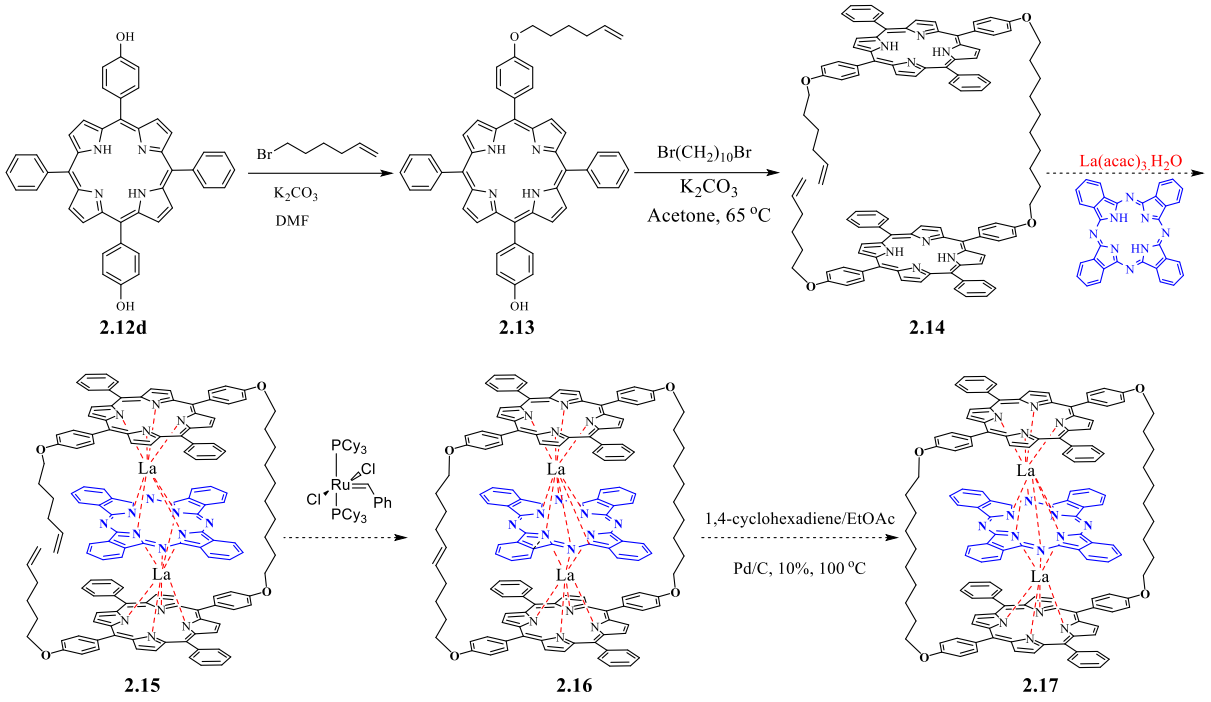

Scheme 59: General synthetic pathways for the synthesis of *trans*-triple decker complex **2.17**.

2.12.1 Functionalisation of *trans*-2.12d

The functionalisation of ***trans*-2.12d** was achieved following the conditions developed in the optimization study conducted for the functionalisation of ***cis*-2.12d** (section 2.11.1), starting with the reaction of 6-bromo-1-hexene in the presence of K_2CO_3 in dry DMF under N_2 overnight at room temperature (Scheme 60).

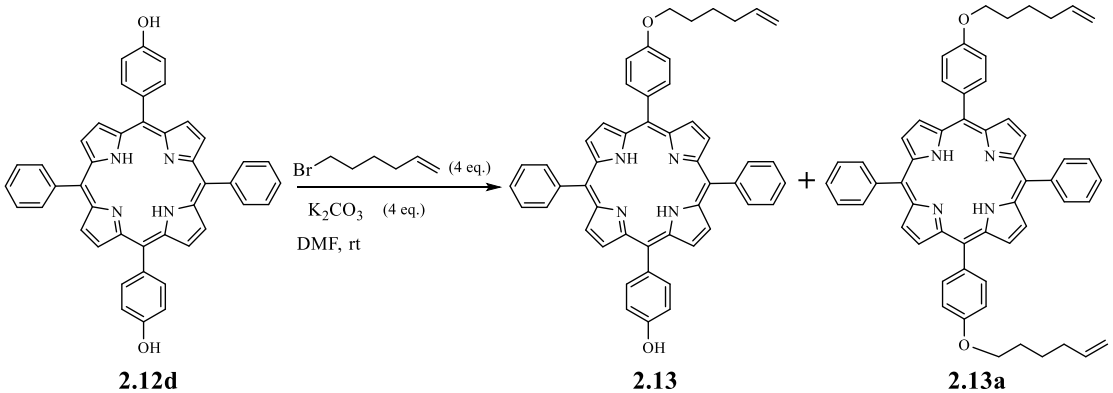

Scheme 60: The preparation of **2.13**.

It is worth mentioning that the progress of the reaction was easily monitored by TLC as the product **2.13** and side product **2.13a** (doubly substituted) have different mobility. After completion, the mixture was worked up and the solvent was removed. The crude mixture was then subjected to column chromatography using DCM 100% as the eluent to collect the first fraction as a *trans*-porphyrin **2.13a** in a 22% yield (R_f = 0.8) (Scheme 60), and the desired product **2.13** as second fraction in a 39 % yield (R_f = 0.45) as purple crystals. The identity of **2.13** was confirmed by a combination of $^1H/^{13}C$-NMR spectroscopy and MALDI-tof MS.

2.12.2 Synthesis of porphyrin dyad 2.14 from porphyrin 2.13

The coupling of the porphyrins was carried out in the presence of K_2CO_3 and 1,10-dibromodecane in acetone at 65 °C in a sealed tube (Scheme 61). The progress of the reaction was monitored by TLC which showed the formation of dyad **2.14** and the expected side product $TPPO(CH_2)_{10}Br$ as confirmed by MALDI-tof MS.

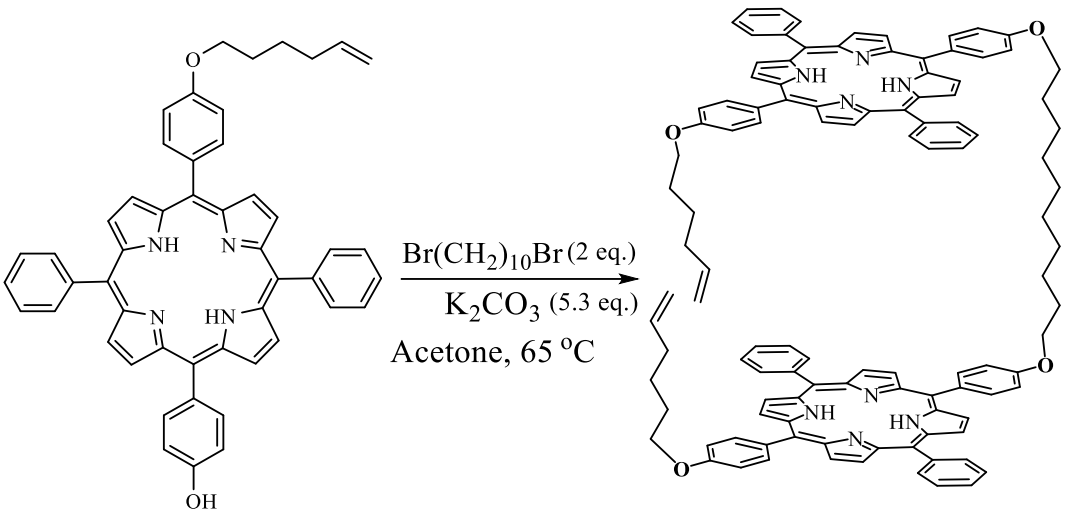

2.13 **2.14**

Scheme 61: Synthesis of porphyrin dyad **2.14**.

After 10 days, the crude precipitated during the reaction and the TLC showed one spot on the baseline which could not be eluted with any solvent system. Work-up to dispose of inorganic material failed as the crude was not soluble enough in the organic layer. Direct

filtration was also not successful because the precipitate adhered to the filter paper making it difficult to collect an adequate amount of the material. The collected material was obtained in very low yield (~10%) and was insoluble in common organic solvents including DMSO, preventing full characterisation.

The outcome of this reaction was unexpected compared to the previously prepared porphyrin dyad **2.57**, which was obtained in a good yield and high solubility. However, it has been observed in our group that some simple porphyrin dimers have low solubility when crystalline. Thus, this route was abandoned, and alternative synthetic pathways were explored due to the limited time available, and the low yield obtained from this dyad reaction.

2.13 Alternative pathway based on 5,15-di-(*p*-5-hexen-1-oxyphenyl) porphyrin 2.13a

After encountering difficulties in the purification and characterization of porphyrin dyad **2.14**, a new pathway for the preparation of *trans* TDs was explored. This route was designed to use *trans*-di-(*p*-5-hexen-1-oxyphenyl) porphyrin **2.13a** as a starting material which was previously obtained as a side product from mono-(*p*-5-hexen-1-oxyphenyl) porphyrin **2.13** reaction. With this in hand, it was to be directly used to react with phthalocyanine and lanthanum ions to form (unbridged) triple decker complex **2.61**. Followed by a metathesis reaction to give bridged triple decker **2.62** and then reduction of the obtained alkenes would afford the targeted complex **2.17**, as detailed in scheme 62.

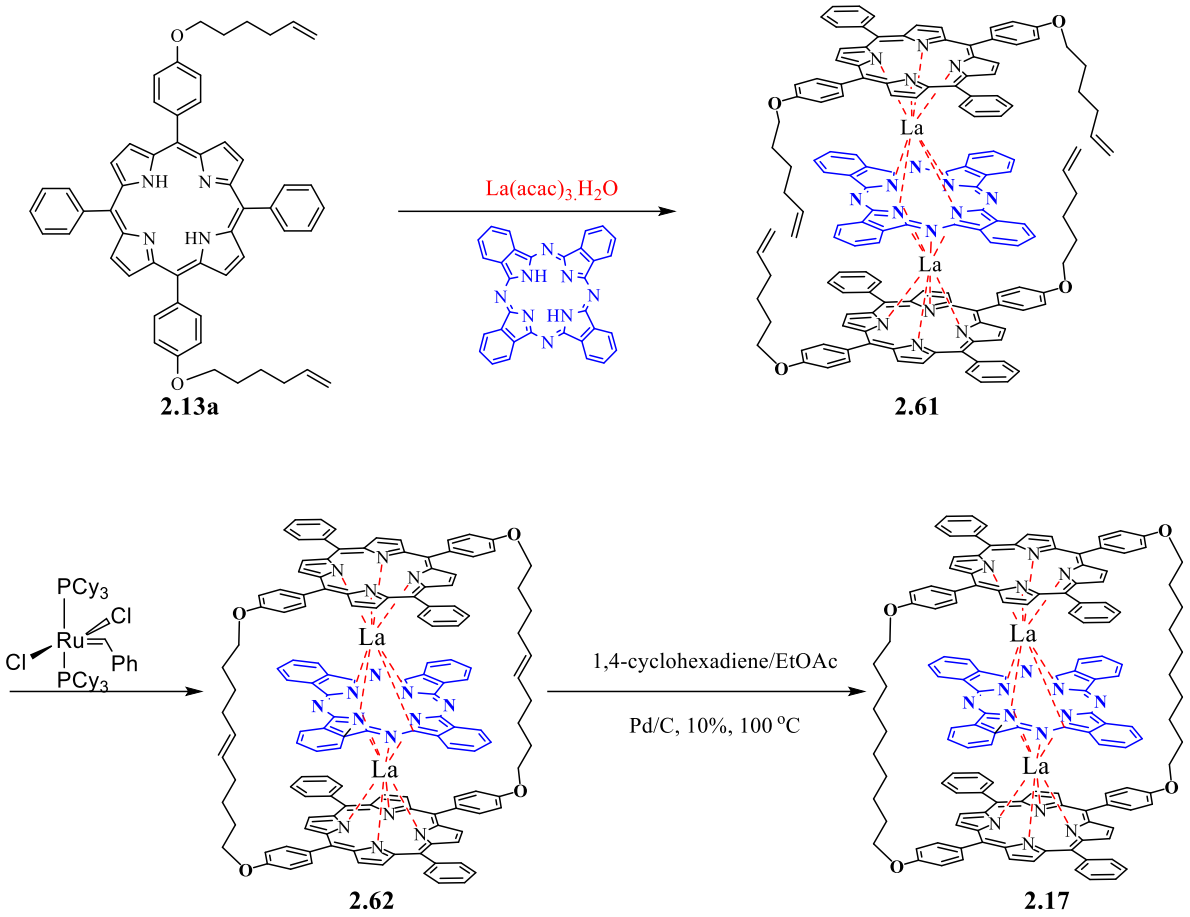

Scheme 62: Alternative synthetic pathway for the synthesis of triple decker complex **2.17** without clipping.

2.13.1 Synthesis of unbridged triple decker 2.61

The synthesis of the open triple decker was attempted following a modified procedure by our group. Thus, a mixture of porphyrin **2.13a** and Pc were refluxed in 1-pentanol for 24 h under N_2, followed by the addition of lanthanum acac.

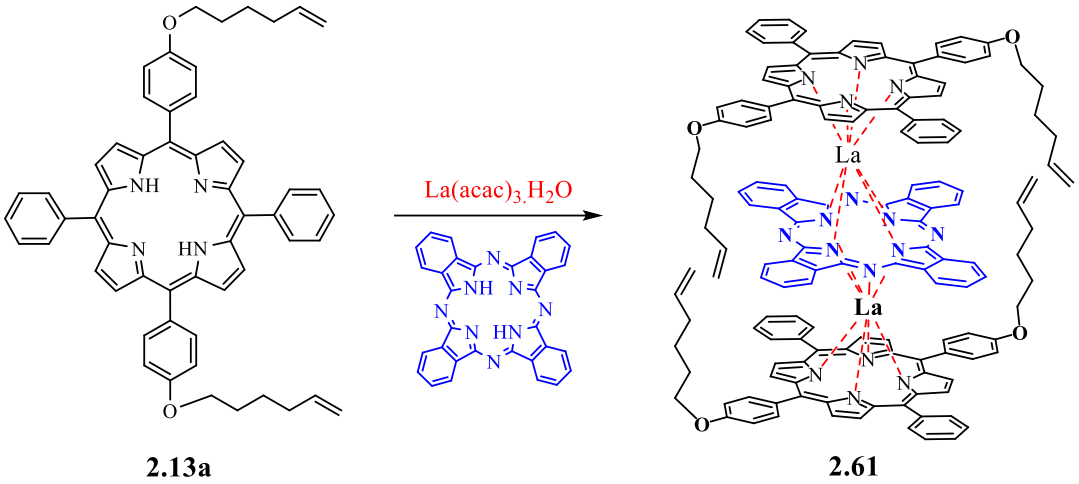

Scheme 63: Synthesis of unbridged TD **2.61**.

After 8 h, the formation of the desired product **2.61** was detected as a brown spot by TLC. The reaction was cooled to room temperature and the solvent removed to afford a dark solid which was dry loaded onto column chromatography with petroleum ether as initial mobile phase then DCM: Petroleum ether (3:1) as the eluent system. Although this solvent system showed reasonable separation on TLC, **2.61** was collected with traces of **2.13a**. This is because the porphyrin **2.13a** partially crystallized within the column dry loading process, impeding proper separation. However, when using (DCM: Petroleum ether 1:1) solvent system for wet column loading, a pure sample of **2.61** was collected. Crystallization from DCM:MeOH gave the desired product **2.61** in a 62% yield as brown crystals.

Identification of the product **2.61** was confirmed by MALDI-tof MS (Figure 37) and $^{1}H/^{13}C$ NMR spectroscopy. Its ^{1}H-NMR spectrum (Figure 38) shows the porphyrin β protons with a typical splitting pattern for *trans* configuration since it is symmetric. Signals at 8.40-8.32 ppm showed the overlapping of meta inner (unsubstituted phenyl) protons with Pc protons where the other signals were observed as expected. Moreover, the COSY spectrum reveals the correlations between the inner and outer protons of the aromatic substituents, confirming which protons are part of the substituted and unsubstituted phenyl rings (Figure 39).

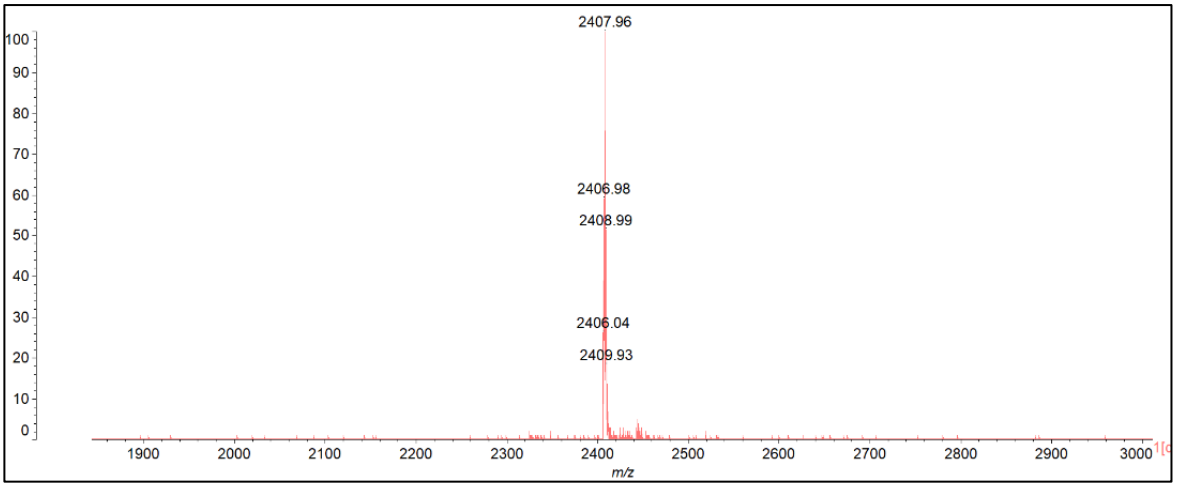

Figure 37: MALDI-tof MS confirms the formation of TD **2.61**.

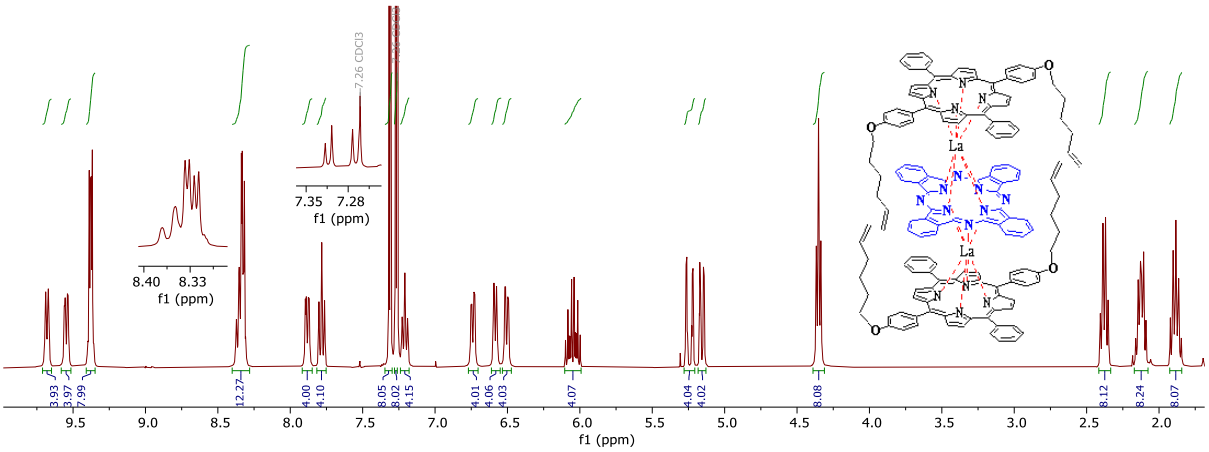

Figure 38: ^{1}H-NMR spectrum of unbridged TD **2.61**.

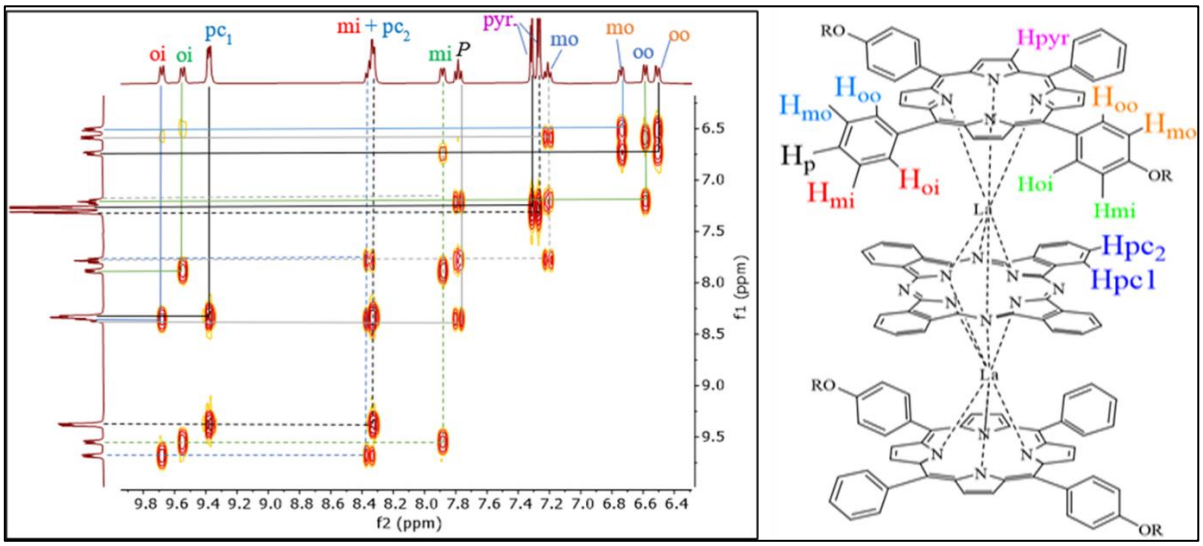

Figure 39: The aromatic region of the ^{1}H-^{1}H COSY spectrum of TD **2.61** in $CDCl_3$.

2.13.2 Cyclisation of triple decker 2.61

Cyclisation of triple decker complex **2.61** to form the cyclic triple decker **2.62** was achieved by metathesis reaction. This step aimed to enhance the structure's rigidity by introducing new linkers at the 5- and 15- positions of the *meso* porphyrins. Notably, this reaction differs from the previous reaction on the *cis* triple-decker **2.59**, which resulted in a mixture of the starting material **2.58a** and the desired product **2.59** (presumably one isomer of) (see section **2.11.3**). For this reaction, we anticipated that the presence of alkene chains in a *trans*-arrangement would facilitate a smooth cyclisation without the same complication (Scheme 64).

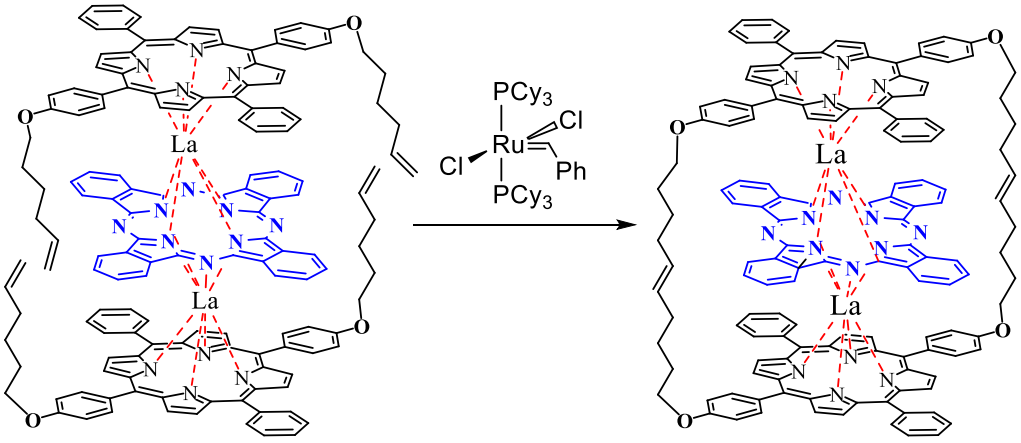

2.61 **2.62**

Scheme 64: Synthesis of **2.62**.

Practically, the open triple decker **2.61** was dissolved in dry DCM and stirred at room temperature under N_2. Separately, the 1st generation of Grubbs catalyst was dissolved in dry DCM and transferred to the mixture. The reaction was monitored by TLC and, after 6 h, was complete as confirmed by the MALDI-tof MS. The catalyst and solids were filtered off, and the solvent removed under high vacuum. After crystallisation (DCM: MeOH, 1:1), the pure cyclic triple decker **2.62** was obtained in an excellent 96% yield. The identity of **2.62** was confirmed by a combination of NMR spectroscopy and MALDI-tof MS (Figure 41). ^{1}H-NMR

spectroscopy revealed (presumably) a mixture of *cis*/*trans* isomers in the new double bonds (Figure 40).

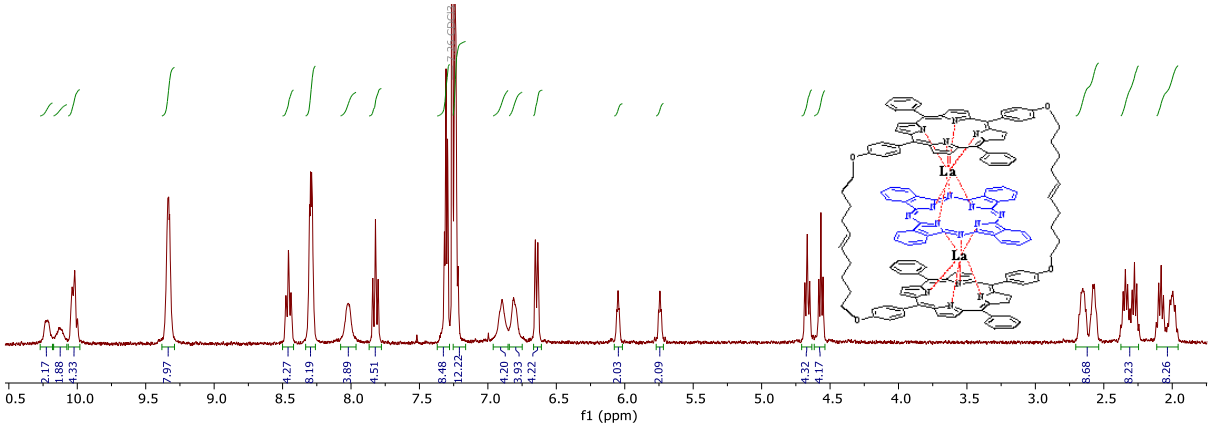

Figure 40: ^{1}H-NMR spectrum of linked triple decker **2.62**.

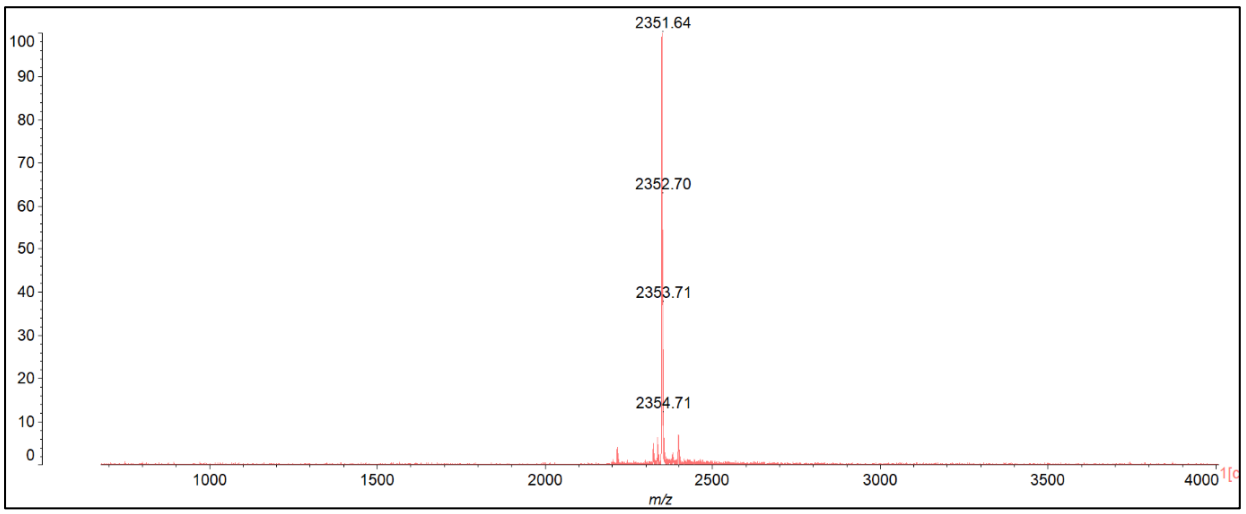

Figure 41: MALDI-tof MS of linked triple decker **2.62**.

2.13.3 Hydrogenation of *trans*-triple decker complex 2.62

The alkene bonds in the cyclic triple decker **2.62** were required to be reduced in order to increase the symmetry of the complex. Previously, we have successfully reduced the alkene bond on *cis* triple decker **2.59** using a reliable method by Felix *et al.*[106] This method had proven effective, selectively reducing the olefinic bonds without compromising the integrity of the complex structure or introducing unwanted side reactions.

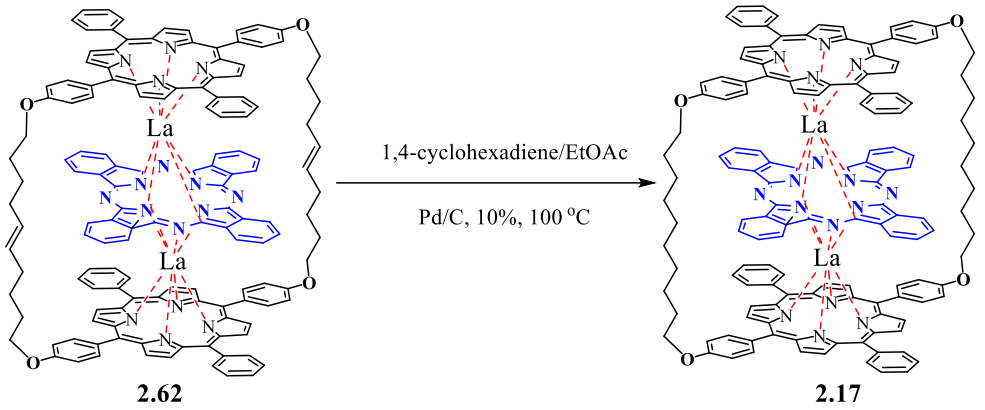

2.62 **2.17**

Scheme 65: Synthesis of symmetrical TD **2.17**.

The reduction reaction was monitored by ^{1}H-NMR spectroscopy. After 24 hours, ^{1}H NMR analysis indicated that the reduction was complete. Notably, the ^{1}H-NMR spectra revealed no evidence of side products, suggesting that the reduction proceeded with remarkable selectivity and efficiency. This was an encouraging outcome, as the absence of side products significantly simplifies the purification process and ensures the high purity of the final product **2.17**. The catalyst was filtered off, and the solvents evaporated, resulting in the isolation of pure **2.17** in an 86% yield after crystallisation.

The identity of the desired product **2.17** was confirmed by ^{1}H-NMR spectroscopy, comparing with the previous *cis* TD **2.60**. They show close similarity, with the main difference being in the porphyrin β protons. As anticipated based on their distinct regiochemistry, in **2.17** the porphyrin β protons show a typical *trans* splitting pattern, whereas in **2.60**, it exhibited a typical *cis* splitting pattern as can be seen in the figure 42.

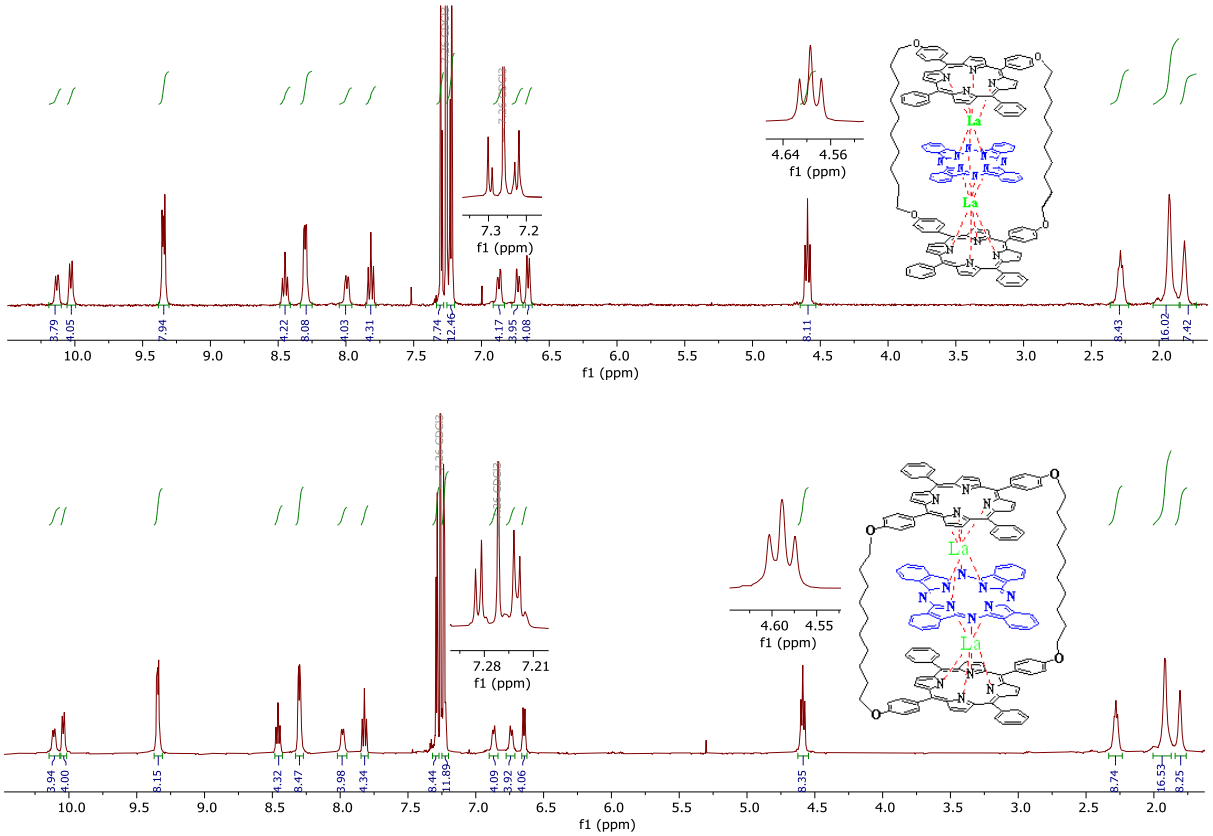

Figure 42: ^{1}H-NMR spectral comparison obtained for **2.60** and **2.17**.

Additionally, the identity of TD **2.17** was confirmed by MALDI-tof mass spectrometry, which indicated a single cluster at *m/z* 2355.47 corresponding to the molecular ion of the complex (Figure 43).

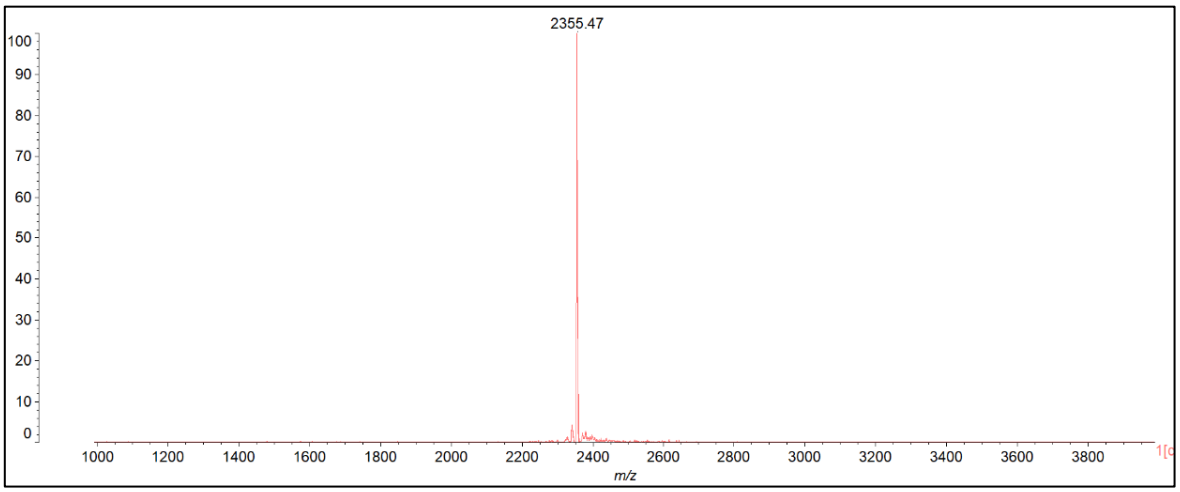

Figure 43: MALDI-tof MS of linked/cyclic triple decker **2.17**.

Finally, further confirmation of the formation of triple decker complex **2.17** was obtained through X-ray crystallography which was compared with the previously obtained *cis* complex **2.60**. Their crystallography results, performed and analysed by UEA collaborator Dr David Hughes, are subtley different (Figure 44). The *trans* complex **2.17** shows porphyrin rings are slightly tilted, giving them an umbrella-like shape while the phthalocyanine is planar. In the *cis* complex **2.60**, the phthalocyanine group appears slightly saddle-shaped, with isoindole groups tilted alternately (by about 5.53°) to one side and the other (Figure 44).

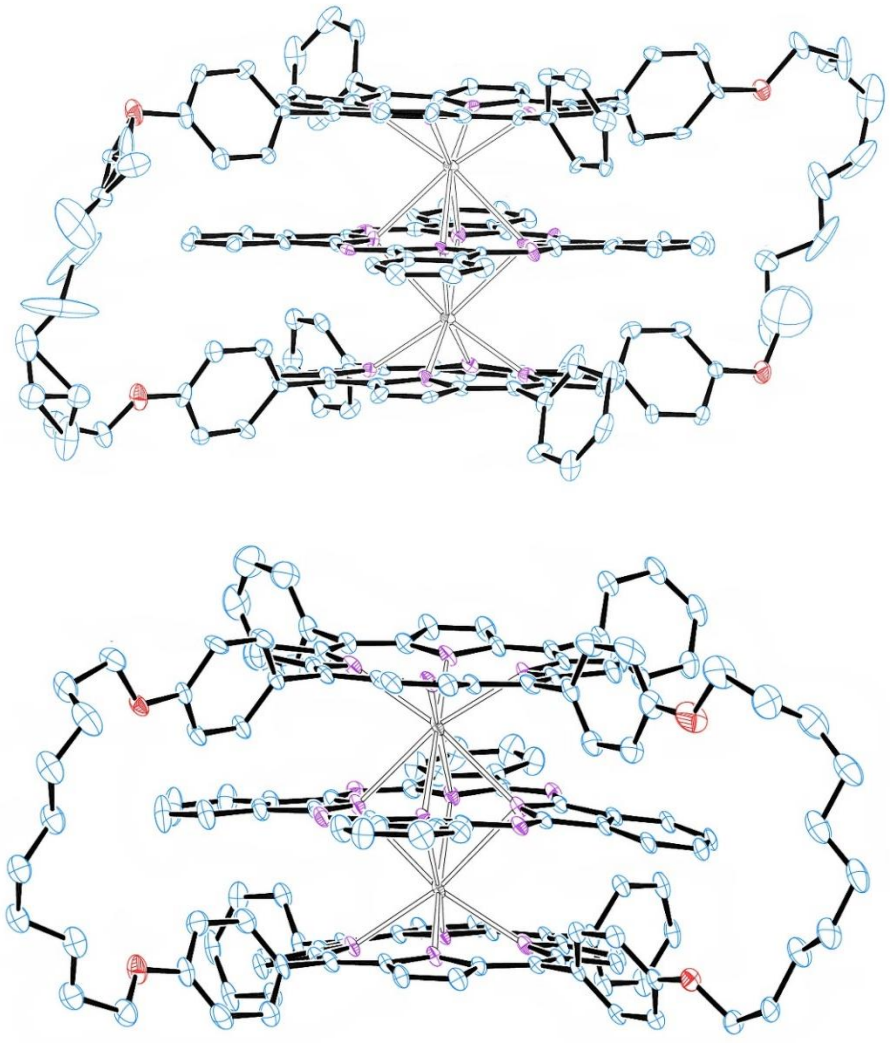

Figure 44: X-ray structures of triple decker complexes **2.17** and **2.60.**

2.13.4 Removal of metal ions

The ultimate goal of the long-term project is to design a strategy that could be applied to strap the bridged porphyrin around a complementary macrocycle (like a Pc) that is itself part of a larger system such that removal of the metals gives a rotaxane or catenane. The successful formation of complex **2.17** allowed the initial investigation on demetallation and see whether the porphyrins remained stable to the demethylation conditions (expected) and whether the unsubstituted Pc could be trapped within the cyclic porphyrin dimer (not expected for this model system). A test reaction aimed at removing the lanthanum ions from complex **2.17** was attempted using TFA (Scheme 66).

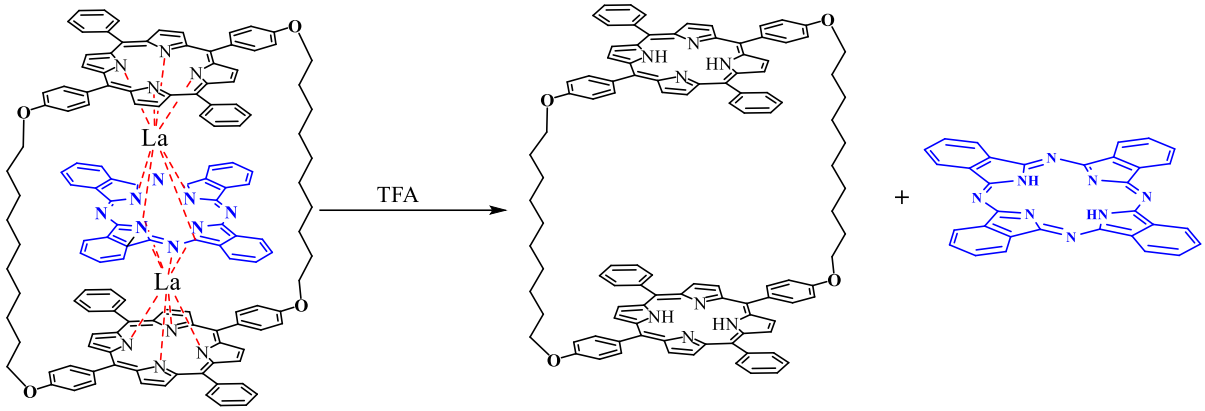

2.17 **2.63**

Scheme 66: Removal of lanthanum ions from **2.17**.

Cyclic triple-decker **2.17** was dissolved in DCM and stirred at room temperature for 5 minutes. A few drops of TFA were added to the mixture which turned green. After 5 minutes, the reaction was neutralised with potassium carbonate and TLC analysis revealed three different spots indicating the removal of lanthanum ions along with Pc and the starting material **2.17** as confirmed by MALDI-tof MS (Figure 45). As expected, the MALDI-tof MS showed no evidence of Pc being trapped within the cyclic demetallated porphyrin dimer **2.63**. The

absence of substituents acting as molecular 'stoppers' in Pc allows it to escape from the cyclic structure.

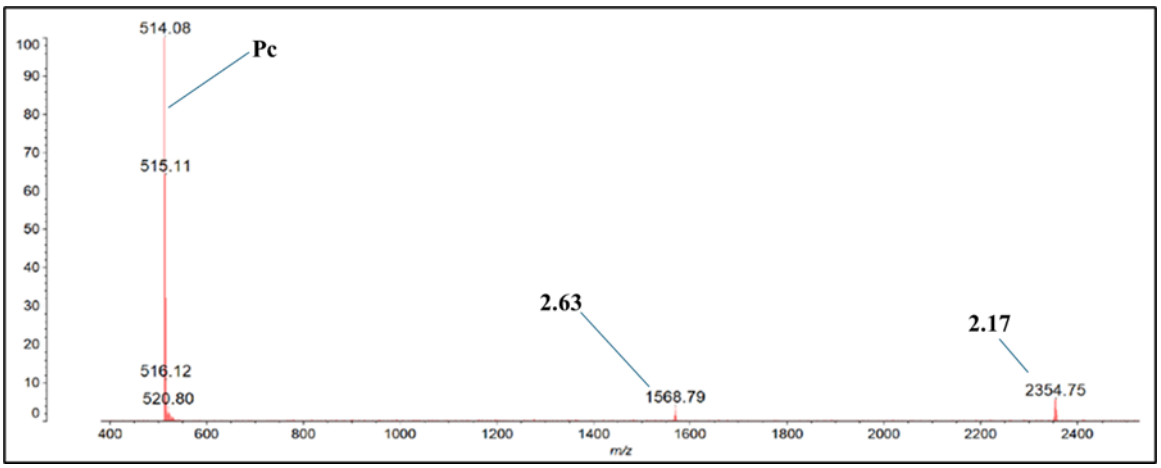

Figure 45: MALDI-tof MS obtained for the removal of lanthanum ions from **2.17** after 5 minutes.

Conclusion and future work

Many challenges were encountered in the synthesis of *trans* porphyrins as building blocks for the project (where a major part of the project's time was committed). Although the synthesis was explored with a wide variety of substituents, including electron-poor and electron-rich aromatics and bulky groups in various positions like 3,5-dimethylbenzaldehyde and 4-*tert*-butylbenzaldehyde, scrambling of these substituents still occurred in most cases. The only exceptions were the pentafluorophenyl- and mesityl porphyrins which were successfully obtained without scrambling but found to be not suitable for the formation of the triple decker complexes. The synthetic strategy was redesigned several times, and the target *trans* porphyrin was obtained through a statistical method, followed by demethylation, to successfully purify it from the *cis* isomer.

However, within the project's later stages, a successful development was made to overcome the scrambling issue by introducing temporary blocking groups (bromides) resulting

in *trans* porphyrin without scrambling. The removal of these groups in *trans*-porphyrin **2.54** and **2.55** resulted in the formation of porphyrin **2.44**. Consequently, this strategy is highly promising for the synthesis of *trans*-porphyrins.[107]

cis-TPP(OH)$_2$ ***cis*-2.12d** emerged as a side product that was not initially targeted in the project. Its high yield and similarity to *trans*-TPP(OH)$_2$ ***trans*-2.12d** made it useful for examining reaction conditions before using *trans*-TPP(OH)$_2$ because of the latter's low yield and the difficulties in its preparation. Successful formation of triple decker complex **2.60** based on linked *cis*-porphyrins was proven by extensive analytical tools, including NMR, MALDI-tof, UV and unambiguously through X-ray crystallography.

The original plan for building the triple decker complex **2.17** through a clipping strategy was complicated and hampered due to the low yield and very low solubility of the intermediate porphyrin dyad **2.14**. An uncontrolled strategy proved to be more efficient. This approach successfully yielded the open triple decker **2.61** in a good yield which was subsequently linked from two sides using a metathesis reaction. The X-ray crystallography confirmed the formation of the final triple decker **2.17** after the alkene reduction reaction. Finally, the removal of lanthanum metals from **2.17** was successful but resulted in the removal of the phthalocyanine as expected. This can be overcome in the future work by exploring the introduction of new phthalocyanine derivatives bearing bulky groups to prevent it escaping after metal removal, potentially resulting in a rotaxane structure.

Experimental Section

Materials and Instrumentation

All starting materials were commercially available and utilized as received unless otherwise stated. Most reaction and distillation steps were performed under N_2 atmosphere and for reactions that were sensitive to air, argon was utilized. To dry organic layers from any remaining water, anhydrous magnesium sulphate was used. Solvents were evaporated using a Buchi rotary evaporator at low pressure. All reactions were investigated using thin layer chromatography (TLC) aluminium sheets coated with silica gel/UV254 and the products were visualized using UV light. For column chromatography, silica gel ((Material Harvest or Merck, particle size 40-63 microns) was employed. All NMR spectra were acquired utilizing a Bruker DPX-400 MHz or Bruker DPX-500 MHz spectrometers, using 5 mm diameter tubes. For ^{13}C NMR, the frequencies used were 101 MHz and 126 MHz. The chemical shifts of signals are reported in ppm as δ downfield from tetramethylsilane (δ = 0.00), whereas coupling constants *J* are quoted in Hertz. The spectra were recorded at room temperature using deuterated chloroform and dichloromethane unless otherwise stated. The IR spectra were obtained using a Perkin-Elmer Spectrum 100 FT-IR spectrometer, and the absorption bands are reported in wavenumbers (cm^{-1}). UV-VIS spectra were recorded using a Perkin Elmer Lamda 35 UV/VIS instrument, specifically in the mentioned solvents. MALDI-tof analyses were conducted using a Shimadzu Biotech Axima Spectrometer. Melting points were measured using a Reichert Thermovar microscope equipped with a thermometer-based temperature control system.

5-Pentafluorophenyldipyrromethane 2.20[108]

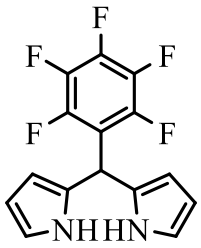

A mixture of pentafluorobenzaldehyde **2.19** (2.82 g, 1.78 mL, 14.4 mmol) and freshly distilled pyrrole (24.1 g, 25 mL, 360 mmol) were degassed by bubbling Ar through it for 30 min. Trifluoroacetic acid (0.11 mL, 0.10 eq.) was added and the solution subsequently stirred under Ar at room temperature for 5 min. NaOH (0.1 M, 250 mL) was used to quench the reaction and then ethyl acetate was added. The organic phase was isolated, washed with water, and then dried over Na_2SO_4. The solvent was removed, and any unreacted pyrrole was further removed under vacuum at 60 °C. The resulting green oil was crystallized using ethanol to yield colourless crystals (0.82 g, 18%). ^{1}H-NMR (400 MHz, $CDCl_3$) δ 8.14 (br-s, 2H), 6.74 (m, 2H), 6.17 – 6.14 (m, 2H), 6.02 (m, 2H), 5.90 (s, 1H). ^{19}F NMR (376 MHz, $CDCl_3$) δ -141.47 (d, J = 21.9 Hz), -155.72 (t, J = 21.0 Hz), -161.19 (td, J = 22.2, 7.9 Hz).

5,15-Bis-(4-methoxyphenyl)-10,20-bis-(pentafluorophenyl)porphyrin 2.23[109]

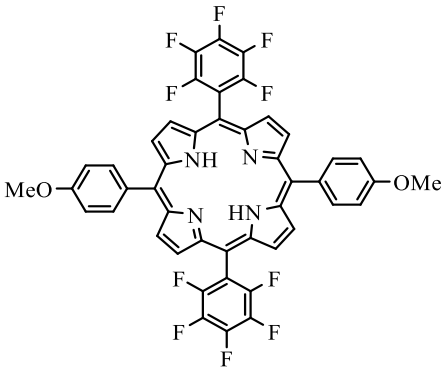

A mixture of pentafluorophenyldipyrromethane **2.20** (0.23 g, 0.74 mmol) and 4-methoxybenzaldehyde **2.22** (0.1 g, 0.74 mmol) were dissolved in dry DCM (50 mL) and stirred

at room temperature. To the mixture, TFA (0.006 mL, 0.1 eq) was added, and the solution was stirred for 20 h. DDQ (0.16 g, 0.70 mmol) was added, and the mixture was stirred for a further 45 min to oxidize porphyrinogen to porphyrin. A few drops of TEA were needed. Then column chromatography was used to isolate the desired product from the black materials using DCM/Pet ether (1:1) as the eluent. The solvent was evaporated, and the resulting purple solid recrystallized from DCM/MeOH to obtain bright purple crystals of **2.23** (0.04 g, 13%). ^{1}H-NMR (400 MHz, $CDCl_3$) δ 8.90 (d, *J* = 4.9 Hz, 4H), 8.71 (d, *J* = 4.9 Hz, 4H), 8.05 (d, *J* = 9.2 Hz, 4H), 7.24 (d, *J* = 9.2 Hz, 4H), 4.04 (s, 6H), -2.89 (s, 2H). ^{19}F NMR (376 MHz, $CDCl_3$) δ -136.80 (dd, *J* = 24.3, 8.7 Hz), -152.48 (t, *J* = 20.6 Hz), -162.10 (td, *J* = 23.9, 8.2 Hz). MALDI-tof MS $(C_{46}H_{24}F_{10}N_4O_2)^+$ *m/z* $[M+]^+$ calcd: 854.17 found: 854.30.

5,15-Bis-(4-hydroxyphenyl)-10,20-bis-(pentafluorophenyl)porphyrin 2.12a[110]

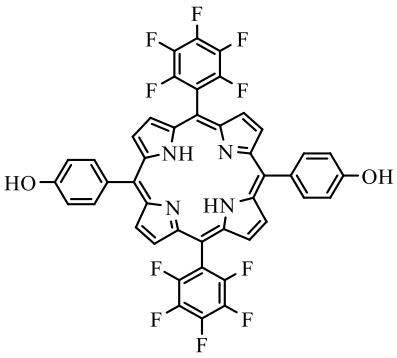

The *trans*-5,15-bis(4-methoxyphenyl)-10,20-bis(pentafluorophenyl)porphyrin **2.23** (0.05 g, 0.058 mmol) and dissolved in 8 mL of DCM under Ar atmosphere. The solution was cooled at -78 ºC and boron tribromide (0.234 mL, 1 M solution in anhydrous CH_2Cl_2, 0.234 mmol) was added slowly. The reaction mixture was allowed to warm to room temperature and stirring continued for 48 h. The mixture was then quenched with ice water, after which it was extracted with DCM and dried over Na_2SO_4. After crystallization from DCM/MeOH, *trans* porphyrin **2.12a** was collected as a purple solid (0.04g 83%). ^{1}H-NMR (400 MHz, $CDCl_3$) δ 8.98 (d, *J* = 4.8 Hz, 4H), 8.79 (d, *J* = 4.8 Hz, 4H), 8.08 (d, *J* = 7.8 Hz, 4H), 7.24 (d, *J* = 7.8 Hz, 4H), 5.24

(s, 2H), -2.83 (s, 2H). ^{19}F NMR (376 MHz, $CDCl_3$) δ -136.75 – -136.90 (m), -152.48 (t, J = 20.7 Hz), -162.06 (td, J = 31.3, 13.7 Hz).

5,10,15,20-Tetra-(pentafluorophenyl) porphyrin 2.24[98],[91]

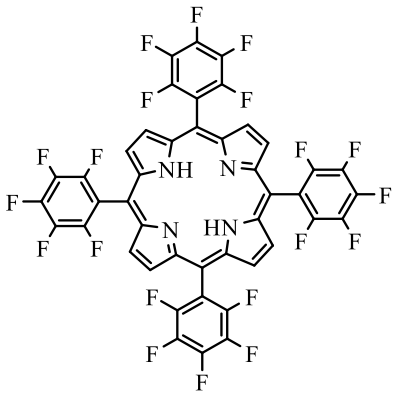

A mixture of 2,3,4,5,6-pentafluorobenzaldehyde **2.19** (0.784 g, 4 mmol) and distilled pyrrole (0.268 g, 4 mmol) were dissolved in dry DCM (300 mL) and stirred under N_2 at room temperature. To the mixture, TFA (0.03 mL, 0.1 eq.) was added dropwise, and the solution stirred for 5 h. After which DDQ (0.908 g, 4 mmol) was added, and the reaction mixture was refluxed and stirred for a further 2 h. Then, the solvent was removed, and the crude purified by column chromatography using DCM/Pet ether (1:5) as the eluent. The product was a purple solid which was recrystallized from DCM/MeOH to obtain bright purple crystals **2.24** (0.20 g, 20%). ^{1}H-NMR (400 MHz, $CDCl_3$) δ 8.92 (s, 8H), -2.91 (s, 2H). MALDI-tof MS $(C_{44}H_{10}F_{20}N_4)^+$ *m/z* $[M]^+$ calcd: 974.05 found: 974.08.

Phthalocyanine [92]

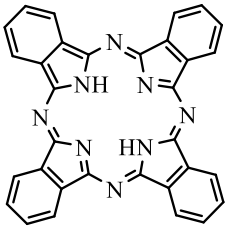

Phthalonitrile (0.5 g, 3.90 mmol) was stirred in refluxing 1-pentanol (10 mL) for 1 h, then lithium (0.05 g, 7.2 mmol) was added to the solution and left for further 1 h. Acetic acid was added (10 mL) and refluxed for 1h. After cooling down, MeOH was added to precipitate the phthalocyanine which was collected as a blue solid (0.2 g, 40 %). UV-vis, λ_{max} (THF/nm (rel. int.)): 336 (0.366); 658 (0.599), 690 (0.547). MALDI-tof MS $(C_{32}H_{18}N_8)^+$ *m/z* $[M]^+$ calcd: 514.17 found: 514.57.

5,10,15,20-Tetra-(mesitylphenyl)porphyrin 2.27[93]

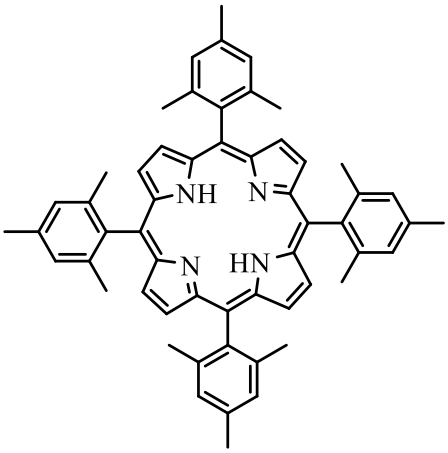

A mixture of mesitaldehyde **2.26** (0.74 g, 5.06 mmol) and pyrrole (0.33 g, 5.06 mmol) were dissolved in dry DCM (500 mL). BF_3•OEt_2 (1.30 mL, 1.25 M solution in anhydrous CH_2Cl_2, 1.63 mmol) was added. The reaction was left to stir for 1h in the dark at room temperature. DDQ (0.90 g, 3.96 mmol) was added, and the mixture stirred at RT for a further 20 min. After the addition of a few drops of Et_3N, the solvent was removed by rotary evaporation. The crude product was purified by column chromatography using hexane/DCM (1:1) as the eluent to yield

5,10,15,20-tetra(mesitylphenyl)porphyrin **2.27** as a purple solid (105 mg, 11%). ^{1}H-NMR (400 MHz, $CDCl_3$) δ 8.61 (s, 8H), 7.27 (s, 8H), 2.62 (s, 12H), 1.85 (s, 24H), -2.51 (s, 2H). MALDI-tof MS $(C_{56}H_{54}N_4)^+$ *m/z* $[M+]^+$ calcd: 782.43 found: 782.21.

5,10,15,20-Tetra-(4-*tert*-butylphenyl)porphyrin 2.29[111]

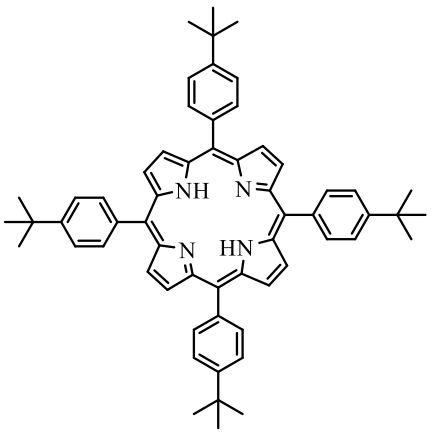

4-*tert*-Butylbenzaldehyde **2.28** (2.33 g, 14.4 mmol) was dissolved and heated at reflux in propionic acid (40 mL). After the mixture started refluxing, distilled pyrrole (1 g, 14.4 mmol) was added dropwise and left to reflux for a further 30 min. After cooling to ambient temperature, methanol (100 mL) was added to the mixture and left in fridge to precipitate overnight. The purple solids were collected by suction filtration and recrystalized from DCM/MeOH affording pure 5,10,15,20-tetra(4-*tert*-butylphenyl)porphyrin **2.29** (0.350 g, 12 %).^{1}H-NMR (400 MHz, $CDCl_3$) δ 8.87 (s, 8H), 8.15 (d, J = 8.3 Hz, 8H), 7.76 (d, J = 8.3 Hz, 8H), 1.61 (s, 36H), -2.74 (s, 2H). UV-vis, λmax (DCM)/nm 420 (0.905); 520 (0.032), 556 (0.018), 597 (0.009), 652 (0.011). MALDI-tof MS $(C_{60}H_{62}N_4)^+$ *m/z* $[M+]^+$ calcd: 838.50 found: 838.30.

5,10,15,20-Tetra-(3,5-dimethylphenyl)porphyrin 2.31[112]

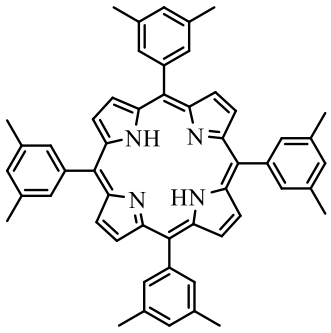

3,5-Dimethylbenzaldehyde **2.30** (2 g, 14.4 mmol) was dissolved and heated at reflux in propionic acid (40 mL). After the mixture started refluxing, distilled pyrrole (1 g, 14.4 mmol) was added dropwise and left to reflux for a further 30 min. After cooling down to ambient temperature, methanol (100 mL) was added to the mixture and left in fridge to precipitate overnight. The purple solids were collected by suction filtration and recrystalized from DCM/MeOH to afford pure **2.31** as purple solid (0.250 g, 10 %).^{1}H-NMR (400 MHz, $CDCl_3$) δ 8.86 (s, 8H), 7.83 (s, 8H), 7.40 (s, 4H), 2.58 (s, 24H), -2.79 (s, 2H). MALDI-tof MS $(C_{52}H_{46}N_4)^+$ *m/z* $[M+]^+$ calcd: 726.37 found: 726.30.

Open Triple decker 2.33

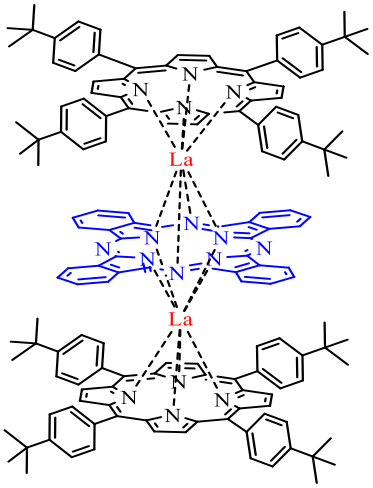

Following a modified version of Cammidge's general procedure,[87] a mixture of 5,10,15,20-tetra(4-*tert*-butylphenyl)porphyrin **2.29** (0.05 g, 0.059 mmol), phthalocyanine (0.015 g, 0.029

mmol) and lanthanum(III) acetylacetonate hydrate (0.051 g, 0.118 mmol) were dissolved in 1-octanol (5 mL) and heated to reflux at 200 °C for 24 h in a sealed tube. The solvent was removed under high vacuum and the resulting solid was purified by column chromatography. The desired compound **2.33** was isolated in the second fraction as dark brown crystals (10 mg, 13%). MP > 350 °C. ^{1}H-NMR (400 MHz, $CDCl_3$) δ 9.44 (dd, *J* = 5.5, 2.9 Hz, 8H), 8.62 (d, *J* = 7.8 Hz, 8H), 8.42 (dd, *J* = 5.5, 2.9 Hz, 8H), 8.05 (d, *J* = 7.8 Hz, 8H), 7.38 (s, 16H), 7.10 (d, *J* = 7.8 Hz, 8H), 6.34 (d, *J* = 7.8 Hz, 8H), 1.64 (s, 72H). ^{13}C-NMR (101 MHz, $CDCl_3$) δ 153.67, 149.45, 148.04, 139.72, 137.00, 133.90, 132.79, 129.96, 128.83, 124.17, 122.29, 120.56, 77.34, 77.02, 76.70, 34.79, 31.81. UV-vis, λ_{max} (DCM)/nm (log ε): 364 (4.85), 422 (5.29), 490 (4.26), 555 (4.11), 612 (4.03), 885 (3.70). IR (KBr, cm^{-1}): 2954, 2829, 2863, 1514, 1462, 1361, 1326, 1266, 1197, 1107, 1066, 985, 880, 851, 808, 795. MALDI-tof MS $(C_{152}H_{136}La_2N_{16})^+$ *m/z* [M+] $^+$ calcd: 2463.93 found: 2463.63.

Open Triple decker 2.34

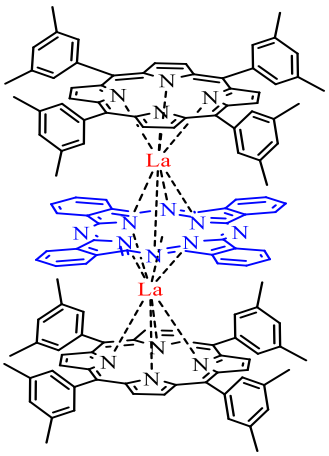

Following a modified version of Cammidge's general procedure,[87] a mixture of 5,10,15,20-tetra(3,5-dimethylphenyl)porphyrin **2.31** (0.05 g, 0.068 mmol), phthalocyanine (0.017 g, 0.034 mmol) and lanthanum (III) acetylacetonate hydrate (0.059 g, 0.136 mmol) were dissolved in 1-octanol (5 mL) and heated to reflux at 200 °C for 24 h in a sealed tube. The solvent was removed under high vacuum and the resulting solid was purified by column chromatography. A desired

product **2.34** was collected in the second fraction as a brown crystal (9 mg, 11 %). MP > 350 ^{o}C. ^{1}H-NMR (400 MHz, $CDCl_3$) δ 9.55 (s, 8H), 9.44 (dd, *J* = 5.4, 3.0 Hz, 8H), 8.32 (dd, *J* = 5.4, 3.0 Hz, 8H), 7.38 (s, 8H), 7.26 (s, 16H), 6.09 (s, 8H), 3.49 (s, 24H), 2.06 (s, 24H). ^{13}C-NMR (101 MHz, $CDCl_3$) δ 147.93, 143.36, 136.93, 134.80, 131.22, 128.52, 123.18, 77.33, 77.22, 77.01, 76.70, 41.35, 22.63, 20.45, 19.44, 14.33. UV-vis, λ_{max} (DCM)/nm (log ε): 363 (4.81), 421 (5.23), 490 (4.17), 553 (4.04), 610 (3.96), 885 (3.63). IR (KBr, cm $^{-1}$): 2918, 2852, 1598, 1330, 1059, 927, 857, 814, 794, 728. MALDI-tof MS $(C_{136}H_{104}La_2N_{16})^+$ *m/z* $[M+]^+$ calcd: 2239.67 found: 2239.60.

5-(4-*tert*-Butylphenyl)dipyrromethane 2.35[108]

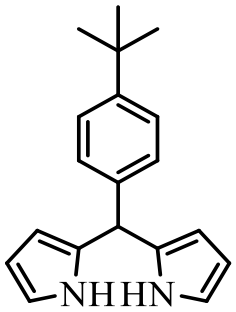

A mixture of 4-*tert*-butylbenzaldehyde **2.28** (1.46 g, 9 mmol) and freshly distilled pyrrole (15 g, 224 mmol) were degassed by bubbling argon through them for 30 min. Trifluoroacetic acid (0.07 mL, 0.10 eq.) was added and the solution stirred under Ar at room temperature for 5 min. NaOH (0.1 M, 250 mL) was used to quench the reaction and then ethyl acetate was added. The organic phase was isolated, washed with water, and then dried over Na_2SO_4. The solvent was removed, and any unreacted pyrrole was further removed under vacuum at 60 ^{o}C. The resulting oil was purified by column chromatography (1:1) DCM/Pet. ether and the resulting solid was recrystalized from hexane to yield colourless crystals (1.12 g, 45%).^{1}H-NMR (400 MHz, $CDCl_3$) δ 7.92 (br-s, 2H), 7.33 (d, *J* = 8.4 Hz, 2H), 7.15 (d, *J* = 8.4 Hz, 2H), 6.69 (d, *J* = 1.6 Hz, 2H), 6.16 – 6.14 (m, 2H), 5.94 (m,2H), 5.46 (s, 1H), 1.31 (s, 9H).

5-(3,5-Dimethylphenyl)dipyrromethane 2.38

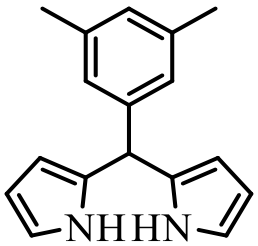

A mixture of 3,5-dimethylbenzaldehyde **2.30** (1.2 g, 9 mmol) and freshly distilled pyrrole (15 g, 224 mmol) were degassed by bubbling argon through them for 30 min. Trifluoroacetic acid (0.07 mL, 0.10 eq.) was added and the solution stirred under Ar at room temperature for 5 min. NaOH (0.1 M, 250 mL) was used to quench the reaction and then ethyl acetate was added. The organic phase was isolated, washed with water, and then dried over Na_2SO_4. The solvent was removed, and any unreacted pyrrole was further removed under vacuum at 60 ^oC. The resulting oil was then purified by column chromatography (1:1) DCM/Pet. ether and the resulting solid was recrystalized from hexane to yield colourless crystals (0.96 g, 43 %) ^{1}H-NMR (400 MHz, $CDCl_3$) δ 7.91 (br-s, 2H), 6.90 (s, 1H), 6.85 (s, 2H), 6.69 (td, J = 2.7, 1.6 Hz, 2H), 6.18 – 6.14 (m, 2H), 5.97-5.90 (m, 2H), 5.40 (s, 1H), 2.28 (s, 6H).

5-Phenyldipyrromethane 2.43[108]

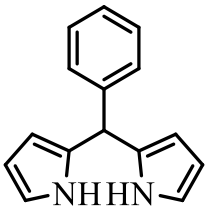

A mixture of benzaldehyde (1.53 g, 1.5 mL, 14.4 mmol) and freshly distilled pyrrole (24.1 g, 25 mL, 360 mmol) were degassed by bubbling argon through them for 30 min. Trifluoroacetic acid (0.11 mL, 0.10 eq.) was added and the solution stirred under Ar at room temperature for 5 min. NaOH (0.1 M, 250 mL) was used to quench the reaction and then ethyl acetate was added. The organic phase was isolated, washed with water, and then dried over Na_2SO_4. The

solvent was removed, and any unreacted pyrrole was further removed under vacuum at 60 ºC. The resulting brown oil was purified using chromatography DCM/Pet. ether (1:1) to give pure crystals of **2.43** (2.25 g, 70%). ^{1}H-NMR (400 MHz, $CDCl_3$) δ 7.94 (br-s, 2H), 7.32 – 7.22 (m, 5H), 6.70 (d, *J* = 2.6, Hz, 2H), 6.16 – 6.14 (m, 2H),5.92 (m, 2H), 5.48 (s, 1H).

5-(4-Methoxyphenyl)dipyrromethane 2.37[108]

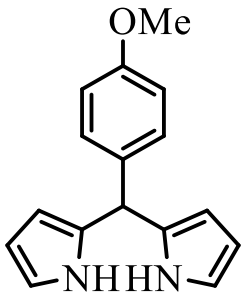

A mixture of 4-methoxybenzaldehyde **2.22** (1.96 g, 1.75 mL, 14.4 mmol) and freshly distilled pyrrole (24.1 g, 25 mL, 360 mmol) were degassed by bubbling argon through them for 30 min. Trifluoroacetic acid (0.11 mL, 0.10 eq.) was added and the solution stirring continued under Ar at room temperature for 5 min. NaOH (0.1 M, 250 mL) was used to quench the reaction and then ethyl acetate was added. The organic phase was isolated, washed with water, and then dried over Na_2SO_4. The solvent and unreacted pyrrole were further removed under vacuum at 60 ºC. The resulting oil was then purified by column chromatography using DCM/Pet. ether (1.5:1) and the resulting solid was recrystalized from ethyl acetate/hexane to yield the product **2.37** as colourless crystals (2.23g, 61%) ^{1}H-NMR (400 MHz, $CDCl_3$) δ 7.90 (br s, 2H), 7.14 (d, *J* = 8.5, 2H), 6.86 (d, *J* = 8.5, 2H,), 6.70 (ddd, *J* = 2.9, 2.7, 1.6 Hz, 2H), 6.17 – 6.14 (m, 2H), 5.93-5.90 (m, 2H), 5.44 (s, 1H), 3.80 (s, 3H).

5-(4-Benzyloxyphenyl)dipyrromethane 2.41

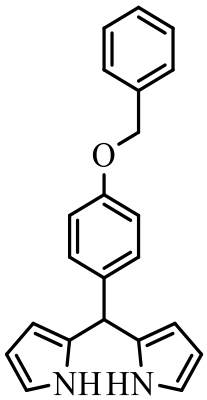

A mixture of 4-benzyloxybenzaldehyde **2.40** (1.9 g, 9 mmol) and freshly distilled pyrrole (15 g, 224 mmol) were degassed by bubbling argon through them for 30 min. Trifluoroacetic acid (0.07 mL, 0.10 eq.) was added and the solution stirred under Ar at room temperature for 5 min. NaOH (0.1 M, 250 mL) was used to quench the reaction and then ethyl acetate was added. The organic phase was isolated, washed with water, and then dried over Na_2SO_4. The solvent was removed, and any unreacted pyrrole was further removed under vacuum at 60 ^oC. The resulting oil was then purified by column chromatography DCM/Pet. ether (1:1) and the resulting solid was recrystalized from hexane to yield colourless crystals (1.61 g, 55%). MP : 115 ^oC; ^{1}H-NMR (400 MHz, $CDCl_3$) δ 7.91 (br-s, 2H), 7.47-7.29 (m, 5H), 7.14 (d, J = 8.6 Hz, 2H), 6.93 (d, J = 8.6 Hz, 2H), 6.69 (d, J = 2.2 Hz, 2H), 6.16 – 6.14 (m, 2H), 5.92 (s, 2H), 5.44 (s, 1H), 5.06 (s, 2H). ^{13}C-NMR (101 MHz, $CDCl_3$) δ 137.60, 135.17, 132.81, 129.44, 128.61, 127.51, 118.07, 117.12, 115.50, 108.44, 108.20, 107.07, 70.09, 43.28. MALDI-tof MS $(C_{22}H_{20}N_2O)^+$ *m/z* $[M+]^+$ calcd: 328.16 found: 328.01.

5,15-(4-Methoxyphenyl) -10,20-diphenylporphyrin 2.44

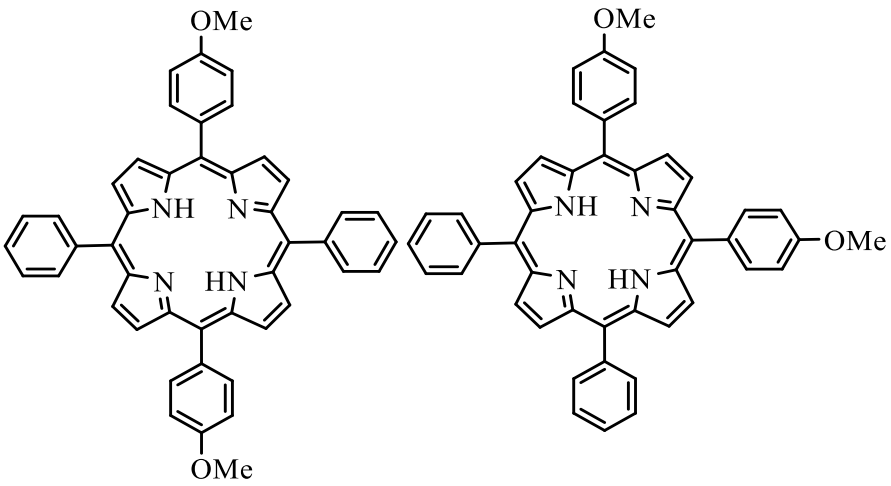

Method A:

4-Methoxydipyrromethane **2.22** (2.52 g, 10 mmol) and benzaldehyde (1.06 g, 10 mmol) were dissolved in dry DCM (1000 mL) and the reaction mixture was stirred under Ar. TFA (1.37 mL, 17.8 mmol) was added slowly at room temperature. After 1.5h, DDQ (2.27 g, 10 mmol) was added, and the mixture stirred for 60 min. The crude was poured onto an alumina pad and eluented with DCM. The solvent was removed to give a dark solid which was redissolved in toluene in the presence of DDQ and heated to reflux for a further 1 h to remove any remaining porphyrinogen. After cooling to room temperature, the solvent was removed, and column chromatography was used to isolate the desired product from the black materials by using DCM/Pet. ether (2:1) as the eluent. The third fraction was collected as a mixture of *trans* and *cis* isomers porphyrin (~1:2) (0.4 g, 12%).

Method B:

Following the Adler procedure,[112] 4-methoxybenzaldehyde **2.22** (6.8 g, 50 mmol) and benzaldehyde (5.3 g, 50 mmol) were dissolved and heated at reflux in propionic acid (200 mL). After the mixture started refluxing, distilled pyrrole (6.7 mL, 6.5 g, 100 mmol) was added dropwise and left for 30 min. After cooling down to ambient temperature, methanol (150 mL)

was added, and the mixture was left in a fridge to precipitate. The purple solids were collected by vacuum filtration, then purified by column chromatography using DCM/pet. ether (2:1) as the eluent. The mixture of *trans/cis* isomers (~1:2) was collected as a third purple fraction (0.8 g, 5 %). ^{1}H-NMR (400 MHz, $CDCl_3$) δ 8.87 (d, *J* = 3.1 Hz, 4H), 8.84 (d, *J* = 3.3 Hz, 4H), 8.22 (d, *J* = 6.0 Hz, 4H), 8.13 (d, *J* = 8.7 Hz, 4H), 7.83 – 7.70 (m, 6H), 7.29 (d, *J* = 8.8 Hz, 4H), 4.10 (s, 6H), -2.76 (s, 2H).

2,4,6-(Tribromo-5-hydroxyphenyl)dipyrromethane 2.48

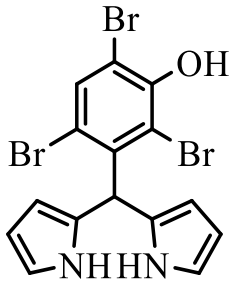

A mixture of 2,4,6-tribromo-5-hydroxybenzaldehyde **2.45** (2 g, 5.57 mmol) and freshly distilled pyrrole (9.38 g, 9.70 mL, 140 mmol) were stirred at room temperature under argon for 20 min. Trifluoroacetic acid (0.04 mL, 0.56 mmol) was added slowly to the mixture and subsequently left stirring for 5 min. NaOH (0.1 M, 250 mL) was added to quench the reaction which was then extracted with ethyl acetate. The organic layer was washed with water (x 3) and dried over anhydrous Na_2SO_4. The solvent was removed under reduced pressure to give a green oil which was chromatographed (silica gel, DCM). Crystallization from DCM/Pet. ether afforded DPM **2.48** as pale-yellow crystals (1.4 g, 53%). MP: 185-187 ^{0}C ; ^{1}H-NMR (400 MHz, $CDCl_3$) δ 8.26 (br-s, 2H), 7.76 (s, 1H), 6.74 (td, *J* = 2.7, 1.5 Hz, 2H), 6.47 (s, 1H), 6.20 (dt, J = 3.5, 2.7 Hz, 2H), 6.09 (ddt, m, 2H). ^{13}C-NMR (101 MHz, $CDCl_3$) δ 139.41, 128.43, 117.04, 108.90, 107.87, 45.04, IR (KBr, cm^{-1}): 3354, 1537, 1433, 1319, 1266, 1183, 1090, 1031, 868, 820, 775, 712, 665. MALDI-tof MS $(C_{15}H_{11}Br_3N_2O)^+$ m/z $[M-H]^+$ calcd: 470.83 found: 470.62.

5,15-Bis-(2,4,6-tribromo-5-hydroxyphenyl)-10,20-di-(4-methoxyphenyl)porphyrin 2.49

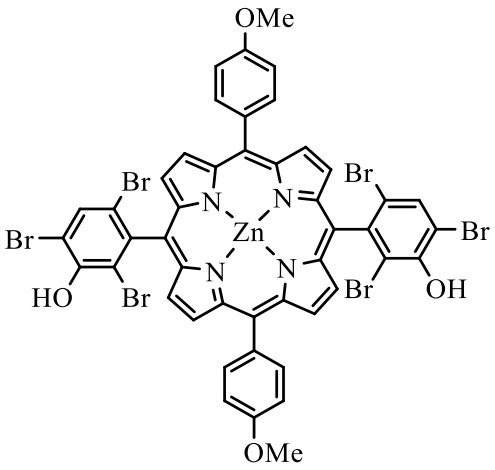

(2,4,6-Tribromo-5-hydroxyphenyl)dipyrromethane **2.48** (0.8 g, 1.69 mmol) and 4-methoxybenzaldehyde **2.22** (0.22 g, 1.69 mmol) were dissolved in anhydrous DCM (200 mL) and stirred under nitrogen. TFA (0.3 mL, 4 mmol) was added slowly at 0 ºC. The solution was stirred with the progress of the reaction monitored by TLC (DCM) as the eluent. After 1.5 h, DDQ (0.38 g, 1.69 mmol) was added, and the mixture stirred for a further 60 min. $Zn(OAc)_2$ (0.45 g, 2,5 mmol) was dissolved in MeOH (30 mL) and added to the mixture. After 12 h, TEA (1 mL) was added, and the solvent removed *via* the rotary evaporator. The resulting solid was purified by short column chromatography using DCM/ethyl acetate (20/1) as the eluent. The solvent was removed, and the residue recrystallized from DCM/MeOH (1:2) afforded the *trans*-Zn **2.49** porphyrin as purple crystals (0.527 g, 50%). MP : 342-345 ^{0}C; ^{1}H-NMR (500 MHz, $CDCl_3$) δ 8.99 (d, *J* = 4.6 Hz, 4H), 8.73 (d, *J* = 4.6 Hz, 4H) , 8.20 (s, 2H), 8.14 (d, *J* = 8.1 Hz, 4H), 7.28 (d, *J* = 8.1 Hz, 4H), 4.10 (s, 6H).;^{13}C NMR (126 MHz, $CDCl_3$) δ 151.45, 151.08, 148.22, 136.04, 133.35, 129.91, 117.78, 113.42, 110.41, 101.24, 77.27, 77.02, 76.76, 55.59, 53.43.; UV-vis, λ_{max} (DCM)/nm (log ε): 424 (4.5), 553 (2.4), 602 (7.6). IR (KBr, cm-1): 3451, 1604, 1493, 1433, 1376, 1335, 1231, 1173, 1061, 993, 953, 853, 795, 718, 683. MALDI-tof MS $(C_{46}H_{26}Br_6N_4O_4Zn)^+$ *m/z* $[M+H]^+$ calcd: 1236.64 found: 1237.27.

5,15-Di-(3-hydroxyphenyl)-10,20-di-(4-methoxyphenyl)porphyrin 2.50

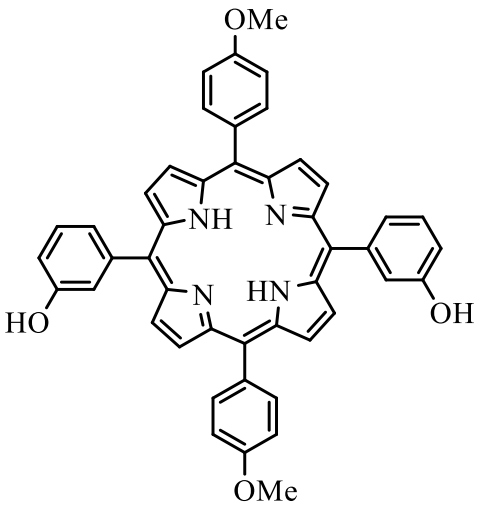

Method A

Porphyrin **2.49** (30 mg, 0.024 mmol) was dissolved in triethylsilane (6 mL) and ~5% mol% palladium dichloride (0.2 mg) was added under argon in a sealed tube. The reaction was heated at 120 ºC for 3 days. The reaction was cooled to room temperature and the solvent evaporated. The resulting green solid was dissolved in DCM and treated with 2-3 drops of concentrated HCl and left stirring overnight to remove any inserted metal(s). Water was added and the mixture extracted with DCM/TEA (2 drops TEA per 100 mL DCM, x 3) dried over anhydrous $MgSO_4$ and the solvent removed under reduced pressure. The crude product was subjected to column chromatography on silica gel with DCM/ethyl acetate (100:0.5) as the eluent. The solvent was removed, and the residue recrystallized from DCM/MeOH (1:2) afforded the porphyrin **2.50** as purple crystals (15 mg, 88%).

Method B

Porphyrin **2.49** (10 mg, 0.08 mmol) was dissolved in triethylsilane (6 mL), and 10% Pd/C (~1 mg) was added under argon in a sealed tube. The reaction was heated at 120 ºC for 3 days. The reaction was cooled to room temperature and then the solvent evaporated. The resulting green

solid was redissolved in DCM and treated with 2-3 drops of concentrated HCl and left stirring overnight to remove inserted metal(s). Water was added and the mixture extracted with DCM/TEA (2 drops TEA per 100 mL DCM, x 3) dried over anhydrous $MgSO_4$ and the solvent removed under reduced pressure. The crude product was subjected to column chromatography on silica gel with DCM/ethyl acetate (100:0.5) as the eluent. The solvent was removed, and the residue recrystallized from DCM/MeOH (1:2) afforded the porphyrin **2.50** as purple crystals (4.5 mg, 79 %). MP : 312-315 ^{0}C; ^{1}H-NMR (500 MHz, methylene chloride-d_2) δ 8.90 (d, J = 4.3 Hz, 4H), 8.89 (d, J = 4.3 Hz, 4H), 8.12 (d, J = 8.3 Hz, 4H), 7.79 (dt, J = 7.5, 1.2 Hz, 2H), 7.69 (br-t, J = 1.2 Hz, 2H), 7.62 (t, J = 7.5 Hz, 2H), 7.31 (d, J = 8.3 Hz, 4H), 7.28 (dd, J = 7.5, 1.2 Hz, 2H), 4.01 (s, 6H), -2.86 (br-s, 2H); ^{13}C-NMR (126 MHz, methylene chloride-d_2) δ 159.7, 154.3, 143.8, 135.37, 134.4, 127.89, 127.75, 122.0, 119.6, 114.8, 112.4, 55.69.; UV-vis, λ_{max} (DCM)/nm (log ε): 421 (4.19), 519 (1.85), 556 (8.98), 596 (5.59), 653 (2.52). MS (MALDI-tof) m/z: [M+] Calcd for $C_{46}H_{34}N_4O_4$ 706.26; Found 706.99 (cluster).

5,15-Bis-(2,4,6-tribromo-5-triflylphenyl)-10,20-di-(4-methoxyphenyl)porphyrin 2.51

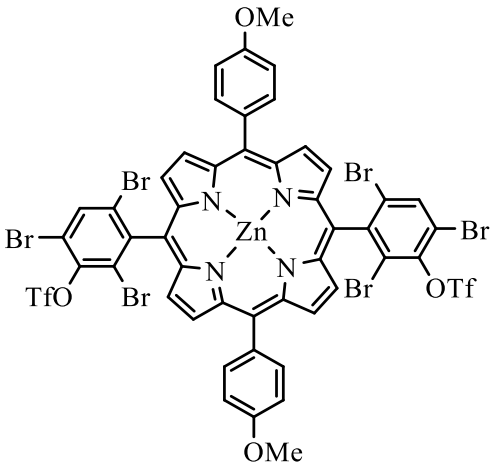

Porphyrin **2.49** (0.1 g, 0.080 mmol) was dissolved in anhydrous DCM (100 mL). Pyridine (0.095 g, 1.19 mmol) was then added, and the reaction mixture was stirred under N_2. Triflic anhydride (0.334 g, 1.25 mmol) was added slowly at 0 °C, and the solution stirred overnight. The mixture was extracted with water and $NaHCO_3$ and then dried over $MgSO_4$. After the

solvent was removed, the resultant solid was redissolved in a mixture of DCM/MeOH in the presence of Zn $(OAc)_2$ to convert the free porphyrin to Zn porphyrin. The reaction was complete after stirring at room temperature for 2.5 hours. The solvent was evaporated, and the mixture purified by column chromatography using 100% DCM to collect the pure porphyrin **2.51** as a purple amorphous solid (0.097 g, 81%). ^{1}H-NMR (400 MHz, $CDCl_3$) δ 9.02 (d, J = 4.7 Hz, 4H), 8.69 (d, J = 4.7 Hz, 4H), 8.39 (2 x s, 2H), 8.15 – 8.12 (m, 4H) 7.29 (d, J = 8.6 Hz, 4H), 4.11 (s, 6H); ^{13}C-NMR (101 MHz, $CDCl_3$) δ 159.5, 151.3, 148.3, 146.1, 135.8, 135.5, 134.4, 133.8, 129.6, 127.8, 124.59, 124.3, 121.7, 117.9, 112.2, 55.6. UV-vis, λ_{max} (DCM)/nm (log ε): 427 (5.6), 554 (4.6), 593 (2.7).

2,6-(Dibromophenyl)dipyrromethane 2.53[102]

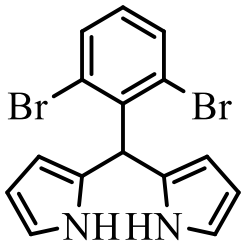

A mixture of 2,6-dibromobenzaldehyde **2.52** (2 g, 7.57 mmol) and freshly distilled pyrrole (12.73 g, 13.16 mL, 190 mmol) were stirred at room temperature under argon for 20 min. Trifluoroacetic acid (0.06 mL, 0.79 mmol) was added slowly to the mixture and left stirring for 5 min. NaOH (0.1 M, 250 mL) was added to quench the reaction then extracted with ethyl acetate. The organic layer was washed with water three times and dried over anhydrous Na_2SO_4. The solvent was then removed by reduced pressure to give brown oil which was chromatographed (Silica gel, hexane: ethyl acetate [30:1]). Crystallization from DCM/Pet. ether afforded pure DPM **2.53** as pure yellow crystals (1.3 g, 45%).^{1}H-NMR (400 MHz, $CDCl_3$) δ 8.30 (s, 2H), 7.58 (d, J = 8.0 Hz, 2H), 6.97 (t, J = 8.0 Hz, 1H), 6.74 (m, 2H), 6.55 (s, 1H), 6.21 (m, 2H), 6.10 (m, 2H). ^{13}C- NMR (101 MHz, $CDCl_3$) δ 139.38, 133.52, 129.42, 129.18, 116.87, 108.77, 107.73, 44.62.

5,15-Bis-(2,6-dibromophenyl)-10,20-di-(4-methoxyphenyl)porphyrin 2.54

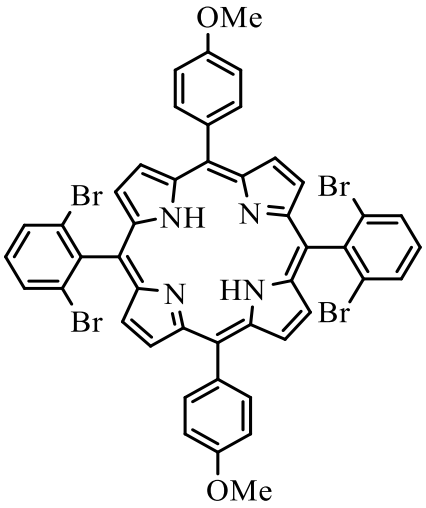

2,6-Dibromophenyldipyrromethane **2.53** (0.381 g, 1 mmol) and 4-methoxybenzaldehyde **2.22** (0.136 g, 1 mmol) were dissolved in anhydrous DCM (100 mL) and stirred under inert atmosphere for 20 minutes. TFA (0.15 mL, 2 mmol) was added slowly to the mixture, at 0 ^{o}C, and stirred with the progress of the reaction monitored by TLC (DCM) as the eluent. After 1.5 h, DDQ (0.22 g, 1 mmol) was added, and the mixture was stirred for 60 min. TEA (1 mL) was added to neutralize the condition. The mixture was eluted through a short silica column using DCM and washed with DCM. Crystallization from DCM/hexane afforded pure *trans*-porphyrin **2.54** as purple crystals (0.28 g, 57 %). MP > 350 ^{0}C. ^{1}H-NMR (400 MHz, $CDCl_3$) δ 8.91 (d, *J* = 4.8 Hz, 4H), 8.67 (d, *J* = 4.8 Hz, 4H), 8.17 (d, *J* = 8.5 Hz, 4H), 8.05 (d, *J* = 8.1 Hz, 4H), 7.56 (t, *J* = 8.1 Hz, 2H), 7.30 (d, *J* = 8.5 Hz, 4H), 4.12 (s, 6H), -2.53 (s, 2H). ^{13}C-NMR (101 MHz, $CDCl_3$) δ 137.09, 131.49, 128.46, 119.69, 112.25, 77.33, 77.01, 76.70, 31.60, 22.66, 14.13. UV-vis, λ_{max} (DCM)/nm (log ε): 519 (3.89) ,556 (3.42) ,596 (3.38), 652 (3.18). IR (KBr, cm^{-1}): 3312, 2836, 2351, 1605, 1547, 1504, 1417, 1343, 1288, 1245, 1172, 1030, 963, 843, 822, 792, 706. MALDI-tof MS $(C_{46}H_{31}Br_4N_4O_2)^+$ *m/z* $[M+H]^+$ calcd: 986.91 found: 986.61.

5,15-Bis-(2,6-dibromophenyl)-10,20-di(4-methoxyphenyl)porphyrin 2.55

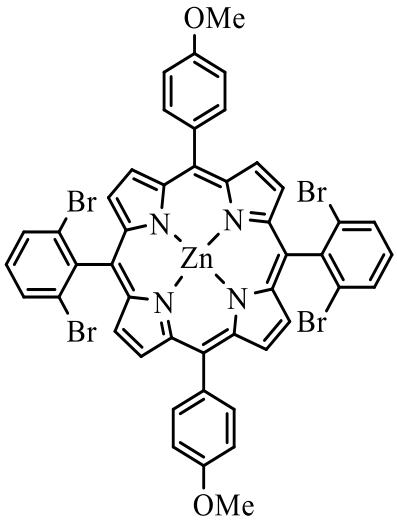

Porphyrin **2.54** (0.2 g, 0.20 mmol) was dissolved in DCM (150 mL). $Zn(OAc)_2$ (0.07 g, 0.3 mmol) in MeOH (15 mL) was added and the mixture heated at reflux overnight. The solvent was evaporated, and the resulting purple solid was redissolved in THF and passed through a silica pad eluting with THF. The solvent was removed and the product crystallized from THF/MeOH (1:2) affording *trans*-Zn porphyrin **2.55** as purple crystals (0.198 g, 94 %). The crystals were of sufficient size and quality for X-ray crystallography. MP > 350 ºC. ^{1}H-NMR (400 MHz, $CDCl_3$) δ 8.98 (d, *J* = 4.6 Hz, 4H), 8.73 (d, *J* = 4.7 Hz, 4H), 8.16 (d, *J* = 8.5 Hz, 4H), 8.03 (d, *J* = 8.1 Hz, 4H), 7.53 (t, *J* = 8.2 Hz, 2H), 7.27 (d, *J* = 7.1 Hz, 4H), 4.09 (s, 6H). ^{13}C-NMR (101 MHz, $CDCl_3$) δ 165.85, 150.95, 148.68, 135.49, 133.77, 131.39, 130.03, 128.44, 119.92, 112.05, 77.33, 77.22, 77.01, 76.70, 31.60, 22.66, 14.13. UV-vis, λ_{max} (DCM)/nm (log ε): 516, (2.95), 552 (3.93) ,594 (3.05). IR (KBr, cm^{-1}): 2956, 2830, 2351, 1806, 1494, 1418, 1336, 1240, 1173, 1065, 994, 791, 711. MALDI-tof MS $(C_{46}H_{28}Br_4N_4O_2Zn_1)^+$ *m/z* [M+] $^+$ calcd: 1047.82 found: 1047.69.

5,15-Diphenyl-10,20-bis-(4-methoxyphenyl)porphyrin 2.44[113]

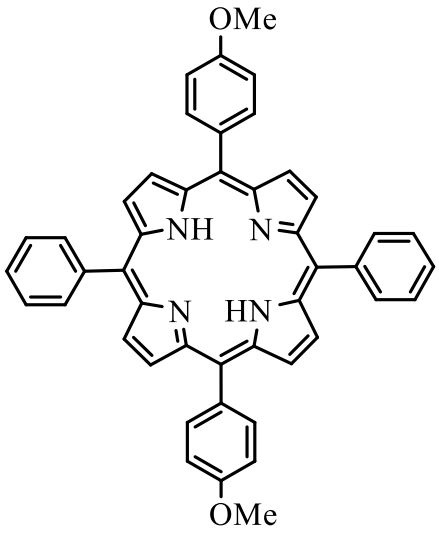

Method A

Porphyrin **2.54** (30 mg, 0.028 mmol), a mixture of (1:1) THF and triethylsilane (6 mL) and 10% Pd/C (~1 mg) was added into a sealed tube. The reaction was heated at 120 ºC for 3 days. After cooling, the solvent was evaporated and the resulting solid redissolved in DCM, treated with 2-3 drops of TEA and the solvent removed under reduced pressure. The crude product which was purified using column chromatography on silica gel with DCM/hexane (1:1) as the eluent. The solvent was removed, and the residue recrystallized from DCM/hexane (1:1) afforded the porphyrin **2.44** as purple crystals (12 mg, 60 %).

Method B

Porphyrin **2.55** (30 mg, 0.028 mmol), a mixture of (1:1) THF and triethylsilane (6 mL) and palladium dichloride (~0.2 mg) were added into a sealed tube. The reaction was heated at 120 ºC for 3 days, cooled down and the solvent evaporated. The resulting green solid was redissolved in DCM and treated with 2-3 drops of concentrated HCl and left stirring overnight to remove any Pd and Zn metals that were inserted into the porphyrin. The mixture was neutralised by adding further DCM and TEA, extracted with water (x 3) and dried over

($MgSO_4$). The solvent was removed under reduced pressure to give a crude product which was purified using column chromatography on silica gel with DCM/hexane (1:1) as the eluent. The solvent was removed, and the residue removed, and the residue recrystallized from DCM/hexane (1:21) afforded the porphyrin **2.44** as purple crystals (14 mg, 74%).^{1}H-NMR (400 MHz, $CDCl_3$) δ 8.87 (d, *J* = 4.8 Hz, 4H), 8.83 (d, *J* = 4.8 Hz, 4H), 8.22 (dd, *J* = 7.7, 1.6 Hz, 4H), 8.13 (d, *J* = 8.6 Hz, 4H), 7.83 – 7.70 (m, 6H), 7.29 (d, *J* = 8.6 Hz, 4H), 4.10 (s, 6H), -2.76 (s, 2H).

5,15-Diphenyl-10,20-bis-(4-hydroxyphenyl)porphyrin 2.12d [98]

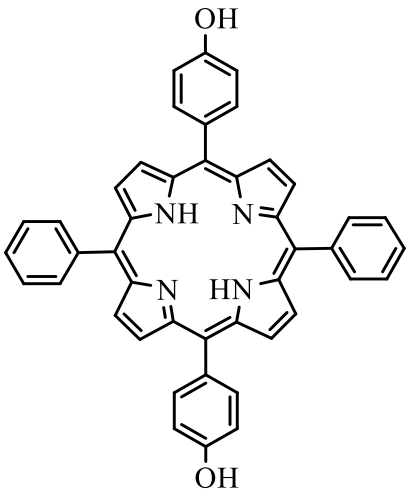

Method A:

Following the Adler method, 4-hydroxybenzaldehyde **2.21** (6.1 g, 50 mmol) and benzaldehyde (5.3 g, 50 mmol) were dissolved and heated at reflux in propionic acid (200 mL). After the mixture started refluxing, distilled pyrrole (6.7 mL, 6.5 g, 100 mmol) was added dropwise and the refluxing continued for a further 30 min. After cooling to ambient temperature, methanol (150 mL) was added, and the mixture was left in a fridge to precipitate. The purple solids were collected by vacuum filtration and then purified by column chromatography using DCM: THF (99.5:0.5) as the eluent. *Trans* isomer **2.12d** was collected as a third purple fraction (0.05 g, 0.03%).

Method B:

The isolated mixture of isomeric porphyrins **2.44** (*trans*+ *cis*) (1 g, 1.48 mmol) was dissolved in dry DCM (40 mL) under Ar. The solution was cooled to -78 ºC and boron tribromide (14.84 mL, 1 M solution in DCM, 14.84 mmol) was added slowly. The reaction mixture was allowed to warm to room temperature and stirring for 48 h. TLC showed complete consumption of the starting materials, so the reaction was quenched with ice water and extracted with ethyl acetate. The organic layer was washed by brine (x 3) and dried over $MgSO_4$. The desired product was isolated by column chromatography using solvent system DCM:THF (99.5:0.5) as the eluent. *Trans* **2.12d** was collected in the first fraction in a 24% yield (0.230 g). ^{1}H-NMR (400 MHz, $CDCl_3$) δ 8.87 (d, *J* = 4.8 Hz, 4H), 8.84 (d, *J* = 4.8 Hz, 4H), 8.21 (dd, *J* = 7.7, 1.7 Hz, 4H), 8.08 (d, *J* = 8.4 Hz, 4H), 7.83 – 7.70 (m, 6H), 7.21 (d, *J* = 8.4 Hz, 4H), -2.78 (s, 2H).

5,10-Diphenyl-15,20-di-(4-hydroxyphenyl)porphyrin 2.12d [98]

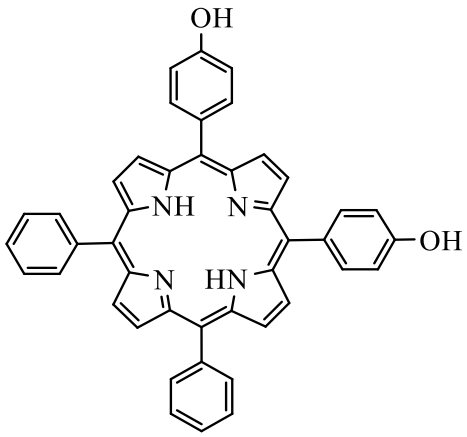

The title compound was collected in the second fraction from the previous reaction (0.590 g, 62%). ^{1}H-NMR (400 MHz, $CDCl_3$) δ 8.87-8.84 (m, 8H), 8.21 (dd, *J* = 7.7, 1.8 Hz, 4H), 8.08 (d, *J* = 8.4 Hz, 4H), 7.82 – 7.70 (m, 6H), 7.22 (d, *J* = 8.4 Hz, 4H), -2.78 (s, 2H).

5-(*p*-5-Hexenyl-1-oxyphenyl)-10-(*p*-hydroxyphenyl)-15,20-diphenylporphyrin 2.56

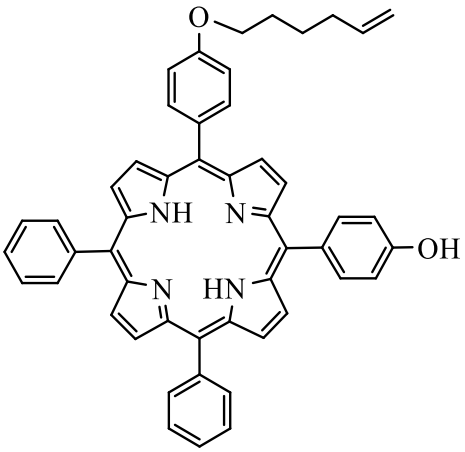

A mixture of 5,10-dihydroxyphenylporphyrin ***cis*-2.12d** (0.2 g, 0.3 mmol), and potassium carbonate (0.17 g, 1.23 mmol) were dissolved in dry DMF (15 mL) under N_2. Then 6-bromo-1-hexene (0.20 g, 1.23 mmol), was added and the mixture stirred at room temperature overnight. The reaction was quenched with water, extracted with DCM and dried over $MgSO_4$. The crude product was purified by column chromatography using DCM affording the desired product **2.56** in the second fraction (95 mg, 43%). MP: 178-180 ^oC. ^{1}H-NMR (400 MHz, $CDCl_3$) δ 8.91 – 8.80 (m, 8H), 8.21 (d, *J* = 5.5 Hz, 4H), 8.11 (d, *J* = 8.5 Hz, 2H), 8.08 (d, *J* = 8.4 Hz, 2H), 7.82 – 7.70 (m, 6H), 7.28 (d, *J* = 8.4 Hz, 2H), 7.14 (d, *J* = 8.4 Hz, 2H), 5.94 (ddt, *J* = 16.9, 10.2, 6.7 Hz, 1H), 5.14 (dd, *J* = 17.1, 1.8 Hz, 1H), 5.07 (dd, *J* = 10.2, 2.2 Hz, 1H), 4.27 (t, *J* = 6.4 Hz, 2H), 2.27 (q, *J* = 7.2 Hz, 2H), 2.07 – 1.95 (m, 2H), 1.76 (m, 2H), -2.77 (s, 2H).^{13}C-NMR (101 MHz, $CDCl_3$) δ 158.96, 155.36, 142.24, 138.63, 135.71, 135.63, 134.80, 134.58, 134.41, 127.69, 126.69, 120.15, 119.96, 119.91, 119.79, 114.88, 113.66, 112.74, 77.35, 77.03, 76.71, 68.10, 33.58, 28.96, 25.53. IR (KBr, cm^{-1}): 2911, 2346, 1604, 1504, 1469, 1347, 1239, 1170, 964, 843, 795, 699.643. UV-vis, λ_{max} (DCM)/nm (log ε): 518 (4.00); 554 (3.70), 594 (3.44), 649 (3.43). MALDI-tof MS $(C_{50}H_{40}N_4O_2)^+$ *m/z* $[M+]^+$ calcd: 728.32 found: 728.48.

Porphyrin dyad 2.57

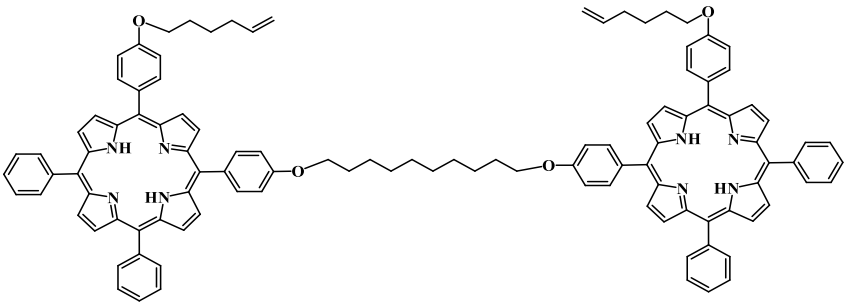

In sealed tube, a mixture of **2.56** (0.100 g, 0.138 mmol), K_2CO_3 (0.094 g, 0.68 mmol) and 1,10-dibromodecane (0.020 g, 0.069 mmol) were dissolved in dry acetone (5 mL) and heated at 65 ^oC for 10 days. The mixture was washed with water, extracted with DCM, dried over $MgSO_4$, and the solvent removed under vacuum to obtain solid material. The pure dyad **2.57** was collected after recrystallization using DCM:MeOH (1:1) (67 mg, 61%). MP: 189-193 ^oC. ^{1}H-NMR (400 MHz, $CDCl_3$) δ 8.93 – 8.87 (m, 8H), 8.84 (s, 8H), 8.23 – 8.19 (m, 8H), 8.11 (dd, *J* = 10.8, 8.5 Hz, 8H), 7.83 – 7.68 (m, 12H), 7.29 (d, *J* = 8.6 Hz, 4H), 7.24 (d, *J* = 8.6 Hz, 4H), 5.92 (ddt, *J* = 16.9, 10.2, 6.7 Hz, 2H), 5.12 (dd, *J* = 17.1, 1.9 Hz, 2H), 5.05 (dd, *J* = 10.2, 2.3, 1.2 Hz, 2H), 4.28 (t, *J* = 6.5 Hz, 4H), 4.20 (t, *J* = 6.4 Hz, 4H), 2.24 (q, *J* = 7.3 Hz, 4H), 2.09 – 1.91 (m, 8H), 1.80 – 1.52 (m, 16H), -2.73 (s, 4H).^{13}C-NMR (101 MHz, $CDCl_3$) δ 159.03, 158.93, 142.27, 138.62, 135.64, 135.61, 134.57, 134.42, 127.66, 126.67, 120.14, 120.10, 119.86, 114.86, 112.76, 112.70, 77.35, 77.23, 77.03, 76.71, 68.36, 68.05, 33.56, 29.70, 29.61, 29.58, 28.93, 26.31, 25.51. IR (KBr, cm^{-1}): 3312, 2912, 2847, 2351, 1600, 1504, 1469, 1348, 1242, 1172, 964, 843, 799,700. UV-vis, λ_{max} (DCM)/nm (log ε): 421 (5.41), 520 (4.06); 557 (3.80), 596 (3.61), 652 (3.52). MALDI-tof MS $(C_{110}H_{98}N_8O_4)^+$ *m/z* $[M+]^+$ calcd: 1595.77 found:1595.61.

Triple Decker 2.58

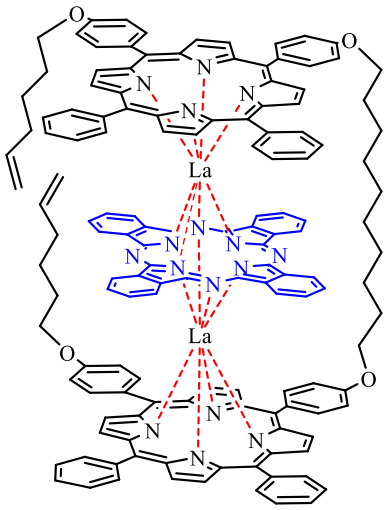

A mixture of porphyrin dyad **2.57** (0.050 g, 0.031 mmol), phthalocyanine (0.016 g, 0.031 mmol) were dissolved in 1-pentanol (8 mL) and heated to reflux for 24 h under N_2. To the homogeneous mixture, lanthanum(III) acetylacetonate hydrate (0.027 g, 0.062 mmol) was added and refluxing continued for a further 2 h. The solvent was removed, and the residue was purified using column chromatography using DCM:hexane (2:1) as the eluent. TD **2.58** was isolated in the second fraction as dark brown crystals (46 mg, 62%). MP > 350 °C. ^{1}H-NMR (400 MHz, $CDCl_3$) δ 10.08 (d, *J* = 8.1 Hz, 2H), 9.98 (m, 4H), 9.91 – 9.81 (m, 2H), 9.35 (dd, *J* = 5.5, 3.0 Hz, 8H), 8.44 (t, *J* = 7.7 Hz, 4H), 8.30 (dd, *J* = 5.5, 3.0 Hz, 8H), 7.98 (d, *J* = 8.1 Hz, 4H), 7.81 (td, *J* = 7.7, 1.2 Hz, 4H), 7.33 – 7.27 (m, 8H), 7.25 – 7.19 (m, 12H), 6.87 (d, *J* = 8.0 Hz, 2H), 6.80 – 6.69 (m, 4H), 6.64 (d, *J* = 7.4 Hz, 4H), 6.55 (dt, *J* = 8.1, 2.8 Hz, 2H), 6.05 (ddt, *J* = 16.9, 10.2, 6.7 Hz, 2H), 5.24 (dd, *J* = 17.1, 1.8 Hz, 2H), 5.18 – 5.11 (m, 2H), 4.60 (t, *J* = 7.3 Hz, 4H), 4.37 (t, *J* = 6.3 Hz, 4H), 2.38 (q, *J* = 7.1 Hz, 4H), 2.33 – 2.24 (m, 4H), 2.17 – 2.10 (m, 4H), 1.97 – 1.79 (m, 16H).^{13}C-NMR (101 MHz, $CDCl_3$) δ 158.92, 157.56, 153.55, 149.13, 142.98, 136.60, 133.31, 130.04, 128.37, 127.09, 125.80, 123.45, 119.89, 114.97, 77.34, 77.22, 77.02, 76.70, 33.73, 29.20, 25.69. UV-vis, λ_{max} (DCM)/nm (log ε): 363 (5.00); 420 (5.41), 491 (4.40), 555 (4.22), 610 (4.15), 888 (3.86). IR (KBr, cm^{-1}): 3043, 2847, 2351, 1806, 1604, 1504,

1469, 1328, 1238, 1173, 1114, 1063, 879, 794. MALDI-tof MS $(C_{142}H_{110}La_2N_{16}O_4)^+$ *m/z* [M+] $^+$ calcd: 2381.71 found: 2381.79.

Triple Decker 2.59

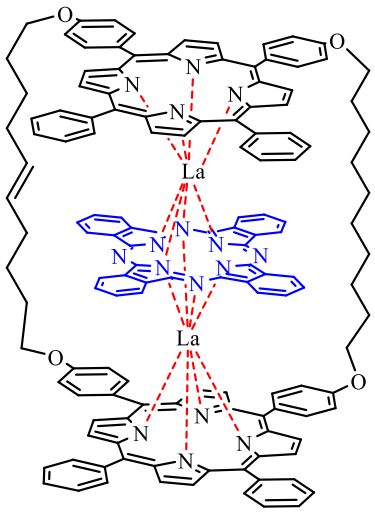

Following a modified version of Grubbs^{TM} metathesis method,[105] TD **2.58** (0.03 g, 0.012 mmol) was dissolved in anhydrous DCM (70 mL) and the reaction mixture was stirred under N_2 for 30 min. A degassed solution of 1st generation Grubbs^{TM} catalyst (5 mg, 0.0058 mmol) in dry DCM (10 mL) was added by cannula and then left stirring at room temperature for 24 h. The reaction was opened to air and left stirring. The solvent was then removed and the resulting dark solid was purified by column chromatography using DCM: hexane (2.5: 1). The desired compound **2.59** was then collected as the first fraction. After crystallization from DCM:MeOH, a dark brown solid was collected (6 mg, 20%). MP > 350 °C. ^{1}H-NMR (400 MHz, $CDCl_3$) δ 10.30 – 10.09 (m, 4H), 10.02 (d, *J* = 7.2 Hz, 4H), 9.34 (dd, *J* = 8.1, 2.8 Hz, 8H), 8.45 (t, *J* = 7.6 Hz, 4H), 8.30 (dd, *J* = 8.1, 2.8 Hz, 8H), 8.05-7.96 (m, 4H), 7.82 (t, *J* = 7.8 Hz, 4H), 7.34 – 7.28 (m, 8H), 7.23 (d, *J* = 5.5 Hz, 12H), 6.87 (d, *J* = 8.9 Hz, 4H), 6.81 (s, 2H), 6.73 (d, *J* = 8.1 Hz, 2H), 6.66 (d, *J* = 7.3 Hz, 4H), 6.06 (s, 1H), 5.75 (s, 1H), 4.67 (t, *J* = 7.2 Hz, 2H), 4.58 (q, J = 7.3 Hz, 6H), 2.72 – 2.49 (m, 4H), 2.36 – 2.24 (m, 8H), 2.14 – 1.99 (m, 4H), 1.96 – 1.77 (m, 12H). ^{13}C-NMR (101 MHz, $CDCl_3$) δ 130.03, 125.79, 123.91, 122.78, 120.60, 77.34,

77.22, 77.02, 76.70, 31.60, 22.66, 14.13. UV-vis, λ_{max} (DCM)/nm (log ε): 363 (4.91); 420 (5.35), 490 (4.33), 554 (4.16), 608 (4.11), 888 (3.76). IR (KBr, cm^{-1}): 2351, 1603, 1501, 1465, 1328, 1227, 1173, 1059, 982, 795. MALDI-tof MS $(C_{140}H_{106}La_2N_{16}O_4)^+$ *m/z* $[M+]^+$ calcd: 2353.67 found: 2353.64.

***Cis* Cyclic Triple Decker 2.60**

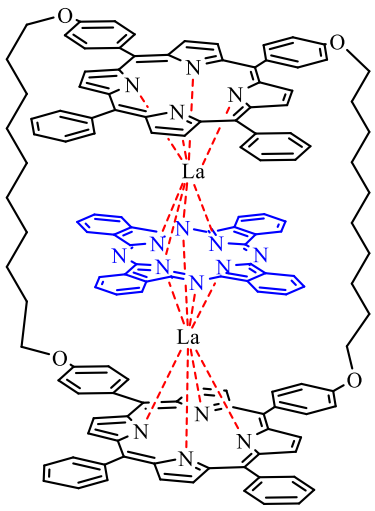

Following a procedure developed by Felix *et al*,[106] a mixture of TD **2.59** (10 mg, 4.3 μmol) and Pd/C 10% (5 mg) were dissolved in a mixture of EtOAc (1 mL) and 1,4-cyclohexadiene (1 mL, 10.9 mmol) in a sealed tube. The reaction mixture was heated in an oil bath at 100˚C for 6 h. After cooling to room temperature, the mixture was filtered and the solvent removed to obtain pure **2.60** as a dark brown solid (8 mg, 80%). MP > 350 ºC. ^{1}H-NMR (400 MHz, $CDCl_3$) δ 10.13 (d, *J* = 8.5 Hz, 4H), 10.03 (d, *J* = 7.4 Hz, 4H), 9.35 (dd, *J* = 5.7, 3.0 Hz, 8H), 8.45 (t, J = 7.6 Hz, 4H), 8.30 (dd, *J* = 5.7, 3.0 Hz, 8H), 7.99 (d, *J* = 8.5 Hz, 4H), 7.82 (t, *J* = 7.8 Hz, 4H), 7.30 (d, *J* = 4.4 Hz, 8H), 7.22 (d, *J* = 4.4 Hz, 12H), 6.87 (d, *J* = 7.6 Hz, 4H), 6.73 (d, *J* = 8.0 Hz, 4H), 6.66 (d, *J* = 7.6 Hz, 4H), 4.59 (t, *J* = 7.3 Hz, 8H), 2.29 (s, 8H), 2.00 – 1.87 (m, 24H). ^{13}C-NMR (101 MHz, $CDCl_3$) δ 158.79, 148.78, 142.99, 136.56, 130.03, 128.54, 126.11, 123.43, 120.10, 89.46, 77.33, 77.22, 77.02, 76.70, 68.64, 29.40, 29.20, 28.59, 26.86, 1.20. IR (KBr, cm^{-1}): 3049, 2924, 2837, 2346, 1605, 1513, 1463, 1328, 1240, 1174, 1065, 982, 880,

794, 727, 624. UV-vis, λ_{max} (DCM)/nm (log ε): 363 (4.89); 488 (4.34), 554 (4.15), 613 (4.06), 886 (3.81). MALDI-tof MS $(C_{140}H_{108}La_2N_{16}O_4)^+$ *m/z* $[M+]^+$ calcd: 2355.69 found: 2355.36.

5,10(*p*-5-Hexenyl-1-oxyphenyl)-15,20-diphenylporphyrin 2.56a

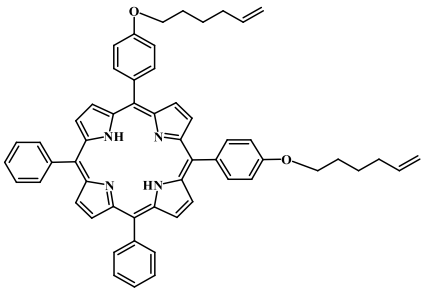

This compound was collected from the previous reaction and obtained as the first fraction. After crystallization using DCM:MeOH (1:2), **2.56a** was collected as purple crystals (78 mg, 31 %). MP: 175-178 ºC. ^{1}H-NMR (400 MHz, $CDCl_3$) δ 8.88 – 8.83 (m, 8H), 8.22 (dd, *J* = 7.7, 1.8 Hz, 4H), 8.11 (d, J = 8.5 Hz, 4H), 7.82 – 7.70 (m, 6H), 7.27 (d, J = 8.8 Hz, 4H), 5.94 (ddt, J = 17.0, 10.2, 6.7 Hz, 2H), 5.14 (dd, *J* = 17.1, 1.8 Hz, 2H), 5.06 (ddt, J = 10.2, 2.3, 1.2 Hz, 2H), 4.26 (t, J = 6.4 Hz, 4H), 2.27 (q, J = 7.2 Hz, 4H), 2.07 – 1.95 (m, 4H), 1.76 (m, 4H), -2.75 (s, 2H). ^{13}C-NMR (101 MHz, $CDCl_3$) δ 157.90, 141.22, 137.58, 134.57, 133.52, 133.39, 126.62, 125.63, 119.05, 118.81, 113.82, 111.67, 76.29, 76.17, 75.97, 75.65, 67.04, 32.53, 27.91, 24.48. UV-vis, λ_{max} (DCM)/nm (log ε): 518 (4.39); 555 (4.11), 594 (3.84), 651 (3.79). IR (KBr, cm^{-1}): 3312, 2911, 2351, 1598, 1504, 1469, 1348, 1282, 1241, 1172, 1106, 1070, 979, 964, 906, 844, 797, 732, 685. MALDI-tof MS $(C_{56}H_{50}N_4O_2)^+$ *m/z* $[M]^+$ calcd: 810.39 found: 810.32.

5-(*p*-5-Hexenyloxyphenyl)-15-(*p*-hydroxyphenyl)-10,20-diphenylporphyrin 2.13

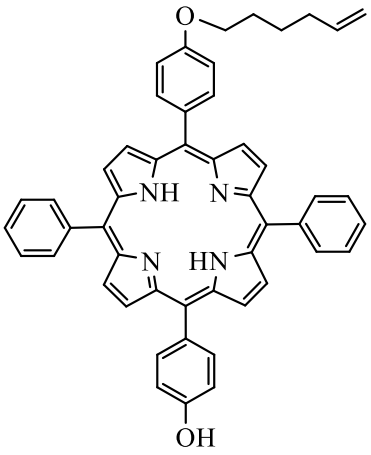

A mixture of 5,15-di(*p*-hydroxyphenyl)porphyrin **2.12d-*trans*** (0.3 g, 0.464 mmol), and potassium carbonate (0.256 g, 1.86 mmol) were dissolved in dry DMF (20 mL) under N_2. 6-Bromo-1-hexene (0.3 g, 1.86 mmol) was added and the mixture was left stirring at room temperature overnight. The reaction was quenched by water, extracted with DCM and dried over $MgSO_4$. The crude product was purified by column chromatography using DCM affording the desired product **2.13** in the second fraction (0.130 g, 39%). MP: 202-205 ºC. ^{1}H-NMR (400 MHz, $CDCl_3$) δ 8.92 – 8.83 (m, 8H), 8.23 (dd, *J* = 7.6, 1.7 Hz, 4H), 8.12 (d, *J* = 8.5 Hz, 2H), 8.05 (d, *J* = 8.5 Hz, 2H), 7.85 – 7.73 (m, 6H), 7.28 (d, *J* = 8.4 Hz, 2H), 7.13 (d, *J* = 8.4 Hz, 2H), 5.94 (ddt, *J* = 16.9, 10.2, 6.6 Hz, 1H), 5.14 (dd, *J* = 17.1, 1.9 Hz, 1H), 5.09 – 5.04 (m, 1H), 4.25 (t, *J* = 6.4 Hz, 2H), 2.27 (q, *J* = 7.4 Hz, 2H), 2.06 – 1.95 (m, 2H), 1.75 (dq, *J* = 10.0, 7.5 Hz, 2H), -2.75 (s, 2H). ^{13}C-NMR (101 MHz, $CDCl_3$) δ 158.96, 155.33, 142.27, 138.64, 135.70, 135.63, 134.78, 134.58, 134.39, 127.70, 126.69, 120.08, 120.04, 119.66, 114.88, 113.66, 112.75, 77.35, 77.03, 76.71, 68.10, 33.58, 28.96, 25.53. UV-vis, λmax (DCM)/nm (log ε): 420 (5.28), 518 (3.78); 553 (3.41), 595 (3.00), 650 (2.90). IR (KBr, cm^{-1}): 3312, 2919, 2842, 2702, 2346, 1600, 1503, 1469, 1347, 1242, 1169, 964, 843. MALDI-tof MS $(C_{50}H_{40}N_4O_2)^+$ *m/z* $[M]^+$ calcd: 728.32 found: 728.53.

5,15-(*p*-5-Hexenyloxyphenyl)-10,20-diphenylporphyrin 2.13a

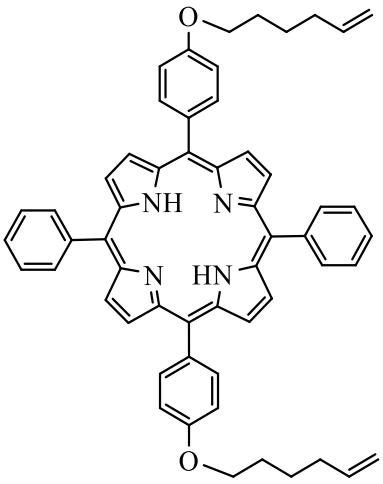

This compound was collected from the previous reaction and isolated from the first fraction. After crystallization using DCM:MeOH (1:2), **2.13a** was collected as purple crystals (0.073 g, 22%). MP: 242-246 °C. ^{1}H-NMR (400 MHz, $CDCl_3$) δ 8.88 (d, *J* = 4.8 Hz, 4H), 8.84 (d, *J* = 4.8 Hz, 4H), 8.22 (dd, *J* = 7.7, 1.7 Hz, 4H), 8.11 (d, *J* = 8.5 Hz, 4H), 7.83 – 7.70 (m, 6H), 7.27 (d, *J* = 8.5 Hz, 4H), 5.94 (ddt, *J* = 16.9, 10.2, 6.6 Hz, 2H), 5.14 (dq, *J* = 17.1, 1.6 Hz, 2H), 5.06 (ddt, *J* = 10.2, 2.3, 1.2 Hz, 2H), 4.26 (t, *J* = 6.4 Hz, 4H), 2.26 (q, *J* = 7.2 Hz, 4H), 2.01 (dq, *J* = 8.5, 6.5 Hz, 4H), 1.81 – 1.69 (m, 4H), -2.75 (s, 2H). ^{13}C-NMR (101 MHz, $CDCl_3$) δ 158.95, 142.30, 138.63, 135.62, 134.57, 134.41, 127.67, 126.67, 119.98, 114.87, 112.73, 77.34, 77.22, 77.02, 76.70, 68.10, 33.58, 28.96, 25.53. UV-vis, λ_{max} (DCM)/nm (log ε): 420 (5.47), 518 (3.86); 553 (3.60), 594 (3.20), 650 (3.08). IR (KBr, cm^{-1}): 3312, 3028, 2917, 2863, 2832, 2708, 2537, 2351, 1883, 1821, 1595, 1504, 1463, 1349, 1280, 1242, 1174, 1107, 1069, 981, 965, 906, 841, 734, 618. MALDI-tof MS $(C_{56}H_{50}N_4O_2)^+$ *m/z* $[M]^+$ calcd: 810.39 found: 810.31.

***Trans* Open Triple Decker 2.61**

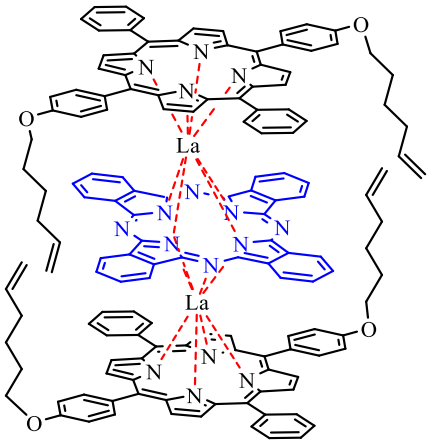

A mixture of porphyrin **2.13a** (0.050 g, 0.061 mmol) and phthalocyanine (0.03 g, 0.058 mmol) were heated in 1-pentanol (12 mL) to reflux for 24 h under N_2. To the homogeneous mixture, lanthanum (III) acetylacetonate hydrate (0.06 g, 0.137 mmol) was added and refluxing continued for a further 8 h. The solvent was removed, and the residue was purified by column chromatography using DCM:Pet. ether (1:1). The title compound **2.61** was isolated as the second fraction as dark brown crystals (46 mg, 62%). MP > 350 °C. ^{1}H-NMR (400 MHz, $CDCl_3$) δ 9.68 (d, *J* = 7.4 Hz, 4H), 9.55 (dd, *J* = 8.2, 2.3 Hz, 4H), 9.38 (dd, *J* = 5.5, 2.9 Hz, 8H), 8.40 – 8.31 (m, 12H), 7.88 (dd, *J* = 8.2, 2.8 Hz, 4H), 7.78 (t, *J* = 7.8 Hz, 4H), 7.31 (d, *J* = 4.3 Hz, 8H), 7.27 (d, *J* = 4.3 Hz, 8H), 7.21 (t, *J* = 7.8 Hz, 4H), 6.74 (dd, *J* = 8.2, 2.8 Hz, 4H), 6.58 (d, *J* = 7.3 Hz, 4H), 6.51 (dd, *J* = 8.2, 2.8 Hz, 4H), 6.05 (ddt, *J* = 16.9, 10.2, 6.7 Hz, 4H), 5.29 – 5.20 (m, 4H), 5.16 (ddt, *J* = 10.1, 2.3, 1.2 Hz, 4H), 4.35 (t, *J* = 6.3 Hz, 8H), 2.38 (q, *J* = 7.1 Hz, 8H), 2.19 – 2.11 (m, 8H), 1.93 – 1.87 (m, 8H). ^{13}C-NMR (101 MHz, $CDCl_3$) δ 158.41, 153.62, 148.21, 147.78, 142.97, 138.74, 136.71, 135.23, 134.49, 134.12, 133.58, 133.20, 130.09, 128.60, 128.41, 127.03, 125.77, 123.60, 120.10, 120.05, 114.97, 112.42, 111.02, 77.35, 77.03, 76.71, 68.12, 33.72, 29.18, 25.67. UV-vis, λ_{max} (DCM)/nm (log ε): 360 (4.88); 421 (5.31), 489 (4.29), 554 (4.11), 610 (4.02), 889 (3.73). IR (KBr, cm^{-1}): 3028, 2917, 2346, 1806,

1728, 1605, 1514, 1463, 1328, 1241, 1174, 1113, 1066, 989, 911, 880, 845, 798, 623. MALDI-tof MS $(C_{144}H_{112}La_2N_{16}O_4)^+$ *m/z* $[M]^+$ calcd: 2407.72 found: 2407.96.

***Trans* Closed Triple Decker 2.62**

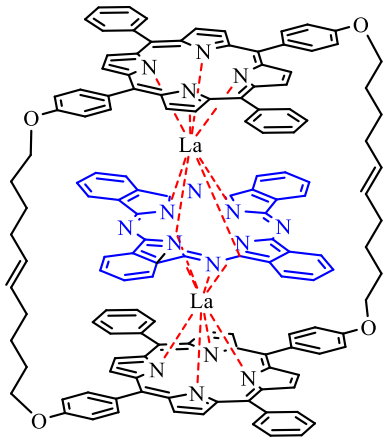

Following a modified version of Grubbs™ metathesis method,[105] *trans* open TD **2.61** (0.078 g, 0.032 mmol) was dissolved in dry DCM (170 mL) and the reaction mixture stirred under N_2 for 30 min. A degassed solution of 1st generation of Grubbs™ catalyst (6 mg, 0.0072 mmol) in dry DCM (15 mL) was added by cannula. The mixture left stirring at room temperature for 8 h. After completion, the reaction was opened to air then passed through short silica pad and washed with DCM. The solvent was removed *via* rotary evaporator and the resulting dark solid crystallised using DCM:hexane affording **2.62** as a dark brown solid (73 mg, 96%). MP > 350 °C. ^{1}H-NMR (400 MHz, $CDCl_3$) δ 10.22 (s, 2H), 10.13 (s, 2H), 10.02 (s, 4H), 9.34 (dd, *J* = 5.6, 2.9 Hz, 8H), 8.46 (t, *J* = 7.7 Hz, 4H), 8.29 (dd, *J* = 5.7, 2.8 Hz, 8H), 8.02 (s, 4H), 7.82 (t, *J* = 7.8 Hz, 4H), 7.31 (td, *J* = 4.7, 1.3 Hz, 8H), 7.25 – 7.19 (m, 12H), 6.90 (s, 4H), 6.81 (s, 4H), 6.64 (d, *J* = 7.3 Hz, 4H), 6.05 (s, 2H), 5.74 (s, 2H), 4.67 (t, *J* = 7.2 Hz, 4H), 4.57 (t, *J* = 6.3 Hz, 4H), 2.77 – 2.48 (m, 8H), 2.30 (dq, *J* = 26.5, 6.7 Hz, 8H), 2.04 (dt, *J* = 34.6, 7.2 Hz, 8H).^{13}C-NMR (101 MHz, $CDCl_3$) δ 159.14, 154.70, 148.23, 143.11, 137.54, 135.05, 130.02, 128.28, 124.59, 77.33, 77.01, 76.70, 69.10. UV-vis, λmax (DCM)/nm (log ε): 360 (4.91); 421 (5.30), 491 (4.32), 554 (4.15), 609 (4.08), 889 (3.79). IR (KBr, cm^{-1}): 3059, 2917, 2516, 2351, 1806,

1604, 1504, 1463, 1329, 1239, 1175, 1059, 982, 793. MALDI-tof MS $(C_{140}H_{104}La_2N_{16}O_4)^+$ *m/z* $[M]^+$ calcd: 2351.66 found: 2351.64.

***Trans* Closed Triple Decker 2.17**

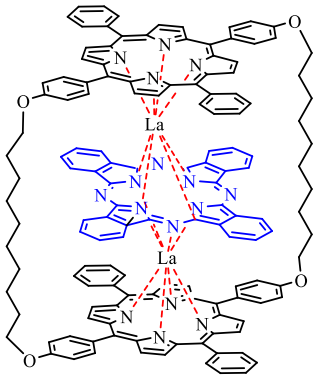

Following a procedure developed by Felix *et al*,[106] *trans* closed TD **2.62** (15 mg, 6.3 µmol) and Pd/C 10% (6 mg) were mixed in EtOAc (1 mL) and 1,4-cyclohexadiene (1 mL, 10.9 mmol) in a sealed tube. The reaction mixture was heated in an oil bath at 100 ºC for 24 h. After cooling to room temperature, the mixture was filtered and the solvent was then removed to obtain pure **2.17** as a dark solid in (13 mg, 86%). MP > 350 ºC. ^{1}H-NMR (500 MHz, $CDCl_3$) δ 10.11 (d, *J* = 8.0 Hz, 4H), 10.04 (d, *J* = 7.8 Hz, 4H), 9.35 (dd, *J* = 5.3, 2.9 Hz, 8H), 8.46 (t, *J* = 7.3 Hz, 4H), 8.30 (dd, *J* = 5.3, 2.9 Hz, 8H), 7.98 (d, *J* = 7.8 Hz, 4H), 7.82 (t, *J* = 7.3 Hz, 4H), 7.29 (d, *J* = 4.2 Hz, 8H), 7.23 (d, *J* = 4.2 Hz, 12H), 6.87 (d, *J* = 7.8 Hz, 4H), 6.74 (d, *J* = 7.8 Hz, 4H), 6.64 (d, *J* = 7.0 Hz, 4H), 4.59 (t, *J* = 7.2 Hz, 8H), 2.43 – 2.21 (m, 8H), 1.92 (s, 16H), 1.81 (s, 8H). ^{13}C-NMR (126 MHz, $CDCl_3$) δ 158.61, 153.52, 147.99, 147.70, 143.06, 136.57, 130.04, 128.28, 127.10, 125.79, 123.44, 119.99, 119.78, 77.27, 77.02, 76.77, 68.72, 31.60, 29.44, 29.27, 28.55, 26.63, 22.67, 14.13. UV-vis, λ_{max} (DCM)/nm (log ε): 362 (4.99); 421 (5.38), 488 (4.43), 555 (4.23), 609 (4.17), 887 (3.89). IR (KBr, cm^{-1}): 3059, 2919, 2847, 2351, 1803, 1604, 1503, 1462, 1328, 1241, 1174, 982, 794. MALDI-tof MS $(C_{140}H_{108}La_2N_{16}O_4)^+$ *m/z* $[M]^+$ calcd: 2355.69 found: 2355.47.

References

[1] R. P. Feynman, *Int. J. Eng. Sci* **1960**, *23*, 22–36.

[2] M. Schulz, *Nature* **1999**, *399*, 729–730.

[3] J. M. Lehn, *Angew. Chem. Int. Ed.* **1988**, *27*, 89–112.

[4] E. Fischer, *Ber. Dtsch. Chem. Ges.* **1894**, *27*, 2985–2993.

[5] C. J. Pedersen, *J. Am. Chem. Soc.* **1967**, *89*, 7017–7036.

[6] D. J. Cram, J. M. Cram, *Science (1979)* **1974**, *183*, 803–809.

[7] Y. Timsit, D. Moras, *EMBO J.* **1994**, *13*, 2737–2746.

[8] K. Ariga, T. Kunitake, *Supramolecular Chemistry – Fundamentals and Applications*, Springer, Heidelberg, **2006**.

[9] J. Sauvage, *Angew. Chem. Int. Ed.* **2017**, *56*, 11080–11093.

[10] C. J. Bruns, J. F. Stoddart, *The Nature of the Mechanical Bond*, Wiley, Hoboken, NJ, **2016**.

[11] B. L. Feringa, *Angew. Chem. Int. Ed.* **2017**, *56*, 11060–11078.

[12] P. Wu, B. Dharmadhikari, P. Patra, X. Xiong, *Nanoscale Adv.* **2022**, *4*, 3418–3461.

[13] J. L. Mann, A. C. Yu, G. Agmon, E. A. Appel, *Biomater. Sci.* **2018**, *6*, 10–37.

[14] M. J. Webber, R. Langer, *Chem Soc Rev* **2017**, *46*, 6600–6620.

[15] J. F. Stoddart, *Chem.Soc.Rev.* **2009**, *38*, 1802–1820.

[16] C. Yang, H. Chen, *ACS Appl. Nano Mater.* **2022**, *5*, 13874–13886.

[17] J. E. Beves, B. A. Blight, C. J. Campbell, D. A. Leigh, R. T. McBurney, *Angew. Chem. Int. Ed.* **2011**, *50*, 9260–9327.

[18] D. A. Leigh, G. Gil-ramírez, D. A. Leigh, A. J. Stephens, *Angew. Chem. Int. Ed.* **2015**, *54*, 6110–6150.

[19] E. Wasserman, *J. Am. Chem. Soc.* **1960**, *82*, 4433–4434.

[20] I. T. Harrison, S. Harrison, *J. Am. Chem. Soc.* **1967**, *3789*, 5723–5724.

[21] G. Schill, A. Lüttringhaus, *Angew. Chem. Int. Ed.* **1964**, *3*, 546–547.

[22] G. Schill, H. Zollenkopf, *Justus Liebigs Ann. Chem.* **1969**, *721*, 53–74.

[23] C. O. Dietrich-Buchecker, J. P. Sauvage, J. P. Kintzinger, *Tetrahedron Lett.* **1983**, *24*, 5095–5098.

[24] B. Mohr, M. Weck, J. P. Sauvage, R. H. Grubbs, *Angew. Chem. Int. Ed.* **1997**, *36*, 1308–1310.

[25] C. Wu, P. R. Lecavalier, Y. X. Shen, H. W. Gibson, *Chem. Mater.* **1991**, *3*, 569–572.

[26] V. Aucagne, K. D. Hänni, D. A. Leigh, P. J. Lusby, D. B. Walker, *J. Am. Chem. Soc.* **2006**, *128*, 2186–2187.

[27] S. M. Goldup, D. A. Leigh, T. Long, P. R. McGonigal, M. D. Symes, J. Wu, *J. Am. Chem. Soc.* **2009**, *131*, 15924–15929.

[28] P. R. Ashton, T. T. Goodnow, A. E. Kaifer, M. V. Reddington, A. M. Z. Slawin, N. Spencer, J. F. Stoddart, C. Vicent, D. J. Williams, *Angew. Chem. Int. Ed.* **1989**, *28*, 1396–1399.

[29] J. A. Bravo, F. M. Raymo, J. F. Stoddart, A. J. P. White, D. J. Williams, *Eur. J. Org. Chem.* **1998**, 2565–2571.

[30] M. Xue, Y. Yang, X. Chi, X. Yan, F. Huang, *Chem. Rev.* **2015**, *115*, 7398–7501.

[31] C. A. Schalley, K. Beizai, F. Vögtle, *Acc. Chem. Res.* **2001**, *34*, 465–476.

[32] J. T. Wilmore, P. D. Beer, *Adv. Mater.* **2024**, *36*, 1–41.

[33] A. Saura-Sanmartin, *Eur. J. Org. Chem.* **2023**, *26*, 1–10.

[34] Y. C. Tse, H. Y. Au-Yeung, *Chem Asian J.* **2023**, *18*, 1–16.

[35] M. Ptaszek, *Prog. Mol. Biol. Transl. Sci.* **2013**, *113*, 59–108.

[36] W. S. Caughey, G. A. Smythe, D. H. O'keeffe, J. E. Maskasky, M. L. Smith, *J. Biol. Chem.* **1975**, *250*, 7602–7622.

[37] M. R. Moore, *An Historical Introduction to Porphyrin and Chlorophyll Synthesis. In Tetrapyrroles: Birth, Life and Death*, Springer, New York, **2009**.

[38] R. A. Sheldon, *Metalloporphyrins in Catalytic Oxidations, Marcel Dekker, New York,* **1994**.

[39] R. Guilard, K. M. Kadish, K. M. Smith, *The Porphyrin Handbook.*, Academic Press, New York, **2000**.

[40] P. J. Brothers, *Chem. Commun.* **2008**, 2090–2102.

[41] T. D. Lash, S. A. Jones, G. M. Ferrence, *J. Am. Chem. Soc.* **2010**, *132*, 12786–12787.

[42] J. Hollingsworth, *Louisiana State University*, **2012**.

[43] J. E. Merritt, K. L. Loening, *Pure & Appl. Chem.* **1979**, *51*, 2251–2304.

[44] D. K. Lavallee, *Synth. React. Inorg. Met.-Org. Chem.* **1982**, *12*, 323–324.

[45] M. Gouterman, G. H. Wagnière, L. C. Snyder, *J. Mol. Spectrosc.* **1963**, *11*, 108–127.

[46] J. S. Lindsey, I. C. Schreiman, H. C. Hsu, P. C. Kearney, A. M. Marguerettaz, *J. Org. Chem.* **1987**, *52*, 827–836.

[47] S. Lindsey, E. Johnson, *Tetrahedron* **1994**, *50*, 8941–8968.

[48] P. Rothemund, *J. Am. Chem. Soc.* **1935**, *57*, 2010–2011.

[49] P. Rothemund, A. R. Menotti, *J. Am. Chem. Soc.* **1941**, *63*, 267–270.

[50] M. Calvin, R. H. Ball, S. Aronoff, *J. Am. Chem. Soc.* **1943**, *65*, 2259.

[51] A. D. Adler, F. R. Longo, D. John, J. Goldmacher, J. Assour, L. Korsakoff, *J. Org. Chem.* **1967**, *32*, 476.

[52] J. S. Lindsey, H. C. Hsu, I. C. Schreiman, *Tetrahedron Lett.* **1986**, *27*, 4969–4970.

[53] R. G. Little, J. A. Anton, P. A. Loach, J. A. Ibers, *J. Heterocycl. Chem.* **1975**, *12*, 343–349.

[54] G. G. Meng, B. R. James, K. A. Skov, M. Korbelik, *CAN. J. CHEM.* **1994**, *72*, 2447–2457.

[55] G. P. Arsenault, E. Bullock, S. F. MacDonald, *J. Am. Chem. Soc.* **1960**, *82*, 4384–4389.

[56] L. Yu, K. Muthukumaran, I. V. Sazanovich, C. Kirmaier, E. Hindin, J. R. Diers, P. D. Boyle, D. F. Bocian, D. Holten, J. S. Lindsey, *Inorg. Chem.* **2003**, *42*, 6629–6647.

[57] P. D. Rao, S. Dhanalekshmi, B. J. Littler, J. S. Lindsey, *J. Org. Chem.* **2000**, *65*, 7323–7344.

[58] C. H. Lee, J. S. Lindsey, *Tetrahedron* **1994**, *50*, 11427–11440.

[59] B. J. Littler, Y. Ciringh, J. S. Lindsey, *J. Org. Chem.* **1999**, *64*, 2864–2872.

[60] P. D. Rao, B. J. Littler, G. R. Geier, J. S. Lindsey, *J. Org. Chem.* **2000**, *65*, 1084–1092.

[61] A. Nowak-Król, R. Plamont, G. Canard, J. A. Edzang, D. T. Gryko, T. Balaban, *Chem. Eur. J.* **2015**, *21*, 1488–1498.

[62] B. Koszarna, D. T. Gryko, *J. Org. Chem.* **2006**, *71*, 3707–3717.

[63] S. Mondal, T. Pain, K. Sahu, S. Kar, *ACS Omega* **2021**, *6*, 22922–22936.

[64] S. Mondal, K. Sahu, B. Patra, S. Jena, H. S. Biswal, S. Kar, *Dalton Trans.* **2020**, *49*, 1424–1432.

[65] A. Braun, J. Tcherniac, *Ber. dtsch. chem. Ges.* **1907**, *40*, 2709–2714.

[66] J. A. Faiz, V. Heitz, J. P. Sauvage, *Chem.Soc.Rev.* **2009**, *38*, 422–442.

[67] K. Chichak, M. C. Walsh, N. R. Branda, *Chem. Commun.* **2000**, 847–848.

[68] M. J. Gunter, N. Bampos, D. Johnstone, J. K. M. Sanders, *New J. Chem.* **2001**, *25*, 166–173.

[69] K. Li, D. I. Schuster, D. M. Guldi, M. Á. Herranz, L. Echegoyen, *J. Am. Chem. Soc.* **2004**, *126*, 3388–3389.

[70] P. R. Ashton, M. R. Johnston, J. F. Stoddart, M. S. Toltey, J. W. Wheeler, *J. Chem. Soc., Chem. Commun.* **1992**, 1128–1131.

[71] J. C. Chambron, V. Heitz, J. P. Sauvage, *J. Chem. Soc., Chem. Commun.* **1992**, 1131–1133.

[72] M. J. Langton, J. D. Matichak, A. L. Thompson, H. L. Anderson, *Chem. Sci.* **2011**, *2*, 1897–1901.

[73] S. Durot, J. Taesch, V. Heitz, *Chem. Rev.* **2014**, *114*, 8542–8578.

[74] M. J. Gunter, *Eur. J. Org. Chem.* **2004**, 1655–1673.

[75] M. J. Gunter, S. M. Farquhar, K. M. Mullen, *New J. C hem.* **2004**, *28*, 1443–1449.

[76] K. M. Mullen, K. D. Johnstone, D. Nath, N. Bampos, J. K. M. Sanders, M. J. Gunter, *Org. Biomol. Chem.* **2009**, *7*, 293–303.

[77] Y. C. Tse, R. Hein, E. J. Mitchell, Z. Zhang, P. D. Beer, *Chem. Eur. J.* **2021**, *27*, 14550 – 14559.

[78] Y. Miyazaki, C. Kahlfuss, A. Ogawa, T. Matsumoto, J. A. Wytko, K. Oohora, T. Hayashi, J. Weiss, *Chem. Eur.J.* **2017**, *23*, 13579–13582.

[79] L. De Juan-Fernández, P. W. Münich, A. Puthiyedath, B. Nieto-Ortega, S. Casado, L. Ruiz-González, E. M. Pérez, D. M. Guldi, *Chem. Sci.* **2018**, *9*, 6779–6784.

[80] S. Yamamoto, H. Iida, E. Yashima, *Angew. Chem. Int. Ed.* **2013**, *52*, 6849–6853.

[81] N. Ousaka, S. Yamamoto, H. Iida, T. Iwata, S. Ito, R. Souza, Y. Hijikata, S. Irle, E. Yashima, *J. Org. Chem.* **2021**, *86*, 10501–10516.

[82] R. Djemili, S. Adrouche, S. Durot, V. Heitz, *J. Org. Chem.* **2023**, *88*, 14760–14766.

[83] L. Schoepff, L. Kocher, S. Durot, V. Heitz, *J. Org. Chem.* **2017**, *82*, 5845–5851.

[84] A. G. Martynov, Y. Horii, K. Katoh, Y. Bian, J. Jiang, M. Yamashita, Y. G. Gorbunova, *Chem Soc Rev* **2022**, *51*, 9262–9339.

[85] H. Wang, K. Wang, Y. Bian, J. Jiang, N. Kobayashi, *Chemical Communications* **2011**, *47*, 6879–6881.

[86] K. P. Birin, Y. G. Gorbunova, A. Yu. Tsivadze, *J Porphyr Phthalocyanines* **2009**, *13*, 283–290.

[87] D. González-Lucas, S. C. Soobrattee, D. L. Hughes, G. J. Tizzard, S. J. Coles, A. N. Cammidge, *Chem. Eur.J.* **2020**, *26*, 10724–10728.

[88] G. R. Geier, J. S. Lindsey, *Tetrahedron* **2004**, *60*, 11435–11444.

[89] F. L. Benton, T. E. Dillon, *J Am Chem Soc* **1942**, *64*, 1128–1129.

[90] J. F. W. McOmie, M. L. Watts, D. E. West, *Tetrahedron* **1968**, *24*, 2289–2292.

[91] S. A. V. Jannuzzi, E. G. R. de Arruda, F. A. Lima, M. A. Ribeiro, C. Brinatti, A. L. B. Formiga, *Chemistry Select* **2016**, *1*, 2235–2243.

[92] N. E. Galanin, G. P. Shaposhnikov, *Russ J Gen Chem* **2012**, *82*, 1734–1739.

[93] J. S. Lindsey, R. W. Wagner, *J. Org. Chem.* **1989**, *54*, 828–836.

[94] K. P. Birin, Y. G. Gorbunova, A. Y. Tsivadze, *Magn.Reson.Chem.* **2010**, *48*, 505–515.

[95] X. Sun, R. Li, D. Wang, J. Dou, P. Zhu, F. Lu, C. Ma, C. F. Choi, D. Y. Y. Cheng, D. K. P. Ng, N. Kobayashi, J. Jiang, *Eur. J. Inorg. Chem.* **2004**, 3806–3813.

[96] N. Datta-Gupta, D. Malakar, L. Rice, S. Rivers, *J. Heterocycl. Chem.* **1987**, *24*, 629–632.

[97] A. Nowak-Krl, R. Plamont, G. Canard, J. A. Edzang, D. T. Gryko, T. S. Balaban, *Chem. Eur. J.* **2015**, *21*, 1488–1498.

[98] J. A. E. Guzmán, H. Zhang, E. Rivera, M. Lavertu, X. X. Zhu, *ACS Appl. Polym. Mater.* **2021**, *3*, 3659–3665.

[99] C. Zhang, H. Pan, C. Chen, Y. Zhou, *ACS Macro Lett.* **2022**, *11*, 434–440.

[100] D. Villemin, B. Nechab, *J. Chem. Res.* **2000**, 432–434.

[101] A. N. Cammidge, K. V. L. Crépy, *J. Org. Chem.* **2003**, *68*, 6832–6835.

[102] H. Lu, C. Li, H. Jiang, C. L. Lizardi, X. P. Zhang, *Angew. Chem. Int. Ed.* **2014**, *53*, 7028–7032.

[103] X. Sun, D. Li, G. Chen, J. Zhang, *Dyes and Pigments* **2006**, *71*, 118–122.

[104] L. Rogers, E. Burke-Murphy, M. O. Senge, *Eur. J. Org. Chem.* **2014**, 4283–4294.

[105] M. Scholl, S. Ding, C. W. Lee, R. H. Grubbs, *Org. Lett.* **1999**, *1*, 953–956.

[106] A. M. Felix, E. P. Heimer, T. J. Lambros, C. Tzougraki, J. Meienhofer, *J. Org. Chem.* **1978**, *43*, 4194–4196.

[107] M. H. Alshammari, S. M. N. Alhunayhin, D. L. Hughes, I. Chambrier, A. N. Cammidge, *Org. Lett.* **2024**, *26*, 1561–1565.

[108] P. D. Rao, B. J. Littler, G. R. Geier, J. S. Lindsey, *J. Org. Chem.* **2000**, *65*, 1084–1092.

[109] M. Suzuki, A. Osuka, *Org. Lett.* **2003**, *5*, 3943–3946.

[110] D. G. Lucas, *University of East Anglia* **2014**.

[111] G. Lu, X. Zhang, X. Cai, Y. Fang, M. Zhu, W. Zhu, Z. Ou, K. M. Kadish, *J. Porphyrins Phthalocyanines* **2013**, *17*, 1–13.

[112] E. E. Bonfantini, A. K. Burrell, W. M. Campbell, M. J. Crossley, J. J. Gosper, M. M. Harding, D. L. Officer, D. C. W. Reid, *J. Porphyrins Phthalocyanines* **2002**, *6*, 708–719.

[113] B. Shi, R. W. Boyle, *J. Chem. Soc., Perkin Trans.* **2002**, 1397–1400.

Appendix

OL | Organic Letters

pubs.acs.org/OrgLett

Letter

Scramble-Free Synthesis of Unhindered *trans*-A_2B_2-Mesoaryl Porphyrins via Bromophenyl Dipyrromethanes

Muteb H. Alshammari, Sultanah M. N. Alhunayhin, David L. Hughes, Isabelle Chambrier, and Andrew N. Cammidge*

Cite This: https://doi.org/10.1021/acs.orglett.3c04215

Read Online

ACCESS | Metrics & More | Article Recommendations | Supporting Information

ABSTRACT: *Trans*-disubstituted porphyrins are highly valuable intermediates across diverse fields, but they pose a significant synthesis challenge in some cases due to scrambling and formation of complex mixtures. Conditions that minimize scrambling also lower yields, but steric hindrance around the meso-aryl substituent can effectively suppress scrambling altogether. Here we report a straightforward approach to valuable trans-A_2B_2 porphyrin intermediates that are otherwise very difficult to obtain, through use of removable blocking bromide substituents.

The synthetic chemistry of porphyrins was first revolutionized by Adler and Longo's simple procedure that permitted easy access to *meso*-aryl porphyrins in a single step from pyrrole and aromatic aldehydes by refluxing in propionic acid open to air.[1] The general methodology was subsequently refined and expanded by Lindsey and co-workers who, among many other developments, introduced higher yielding protocols that employed milder acidic conditions in organic solvents to allow the incorporation of more sensitive substrates (Scheme 1).[2]

Scheme 1. Direct Synthesis of *meso*-Aryl Porphyrins

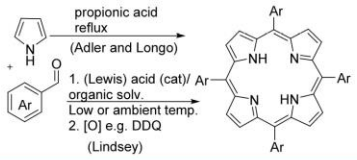

Unsymmetrically substituted derivatives can be accessed through a mixed condensation of pyrrole with two different aldehydes. As expected, reactions of this type produce a complex mixture with low yields of the individual products isolated after challenging separations. The reactions can be useful for synthesis of A_3B type porphyrins, and we have exploited this in our own work for building symmetrical diporphyrins as precursors to multidecker systems,[3] and unsymmetrical chromophore dyads.[4] The strategy is rarely useful for A_2B_2 derivatives where both AABB (*cis*) and ABAB (*trans*) isomers are formed. The *trans* isomers are highly valued intermediates and have been widely employed across diverse fields including supra-/supermolecule construction and catalysis.[5−7] A rational approach to the synthesis of *trans*-ABAB porphyrins exists[6] whereby a preformed dipyrromethane is condensed with a different aldehyde. The synthesis, which follows from MacDonald's original use of a dipyrromethane dialdehyde + dipyrromethane,[8] is widely employed and is highly successful in selected cases. However, a major problem that is inevitably encountered in these syntheses is that of scrambling, whereby acidolysis of dipyrromethane and/or higher oligomers (essentially reverse condensation) leads to a set of products identical to that expected from a simple mixed condensation with two aldehydes. The reaction has been carefully and systematically investigated, and conditions have been developed to minimize scrambling. Typically, conditions that minimize scrambling have a negative impact on yield, but a key observation is that significant steric hindrance around the *meso*-aryl substituent can effectively suppress scrambling altogether (Scheme 2).[6] In many cases this is a benefit because the same bulky substituents aid the porphyrin solubility (useful in supra- and supermolecule construction and characterization) and can affect the environment above and below the porphyrin plane around the axial position of any incorporated metal ion, a feature that can be exploited in catalysis.[9]

In our ongoing work on heteroleptic triple-decker porphyrin−phthalocyanine complexes[3] we required efficient

Received: December 15, 2023
Revised: January 24, 2024
Accepted: February 14, 2024

Scheme 2. Efficient Rational Synthesis of *trans*A_2B_2*meso*-Aryl Porphyrins Using a Dipyrromethane Bearing a Sterically Hindered Aryl (e.g., Mesityl, Top) and Inefficient Synthesis Due to Scrambling When Unhindered Aryl Substituents Are Employed (Bottom)[6b]

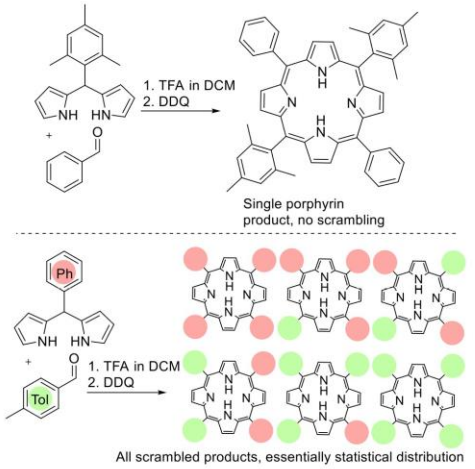

Scheme 3. Attempted Synthesis of *trans*-Dimethoxyphenyl Porphyrin 2 Is Inefficient Due to Scrambling and Favors *cis*-Isomer Production (Top); Lightly Functionalized Opposite-Opposite *trans*-Substituted Porphyrins Like the Target 4 (Bottom) Are Not Accessible

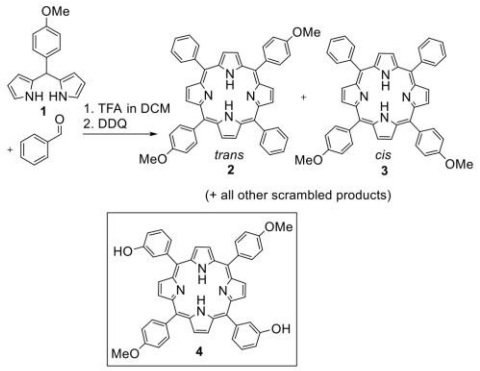

syntheses of differentially substituted *trans* ABAB-*meso*-aryl porphyrins suitable for further elaboration at either of the 5,15-positions only, or separately at the 5,15- and then 10,20-positions. The planned chemistry is one example where the use of sterically hindered aryl substituents cannot be used, because the hindrance required for efficient *trans*-porphyrin synthesis prevents the subsequent face-to-face assembly of multidecker complexes. Here even fluorine substituents on the 2,6-positions prevent face-to-face assembly and essentially only hydrogen can be accommodated. However, porphyrins bearing only remote functionality (3- and 4-positions) are valuable for elaboration in many other areas also, for example to build oligomers and polymers, and for attachment to complementary organic and inorganic species and surfaces.[10] We particularly targeted *trans*-porphyrins bearing opposite pairs of hydroxyl and/or methoxy groups, knowing the latter can be selectively hydrolyzed to reveal phenolic residues following alkylation of the first pair of phenols and therefore provide valuable versatility for further stepwise elaboration. *trans*-Bis(4-methoxyphenyl)porphyrin **2** can be prepared using the dipyrromethane route, but the outcome is similar to the standard mixed porphyrin synthesis from aldehyde precursors. The reactions yielded the full mixture of scrambled products from which the dimethoxy isomeric mixture can be isolated in low (5−12%) yield (Scheme 3). The isomers cannot be separated, but NMR analysis of the mixture shows that the ratio of isomers is between 2:1 and 1:1 (Supporting Information). Hydrolysis allows careful separation of the isomeric diols and reveals the major isomer to be *cis* (5,10-). The presence of the activating methoxy substituent no doubt accelerates acidolysis. The reason for domination of the *cis*-isomer over *trans* is less clear, but the result is consistent with reported direct synthesis of di(4-hydroxyphenyl)porphyrins where the *cis*-isomer is also formed preferentially.[11] The differentially substituted *trans* di(4-methoxyphenyl)-di(3-hydroxyphenyl)porphyrin **4** is unknown, and there is no obvious direct synthesis possible. Our brief investigation of mixed cyclizations confirmed that separation of the porphyrin mixture, and particularly the isomers, would be impractical.

While multistep synthesis via cross-coupling strategies is possible,[12] we reasoned that the most pragmatic solution to overcoming the scrambling issue would be to employ steric blocking groups that could later be removed after guiding efficient dipyromethane + aldehyde porphyrin synthesis without scrambling. The success of the sequence would rely on the ready availability of suitable precursors, so that the overall effectiveness of the sequence outweighed the inherent low atom economy of protecting group strategies. A survey of suitably designed benzaldehyde derivatives highlighted the potential of 3-hydroxy-2,4,6-tribromobenzaldehyde **5** which is readily available both commercially and from bromination of 3-hydroxybenzaldehyde.[13] We recognized that aldehyde **5** could act as a precursor for both the complex, differentially substituted porphyrin **4**, and the simple (but difficult to access) *trans*-dimethoxyporphyrin **2** via common intermediate *trans*-porphyrin **7**. The sequence is shown in Scheme 4 along with the simple statistical porphyrin synthesis that was employed to generate a suitable model porphyrin **9** for the initial evaluation of deprotection (reduction) conditions.

Unsurprisingly the hindered aldehyde **5** proved to be less reactive than benzaldehyde itself, resulting in a 2% yield of the 3:1 porphyrin **9** alongside tetraphenylporphyrin (TPP) as the major porphyrin product. Nevertheless, sufficient porphyrin **9** was isolated to allow investigation of known reduction conditions employing triethylsilane and palladium chloride catalyst (Scheme 5).[14] Porphyrin **9** and $PdCl_2$ (5 mol %) were heated in triethylsilane at 120 °C in a sealed tube, and the reaction was monitored periodically by analysis of aliquots by MALDI-MS. Reduction proceeded slowly, and it was clear that palladium porphyrin derivatives were also formed in the process. While this is not surprising, and the palladium can be easily removed in the acidic workup, the side reaction effectively removes the palladium catalyst from the system

https://doi.org/10.1021/acs.orglett.3c04215
Org. Lett. XXXX, XXX, XXX−XXX

Scheme 4. Synthesis of Lightly Substituted *Trans* Porphyrins Employing Removable Bromide Substituents To Prevent Scrambling

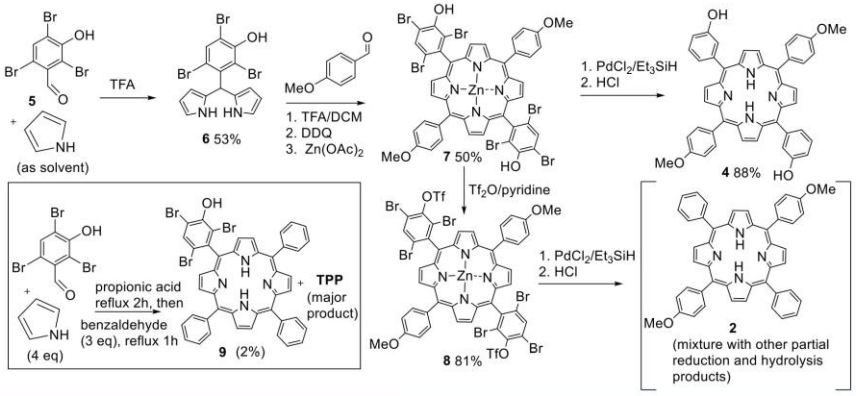

Scheme 5. Reductive Debromination of Porphyrin 9 Using Triethyl Silane and Palladium Chloride

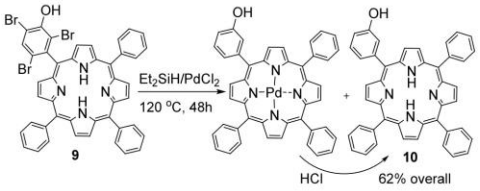

and slows the rate. Nevertheless, mono-(3-hydroxyphenyl)-porphyrin **10** was isolated after workup (HCl) in 62% yield.

The main synthesis of *trans*-porphyrin targets began with straightforward synthesis of dipyrromethane **6** from the reaction of aldehyde **5** with excess pyrrole (used as reactant and solvent). As expected, dipyrromethane **6** proved to be relatively stable and could be stored for several weeks as a crystalline solid in the dark at 0−5 °C without any noticeable degradation. Pleasingly the synthesis of the corresponding *trans*-porphyrin was also smoothly achieved using 4-methoxybenzaldehyde following conditions developed by Lindsey,[2] and it is worth noting this electron-rich, unhindered aldehyde represents one of the most challenging reactants in terms of suppressing scrambling during porphyrin synthesis. However, based on the previous observations during reductive debromination of the model porphyrin **9**, we decided to insert zinc at the end of the reaction in order to prevent palladium sequestration during subsequent reduction. Dipyrromethane **6** and 4-methoxybenzaldehyde were therefore reacted together in DCM (0.85 mM) with TFA catalyst at 0 °C. At the end of the reaction, DDQ was added followed (after 1 h) by addition of $Zn(OAc)_2$. *Trans* porphyrin **7** was isolated as the only observed porphyrin product in a 50% yield. Porphyrin **7** exists as an equilibrated mixture of atropisomers. They appear as two distinct spots by tlc but are essentially identical in ^{1}H NMR spectroscopy. Atropisomer interconversion occurs in minutes at room temperature (tlc).

Reductive debromination of zinc porphyrin **7** was achieved smoothly by using triethylsilane and $PdCl_2$ at 120 °C for 3−5 days. The crude reaction mixture was treated with HCl to remove zinc, neutralized, and separated to give the target differentially substituted *trans* porphyrin **4** in 88% yield. Alternative reduction conditions using formate and palladium, successfully employed by us in other projects for reduction of Ar−X,[15] gave very slow reduction, an observation that likely reflects the effect of the electron-donating hydroxyl group in retarding palladium insertion (oxidative addition) into the Ar−Br bonds.

Conversion of intermediate **7** into *trans* di(methoxyphenyl) porphyrin **2** required reductive removal of both the bromide and hydroxyl substituents and was achieved by first converting the free phenols to triflates using triflic anhydride. Reduction of triflate **8** was attempted by using both $PdCl_2/Et_3SiH$ and Pd/formate conditions. In each case the reduction of both triflate and bromide could be achieved, but the reactions were slow and impractical. Each reaction was monitored periodically by MALDI-MS. Under $PdCl_2/Et_3SiH$ conditions, the MALDI-MS spectra clearly demonstrated initial preferential (faster) removal of bromides but very sluggish aryl triflate reduction (incomplete after 7 days at 120 °C). Reductions using Pd/formate conditions were also inefficient and slow, with evidence for competing triflate hydrolysis at long reaction times. Rather than pursue investigation of alternative conditions to achieve this, more simple, target, we elected to instead use the developed blocking strategy with an alternative bromoaryl aldehyde. Fortunately, 2,6-dibromobenzaldehyde is available. Indeed, it has been previously employed for synthesis of *trans* porphyrins, although not with challenging electron-rich partners.[9] The convenient synthesis of *trans* di-(methoxyphenyl) porphyrin **2** is shown in Scheme 6.

Dipyrromethane **11** was synthesized as reported,[9] and reaction first with 4-methoxybenzaldehyde, then DDQ, and then zinc acetate gave the corresponding *trans* Zn-porphyrin **13** with no evidence for other scrambled products; Scheme 6 (inset) shows the MALDI-MS taken for an aliquot of the reaction mixture, before addition of zinc acetate, with essentially a single signal (cluster at m/z 990.62) corresponding to porphyrin **12**. The zinc porphyrin **13** showed a strong tendency toward crystallization that complicated chromatographic purification. It was found to be more convenient to

https://doi.org/10.1021/acs.orglett.3c04215
Org. Lett. XXXX, XXX, XXX−XXX

Scheme 6. Convenient Synthesis of *trans* Dimethoxyporphyrin 2 (Inset Shows the Single Mass Observed in MALDI-MS of a Sample before Addition of Zinc Acetate), and the X-ray Crystal Structure for Porphyrin 13 (Shown as Elipsoids at 65% Probability, H-Atoms and Molecule of Chloroform Removed for Clarity)

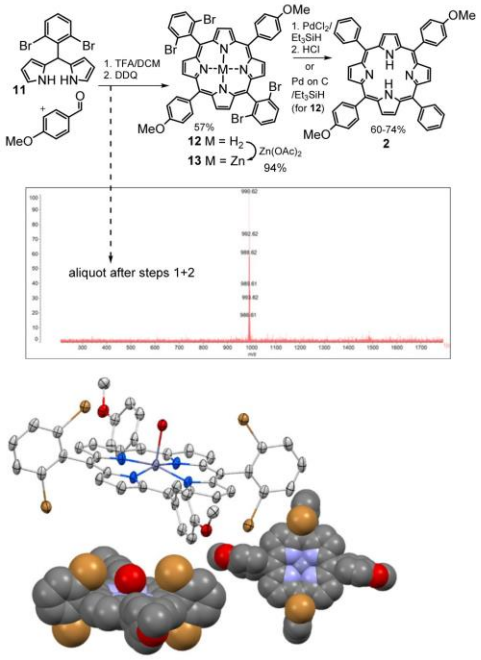

first isolate the metal-free porphyrin **12** (57%) and then insert zinc in a separate step (94%). Crystals of porphyrin **13** suitable for X-ray diffraction were obtained (CCDC 2313839), and the structure is also shown in Scheme 6. The space-filling representations clearly illustrate the effective steric blocking of *meso*-sites provided by the *o*-bromines. Reduction also proceeded smoothly using $PdCl_2/Et_3SIH$ and gave the desired porphyrin **2** in 74% yield after workup (HCl) and straightforward isolation. Direct reductive debromination of metal-free *trans* porphyrin **12** was also investigated by using palladium on carbon. Pleasingly the reduction works well, again employing triethylsilane, giving porphyrin **2** in 60% yield.

In conclusion, we have developed a straightforward approach to valuable *trans*-A_2B_2 porphyrin intermediates that are otherwise very difficult to obtain by direct methods. Access to such porphyrins, which bear remote functionality but lack excessive steric blocking on the porphyrin core, opens the potential for wide application, particularly in super/supramolecule construction and surface grafting.

■ ASSOCIATED CONTENT

Data Availability Statement

The data underlying this study are available in the published article and its Supporting Information.

Supporting Information

The Supporting Information is available free of charge at https://pubs.acs.org/doi/10.1021/acs.orglett.3c04215.

Experimental and characterization data for synthesized compounds plus crystallography details for porphyrin **13** (PDF)

Accession Codes

CCDC 2313839 contains the supplementary crystallographic data for this paper. These data can be obtained free of charge via www.ccdc.cam.ac.uk/data_request/cif, or by emailing data_request@ccdc.cam.ac.uk, or by contacting The Cambridge Crystallographic Data Centre, 12 Union Road, Cambridge CB2 1EZ, UK; fax: +44 1223 336033.

■ AUTHOR INFORMATION

Corresponding Author

Andrew N. Cammidge − *School of Chemistry, University of East Anglia, Norwich NR4 7TJ, U.K.;* orcid.org/0000-0001-7912-4310; Email: a.cammidge@uea.ac.uk

Authors

Muteb H. Alshammari − *School of Chemistry, University of East Anglia, Norwich NR4 7TJ, U.K.*

Sultanah M. N. Alhunayhin − *School of Chemistry, University of East Anglia, Norwich NR4 7TJ, U.K.*

David L. Hughes − *School of Chemistry, University of East Anglia, Norwich NR4 7TJ, U.K.*

Isabelle Chambrier − *School of Chemistry, University of East Anglia, Norwich NR4 7TJ, U.K.*

Complete contact information is available at: https://pubs.acs.org/10.1021/acs.orglett.3c04215

Author Contributions

M.A. and S.A. performed the experimental synthetic work with equal contribution. I.C. and D.L.H. performed X-ray crystallographic analysis. A.C. conceived and led the research and prepared the manuscript draft.

Notes

The authors declare no competing financial interest.

■ ACKNOWLEDGMENTS

Financial support is gratefully acknowledged from Northern Border University (MA) and Almajmaah University (SA).

■ REFERENCES

(1) Adler, A. D.; Longo, F. R.; Finarelli, J. D.; Goldmacher, J.; Assour, J.; Korsakoff, L. A simplified synthesis of *meso*-tetraphenylporphin. *J. Org. Chem.* **1967**, *32*, 476.

(2) Lindsey, J. S.; Schreiman, I. C.; Hsu, H. C.; Kearney, P. C.; Marguerettaz, A. M. Rothemund and Adler-Longo reactions revisited: synthesis of tetraphenylporphyrins under equilibrium conditions. *J. Org. Chem.* **1987**, *52*, 827−836.

(3) González-Lucas, D.; Soobrattee, S. C.; Hughes, D. L.; Tizzard, G. J.; Coles, S. J.; Cammidge, A. N. Straightforward and controlled synthesis of porphyrin-phthalocyanine-porphyrin heteroleptic triple-decker assemblies. *Chem.—Eur. J.* **2020**, *26*, 10724−10728.

(4) Bressan, G.; Cammidge, A. N.; Jones, G. A.; Heisler, I. A.; González-Lucas, D.; Remiro-Buenamañana, S.; Meech, S. R. Electronic Energy Transfer in a subphthalocyanine-Zn porphyrin dimer studied by linear and nonlinear ultrafast spectroscopy. *J. Phys. Chem.* **2019**, *123*, 5724−5733.

(5) Marschner, S. M.; Haldar, R.; Fuhr, O.; Wöll, W.; Bräse, S. Modular synthesis of trans-A2B2-porphyrins with terminal esters: systematically extending the scope of linear linkers for porphyrin-based MOFs. *Chem.—Eur. J.* **2021**, *27*, 1390−1401 and references therein.
(6) (a) Littler, B. J.; Ciringh, Y.; Lindsey, J. S. Investigation of conditions giving minimal scrambling in the synthesis of trans-porphyrins from dipyrromethanes and aldehydes. *J. Org. Chem.* **1999**, *64*, 2864−2872 and references therein. (b) Geier, G. R., III; Littler, B. J.; Lindsey, J. S. Investigation of porphyrin-forming reactions. Part 3. The origin of scrambling in dipyromethane + aldehyde condensations yielding *trans*-A_2B_2-tetraarylporphyrins. *J. Chem. Soc., Perkin Trans.* **2001**, *2*, 701−711.
(7) Zwick, P.; Dulić, D.; van der Zant, H. S. J.; Mayor, M. Poprhyrins as building blocks for single-molecule devices. *Nanoscale* **2021**, *13*, 15500−15525.
(8) (a) Arsenault, G. P.; Bullock, E.; MacDonald, S. F. Pyrromethanes and porphyrins therefrom. *J. Am. Chem. Soc.* **1960**, *82*, 4384−4389. (b) Lash, T. D. What's in a name? The MacDonald condensation. *J. Porphyrins Phthalocyanines* **2016**, *20*, 855−888.
(9) Lu, H.; Li, C.; Jiang, H.; Lizardi, C. L.; Zhang, X. P. Chemoselective amination of propargylic C(sp^3)-H bonds by cobalt(II)-based metalloradical catalysis. *Angew. Chem.Int. Ed.* **2014**, *53*, 7028−7032.
(10) (a) Walter, M. G.; Rudine, A. B.; Wamser, C. C. Porphyrins and phthalocyanines in solar photovoltaic cells. *J. Porphyrins Phthalocyanines* **2010**, *14*, 759−792. (b) Day, N. U.; Wamser, C. C.; Walter, M. G. Porphyrin polymers and organic frameworks. *Polym. Int.* **2015**, *64*, 833−857.
(11) Esquivel Guzmán, J. A.; Zhang, H.; Rivera, E.; Lavertu, M.; Zhu, X.-X. Porphyrin-based polyesters synthesized by enzymatic catalysis. *ACS Appl. Polym. Mater.* **2021**, *3*, 3659−3665.
(12) Shi, B.; Boyle, R. W. Synthesis of unsymmetrically substituted meso-phenylporphyrins by Suzuki cross coupling reactions. *J. Chem. Soc., Perkin Trans.* **2002**, *1*, 1397−1400.
(13) Osuna, M. R.; Aguirre, G.; Somanathan, R.; Molins, E. Asymmetric synthesis of amathamides A and B: novel alkaloids isolated from *Amathia wilsoni*. *Tetrahedron Asymm.* **2002**, *13*, 2261−2266.
(14) Villemin, D.; Nechab, B. Rapid and efficient palladium catalysed reduction of aryl halides by triethylsilane under microwave irradiation. *J. Chem. Res. (S)* **2000**, *2000*, 432−434.
(15) Cammidge, A. N.; Crépy, K. C. Application of the Suzuki reaction as the key step in the synthesis of a novel atropisomeric biphenyl derivative for use as a liquid crystal dopant. *J. Org. Chem.* **2003**, *68*, 6832−6835.

https://doi.org/10.1021/acs.orglett.3c04215
Org. Lett. XXXX, XXX, XXX−XXX

Crystal data and structure refinement for

La_2-triple-decked-phthal-porph-phthal with two O-$(CH_2)_{10}$-O bridges

---

Identification code	isabf1405
Elemental formula	C150.60 H117.20 Cl8.72 La2 N16 O4
Formula weight	2801.94
Crystal system, space group	Triclinic, P-1 (no. 2)
Unit cell dimensions	a = 17.0068(2) Å α = 94.4090(10) ° b = 20.0472(2) Å β = 109.6790(10) ° c = 21.9704(2) Å γ = 110.3770(10) °
Volume	6449.80(13) $Å^3$
Z, Calculated density	2, 1.443 Mg/m^3
F(000)	2854
Absorption coefficient	7.213 mm^{-1}
Temperature	100(2) K
Wavelength	1.54184 Å
Crystal colour, shape	purple block
Crystal size	0.58 x 0.38 x 0.32 mm
Crystal mounting:	on a small loop, in oil, fixed in cold N_2 stream

On the diffractometer:

Theta range for data collection	7.663 to 69.997 °

Limiting indices	-20<=h<=20, -24<=k<=24, -26<=l<=25
Completeness to theta = 67.684	99.4 %
Absorption correction	Semi-empirical from equivalents
Max. and min. transmission	1.00000 and 0.43022
Reflections collected (not including absences)	87504
No. of unique reflections	24113 [R(int) for equivalents = 0.073]
No. of 'observed' reflections ($I > 2\sigma_I$)	22192
Structure determined by:	dual methods, in SHELXT
Refinement:	Full-matrix-block least-squares on F^2, in SHELXL
Data / restraints / parameters	24113 / 0 / 1654
Goodness-of-fit on F^2	1.021
Final R indices ('observed' data)	$R_1 = 0.066$, $wR_2 = 0.180$
Final R indices (all data)	$R_1 = 0.069$, $wR_2 = 0.184$
Reflections weighted: $w = [\sigma^2(Fo^2)+(0.1167P)^2+21.8436P]^{-1}$ where $P=(Fo^2+2Fc^2)/3$	
Extinction coefficient	n/a
Largest diff. peak and hole	2.86 and -1.92 e.Å^{-3}
Location of largest difference peak	near La(2)

Table 1. Atomic coordinates (x 10^5) and equivalent isotropic displacement parameters ($Å^2$ x 10^4). U(eq) is defined as one third of the trace of the orthogonalized Uij tensor. E.s.ds are in parentheses.

	x	y	z	U(eq)	S.o.f.#
N(1)	41040(30)	14140(20)	58640(20)	204(8)	
C(2)	43530(30)	14540(30)	53250(20)	213(9)	
C(3)	36870(40)	15900(30)	47950(30)	291(11)	
C(4)	30390(40)	16250(30)	50140(30)	299(11)	
C(5)	32920(30)	15070(30)	56790(20)	234(10)	
C(6)	27720(30)	14570(30)	60680(20)	243(10)	
C(661)	19090(40)	15730(30)	57770(30)	273(11)	
C(662)	11390(40)	10380(40)	52840(40)	458(15)	
C(663)	3390(50)	11440(50)	50190(40)	600(20)	
C(664)	3060(50)	17980(40)	52480(40)	537(18)	
C(665)	10530(50)	23230(40)	57220(40)	564(19)	
C(666)	18650(40)	22200(30)	59890(30)	403(14)	
N(11)	37090(30)	11380(20)	70410(20)	212(8)	
C(12)	29540(30)	12660(30)	66900(20)	228(10)	
C(13)	23460(40)	11320(30)	70370(30)	268(10)	
C(14)	27350(40)	9140(30)	75900(30)	280(11)	
C(15)	35790(30)	9090(30)	75870(20)	230(10)	
C(16)	41680(30)	6720(30)	80650(20)	229(10)	
C(161)	39110(40)	4350(30)	86200(30)	260(10)	
C(162)	31190(40)	-1850(30)	84910(30)	304(11)	
C(163)	29090(40)	-4410(30)	90070(30)	363(13)	
C(164)	34800(40)	-1000(40)	96560(30)	397(14)	
C(165)	42560(40)	5260(30)	97920(30)	362(13)	
C(166)	44680(40)	7930(30)	92750(20)	285(11)	
N(21)	52910(30)	7650(20)	75521(19)	201(8)	
C(22)	49460(30)	5950(20)	80300(20)	195(9)	
C(23)	54970(40)	3040(30)	84950(20)	240(10)	
C(24)	61640(40)	2890(30)	82830(20)	248(10)	
C(25)	60200(30)	5650(20)	76870(20)	204(9)	
C(26)	65290(30)	5820(30)	72890(20)	229(10)	
C(261)	73110(40)	3590(30)	75480(20)	243(10)	

C(262) 72260(40) -3560(30) 73880(30) 370(13)
C(263) 79450(50) -5580(30) 76690(40) 482(16)
C(264) 87790(40) -370(30) 81200(30) 384(13)
C(265) 88760(40) 6740(30) 82710(30) 348(12)
C(266) 81530(40) 8700(30) 79960(30) 308(11)
O(267) 95420(30) -1570(30) 84420(30) 574(13)
C(268) 94860(60) -8920(40) 83860(50) 640(20)
C(269) 104060(50) -8170(40) 88980(40) 575(19)
C(270) 104650(60) -6460(40) 95990(40) 579(19)
C(271) 114280(60) -2730(40) 101230(40) 548(18)
C(272) 119390(50) 5250(40) 101090(40) 507(17)
C(273) 128210(50) 9180(40) 107130(30) 486(16)
C(274) 133870(50) 17030(40) 107010(30) 432(15)
N(31) 56800(30) 10310(20) 63730(20) 203(8)
C(32) 63380(30) 7780(30) 66710(20) 207(9)
C(33) 68000(30) 7200(30) 62320(20) 242(10)
C(34) 64140(30) 9300(30) 56810(30) 242(10)
C(35) 56990(30) 11160(20) 57590(20) 195(9)
C(36) 51060(30) 13410(20) 52810(20) 202(9)
C(361) 52990(30) 14810(30) 46770(20) 204(9)
C(362) 56130(40) 21990(30) 45900(20) 262(10)
C(363) 58210(40) 23580(30) 40520(30) 272(11)
C(364) 57010(30) 18040(30) 35660(20) 217(9)
C(365) 53640(40) 10810(30) 36290(30) 304(11)
C(366) 51760(40) 9300(30) 41830(30) 290(11)
O(367) 59520(20) 20262(18) 30589(16) 248(7)
C(368) 56130(50) 14960(30) 24500(30) 426(15)
C(369) 60220(50) 19110(40) 19990(30) 451(16)
C(370) 70230(60) 20630(40) 21940(40) 520(18)
C(371) 75840(50) 27350(40) 20050(30) 447(15)
C(372) 77790(50) 34520(30) 24380(30) 400(13)
La(1) 52284(2) 17998(2) 70265(2) 157.8(7)
N(41) 51090(30) 28530(20) 78722(19) 193(8)
C(42) 43990(30) 30510(20) 75900(20) 200(9)
C(43) 38340(30) 29510(30) 79780(30) 253(10)
C(44) 30480(40) 30650(30) 79010(30) 318(12)
C(45) 26760(40) 28960(40) 83700(30) 443(15)
C(46) 30540(40) 25970(40) 88910(30) 438(15)
C(47) 38440(40) 24860(30) 89720(30) 345(12)
C(48) 42360(30) 26750(30) 85110(20) 234(10)

C(49) 50430(30) 26350(20) 84390(20) 193(9)
N(50) 56130(30) 24180(20) 88770(19) 203(8)
N(51) 65680(30) 24540(20) 82595(19) 177(7)
C(52) 63420(30) 23760(20) 88020(20) 187(9)
C(53) 70340(30) 22360(20) 93170(20) 207(9)
C(54) 71370(40) 21590(30) 99640(20) 238(10)
C(55) 79280(40) 20920(30) 103520(20) 277(11)
C(56) 85770(40) 20860(30) 101020(30) 273(11)
C(57) 84730(40) 21480(30) 94570(20) 242(10)
C(58) 76800(30) 22270(20) 90650(20) 197(9)
C(59) 73770(30) 23670(20) 84010(20) 182(9)
N(60) 78270(30) 23880(20) 80043(19) 188(8)
N(61) 68830(30) 27750(20) 71344(19) 196(8)
C(62) 75780(30) 25600(20) 74160(20) 182(9)
C(63) 80500(30) 25530(30) 69740(20) 209(9)
C(64) 87800(30) 23680(30) 70120(30) 255(10)
C(65) 90650(40) 24260(30) 64930(30) 353(12)
C(66) 86310(40) 26690(40) 59420(30) 380(13)
C(67) 79040(40) 28490(30) 58970(30) 321(12)
C(68) 76150(30) 27870(30) 64220(20) 222(10)
C(69) 68860(30) 29190(20) 65410(20) 188(9)
N(70) 63250(30) 31600(20) 61096(19) 214(8)
N(71) 53960(30) 31500(20) 67461(19) 200(8)
C(72) 56490(30) 32680(20) 62230(20) 209(9)
C(73) 50540(40) 35560(30) 57660(20) 252(10)
C(74) 50290(40) 37740(30) 51740(30) 336(12)
C(75) 43850(50) 40490(40) 48850(30) 480(17)
C(76) 37670(50) 40820(40) 51550(30) 500(17)
C(77) 37700(50) 38520(40) 57300(30) 384(14)
C(78) 44350(40) 35920(30) 60350(20) 268(11)
C(79) 46520(30) 33330(30) 66470(20) 214(9)
N(80) 41870(30) 32870(20) 70280(20) 215(8)
La(2) 68275(2) 38177(2) 79691(2) 145.5(5)
N(81) 69010(30) 48840(20) 74516(18) 176(7)
C(82) 72800(30) 50280(20) 69890(20) 191(9)
C(83) 68590(40) 54250(30) 65620(20) 241(10)
C(84) 62350(40) 55200(30) 67780(20) 249(10)
C(85) 62670(30) 51860(20) 73380(20) 175(9)
C(86) 57250(30) 51780(20) 77060(20) 184(9)
C(861) 50380(30) 54980(30) 74530(20) 211(9)

C(862) 41230(40) 50610(30) 71340(20) 254(10)
C(863) 35040(40) 53630(30) 68440(30) 313(12)
C(864) 37930(40) 61090(30) 68960(30) 329(13)
C(865) 47020(40) 65510(30) 72300(30) 322(12)
C(866) 53270(40) 62560(30) 75090(20) 251(10)
N(91) 64090(30) 46210(20) 85897(19) 179(7)
C(92) 57830(30) 48960(20) 82800(20) 172(9)
C(93) 52410(30) 49060(30) 86600(20) 211(9)
C(94) 55540(30) 46400(30) 92040(20) 212(9)
C(95) 63030(30) 44820(20) 91670(20) 173(9)
C(96) 68700(30) 42610(20) 96680(20) 180(9)
C(961) 66640(30) 41980(30) 102710(20) 196(9)
C(962) 61410(30) 35170(30) 103510(20) 228(10)
C(963) 59140(40) 34740(30) 109000(30) 270(11)
C(964) 61820(40) 40920(30) 113680(30) 281(11)
C(965) 66920(40) 47650(30) 112910(30) 307(11)
C(966) 69390(40) 48170(30) 107480(30) 269(11)
N(101) 79210(30) 41560(20) 91357(18) 162(7)
C(102) 76380(30) 41380(20) 96610(20) 167(8)
C(103) 82670(30) 40000(20) 102120(20) 190(9)
C(104) 89210(30) 39330(20) 100210(20) 184(9)
C(105) 87220(30) 40420(20) 93540(20) 171(9)
C(106) 92530(30) 40520(20) 89760(20) 180(9)
C(601) 100320(30) 38290(20) 92480(20) 180(9)
C(602) 107450(30) 41850(20) 98570(20) 192(9)
C(603) 114640(30) 39620(30) 101060(20) 209(9)
C(604) 114600(30) 33690(30) 97330(20) 205(9)
C(605) 107630(30) 30140(30) 91180(20) 229(10)
C(606) 100560(30) 32410(30) 88790(20) 213(9)
O(607) 121230(20) 30979(19) 99268(17) 250(7)
C(608) 128440(30) 34330(30) 105700(30) 260(10)
C(609) 134260(40) 29890(30) 106860(30) 306(11)
C(610) 128810(50) 22030(30) 107010(30) 398(14)
N(111) 83920(30) 44140(20) 79901(18) 179(7)
C(112) 91120(30) 42540(20) 83530(20) 188(9)
C(113) 97160(30) 43350(30) 80120(20) 228(10)
C(114) 93620(30) 45350(30) 74450(20) 219(9)
C(115) 85360(30) 46020(20) 74320(20) 188(9)
C(116) 80060(30) 48660(20) 69480(20) 201(9)
C(611) 82080(30) 49970(30) 63490(20) 227(10)

C(612) 89910(40) 55260(30) 63560(30) 310(11)
C(613) 91210(40) 56470(30) 57680(30) 355(13)
C(614) 84610(40) 52460(30) 51690(30) 298(11)
C(615) 76570(40) 47070(30) 51470(30) 343(12)
C(616) 75460(40) 45830(30) 57260(30) 346(12)
O(617) 84860(30) 53200(20) 45619(18) 353(9)
C(618) 93230(40) 57700(40) 45260(30) 400(14)
C(619) 91440(40) 57020(40) 38000(30) 407(14)
C(620) 89140(40) 49470(30) 34270(30) 370(13)
C(621) 84910(40) 48400(30) 26810(30) 341(12)
C(622) 83750(40) 41270(30) 22920(30) 360(12)

C(804) 81930(80) 80900(80) 66180(50) 930(40)
C(806) 64400(90) 75170(50) 66490(40) 920(40)
C(807) 105730(70) -4630(50) 73600(70) 990(40)
C(808) 107830(80) -13570(160) 72350(140) 2900(200)
C(809) 107440(80) -17380(70) 74280(40) 710(40)
C(811) 95430(90) -250(80) 64960(70) 1270(60)

C(801) 29910(60) -3520(40) 58840(40) 576(18)
Cl(82) 27160(20) -7698(13) 65118(15) 986(9)
Cl(83) 21201(15) -5853(18) 51173(12) 967(9)

C(810) 83620(110) 72500(90) 65180(110) 930(60) 0.6
Cl(84) 86050(30) 73210(30) 58020(20) 902(12) 0.6
Cl(85) 74860(40) 74990(30) 65590(30) 989(14) 0.6

C(901) 109980(50) 36180(40) 115590(40) 492(16)
Cl(92) 100176(12) 34791(11) 117276(9) 553(4)
Cl(93) 114960(20) 30290(20) 118120(20) 770(14) 0.751(9)
Cl(94) 110790(70) 27800(50) 113120(60) 720(30)* 0.249(9)

C(904) 95110(100) 7690(70) 69350(90) 1260(50)
Cl(95) 105080(19) 14632(17) 75140(20) 1133(11)
Cl(96) 96480(30) 7060(30) 62729(17) 687(18) 0.518(10)

C(907) 80770(70) 26300(50) 41470(40) 710(20)
Cl(98) 89832(15) 25883(12) 39829(15) 829(7)
Cl(99) 82384(14) 35067(11) 44637(10) 630(5)

- site occupancy, if different from 1.

* - U(iso) ($Å^2$ x 10^4)

Table 2. Molecular dimensions. Bond lengths are in Ångstroms, angles in degrees. E.s.ds are in parentheses.

N(1)-La(1)	2.480(4)	N(41)-La(2)	2.812(4)
N(11)-La(1)	2.472(4)	N(51)-La(2)	2.773(4)
N(21)-La(1)	2.467(4)	N(61)-La(2)	2.722(4)
N(31)-La(1)	2.501(4)	N(71)-La(2)	2.776(4)
La(1)-N(61)	2.729(4)	La(2)-N(91)	2.465(4)
La(1)-N(51)	2.733(4)	La(2)-N(101)	2.476(4)
La(1)-N(71)	2.762(4)	La(2)-N(81)	2.482(4)
La(1)-N(41)	2.810(4)	La(2)-N(111)	2.491(4)
La(1)-La(2)	3.9124(4)		

N(21)-La(1)-N(11)	72.60(13)	N(51)-La(1)-N(41)	59.54(11)
N(21)-La(1)-N(1)	113.12(13)	N(71)-La(1)-N(41)	59.10(11)
N(11)-La(1)-N(1)	72.47(13)	N(21)-La(1)-La(2)	121.59(9)
N(21)-La(1)-N(31)	72.12(13)	N(11)-La(1)-La(2)	124.34(9)
N(11)-La(1)-N(31)	113.02(13)	N(1)-La(1)-La(2)	125.27(9)
N(1)-La(1)-N(31)	72.00(13)	N(31)-La(1)-La(2)	122.60(9)
N(21)-La(1)-N(61)	114.21(9)	N(61)-La(1)-La(2)	44.05(8)
N(11)-La(1)-N(61)	168.18(9)	N(51)-La(1)-La(2)	45.13(8)
N(1)-La(1)-N(61)	111.41(9)	N(71)-La(1)-La(2)	45.21(8)
N(31)-La(1)-N(61)	78.69(9)	N(41)-La(1)-La(2)	45.92(8)
N(21)-La(1)-N(51)	76.46(9)	N(91)-La(2)-N(101)	73.22(12)
N(11)-La(1)-N(51)	113.58(9)	N(91)-La(2)-N(81)	72.40(12)
N(1)-La(1)-N(51)	170.24(9)	N(101)-La(2)-N(81)	113.00(12)
N(31)-La(1)-N(51)	110.76(9)	N(91)-La(2)-N(111)	113.44(13)
N(61)-La(1)-N(51)	61.10(11)	N(101)-La(2)-N(111)	71.94(12)
N(21)-La(1)-N(71)	166.25(9)	N(81)-La(2)-N(111)	71.92(12)
N(11)-La(1)-N(71)	110.50(9)	N(91)-La(2)-N(61)	167.28(9)
N(1)-La(1)-N(71)	80.29(9)	N(101)-La(2)-N(61)	116.79(8)
N(31)-La(1)-N(71)	116.83(9)	N(81)-La(2)-N(61)	108.26(9)
N(61)-La(1)-N(71)	60.53(12)	N(111)-La(2)-N(61)	78.23(9)
N(51)-La(1)-N(71)	90.25(11)	N(91)-La(2)-N(51)	116.85(8)
N(21)-La(1)-N(41)	109.87(9)	N(101)-La(2)-N(51)	78.92(8)
N(11)-La(1)-N(41)	78.44(9)	N(81)-La(2)-N(51)	167.31(9)
N(1)-La(1)-N(41)	116.33(9)	N(111)-La(2)-N(51)	109.53(8)
N(31)-La(1)-N(41)	168.05(9)	N(61)-La(2)-N(51)	60.69(11)
N(61)-La(1)-N(41)	89.97(12)	N(91)-La(2)-N(71)	107.93(9)

N(101)-La(2)-N(71)	166.76(9)	N(51)-La(2)-N(41)	59.06(11)
N(81)-La(2)-N(71)	79.42(9)	N(71)-La(2)-N(41)	58.91(11)
N(111)-La(2)-N(71)	118.03(9)	N(91)-La(2)-La(1)	124.41(9)
N(61)-La(2)-N(71)	60.43(12)	N(101)-La(2)-La(1)	123.17(8)
N(51)-La(2)-N(71)	89.11(11)	N(81)-La(2)-La(1)	123.78(9)
N(91)-La(2)-N(41)	78.75(9)	N(111)-La(2)-La(1)	122.15(9)
N(101)-La(2)-N(41)	109.30(9)	N(61)-La(2)-La(1)	44.21(9)
N(81)-La(2)-N(41)	117.71(9)	N(51)-La(2)-La(1)	44.30(8)
N(111)-La(2)-N(41)	167.05(9)	N(71)-La(2)-La(1)	44.90(8)
N(61)-La(2)-N(41)	90.08(12)	N(41)-La(2)-La(1)	45.88(8)

La(1)-N(41)-La(2)	88.20(11)	La(2)-N(61)-La(1)	91.74(12)
La(1)-N(51)-La(2)	90.57(11)	La(1)-N(71)-La(2)	89.90(11)

N(1)-C(5)	1.385(6)	C(163)-C(164)	1.378(9)
N(1)-C(2)	1.386(6)	C(164)-C(165)	1.389(9)
C(2)-C(36)	1.407(7)	C(165)-C(166)	1.393(7)
C(2)-C(3)	1.444(7)	N(21)-C(22)	1.376(6)
C(3)-C(4)	1.362(8)	N(21)-C(25)	1.380(6)
C(4)-C(5)	1.441(7)	C(22)-C(23)	1.446(6)
C(5)-C(6)	1.408(7)	C(23)-C(24)	1.371(7)
C(6)-C(12)	1.409(7)	C(24)-C(25)	1.439(6)
C(6)-C(661)	1.499(7)	C(25)-C(26)	1.417(7)
C(661)-C(666)	1.380(8)	C(26)-C(32)	1.407(7)
C(661)-C(662)	1.388(9)	C(26)-C(261)	1.496(7)
C(662)-C(663)	1.386(9)	C(261)-C(266)	1.393(8)
C(663)-C(664)	1.394(11)	C(261)-C(262)	1.394(7)
C(664)-C(665)	1.347(11)	C(262)-C(263)	1.385(8)
C(665)-C(666)	1.402(9)	C(263)-C(264)	1.396(10)
N(11)-C(15)	1.376(6)	C(264)-O(267)	1.366(7)
N(11)-C(12)	1.380(6)	C(264)-C(265)	1.376(8)
C(12)-C(13)	1.447(7)	C(265)-C(266)	1.380(7)
C(13)-C(14)	1.360(7)	O(267)-C(268)	1.437(8)
C(14)-C(15)	1.441(7)	C(268)-C(269)	1.535(10)
C(15)-C(16)	1.424(7)	C(269)-C(270)	1.515(11)
C(16)-C(22)	1.410(7)	C(270)-C(271)	1.521(12)
C(16)-C(161)	1.486(7)	C(271)-C(272)	1.540(10)
C(161)-C(166)	1.390(8)	C(272)-C(273)	1.519(11)
C(161)-C(162)	1.400(8)	C(273)-C(274)	1.541(10)
C(162)-C(163)	1.382(7)	C(274)-C(610)	1.531(6)

N(31)-C(32)	1.375(6)	C(56)-C(57)	1.389(7)
N(31)-C(35)	1.382(6)	C(57)-C(58)	1.404(7)
C(32)-C(33)	1.454(7)	C(58)-C(59)	1.460(6)
C(33)-C(34)	1.347(7)	C(59)-N(60)	1.335(6)
C(34)-C(35)	1.449(7)	N(60)-C(62)	1.331(6)
C(35)-C(36)	1.414(7)	N(61)-C(69)	1.359(6)
C(36)-C(361)	1.494(6)	N(61)-C(62)	1.366(6)
C(361)-C(366)	1.395(7)	C(62)-C(63)	1.456(6)
C(361)-C(362)	1.402(7)	C(63)-C(64)	1.394(7)
C(362)-C(363)	1.371(7)	C(63)-C(68)	1.401(7)
C(363)-C(364)	1.389(7)	C(64)-C(65)	1.379(8)
C(364)-O(367)	1.374(5)	C(65)-C(66)	1.410(8)
C(364)-C(365)	1.397(7)	C(66)-C(67)	1.380(8)
C(365)-C(366)	1.389(7)	C(67)-C(68)	1.394(7)
O(367)-C(368)	1.444(6)	C(68)-C(69)	1.454(7)
C(368)-C(369)	1.532(8)	C(69)-N(70)	1.350(6)
C(369)-C(370)	1.517(11)	N(70)-C(72)	1.337(6)
C(370)-C(371)	1.534(9)	N(71)-C(72)	1.366(6)
C(371)-C(372)	1.526(9)	N(71)-C(79)	1.391(6)
C(372)-C(622)	1.515(6)	C(72)-C(73)	1.476(7)
N(41)-C(42)	1.367(6)	C(73)-C(78)	1.387(8)
N(41)-C(49)	1.378(6)	C(73)-C(74)	1.396(7)
C(42)-N(80)	1.337(6)	C(74)-C(75)	1.382(8)
C(42)-C(43)	1.462(7)	C(75)-C(76)	1.386(10)
C(43)-C(44)	1.389(7)	C(76)-C(77)	1.377(9)
C(43)-C(48)	1.404(7)	C(77)-C(78)	1.398(7)
C(44)-C(45)	1.386(8)	C(78)-C(79)	1.457(7)
C(45)-C(46)	1.400(9)	C(79)-N(80)	1.318(6)
C(46)-C(47)	1.392(8)	N(81)-C(82)	1.374(6)
C(47)-C(48)	1.396(7)	N(81)-C(85)	1.374(6)
C(48)-C(49)	1.462(7)	C(82)-C(116)	1.410(6)
C(49)-N(50)	1.335(6)	C(82)-C(83)	1.444(6)
N(50)-C(52)	1.335(6)	C(83)-C(84)	1.362(7)
N(51)-C(52)	1.374(6)	C(84)-C(85)	1.440(6)
N(51)-C(59)	1.380(6)	C(85)-C(86)	1.413(6)
C(52)-C(53)	1.459(6)	C(86)-C(92)	1.409(6)
C(53)-C(58)	1.392(7)	C(86)-C(861)	1.492(6)
C(53)-C(54)	1.400(7)	C(861)-C(862)	1.379(7)
C(54)-C(55)	1.388(7)	C(861)-C(866)	1.406(7)
C(55)-C(56)	1.391(8)	C(862)-C(863)	1.390(7)

C(863)-C(864)	1.384(8)	C(602)-C(603)	1.402(6)
C(864)-C(865)	1.377(9)	C(603)-C(604)	1.387(7)
C(865)-C(866)	1.383(7)	C(604)-O(607)	1.374(5)
N(91)-C(92)	1.369(6)	C(604)-C(605)	1.388(7)
N(91)-C(95)	1.375(6)	C(605)-C(606)	1.386(7)
C(92)-C(93)	1.441(6)	O(607)-C(608)	1.437(6)
C(93)-C(94)	1.365(7)	C(608)-C(609)	1.521(7)
C(94)-C(95)	1.443(6)	C(609)-C(610)	1.535(8)
C(95)-C(96)	1.413(6)	N(111)-C(112)	1.377(6)
C(96)-C(102)	1.416(6)	N(111)-C(115)	1.384(6)
C(96)-C(961)	1.484(6)	C(112)-C(113)	1.437(6)
C(961)-C(966)	1.387(7)	C(113)-C(114)	1.347(7)
C(961)-C(962)	1.408(7)	C(114)-C(115)	1.448(7)
C(962)-C(963)	1.385(7)	C(115)-C(116)	1.413(6)
C(963)-C(964)	1.375(8)	C(116)-C(611)	1.487(6)
C(964)-C(965)	1.387(8)	C(611)-C(612)	1.378(8)
C(965)-C(966)	1.390(7)	C(611)-C(616)	1.404(8)
N(101)-C(102)	1.389(6)	C(612)-C(613)	1.407(8)
N(101)-C(105)	1.390(6)	C(613)-C(614)	1.361(8)
C(102)-C(103)	1.440(6)	C(614)-O(617)	1.366(6)
C(103)-C(104)	1.359(6)	C(614)-C(615)	1.399(8)
C(104)-C(105)	1.441(6)	C(615)-C(616)	1.376(7)
C(105)-C(106)	1.414(6)	O(617)-C(618)	1.427(7)
C(106)-C(112)	1.424(6)	C(618)-C(619)	1.506(8)
C(106)-C(601)	1.493(6)	C(619)-C(620)	1.517(9)
C(601)-C(602)	1.389(7)	C(620)-C(621)	1.515(8)
C(601)-C(606)	1.400(7)	C(621)-C(622)	1.521(8)

C(5)-N(1)-C(2)	106.6(4)	C(5)-C(6)-C(661)	117.0(4)
C(5)-N(1)-La(1)	122.6(3)	C(12)-C(6)-C(661)	116.4(4)
C(2)-N(1)-La(1)	122.9(3)	C(666)-C(661)-C(662)	118.4(5)
N(1)-C(2)-C(36)	125.8(4)	C(666)-C(661)-C(6)	120.6(5)
N(1)-C(2)-C(3)	109.2(4)	C(662)-C(661)-C(6)	121.0(5)
C(36)-C(2)-C(3)	124.9(4)	C(663)-C(662)-C(661)	120.9(7)
C(4)-C(3)-C(2)	107.4(4)	C(662)-C(663)-C(664)	119.8(7)
C(3)-C(4)-C(5)	107.2(4)	C(665)-C(664)-C(663)	119.7(6)
N(1)-C(5)-C(6)	125.2(4)	C(664)-C(665)-C(666)	120.8(7)
N(1)-C(5)-C(4)	109.5(4)	C(661)-C(666)-C(665)	120.4(6)
C(6)-C(5)-C(4)	125.3(5)	C(15)-N(11)-C(12)	106.4(4)
C(5)-C(6)-C(12)	126.5(5)	C(15)-N(11)-La(1)	123.4(3)

C(12)-N(11)-La(1) 122.9(3)
N(11)-C(12)-C(6) 125.4(4)
N(11)-C(12)-C(13) 109.7(4)
C(6)-C(12)-C(13) 124.8(4)
C(14)-C(13)-C(12) 106.8(4)
C(13)-C(14)-C(15) 107.3(4)
N(11)-C(15)-C(16) 125.3(4)
N(11)-C(15)-C(14) 109.8(4)
C(16)-C(15)-C(14) 124.8(4)
C(22)-C(16)-C(15) 125.3(4)
C(22)-C(16)-C(161) 116.8(4)
C(15)-C(16)-C(161) 117.8(4)
C(166)-C(161)-C(162) 118.6(5)
C(166)-C(161)-C(16) 121.3(5)
C(162)-C(161)-C(16) 120.0(5)
C(163)-C(162)-C(161) 120.4(5)
C(164)-C(163)-C(162) 120.8(6)
C(163)-C(164)-C(165) 119.5(5)
C(164)-C(165)-C(166) 120.1(5)
C(161)-C(166)-C(165) 120.5(5)
C(22)-N(21)-C(25) 106.9(4)
C(22)-N(21)-La(1) 122.7(3)
C(25)-N(21)-La(1) 122.1(3)
N(21)-C(22)-C(16) 126.4(4)
N(21)-C(22)-C(23) 109.3(4)
C(16)-C(22)-C(23) 124.4(4)
C(24)-C(23)-C(22) 107.2(4)
C(23)-C(24)-C(25) 106.8(4)
N(21)-C(25)-C(26) 126.2(4)
N(21)-C(25)-C(24) 109.7(4)
C(26)-C(25)-C(24) 124.0(4)
C(32)-C(26)-C(25) 124.8(4)
C(32)-C(26)-C(261) 118.5(4)
C(25)-C(26)-C(261) 116.7(4)
C(266)-C(261)-C(262) 117.6(5)
C(266)-C(261)-C(26) 119.6(4)
C(262)-C(261)-C(26) 122.7(5)
C(263)-C(262)-C(261) 121.5(6)
C(262)-C(263)-C(264) 119.6(5)
O(267)-C(264)-C(265) 114.5(6)
O(267)-C(264)-C(263) 126.2(5)
C(265)-C(264)-C(263) 119.2(5)
C(264)-C(265)-C(266) 120.8(6)
C(265)-C(266)-C(261) 121.1(5)
C(264)-O(267)-C(268) 119.2(6)
O(267)-C(268)-C(269) 103.9(6)
C(270)-C(269)-C(268) 111.4(7)
C(269)-C(270)-C(271) 114.8(7)
C(270)-C(271)-C(272) 114.9(6)
C(273)-C(272)-C(271) 113.1(6)
C(272)-C(273)-C(274) 115.0(5)
C(610)-C(274)-C(273) 111.9(5)
C(32)-N(31)-C(35) 107.0(4)
C(32)-N(31)-La(1) 122.2(3)
C(35)-N(31)-La(1) 123.1(3)
N(31)-C(32)-C(26) 126.4(4)
N(31)-C(32)-C(33) 109.0(4)
C(26)-C(32)-C(33) 124.5(4)
C(34)-C(33)-C(32) 107.5(4)
C(33)-C(34)-C(35) 107.4(4)
N(31)-C(35)-C(36) 125.4(4)
N(31)-C(35)-C(34) 109.1(4)
C(36)-C(35)-C(34) 125.5(4)
C(2)-C(36)-C(35) 125.9(4)
C(2)-C(36)-C(361) 116.8(4)
C(35)-C(36)-C(361) 117.3(4)
C(366)-C(361)-C(362) 117.3(4)
C(366)-C(361)-C(36) 123.3(4)
C(362)-C(361)-C(36) 119.4(4)
C(363)-C(362)-C(361) 121.6(5)
C(362)-C(363)-C(364) 120.5(5)
O(367)-C(364)-C(363) 115.6(4)
O(367)-C(364)-C(365) 125.1(4)
C(363)-C(364)-C(365) 119.3(4)
C(366)-C(365)-C(364) 119.5(5)
C(365)-C(366)-C(361) 121.7(5)
C(364)-O(367)-C(368) 118.5(4)
O(367)-C(368)-C(369) 105.4(5)
C(370)-C(369)-C(368) 113.0(6)
C(369)-C(370)-C(371) 116.1(6)

C(372)-C(371)-C(370) 112.9(5)
C(622)-C(372)-C(371) 114.5(4)
C(42)-N(41)-C(49) 107.1(4)
C(42)-N(41)-La(1) 114.7(3)
C(49)-N(41)-La(1) 112.5(3)
C(42)-N(41)-La(2) 116.3(3)
C(49)-N(41)-La(2) 117.4(3)
N(80)-C(42)-N(41) 127.8(4)
N(80)-C(42)-C(43) 121.2(4)
N(41)-C(42)-C(43) 110.9(4)
C(44)-C(43)-C(48) 121.3(5)
C(44)-C(43)-C(42) 133.2(5)
C(48)-C(43)-C(42) 105.6(4)
C(45)-C(44)-C(43) 117.5(5)
C(44)-C(45)-C(46) 121.7(5)
C(47)-C(46)-C(45) 120.9(5)
C(46)-C(47)-C(48) 117.6(5)
C(47)-C(48)-C(43) 120.9(5)
C(47)-C(48)-C(49) 132.7(5)
C(43)-C(48)-C(49) 106.3(4)
N(50)-C(49)-N(41) 127.2(4)
N(50)-C(49)-C(48) 122.8(4)
N(41)-C(49)-C(48) 110.1(4)
C(52)-N(50)-C(49) 122.2(4)
C(52)-N(51)-C(59) 107.5(4)
C(52)-N(51)-La(1) 118.6(3)
C(59)-N(51)-La(1) 118.0(3)
C(52)-N(51)-La(2) 113.0(3)
C(59)-N(51)-La(2) 107.9(3)
N(50)-C(52)-N(51) 127.5(4)
N(50)-C(52)-C(53) 122.6(4)
N(51)-C(52)-C(53) 109.9(4)
C(58)-C(53)-C(54) 121.9(4)
C(58)-C(53)-C(52) 106.5(4)
C(54)-C(53)-C(52) 131.5(5)
C(55)-C(54)-C(53) 116.8(5)
C(54)-C(55)-C(56) 121.4(5)
C(57)-C(56)-C(55) 122.2(5)
C(56)-C(57)-C(58) 116.7(5)
C(53)-C(58)-C(57) 121.0(4)
C(53)-C(58)-C(59) 106.5(4)
C(57)-C(58)-C(59) 132.3(4)
N(60)-C(59)-N(51) 127.1(4)
N(60)-C(59)-C(58) 123.3(4)
N(51)-C(59)-C(58) 109.6(4)
C(62)-N(60)-C(59) 123.0(4)
C(69)-N(61)-C(62) 108.3(4)
C(69)-N(61)-La(2) 116.7(3)
C(62)-N(61)-La(2) 113.8(3)
C(69)-N(61)-La(1) 112.3(3)
C(62)-N(61)-La(1) 113.4(3)
N(60)-C(62)-N(61) 127.7(4)
N(60)-C(62)-C(63) 122.7(4)
N(61)-C(62)-C(63) 109.6(4)
C(64)-C(63)-C(68) 120.9(4)
C(64)-C(63)-C(62) 133.1(5)
C(68)-C(63)-C(62) 106.0(4)
C(65)-C(64)-C(63) 118.0(5)
C(64)-C(65)-C(66) 120.9(5)
C(67)-C(66)-C(65) 121.5(5)
C(66)-C(67)-C(68) 117.5(5)
C(67)-C(68)-C(63) 121.2(5)
C(67)-C(68)-C(69) 132.6(5)
C(63)-C(68)-C(69) 106.2(4)
N(70)-C(69)-N(61) 127.5(4)
N(70)-C(69)-C(68) 122.6(4)
N(61)-C(69)-C(68) 109.8(4)
C(72)-N(70)-C(69) 121.8(4)
C(72)-N(71)-C(79) 107.8(4)
C(72)-N(71)-La(1) 113.3(3)
C(79)-N(71)-La(1) 117.0(3)
C(72)-N(71)-La(2) 113.4(3)
C(79)-N(71)-La(2) 114.9(3)
N(70)-C(72)-N(71) 128.4(4)
N(70)-C(72)-C(73) 122.1(4)
N(71)-C(72)-C(73) 109.5(4)
C(78)-C(73)-C(74) 120.9(5)
C(78)-C(73)-C(72) 106.4(4)
C(74)-C(73)-C(72) 132.7(5)
C(75)-C(74)-C(73) 117.0(5)

C(74)-C(75)-C(76) 121.7(5)
C(77)-C(76)-C(75) 121.8(5)
C(76)-C(77)-C(78) 116.7(6)
C(73)-C(78)-C(77) 121.7(5)
C(73)-C(78)-C(79) 107.0(4)
C(77)-C(78)-C(79) 131.3(5)
N(80)-C(79)-N(71) 127.6(4)
N(80)-C(79)-C(78) 123.1(4)
N(71)-C(79)-C(78) 109.3(4)
C(79)-N(80)-C(42) 122.2(4)
C(82)-N(81)-C(85) 107.1(4)
C(82)-N(81)-La(2) 122.8(3)
C(85)-N(81)-La(2) 124.0(3)
N(81)-C(82)-C(116) 126.8(4)
N(81)-C(82)-C(83) 109.3(4)
C(116)-C(82)-C(83) 123.8(4)
C(84)-C(83)-C(82) 107.0(4)
C(83)-C(84)-C(85) 107.3(4)
N(81)-C(85)-C(86) 126.4(4)
N(81)-C(85)-C(84) 109.3(4)
C(86)-C(85)-C(84) 124.3(4)
C(92)-C(86)-C(85) 125.5(4)
C(92)-C(86)-C(861) 118.6(4)
C(85)-C(86)-C(861) 115.9(4)
C(862)-C(861)-C(866) 118.9(4)
C(862)-C(861)-C(86) 121.3(4)
C(866)-C(861)-C(86) 119.7(4)
C(861)-C(862)-C(863) 120.4(5)
C(864)-C(863)-C(862) 120.4(5)
C(865)-C(864)-C(863) 119.6(5)
C(864)-C(865)-C(866) 120.6(5)
C(865)-C(866)-C(861) 120.1(5)
C(92)-N(91)-C(95) 107.0(4)
C(92)-N(91)-La(2) 122.3(3)
C(95)-N(91)-La(2) 120.0(3)
N(91)-C(92)-C(86) 125.2(4)
N(91)-C(92)-C(93) 109.6(4)
C(86)-C(92)-C(93) 125.1(4)
C(94)-C(93)-C(92) 107.1(4)
C(93)-C(94)-C(95) 106.8(4)
N(91)-C(95)-C(96) 125.8(4)
N(91)-C(95)-C(94) 109.4(4)
C(96)-C(95)-C(94) 124.7(4)
C(95)-C(96)-C(102) 125.9(4)
C(95)-C(96)-C(961) 116.1(4)
C(102)-C(96)-C(961) 117.9(4)
C(966)-C(961)-C(962) 118.8(4)
C(966)-C(961)-C(96) 120.3(4)
C(962)-C(961)-C(96) 120.7(4)
C(963)-C(962)-C(961) 119.9(5)
C(964)-C(963)-C(962) 120.9(5)
C(963)-C(964)-C(965) 119.5(5)
C(964)-C(965)-C(966) 120.4(5)
C(961)-C(966)-C(965) 120.4(5)
C(102)-N(101)-C(105) 106.4(4)
C(102)-N(101)-La(2) 121.8(3)
C(105)-N(101)-La(2) 125.0(3)
N(101)-C(102)-C(96) 125.8(4)
N(101)-C(102)-C(103) 109.6(4)
C(96)-C(102)-C(103) 124.6(4)
C(104)-C(103)-C(102) 107.1(4)
C(103)-C(104)-C(105) 107.9(4)
N(101)-C(105)-C(106) 124.4(4)
N(101)-C(105)-C(104) 109.0(4)
C(106)-C(105)-C(104) 126.6(4)
C(105)-C(106)-C(112) 125.9(4)
C(105)-C(106)-C(601) 117.7(4)
C(112)-C(106)-C(601) 116.4(4)
C(602)-C(601)-C(606) 117.9(4)
C(602)-C(601)-C(106) 122.6(4)
C(606)-C(601)-C(106) 119.4(4)
C(601)-C(602)-C(603) 121.7(4)
C(604)-C(603)-C(602) 118.9(4)
O(607)-C(604)-C(603) 124.2(4)
O(607)-C(604)-C(605) 115.4(4)
C(603)-C(604)-C(605) 120.3(4)
C(606)-C(605)-C(604) 120.0(4)
C(605)-C(606)-C(601) 121.1(4)
C(604)-O(607)-C(608) 117.5(4)
O(607)-C(608)-C(609) 106.8(4)

C(608)-C(609)-C(610)	111.4(5)	C(612)-C(611)-C(616)	116.6(5)
C(274)-C(610)-C(609)	113.1(5)	C(612)-C(611)-C(116)	124.6(5)
C(112)-N(111)-C(115)	106.6(4)	C(616)-C(611)-C(116)	118.7(5)
C(112)-N(111)-La(2)	123.5(3)	C(611)-C(612)-C(613)	121.8(5)
C(115)-N(111)-La(2)	121.5(3)	C(614)-C(613)-C(612)	120.4(5)
N(111)-C(112)-C(106)	125.7(4)	C(613)-C(614)-O(617)	126.5(5)
N(111)-C(112)-C(113)	109.5(4)	C(613)-C(614)-C(615)	119.0(5)
C(106)-C(112)-C(113)	124.8(4)	O(617)-C(614)-C(615)	114.4(5)
C(114)-C(113)-C(112)	107.7(4)	C(616)-C(615)-C(614)	120.0(5)
C(113)-C(114)-C(115)	107.3(4)	C(615)-C(616)-C(611)	122.1(5)
N(111)-C(115)-C(116)	126.1(4)	C(614)-O(617)-C(618)	119.0(5)
N(111)-C(115)-C(114)	108.9(4)	O(617)-C(618)-C(619)	106.2(5)
C(116)-C(115)-C(114)	124.9(4)	C(618)-C(619)-C(620)	115.0(5)
C(82)-C(116)-C(115)	124.4(4)	C(621)-C(620)-C(619)	113.7(5)
C(82)-C(116)-C(611)	115.7(4)	C(620)-C(621)-C(622)	114.8(5)
C(115)-C(116)-C(611)	119.8(4)	C(372)-C(622)-C(621)	114.0(4)
C(807)-C(808)	1.96(3)	C(809)-C(808)-C(807)	136(2)
C(808)-C(809)	0.89(4)		
C(801)-Cl(83)	1.722(9)	Cl(83)-C(801)-Cl(82)	116.8(5)
C(801)-Cl(82)	1.780(8)		
C(810)-Cl(85)	1.75(2)	Cl(85)-C(810)-Cl(84)	117.5(10)
C(810)-Cl(84)	1.76(2)		
C(901)-Cl(93)	1.702(8)	Cl(93)-C(901)-Cl(92)	114.2(4)
C(901)-Cl(92)	1.762(7)		
C(904)-Cl(96)	1.551(16)	Cl(96)-C(904)-Cl(95)	106.5(8)
C(904)-Cl(95)	1.750(15)		
C(907)-Cl(98)	1.724(10)	Cl(98)-C(907)-Cl(99)	113.4(5)
C(907)-Cl(99)	1.731(9)		

Table 3. Anisotropic displacement parameters ($Å^2$ x 10^4) for the expression:

$\exp \{-2\pi^2(h^2a^{*2}U_{11} + ... + 2hka^*b^*U_{12})\}$

E.s.ds are in parentheses.

	U_{11}	U_{22}	U_{33}	U_{23}	U_{13}	U_{12}
N(1)	250(20)	163(19)	280(20)	96(15)	157(17)	106(16)

C(2) 290(20) 190(20) 200(20) 75(18) 121(19) 96(19)
C(3) 330(30) 380(30) 270(30) 190(20) 160(20) 190(20)
C(4) 300(30) 410(30) 280(30) 200(20) 140(20) 210(20)
C(5) 270(20) 220(20) 290(20) 123(19) 140(20) 150(20)
C(6) 270(20) 230(20) 270(20) 102(19) 120(20) 120(20)
C(661) 310(30) 340(30) 310(30) 170(20) 180(20) 200(20)
C(662) 380(30) 410(40) 590(40) 130(30) 140(30) 200(30)
C(663) 370(40) 630(50) 730(50) 180(40) 70(30) 250(30)
C(664) 400(40) 690(50) 700(50) 340(40) 220(30) 380(40)
C(665) 540(40) 530(40) 720(50) 160(40) 160(40) 400(40)
C(666) 370(30) 350(30) 540(40) 120(30) 140(30) 240(30)
N(11) 250(20) 179(19) 280(20) 133(16) 159(17) 102(16)
C(12) 240(20) 210(20) 300(20) 104(19) 140(20) 117(19)
C(13) 310(30) 320(30) 350(30) 180(20) 230(20) 200(20)
C(14) 350(30) 310(30) 340(30) 160(20) 230(20) 190(20)
C(15) 320(30) 190(20) 240(20) 121(18) 150(20) 120(20)
C(16) 330(30) 170(20) 230(20) 92(18) 140(20) 110(20)
C(161) 350(30) 250(30) 300(30) 160(20) 190(20) 170(20)
C(162) 350(30) 300(30) 350(30) 170(20) 190(20) 160(20)
C(163) 380(30) 370(30) 450(30) 260(30) 250(30) 150(30)
C(164) 500(30) 490(40) 420(30) 310(30) 320(30) 260(30)
C(165) 460(30) 430(30) 270(30) 160(20) 190(20) 190(30)
C(166) 390(30) 270(30) 260(20) 130(20) 170(20) 140(20)
N(21) 300(20) 154(18) 243(19) 123(15) 140(17) 144(16)
C(22) 290(20) 130(20) 220(20) 93(17) 135(19) 90(18)
C(23) 350(30) 210(20) 240(20) 142(19) 150(20) 140(20)
C(24) 350(30) 210(20) 280(20) 140(20) 150(20) 190(20)
C(25) 290(20) 120(20) 270(20) 96(18) 130(20) 129(18)
C(26) 270(20) 160(20) 330(30) 100(19) 150(20) 123(19)
C(261) 340(30) 230(20) 290(20) 140(20) 180(20) 200(20)
C(262) 380(30) 250(30) 540(40) 90(20) 160(30) 200(20)
C(263) 530(40) 290(30) 800(50) 180(30) 290(40) 320(30)
C(264) 370(30) 400(30) 510(30) 190(30) 160(30) 290(30)
C(265) 330(30) 340(30) 440(30) 130(20) 120(20) 240(20)
C(266) 410(30) 280(30) 360(30) 130(20) 180(20) 240(20)
O(267) 510(30) 400(30) 910(40) 220(20) 170(30) 360(20)
C(268) 650(50) 440(40) 930(60) 210(40) 180(40) 440(40)
C(269) 600(40) 540(40) 740(50) 190(40) 180(40) 460(40)
C(270) 690(50) 480(40) 860(60) 300(40) 410(40) 420(40)
C(271) 820(50) 390(40) 690(50) 260(30) 440(40) 350(40)

C(272) 710(50) 430(40) 620(40) 300(30) 350(40) 380(40)
C(273) 750(50) 470(40) 520(40) 290(30) 330(40) 440(40)
C(274) 580(40) 420(30) 500(40) 190(30) 220(30) 390(30)
N(31) 260(20) 179(19) 280(20) 125(16) 155(17) 142(16)
C(32) 240(20) 170(20) 280(20) 106(18) 128(19) 127(19)
C(33) 300(30) 230(20) 290(20) 82(19) 160(20) 170(20)
C(34) 330(30) 200(20) 320(30) 94(19) 220(20) 140(20)
C(35) 270(20) 140(20) 240(20) 73(17) 163(19) 100(18)
C(36) 280(20) 140(20) 230(20) 88(17) 147(19) 81(18)
C(361) 260(20) 200(20) 210(20) 97(18) 124(19) 105(19)
C(362) 440(30) 200(20) 260(20) 124(19) 210(20) 170(20)
C(363) 420(30) 200(20) 300(30) 140(20) 210(20) 160(20)
C(364) 300(20) 230(20) 210(20) 122(18) 145(19) 140(20)
C(365) 480(30) 130(20) 300(30) 46(19) 230(20) 50(20)
C(366) 420(30) 180(20) 280(30) 60(20) 200(20) 80(20)
O(367) 390(19) 203(17) 236(17) 106(13) 215(15) 112(15)
C(368) 740(40) 260(30) 300(30) 40(20) 330(30) 100(30)
C(369) 730(50) 450(40) 330(30) 180(30) 380(30) 240(30)
C(370) 850(50) 430(40) 660(40) 270(30) 560(40) 400(40)
C(371) 710(40) 460(40) 510(40) 230(30) 460(30) 370(30)
C(372) 540(40) 430(30) 420(30) 180(30) 300(30) 270(30)
La(1) 235.3(14) 142.4(13) 188.6(13) 103.1(10) 127.5(10) 123.5(10)
N(41) 300(20) 175(19) 193(18) 83(15) 137(16) 148(16)
C(42) 260(20) 160(20) 240(20) 60(18) 123(19) 124(19)
C(43) 290(30) 220(20) 300(30) 40(20) 150(20) 120(20)
C(44) 320(30) 450(30) 300(30) 130(20) 160(20) 250(30)
C(45) 320(30) 730(50) 450(30) 140(30) 240(30) 310(30)
C(46) 390(30) 680(40) 360(30) 140(30) 240(30) 240(30)
C(47) 340(30) 500(30) 290(30) 120(20) 190(20) 190(30)
C(48) 280(20) 250(20) 240(20) 70(19) 150(20) 140(20)
C(49) 270(20) 150(20) 200(20) 49(17) 116(19) 111(18)
N(50) 250(20) 188(19) 223(19) 109(15) 146(16) 89(16)
N(51) 238(19) 174(19) 225(19) 111(15) 154(16) 130(16)
C(52) 230(20) 140(20) 220(20) 61(17) 104(18) 92(18)
C(53) 280(20) 130(20) 240(20) 93(17) 113(19) 95(18)
C(54) 360(30) 200(20) 240(20) 133(19) 160(20) 140(20)
C(55) 430(30) 200(20) 220(20) 147(19) 100(20) 150(20)
C(56) 340(30) 220(20) 290(30) 140(20) 80(20) 170(20)
C(57) 330(30) 180(20) 280(20) 124(19) 120(20) 150(20)
C(58) 280(20) 130(20) 230(20) 104(17) 125(19) 106(18)

C(59) 230(20) 130(20) 230(20) 65(17) 100(18) 91(17)
N(60) 252(19) 148(18) 231(19) 84(15) 127(16) 115(16)
N(61) 320(20) 155(18) 202(19) 80(15) 141(17) 147(16)
C(62) 210(20) 120(20) 270(20) 86(17) 120(19) 88(17)
C(63) 250(20) 170(20) 230(20) 45(18) 142(19) 64(18)
C(64) 280(20) 250(20) 320(30) 70(20) 180(20) 140(20)
C(65) 340(30) 430(30) 450(30) 130(30) 250(30) 240(30)
C(66) 420(30) 560(40) 330(30) 180(30) 260(30) 250(30)
C(67) 380(30) 410(30) 320(30) 180(20) 260(20) 180(20)
C(68) 300(20) 180(20) 240(20) 65(18) 140(20) 119(19)
C(69) 300(20) 120(20) 200(20) 76(17) 141(19) 105(18)
N(70) 300(20) 174(19) 217(19) 106(15) 130(17) 111(17)
N(71) 300(20) 188(19) 216(19) 108(15) 149(17) 153(17)
C(72) 310(20) 150(20) 220(20) 74(18) 121(19) 130(19)
C(73) 390(30) 200(20) 220(20) 84(19) 120(20) 170(20)
C(74) 540(30) 370(30) 310(30) 210(20) 250(30) 320(30)
C(75) 740(50) 670(40) 340(30) 330(30) 280(30) 510(40)
C(76) 690(40) 730(50) 370(30) 280(30) 210(30) 570(40)
C(77) 550(40) 500(40) 290(30) 150(30) 180(30) 400(30)
C(78) 410(30) 230(30) 240(20) 90(20) 130(20) 200(20)
C(79) 260(20) 180(20) 200(20) 45(18) 58(19) 104(19)
N(80) 280(20) 188(19) 250(20) 72(16) 110(17) 153(17)
La(2) 217.3(12) 139.7(12) 173.2(12) 99.6(9) 123.1(10) 118.5(10)
N(81) 263(19) 160(18) 205(18) 115(15) 143(16) 131(16)
C(82) 250(20) 180(20) 220(20) 98(18) 137(19) 123(18)
C(83) 350(30) 270(30) 260(20) 190(20) 190(20) 210(20)
C(84) 390(30) 290(30) 240(20) 170(20) 200(20) 240(20)
C(85) 230(20) 140(20) 220(20) 77(17) 113(18) 117(18)
C(86) 260(20) 150(20) 210(20) 101(17) 107(18) 124(18)
C(861) 300(20) 280(20) 210(20) 147(19) 174(19) 210(20)
C(862) 320(30) 300(30) 280(20) 150(20) 190(20) 200(20)
C(863) 300(30) 520(30) 300(30) 200(20) 190(20) 270(30)
C(864) 490(30) 540(40) 310(30) 300(30) 300(30) 440(30)
C(865) 550(40) 350(30) 340(30) 250(20) 290(30) 340(30)
C(866) 390(30) 250(30) 260(20) 130(20) 190(20) 220(20)
N(91) 250(19) 155(18) 232(19) 118(15) 139(16) 134(15)
C(92) 230(20) 140(20) 200(20) 75(17) 100(18) 107(18)
C(93) 270(20) 220(20) 260(20) 123(19) 150(20) 158(19)
C(94) 280(20) 230(20) 260(20) 122(19) 180(20) 160(20)
C(95) 250(20) 140(20) 200(20) 91(17) 120(18) 117(18)

C(96) 260(20) 150(20) 220(20) 115(17) 165(19) 105(18)
C(961) 250(20) 240(20) 220(20) 139(18) 139(19) 179(19)
C(962) 310(20) 220(20) 250(20) 123(19) 170(20) 140(20)
C(963) 330(30) 350(30) 300(30) 220(20) 210(20) 210(20)
C(964) 390(30) 430(30) 270(30) 230(20) 250(20) 300(30)
C(965) 470(30) 380(30) 270(30) 140(20) 220(20) 300(30)
C(966) 400(30) 250(30) 290(30) 170(20) 210(20) 190(20)
N(101) 218(18) 147(18) 218(18) 86(14) 140(15) 121(15)
C(102) 240(20) 140(20) 210(20) 97(17) 131(18) 122(17)
C(103) 290(20) 180(20) 220(20) 141(18) 172(19) 147(19)
C(104) 250(20) 180(20) 220(20) 125(18) 125(18) 138(18)
C(105) 230(20) 120(20) 220(20) 93(17) 109(18) 108(17)
C(106) 220(20) 140(20) 220(20) 77(17) 107(18) 83(17)
C(601) 230(20) 180(20) 230(20) 139(18) 156(18) 114(18)
C(602) 270(20) 160(20) 250(20) 113(18) 163(19) 132(19)
C(603) 230(20) 220(20) 240(20) 98(18) 126(19) 119(19)
C(604) 230(20) 210(20) 270(20) 140(19) 129(19) 145(19)
C(605) 300(20) 240(20) 260(20) 81(19) 150(20) 180(20)
C(606) 260(20) 230(20) 220(20) 96(18) 121(19) 133(19)
O(607) 265(17) 249(18) 307(18) 84(14) 98(14) 193(15)
C(608) 240(20) 300(30) 300(30) 110(20) 100(20) 170(20)
C(609) 350(30) 310(30) 320(30) 130(20) 80(20) 220(20)
C(610) 540(40) 360(30) 510(30) 210(30) 270(30) 330(30)
N(111) 217(19) 192(19) 219(19) 124(15) 137(16) 117(15)
C(112) 250(20) 160(20) 200(20) 66(17) 96(18) 115(18)
C(113) 280(20) 240(20) 290(20) 120(20) 170(20) 180(20)
C(114) 280(20) 270(20) 230(20) 136(19) 171(19) 150(20)
C(115) 270(20) 170(20) 200(20) 97(17) 133(19) 121(18)
C(116) 270(20) 180(20) 240(20) 91(18) 152(19) 133(19)
C(611) 340(30) 250(20) 260(20) 174(19) 170(20) 240(20)
C(612) 340(30) 350(30) 320(30) 160(20) 180(20) 150(20)
C(613) 340(30) 360(30) 450(30) 230(30) 240(30) 130(20)
C(614) 440(30) 400(30) 280(30) 200(20) 240(20) 290(30)
C(615) 390(30) 390(30) 260(30) 90(20) 160(20) 120(20)
C(616) 390(30) 350(30) 320(30) 150(20) 200(20) 90(20)
O(617) 400(20) 480(20) 304(19) 221(17) 238(17) 194(19)
C(618) 400(30) 470(40) 360(30) 190(30) 230(30) 110(30)
C(619) 450(30) 450(30) 370(30) 180(30) 280(30) 110(30)
C(620) 400(30) 490(40) 440(30) 220(30) 290(30) 280(30)
C(621) 380(30) 410(30) 430(30) 210(30) 290(30) 230(30)

C(622) 430(30) 430(30) 370(30) 160(30) 250(30) 220(30)

C(804) 920(70) 1280(100) 500(50) 50(50) 30(50) 610(80)
C(806) 1540(100) 410(40) 650(50) 210(40) 670(60) -70(50)
C(807) 780(60) 550(50) 1910(130) 660(70) 760(80) 260(50)
C(808) 210(50) 3100(300) 3600(300) -2700(300) 520(100) -330(90)
C(809) 1000(80) 1160(90) 240(30) 40(40) 10(40) 970(80)
C(811) 960(80) 1200(110) 1410(110) -700(90) 620(80) 220(70)

C(801) 610(40) 490(40) 730(50) 120(40) 320(40) 290(40)
Cl(82) 1560(30) 509(12) 1130(20) 283(12) 910(20) 291(14)
Cl(83) 506(11) 1440(20) 749(14) -276(15) 185(10) 328(13)

C(810) 650(90) 460(80) 1500(170) 390(100) 280(100) 110(70)
Cl(84) 870(30) 940(30) 1030(30) 280(20) 340(20) 520(20)
Cl(85) 1100(40) 720(30) 1040(30) 310(20) 240(30) 390(30)

C(901) 540(40) 450(40) 570(40) 100(30) 380(30) 130(30)
Cl(92) 483(9) 630(11) 494(9) -12(8) 209(7) 171(8)
Cl(93) 870(20) 920(20) 1030(30) 600(20) 590(20) 640(20)

C(904) 1140(100) 750(80) 2230(170) 260(90) 1010(110) 430(70)
Cl(95) 717(15) 928(19) 1950(30) 220(20) 718(19) 373(14)
Cl(96) 680(30) 1040(40) 430(20) 214(19) 262(17) 390(20)

C(907) 990(70) 600(50) 550(50) 240(40) 380(50) 230(50)
Cl(98) 571(11) 573(12) 1230(20) 139(12) 263(12) 203(10)
Cl(99) 645(11) 596(11) 667(11) 213(9) 278(9) 232(9)

Table 4. Hydrogen coordinates (x 10^4) and isotropic displacement parameters ($Å^2$ x 10^3). All hydrogen atoms were included in idealised positions with U(iso)'s set at 1.2*U(eq) of the parent carbon atoms.

	x	y	z	U(iso)	S.o.f.#
H(3)	3699	1645	4373	35	
H(4)	2517	1711	4772	36	
H(662)	1160	592	5126	55	
H(663)	-184	773	4684	72	
H(664)	-240	1874	5069	64	
H(665)	1028	2768	5877	68	
H(666)	2389	2599	6317	48	
H(13)	1783	1186	6904	32	
H(14)	2495	789	7918	34	
H(162)	2724	-431	8046	36	
H(163)	2365	-857	8913	44	
H(164)	3344	-291	10007	48	
H(165)	4644	771	10238	43	
H(166)	4997	1224	9371	34	
H(23)	5413	151	8875	29	
H(24)	6631	127	8490	30	
H(262)	6662	-712	7078	44	
H(263)	7871	-1050	7556	58	
H(265)	9446	1033	8568	42	
H(266)	8231	1361	8113	37	
H(26A)	9401	-1101	7934	77	
H(26B)	8977	-1206	8492	77	
H(26C)	10487	-1278	8822	69	
H(26D)	10903	-423	8839	69	
H(27A)	10150	-1107	9711	70	
H(27B)	10135	-329	9616	70	
H(27C)	11783	-556	10066	66	
H(27D)	11402	-287	10566	66	
H(27E)	12076	534	9706	61	
H(27F)	11538	789	10083	61	
H(27G)	13200	631	10755	58	

H(27H)	12675	931	11112	58
H(27I)	13969	1901	11094	52
H(27J)	13532	1697	10301	52
H(33)	7286	563	6319	29
H(34)	6581	953	5309	29
H(362)	5685	2584	4911	31
H(363)	6048	2850	4012	33
H(365)	5265	696	3294	36
H(366)	4959	438	4227	35
H(36A)	4940	1295	2245	51
H(36B)	5810	1089	2534	51
H(36C)	5680	1623	1537	54
H(36D)	5949	2380	2014	54
H(37A)	7070	1630	1986	62
H(37B)	7302	2122	2680	62
H(37C)	8169	2709	2044	54
H(37D)	7251	2728	1536	54
H(37E)	7192	3487	2380	48
H(37F)	8078	3444	2908	48
H(44)	2776	3253	7540	38
H(45)	2151	2984	8337	53
H(46)	2768	2469	9194	53
H(47)	4106	2289	9328	41
H(54)	6687	2153	10130	29
H(55)	8028	2048	10796	33
H(56)	9110	2038	10382	33
H(57)	8917	2138	9289	29
H(64)	9073	2207	7385	31
H(65)	9561	2302	6508	42
H(66)	8844	2708	5592	46
H(67)	7611	3009	5523	39
H(74)	5436	3736	4978	40
H(75)	4365	4220	4491	58
H(76)	3330	4268	4938	60
H(77)	3341	3869	5911	46
H(83)	6991	5589	6200	29
H(84)	5849	5763	6594	30
H(862)	3915	4551	7112	30
H(863)	2879	5055	6608	38
H(864)	3367	6314	6702	39

H(865)	4901	7064	7269	39
H(866)	5953	6566	7738	30
H(93)	4758	5067	8553	25
H(94)	5322	4573	9543	25
H(962)	5943	3087	10028	27
H(963)	5570	3012	10955	32
H(964)	6018	4057	11740	34
H(965)	6875	5193	11611	37
H(966)	7298	5280	10704	32
H(103)	8231	3964	10632	23
H(104)	9422	3831	10280	22
H(602)	10745	4591	10111	23
H(603)	11947	4213	10524	25
H(605)	10770	2614	8860	27
H(606)	9580	2993	8458	26
H(60A)	12591	3431	10915	31
H(60B)	13214	3945	10585	31
H(60C)	13956	3223	11112	37
H(60D)	13656	2983	10328	37
H(61A)	12738	2207	11102	48
H(61B)	12297	2001	10309	48
H(113)	10267	4261	8160	27
H(114)	9608	4617	7115	26
H(612)	9456	5816	6769	37
H(613)	9673	6010	5790	43
H(615)	7188	4427	4732	41
H(616)	7003	4206	5703	42
H(61C)	9809	5602	4748	48
H(61D)	9515	6283	4744	48
H(61E)	9690	6050	3755	49
H(61F)	8634	5849	3589	49
H(62A)	9477	4855	3547	44
H(62B)	8487	4581	3569	44
H(62C)	8876	5249	2547	41
H(62D)	7887	4863	2557	41
H(62E)	8106	4113	1812	43
H(62F)	8983	4117	2392	43
H(80A)	3239	184	6043	69
H(80B)	3484	-472	5827	69

H(81A)	8207	6738	6565	112	0.6
H(81B)	8925	7555	6905	112	0.6
H(90A)	10832	3570	11076	59	
H(90B)	11449	4122	11780	59	
H(90C)	9407	303	7081	151	
H(90D)	8980	893	6880	151	
H(90E)	7973	2324	4468	85	
H(90F)	7523	2423	3733	85	

- site occupancy, if different from 1.

Table 5. Torsion angles, in degrees. E.s.ds are in parentheses.

C(5)-N(1)-C(2)-C(36)	-175.6(5)	N(11)-C(12)-C(13)-C(14)	-0.9(6)
La(1)-N(1)-C(2)-C(36)	34.7(6)	C(6)-C(12)-C(13)-C(14)	175.7(5)
C(5)-N(1)-C(2)-C(3)	1.2(5)	C(12)-C(13)-C(14)-C(15)	-0.2(6)
La(1)-N(1)-C(2)-C(3)	-148.5(3)	C(12)-N(11)-C(15)-C(16)	175.8(5)
N(1)-C(2)-C(3)-C(4)	-0.5(6)	La(1)-N(11)-C(15)-C(16)	-33.5(6)
C(36)-C(2)-C(3)-C(4)	176.3(5)	C(12)-N(11)-C(15)-C(14)	-1.8(5)
C(2)-C(3)-C(4)-C(5)	-0.3(6)	La(1)-N(11)-C(15)-C(14)	149.0(3)
C(2)-N(1)-C(5)-C(6)	175.7(5)	C(13)-C(14)-C(15)-N(11)	1.3(6)
La(1)-N(1)-C(5)-C(6)	-34.5(6)	C(13)-C(14)-C(15)-C(16)	-176.3(5)
C(2)-N(1)-C(5)-C(4)	-1.4(5)	N(11)-C(15)-C(16)-C(22)	-4.0(8)
La(1)-N(1)-C(5)-C(4)	148.4(3)	C(14)-C(15)-C(16)-C(22)	173.2(5)
C(3)-C(4)-C(5)-N(1)	1.0(6)	N(11)-C(15)-C(16)-C(161)	-179.2(4)
C(3)-C(4)-C(5)-C(6)	-176.0(5)	C(14)-C(15)-C(16)-C(161)	-2.1(7)
N(1)-C(5)-C(6)-C(12)	-3.8(8)	C(22)-C(16)-C(161)-C(166)	65.7(6)
C(4)-C(5)-C(6)-C(12)	172.8(5)	C(15)-C(16)-C(161)-C(166)	-118.7(6)
N(1)-C(5)-C(6)-C(661)	-179.8(5)	C(22)-C(16)-C(161)-C(162)	-110.8(6)
C(4)-C(5)-C(6)-C(661)	-3.2(8)	C(15)-C(16)-C(161)-C(162)	64.9(6)
C(5)-C(6)-C(661)-C(666)	-104.0(6)	C(166)-C(161)-C(162)-C(163)	-1.3(8)
C(12)-C(6)-C(661)-C(666)	79.6(7)	C(16)-C(161)-C(162)-C(163)	175.3(5)
C(5)-C(6)-C(661)-C(662)	75.4(7)	C(161)-C(162)-C(163)-C(164)	-1.1(9)
C(12)-C(6)-C(661)-C(662)	-101.0(6)	C(162)-C(163)-C(164)-C(165)	2.6(9)
C(666)-C(661)-C(662)-C(663)	-1.1(10)	C(163)-C(164)-C(165)-C(166)	-1.8(9)
C(6)-C(661)-C(662)-C(663)	179.5(6)	C(162)-C(161)-C(166)-C(165)	2.1(8)
C(661)-C(662)-C(663)-C(664)	0.2(12)	C(16)-C(161)-C(166)-C(165)	-174.4(5)
C(662)-C(663)-C(664)-C(665)	0.3(12)	C(164)-C(165)-C(166)-C(161)	-0.6(9)
C(663)-C(664)-C(665)-C(666)	0.1(12)	C(25)-N(21)-C(22)-C(16)	-176.6(5)
C(662)-C(661)-C(666)-C(665)	1.5(10)	La(1)-N(21)-C(22)-C(16)	34.6(6)
C(6)-C(661)-C(666)-C(665)	-179.1(6)	C(25)-N(21)-C(22)-C(23)	2.2(5)
C(664)-C(665)-C(666)-C(661)	-1.0(12)	La(1)-N(21)-C(22)-C(23)	-146.6(3)
C(15)-N(11)-C(12)-C(6)	-175.0(5)	C(15)-C(16)-C(22)-N(21)	3.3(8)
La(1)-N(11)-C(12)-C(6)	34.1(7)	C(161)-C(16)-C(22)-N(21)	178.6(4)
C(15)-N(11)-C(12)-C(13)	1.6(5)	C(15)-C(16)-C(22)-C(23)	-175.3(5)
La(1)-N(11)-C(12)-C(13)	-149.4(3)	C(161)-C(16)-C(22)-C(23)	0.0(7)
C(5)-C(6)-C(12)-N(11)	4.2(8)	N(21)-C(22)-C(23)-C(24)	-1.1(6)
C(661)-C(6)-C(12)-N(11)	-179.8(5)	C(16)-C(22)-C(23)-C(24)	177.7(5)
C(5)-C(6)-C(12)-C(13)	-171.9(5)	C(22)-C(23)-C(24)-C(25)	-0.4(6)
C(661)-C(6)-C(12)-C(13)	4.1(7)	C(22)-N(21)-C(25)-C(26)	174.1(5)

La(1)-N(21)-C(25)-C(26) -36.9(6)
C(22)-N(21)-C(25)-C(24) -2.5(5)
La(1)-N(21)-C(25)-C(24) 146.6(3)
C(23)-C(24)-C(25)-N(21) 1.8(6)
C(23)-C(24)-C(25)-C(26) -174.8(5)
N(21)-C(25)-C(26)-C(32) -3.1(8)
C(24)-C(25)-C(26)-C(32) 173.0(5)
N(21)-C(25)-C(26)-C(261) 178.2(4)
C(24)-C(25)-C(26)-C(261) -5.7(7)
C(32)-C(26)-C(261)-C(266) 96.8(6)
C(25)-C(26)-C(261)-C(266) -84.4(6)
C(32)-C(26)-C(261)-C(262) -86.7(6)
C(25)-C(26)-C(261)-C(262) 92.0(6)
C(266)-C(261)-C(262)-C(263) 1.0(9)
C(26)-C(261)-C(262)-C(263) -175.6(6)
C(261)-C(262)-C(263)-C(264) -0.6(11)
C(262)-C(263)-C(264)-O(267) 179.1(7)
C(262)-C(263)-C(264)-C(265) -0.8(10)
O(267)-C(264)-C(265)-C(266) -178.2(6)
C(263)-C(264)-C(265)-C(266) 1.7(10)
C(264)-C(265)-C(266)-C(261) -1.2(9)
C(262)-C(261)-C(266)-C(265) -0.1(8)
C(26)-C(261)-C(266)-C(265) 176.6(5)
C(265)-C(264)-O(267)-C(268) 172.2(7)
C(263)-C(264)-O(267)-C(268) -7.7(11)
C(264)-O(267)-C(268)-C(269) -170.7(6)
O(267)-C(268)-C(269)-C(270) 72.2(9)
C(268)-C(269)-C(270)-C(271) -156.8(6)
C(269)-C(270)-C(271)-C(272) 71.2(8)
C(270)-C(271)-C(272)-C(273) 169.2(6)
C(271)-C(272)-C(273)-C(274) 176.3(6)
C(272)-C(273)-C(274)-C(610) 63.4(7)
C(35)-N(31)-C(32)-C(26) -176.8(5)
La(1)-N(31)-C(32)-C(26) 32.9(6)
C(35)-N(31)-C(32)-C(33) 1.4(5)
La(1)-N(31)-C(32)-C(33) -148.8(3)
C(25)-C(26)-C(32)-N(31) 4.9(8)
C(261)-C(26)-C(32)-N(31) -176.5(5)
C(25)-C(26)-C(32)-C(33) -173.1(5)
C(261)-C(26)-C(32)-C(33) 5.5(7)
N(31)-C(32)-C(33)-C(34) -0.5(6)
C(26)-C(32)-C(33)-C(34) 177.8(5)
C(32)-C(33)-C(34)-C(35) -0.6(6)
C(32)-N(31)-C(35)-C(36) 177.5(4)
La(1)-N(31)-C(35)-C(36) -32.6(6)
C(32)-N(31)-C(35)-C(34) -1.8(5)
La(1)-N(31)-C(35)-C(34) 148.1(3)
C(33)-C(34)-C(35)-N(31) 1.5(6)
C(33)-C(34)-C(35)-C(36) -177.8(5)
N(1)-C(2)-C(36)-C(35) 4.9(8)
C(3)-C(2)-C(36)-C(35) -171.4(5)
N(1)-C(2)-C(36)-C(361) -174.3(4)
C(3)-C(2)-C(36)-C(361) 9.4(7)
N(31)-C(35)-C(36)-C(2) -5.8(8)
C(34)-C(35)-C(36)-C(2) 173.3(5)
N(31)-C(35)-C(36)-C(361) 173.4(4)
C(34)-C(35)-C(36)-C(361) -7.5(7)
C(2)-C(36)-C(361)-C(366) -110.5(6)
C(35)-C(36)-C(361)-C(366) 70.2(6)
C(2)-C(36)-C(361)-C(362) 69.0(6)
C(35)-C(36)-C(361)-C(362) -110.2(5)
C(366)-C(361)-C(362)-C(363) -2.0(8)
C(36)-C(361)-C(362)-C(363) 178.5(5)
C(361)-C(362)-C(363)-C(364) 1.7(8)
C(362)-C(363)-C(364)-O(367) -178.4(5)
C(362)-C(363)-C(364)-C(365) 0.2(8)
O(367)-C(364)-C(365)-C(366) 176.8(5)
C(363)-C(364)-C(365)-C(366) -1.6(8)
C(364)-C(365)-C(366)-C(361) 1.2(9)
C(362)-C(361)-C(366)-C(365) 0.6(8)
C(36)-C(361)-C(366)-C(365) -179.9(5)
C(363)-C(364)-O(367)-C(368) -162.2(5)
C(365)-C(364)-O(367)-C(368) 19.3(8)
C(364)-O(367)-C(368)-C(369) -179.4(5)
O(367)-C(368)-C(369)-C(370) 75.2(7)
C(368)-C(369)-C(370)-C(371) -153.2(6)
C(369)-C(370)-C(371)-C(372) 73.7(8)
C(370)-C(371)-C(372)-C(622) 176.8(5)
C(49)-N(41)-C(42)-N(80) -179.0(5)
La(1)-N(41)-C(42)-N(80) -53.3(6)

La(2)-N(41)-C(42)-N(80)	47.5(6)	N(51)-C(52)-C(53)-C(58)	-0.4(5)
C(49)-N(41)-C(42)-C(43)	-0.8(5)	N(50)-C(52)-C(53)-C(54)	-3.8(8)
La(1)-N(41)-C(42)-C(43)	124.8(3)	N(51)-C(52)-C(53)-C(54)	175.9(5)
La(2)-N(41)-C(42)-C(43)	-134.3(3)	C(58)-C(53)-C(54)-C(55)	1.6(7)
N(80)-C(42)-C(43)-C(44)	-1.1(9)	C(52)-C(53)-C(54)-C(55)	-174.3(5)
N(41)-C(42)-C(43)-C(44)	-179.5(6)	C(53)-C(54)-C(55)-C(56)	-1.3(7)
N(80)-C(42)-C(43)-C(48)	177.8(4)	C(54)-C(55)-C(56)-C(57)	0.1(8)
N(41)-C(42)-C(43)-C(48)	-0.5(6)	C(55)-C(56)-C(57)-C(58)	0.7(7)
C(48)-C(43)-C(44)-C(45)	0.0(8)	C(54)-C(53)-C(58)-C(57)	-0.7(7)
C(42)-C(43)-C(44)-C(45)	178.8(6)	C(52)-C(53)-C(58)-C(57)	176.1(4)
C(43)-C(44)-C(45)-C(46)	-2.1(10)	C(54)-C(53)-C(58)-C(59)	-176.4(4)
C(44)-C(45)-C(46)-C(47)	2.5(11)	C(52)-C(53)-C(58)-C(59)	0.4(5)
C(45)-C(46)-C(47)-C(48)	-0.7(10)	C(56)-C(57)-C(58)-C(53)	-0.4(7)
C(46)-C(47)-C(48)-C(43)	-1.4(9)	C(56)-C(57)-C(58)-C(59)	173.9(5)
C(46)-C(47)-C(48)-C(49)	-179.9(6)	C(52)-N(51)-C(59)-N(60)	178.7(4)
C(44)-C(43)-C(48)-C(47)	1.7(8)	La(1)-N(51)-C(59)-N(60)	41.4(6)
C(42)-C(43)-C(48)-C(47)	-177.3(5)	La(2)-N(51)-C(59)-N(60)	-59.2(5)
C(44)-C(43)-C(48)-C(49)	-179.4(5)	C(52)-N(51)-C(59)-C(58)	0.0(5)
C(42)-C(43)-C(48)-C(49)	1.6(5)	La(1)-N(51)-C(59)-C(58)	-137.3(3)
C(42)-N(41)-C(49)-N(50)	-177.9(5)	La(2)-N(51)-C(59)-C(58)	122.1(3)
La(1)-N(41)-C(49)-N(50)	55.3(6)	C(53)-C(58)-C(59)-N(60)	-179.0(4)
La(2)-N(41)-C(49)-N(50)	-44.9(6)	C(57)-C(58)-C(59)-N(60)	6.1(8)
C(42)-N(41)-C(49)-C(48)	1.8(5)	C(53)-C(58)-C(59)-N(51)	-0.3(5)
La(1)-N(41)-C(49)-C(48)	-125.0(3)	C(57)-C(58)-C(59)-N(51)	-175.2(5)
La(2)-N(41)-C(49)-C(48)	134.7(3)	N(51)-C(59)-N(60)-C(62)	5.7(7)
C(47)-C(48)-C(49)-N(50)	-3.8(9)	C(58)-C(59)-N(60)-C(62)	-175.8(4)
C(43)-C(48)-C(49)-N(50)	177.5(4)	C(59)-N(60)-C(62)-N(61)	3.7(7)
C(47)-C(48)-C(49)-N(41)	176.6(6)	C(59)-N(60)-C(62)-C(63)	-177.4(4)
C(43)-C(48)-C(49)-N(41)	-2.2(5)	C(69)-N(61)-C(62)-N(60)	178.0(4)
N(41)-C(49)-N(50)-C(52)	-1.2(7)	La(2)-N(61)-C(62)-N(60)	46.5(6)
C(48)-C(49)-N(50)-C(52)	179.2(4)	La(1)-N(61)-C(62)-N(60)	-56.6(5)
C(49)-N(50)-C(52)-N(51)	-8.2(7)	C(69)-N(61)-C(62)-C(63)	-0.9(5)
C(49)-N(50)-C(52)-C(53)	171.6(4)	La(2)-N(61)-C(62)-C(63)	-132.4(3)
C(59)-N(51)-C(52)-N(50)	-180.0(4)	La(1)-N(61)-C(62)-C(63)	124.4(3)
La(1)-N(51)-C(52)-N(50)	-43.0(6)	N(60)-C(62)-C(63)-C(64)	2.2(8)
La(2)-N(51)-C(52)-N(50)	61.1(5)	N(61)-C(62)-C(63)-C(64)	-178.8(5)
C(59)-N(51)-C(52)-C(53)	0.3(5)	N(60)-C(62)-C(63)-C(68)	-177.9(4)
La(1)-N(51)-C(52)-C(53)	137.3(3)	N(61)-C(62)-C(63)-C(68)	1.1(5)
La(2)-N(51)-C(52)-C(53)	-118.7(3)	C(68)-C(63)-C(64)-C(65)	0.4(7)
N(50)-C(52)-C(53)-C(58)	179.8(4)	C(62)-C(63)-C(64)-C(65)	-179.8(5)

C(63)-C(64)-C(65)-C(66)	0.2(9)	C(74)-C(73)-C(78)-C(79)	-179.6(5)
C(64)-C(65)-C(66)-C(67)	-0.6(10)	C(72)-C(73)-C(78)-C(79)	0.2(6)
C(65)-C(66)-C(67)-C(68)	0.3(9)	C(76)-C(77)-C(78)-C(73)	-1.0(9)
C(66)-C(67)-C(68)-C(63)	0.3(8)	C(76)-C(77)-C(78)-C(79)	177.8(6)
C(66)-C(67)-C(68)-C(69)	-179.4(6)	C(72)-N(71)-C(79)-N(80)	178.6(5)
C(64)-C(63)-C(68)-C(67)	-0.6(8)	La(1)-N(71)-C(79)-N(80)	49.6(6)
C(62)-C(63)-C(68)-C(67)	179.5(5)	La(2)-N(71)-C(79)-N(80)	-54.0(6)
C(64)-C(63)-C(68)-C(69)	179.1(4)	C(72)-N(71)-C(79)-C(78)	-1.1(5)
C(62)-C(63)-C(68)-C(69)	-0.8(5)	La(1)-N(71)-C(79)-C(78)	-130.1(3)
C(62)-N(61)-C(69)-N(70)	-178.6(5)	La(2)-N(71)-C(79)-C(78)	126.4(3)
La(2)-N(61)-C(69)-N(70)	-48.6(6)	C(73)-C(78)-C(79)-N(80)	-179.2(5)
La(1)-N(61)-C(69)-N(70)	55.4(5)	C(77)-C(78)-C(79)-N(80)	1.9(9)
C(62)-N(61)-C(69)-C(68)	0.4(5)	C(73)-C(78)-C(79)-N(71)	0.5(6)
La(2)-N(61)-C(69)-C(68)	130.4(3)	C(77)-C(78)-C(79)-N(71)	-178.4(6)
La(1)-N(61)-C(69)-C(68)	-125.5(3)	N(71)-C(79)-N(80)-C(42)	0.7(8)
C(67)-C(68)-C(69)-N(70)	-1.0(9)	C(78)-C(79)-N(80)-C(42)	-179.7(5)
C(63)-C(68)-C(69)-N(70)	179.3(4)	N(41)-C(42)-N(80)-C(79)	2.7(8)
C(67)-C(68)-C(69)-N(61)	179.9(5)	C(43)-C(42)-N(80)-C(79)	-175.3(4)
C(63)-C(68)-C(69)-N(61)	0.2(5)	C(85)-N(81)-C(82)-C(116)	175.2(5)
N(61)-C(69)-N(70)-C(72)	-2.1(7)	La(2)-N(81)-C(82)-C(116)	-31.3(6)
C(68)-C(69)-N(70)-C(72)	179.0(4)	C(85)-N(81)-C(82)-C(83)	-1.0(5)
C(69)-N(70)-C(72)-N(71)	-1.5(8)	La(2)-N(81)-C(82)-C(83)	152.5(3)
C(69)-N(70)-C(72)-C(73)	177.8(4)	N(81)-C(82)-C(83)-C(84)	0.5(6)
C(79)-N(71)-C(72)-N(70)	-179.4(5)	C(116)-C(82)-C(83)-C(84)	-175.8(5)
La(1)-N(71)-C(72)-N(70)	-48.3(6)	C(82)-C(83)-C(84)-C(85)	0.1(6)
La(2)-N(71)-C(72)-N(70)	52.3(6)	C(82)-N(81)-C(85)-C(86)	-178.9(4)
C(79)-N(71)-C(72)-C(73)	1.2(5)	La(2)-N(81)-C(85)-C(86)	28.1(6)
La(1)-N(71)-C(72)-C(73)	132.3(3)	C(82)-N(81)-C(85)-C(84)	1.0(5)
La(2)-N(71)-C(72)-C(73)	-127.1(3)	La(2)-N(81)-C(85)-C(84)	-152.0(3)
N(70)-C(72)-C(73)-C(78)	179.7(5)	C(83)-C(84)-C(85)-N(81)	-0.7(6)
N(71)-C(72)-C(73)-C(78)	-0.9(6)	C(83)-C(84)-C(85)-C(86)	179.2(5)
N(70)-C(72)-C(73)-C(74)	-0.6(9)	N(81)-C(85)-C(86)-C(92)	4.2(8)
N(71)-C(72)-C(73)-C(74)	178.9(6)	C(84)-C(85)-C(86)-C(92)	-175.7(5)
C(78)-C(73)-C(74)-C(75)	2.2(9)	N(81)-C(85)-C(86)-C(861)	-175.8(4)
C(72)-C(73)-C(74)-C(75)	-177.6(6)	C(84)-C(85)-C(86)-C(861)	4.4(7)
C(73)-C(74)-C(75)-C(76)	-2.4(11)	C(92)-C(86)-C(861)-C(862)	-74.0(6)
C(74)-C(75)-C(76)-C(77)	0.9(12)	C(85)-C(86)-C(861)-C(862)	105.9(5)
C(75)-C(76)-C(77)-C(78)	0.9(11)	C(92)-C(86)-C(861)-C(866)	109.2(5)
C(74)-C(73)-C(78)-C(77)	-0.5(8)	C(85)-C(86)-C(861)-C(866)	-70.9(6)
C(72)-C(73)-C(78)-C(77)	179.3(5)	C(866)-C(861)-C(862)-C(863)	3.2(7)

C(86)-C(861)-C(862)-C(863) -173.6(4)
C(861)-C(862)-C(863)-C(864) -2.8(7)
C(862)-C(863)-C(864)-C(865) 0.9(8)
C(863)-C(864)-C(865)-C(866) 0.4(8)
C(864)-C(865)-C(866)-C(861) 0.0(8)
C(862)-C(861)-C(866)-C(865) -1.9(7)
C(86)-C(861)-C(866)-C(865) 175.0(4)
C(95)-N(91)-C(92)-C(86) 173.3(4)
La(2)-N(91)-C(92)-C(86) -42.5(6)
C(95)-N(91)-C(92)-C(93) -2.1(5)
La(2)-N(91)-C(92)-C(93) 142.1(3)
C(85)-C(86)-C(92)-N(91) 3.7(7)
C(861)-C(86)-C(92)-N(91) -176.4(4)
C(85)-C(86)-C(92)-C(93) 178.5(5)
C(861)-C(86)-C(92)-C(93) -1.6(7)
N(91)-C(92)-C(93)-C(94) 0.5(5)
C(86)-C(92)-C(93)-C(94) -174.9(5)
C(92)-C(93)-C(94)-C(95) 1.3(5)
C(92)-N(91)-C(95)-C(96) -173.4(4)
La(2)-N(91)-C(95)-C(96) 41.4(6)
C(92)-N(91)-C(95)-C(94) 2.9(5)
La(2)-N(91)-C(95)-C(94) -142.2(3)
C(93)-C(94)-C(95)-N(91) -2.7(5)
C(93)-C(94)-C(95)-C(96) 173.8(4)
N(91)-C(95)-C(96)-C(102) -0.6(8)
C(94)-C(95)-C(96)-C(102) -176.5(5)
N(91)-C(95)-C(96)-C(961) 175.4(4)
C(94)-C(95)-C(96)-C(961) -0.4(7)
C(95)-C(96)-C(961)-C(966) -78.3(6)
C(102)-C(96)-C(961)-C(966) 98.0(5)
C(95)-C(96)-C(961)-C(962) 97.8(5)
C(102)-C(96)-C(961)-C(962) -85.8(6)
C(966)-C(961)-C(962)-C(963) -0.4(7)
C(96)-C(961)-C(962)-C(963) -176.6(4)
C(961)-C(962)-C(963)-C(964) 1.0(7)
C(962)-C(963)-C(964)-C(965) -0.6(8)
C(963)-C(964)-C(965)-C(966) -0.5(8)
C(962)-C(961)-C(966)-C(965) -0.7(7)
C(96)-C(961)-C(966)-C(965) 175.5(5)
C(964)-C(965)-C(966)-C(961) 1.1(8)
C(105)-N(101)-C(102)-C(96) 177.2(4)
La(2)-N(101)-C(102)-C(96) -30.3(6)
C(105)-N(101)-C(102)-C(103) -0.8(5)
La(2)-N(101)-C(102)-C(103) 151.7(3)
C(95)-C(96)-C(102)-N(101) -5.7(8)
C(961)-C(96)-C(102)-N(101) 178.4(4)
C(95)-C(96)-C(102)-C(103) 172.0(4)
C(961)-C(96)-C(102)-C(103) -3.9(7)
N(101)-C(102)-C(103)-C(104) -0.3(5)
C(96)-C(102)-C(103)-C(104) -178.3(4)
C(102)-C(103)-C(104)-C(105) 1.1(5)
C(102)-N(101)-C(105)-C(106) -177.0(4)
La(2)-N(101)-C(105)-C(106) 31.7(6)
C(102)-N(101)-C(105)-C(104) 1.5(5)
La(2)-N(101)-C(105)-C(104) -149.9(3)
C(103)-C(104)-C(105)-N(101) -1.7(5)
C(103)-C(104)-C(105)-C(106) 176.8(4)
N(101)-C(105)-C(106)-C(112) 6.9(7)
C(104)-C(105)-C(106)-C(112) -171.3(5)
N(101)-C(105)-C(106)-C(601) -172.7(4)
C(104)-C(105)-C(106)-C(601) 9.1(7)
C(105)-C(106)-C(601)-C(602) -59.2(6)
C(112)-C(106)-C(601)-C(602) 121.1(5)
C(105)-C(106)-C(601)-C(606) 121.0(5)
C(112)-C(106)-C(601)-C(606) -58.6(6)
C(606)-C(601)-C(602)-C(603) -1.0(7)
C(106)-C(601)-C(602)-C(603) 179.3(4)
C(601)-C(602)-C(603)-C(604) -0.1(7)
C(602)-C(603)-C(604)-O(607) -179.6(4)
C(602)-C(603)-C(604)-C(605) 1.3(7)
O(607)-C(604)-C(605)-C(606) 179.4(4)
C(603)-C(604)-C(605)-C(606) -1.3(7)
C(604)-C(605)-C(606)-C(601) 0.2(7)
C(602)-C(601)-C(606)-C(605) 0.9(7)
C(106)-C(601)-C(606)-C(605) -179.4(4)
C(603)-C(604)-O(607)-C(608) 2.8(7)
C(605)-C(604)-O(607)-C(608) -178.0(4)
C(604)-O(607)-C(608)-C(609) 174.7(4)
O(607)-C(608)-C(609)-C(610) -62.9(6)
C(273)-C(274)-C(610)-C(609) -179.7(4)

C(608)-C(609)-C(610)-C(274) 170.5(4)
C(115)-N(111)-C(112)-C(106) 178.2(4)
La(2)-N(111)-C(112)-C(106) -33.4(6)
C(115)-N(111)-C(112)-C(113) -0.6(5)
La(2)-N(111)-C(112)-C(113) 147.8(3)
C(105)-C(106)-C(112)-N(111) -5.6(8)
C(601)-C(106)-C(112)-N(111) 174.0(4)
C(105)-C(106)-C(112)-C(113) 173.0(5)
C(601)-C(106)-C(112)-C(113) -7.4(7)
N(111)-C(112)-C(113)-C(114) -0.7(6)
C(106)-C(112)-C(113)-C(114) -179.5(4)
C(112)-C(113)-C(114)-C(115) 1.6(6)
C(112)-N(111)-C(115)-C(116) -174.3(5)
La(2)-N(111)-C(115)-C(116) 36.5(6)
C(112)-N(111)-C(115)-C(114) 1.6(5)
La(2)-N(111)-C(115)-C(114) -147.6(3)
C(113)-C(114)-C(115)-N(111) -2.0(6)
C(113)-C(114)-C(115)-C(116) 173.9(5)
N(81)-C(82)-C(116)-C(115) -8.0(8)
C(83)-C(82)-C(116)-C(115) 167.7(5)
N(81)-C(82)-C(116)-C(611) 172.7(4)
C(83)-C(82)-C(116)-C(611) -11.7(7)
N(111)-C(115)-C(116)-C(82) 4.8(8)
C(114)-C(115)-C(116)-C(82) -170.4(5)
N(111)-C(115)-C(116)-C(611) -175.9(4)
C(114)-C(115)-C(116)-C(611) 8.9(7)
C(82)-C(116)-C(611)-C(612) 112.7(6)
C(115)-C(116)-C(611)-C(612) -66.7(7)
C(82)-C(116)-C(611)-C(616) -64.0(6)
C(115)-C(116)-C(611)-C(616) 116.6(5)
C(616)-C(611)-C(612)-C(613) 0.1(8)
C(116)-C(611)-C(612)-C(613) -176.7(5)
C(611)-C(612)-C(613)-C(614) 1.0(9)
C(612)-C(613)-C(614)-O(617) 178.0(5)
C(612)-C(613)-C(614)-C(615) -0.7(8)
C(613)-C(614)-C(615)-C(616) -0.7(9)
O(617)-C(614)-C(615)-C(616) -179.5(5)
C(614)-C(615)-C(616)-C(611) 1.8(9)
C(612)-C(611)-C(616)-C(615) -1.5(8)
C(116)-C(611)-C(616)-C(615) 175.4(5)
C(613)-C(614)-O(617)-C(618) 11.0(8)
C(615)-C(614)-O(617)-C(618) -170.2(5)
C(614)-O(617)-C(618)-C(619) 176.6(5)
O(617)-C(618)-C(619)-C(620) -64.6(7)
C(618)-C(619)-C(620)-C(621) 164.2(5)
C(619)-C(620)-C(621)-C(622) 171.9(5)
C(371)-C(372)-C(622)-C(621) 174.6(4)
C(620)-C(621)-C(622)-C(372) 59.6(6)

Crystal structure analysis of a complex:

La_2-triple-decked-phthal-porph-phthal with two O-$(CH_2)_{10}$-O bridges

Crystal data: $C_{140}H_{108}N_{16}O_4La_2$, $C_{10.6}H_{9.2}Cl_{8.72..}$, M = 2801.94. Triclinic, space group P-1 (no. 2), a = 17.0068(2), b = 20.0472(2), c = 21.9704(2) Å, α = 94.4090(10), β = 109.6790(10), γ = 110.3770(10) °, V = 6449.80(13) $Å^3$. Z = 2, Dc = 1.443 g cm^{-3}, F(000) = 2854, T = 100(2) K, μ(Cu-Kα) = 72.13 cm^{-1}, λ(Cu-Kα) = 1.54184 Å.

The crystal was a purple block. From a sample under oil, one, *ca* 0.32 x 0.38 x 0.58 mm, was mounted on a small loop and fixed in the cold nitrogen stream on a Rigaku Oxford Diffraction XtaLAB Synergy diffractometer, equipped with Cu-Kα radiation, HyPix detector and mirror monochromator. Intensity data were measured by thin-slice ω-scans. Total no. of reflections recorded, to θ_{max} = 70.0°, was 87,504 of which 24,113 were unique (Rint = 0.073); 22,192 were 'observed' with $I > 2\sigma_I$.

Data were processed using the CrysAlisPro-CCD and -RED (1) programs. The structure was determined by the intrinsic phasing routines in the SHELXT program (2A) and refined by full-matrix least-squares methods, on F2's, in SHELXL (2B). In addition to the principal La_2-triple- decker complex, there are several CH_2Cl_2 and other unidentified atoms and small solvent molecules in the cell. The non-hydrogen atoms were refined with anisotropic thermal parameters. Hydrogen atoms were included in idealised positions and their Uiso values were set to ride on the Ueq values of the parent carbon atoms. At the conclusion of the refinement, wR_2 = 0.184 and R_1 = 0.069 (2B) for all 24,113 reflections weighted w = $[\sigma^2(F_o^2) + (0.1167\ P)^2 + 21.8436\ P]^{-1}$ with P = $(F_o^2 + 2F_c^2)/3$; for the 'observed' data only, R_1 = 0.066.

In the final difference map, the highest peak (*ca* 2.9 $eÅ^{-3}$) was near La(2).

Scattering factors for neutral atoms were taken from reference (3). Computer programs used in this analysis have been noted above, and were run through WinGX (4) on a Dell Optiplex 780 PC at the University of East Anglia.

References

(1) Programs CrysAlisPro, Rigaku Oxford Diffraction Ltd., Abingdon, UK (2018).

(2) G. M. Sheldrick, Programs for crystal structure determination (SHELXT), *Acta Cryst.* (2015) A**71**, 3-8, and refinement (SHELXL), *Acta Cryst.* (2008) A**64**, 112-122 and (2015) C**71**, 3-8.

(3) *'International Tables for X-ray Crystallography'*, Kluwer Academic Publishers, Dordrecht (1992). Vol. C, pp. 500, 219 and 193.

(4) L. J. Farrugia, *J. Appl. Cryst.* (2012) **45**, 849–854.

Legends for Figures

Figure 1. View of the La_2-triple-decker complex molecule, showing the three decks and the two bridging links between the outer porphyrin rings, and indicating the atom numbering scheme. Thermal ellipsoids are drawn at the 50% probability level.

Figure 2. View approximately along the La…La central vector.

Notes on the structure

The principal molecule is a porphyrin-phthalocyanine-porphyrin triple-decked complex linked through two lanthanum centres, Figure 1. Each La atom is eight-coordinate with a square-prismatic pattern, with each La sharing a square face. The La–N distances to the outer, porphyrin ligands have an average value of 2.479 Å whereas the La–N(phthal) distances are longer at 2.765 Å. The two porphyrin rings are linked through two -$O(CH_2)_{10}$-O- chains, and viewed along the La…La vector, these chains are 90 ° apart, Figure 2.

In the porphyrin rings, each pyrrole group is tilted slightly (mean values of 7.41 ° and 7.51 °) away from central N_4 ring plane (of that porphyrin ring). The phthalocyanine group has a very slight wavy appearance with the isoindole groups tilted (mean value 5.53 °) alternately to one side and the other.

Crystal data and structure refinement for

La2-triple-decked-phthal-porph-phthal with two O-$(CH_2)_{10}$-O bridges

---

Identification code	isabf1475
Elemental formula	C140 H108 La2 N16 O4, 4($CHCl_3$) plus unresolved solvent molecules
Formula weight	3056.16
Crystal system, space group	Monoclinic, $P2_1$ (no. 4)
Unit cell dimensions	a = 14.71543(11) Å α = 90 ° b = 22.86186(19) Å β = 102.3754(8) ° c = 20.55253(17) Å γ = 90 °
Volume	6753.66(10) $Å^3$
Z, Calculated density	2, 1.503 Mg/m^3
F(000)	3090
Absorption coefficient	7.561 mm^{-1}
Temperature	100(2) K
Wavelength	1.54184 Å
Crystal colour, shape	dark blue cuboid
Crystal size	0.17 x 0.03 x 0.03 mm
Crystal mounting:	on a small loop, in oil, fixed in cold N_2 stream

On the diffractometer:

Theta range for data collection	7.672 to 69.999 °

Limiting indices -13<=h<=17, -27<=k<=27, -25<=l<=24

Completeness to theta = 67.684 99.4 %

Absorption correction Semi-empirical from equivalents

Max. and min. transmission 1.00000 and 0.44975

Reflections collected (not including absences) 50191

No. of unique reflections 22236 [R(int) for equivalents = 0.041]

No. of 'observed' reflections ($I > 2\sigma_I$) 20702

Structure determined by: dual methods, in SHELXT

Refinement: Full-matrix-block least-squares on F^2, in SHELXL

Data / restraints / parameters 22236 / 1 / 1735

Goodness-of-fit on F^2 1.035

Final R indices ('observed' data) $R_1 = 0.050$, $wR_2 = 0.129$

Final R indices (all data) $R_1 = 0.054$, $wR_2 = 0.132$

Reflections weighted:
$w = [\sigma^2(Fo^2)+(0.0641P)^2+16.6288P]^{-1}$ where $P=(Fo^2+2Fc^2)/3$

Absolute structure parameter 0.506(7)

Extinction coefficient n/a

Largest diff. peak and hole 2.85 and -1.17 e.Å^{-3}

Location of largest difference peak near Cl(99)

Table 1. Atomic coordinates (x 10^5) and equivalent isotropic displacement parameters ($Å^2$ x 10^4). U(eq) is defined as one third of the trace of the orthogonalized Uij tensor. E.s.ds are in parentheses.

	x	y	z	U(eq)	S.o.f.#
N(1)	3416(5)	2454(3)	9091(3)	299(15)	
C(2)	2828(6)	2480(3)	9522(4)	307(18)	
C(3)	3342(6)	2682(4)	10159(4)	319(18)	
C(4)	4215(6)	2777(4)	10114(4)	321(18)	
C(5)	4277(5)	2630(4)	9434(3)	234(15)	
C(6)	5110(5)	2640(4)	9194(4)	271(16)	
C(661)	5974(5)	2832(5)	9674(4)	360(20)	
C(662)	6361(6)	2458(5)	10212(4)	460(30)	
C(663)	7196(7)	2623(7)	10629(5)	650(40)	
C(664)	7666(7)	3128(7)	10539(6)	640(40)	
C(665)	7293(6)	3494(6)	9980(6)	600(30)	
C(666)	6422(6)	3351(5)	9562(5)	420(20)	
N(11)	4511(5)	2246(3)	8052(3)	287(14)	
C(12)	5195(5)	2466(3)	8559(4)	242(15)	
C(13)	6076(6)	2466(4)	8333(4)	314(18)	
C(14)	5875(5)	2247(4)	7712(4)	274(17)	
C(15)	4930(6)	2104(3)	7545(4)	271(17)	
C(16)	4473(5)	1810(4)	6965(4)	281(17)	
C(161)	5046(5)	1708(4)	6462(4)	301(17)	
C(162)	4763(7)	1938(4)	5816(4)	360(20)	
C(163)	5325(7)	1820(5)	5339(4)	410(20)	
C(164)	6107(7)	1514(4)	5482(5)	400(20)	
C(165)	6354(6)	1258(4)	6119(4)	342(19)	
C(166)	5821(5)	1332(4)	6588(5)	326(18)	
O(167)	6679(5)	1383(4)	5081(3)	528(18)	
C(168)	6560(30)	1900(20)	4380(20)	2810(220)	
C(169)	6082(11)	1453(6)	4131(11)	1070(70)	
C(170)	5460(8)	1941(5)	3447(6)	540(30)	
C(171)	6183(9)	2222(9)	3152(8)	1190(90)	
C(172)	5724(19)	2723(7)	2668(15)	1630(130)	
N(21)	2904(4)	1727(3)	7191(3)	276(14)	

C(22)	3517(5)	1618(4)	6813(4)	283(17)
C(23)	3105(6)	1252(4)	6263(4)	350(19)
C(24)	2235(6)	1150(4)	6293(4)	328(19)
C(25)	2066(5)	1434(4)	6892(4)	285(17)
C(26)	1278(6)	1406(4)	7153(4)	279(17)
C(261)	429(5)	1133(4)	6729(4)	286(17)
C(262)	-334(6)	1434(4)	6450(4)	323(18)
C(263)	-1131(6)	1179(4)	6037(4)	380(20)
C(264)	-1167(6)	578(5)	5940(5)	450(20)
C(265)	-343(7)	267(5)	6232(5)	480(20)
C(266)	413(7)	518(4)	6603(5)	390(20)
N(31)	1819(4)	1936(3)	8226(3)	251(14)
C(32)	1134(5)	1622(3)	7759(4)	252(16)
C(33)	318(6)	1546(4)	8037(4)	294(17)
C(34)	488(5)	1804(4)	8646(4)	315(18)
C(35)	1428(6)	2029(4)	8761(4)	297(17)
C(36)	1889(6)	2285(4)	9368(4)	287(17)
C(361)	1379(6)	2355(4)	9904(4)	333(18)
C(362)	1182(6)	2918(4)	10130(5)	390(20)
C(363)	662(7)	2962(5)	10623(5)	430(20)
C(364)	366(6)	2516(5)	10926(4)	380(20)
C(365)	604(7)	1948(5)	10738(5)	460(20)
C(366)	1037(6)	1866(5)	10226(4)	390(20)
O(367)	-95(5)	2610(4)	11428(3)	543(19)
C(368)	-479(7)	2180(5)	11700(5)	510(30)
C(369)	-988(11)	2443(8)	12213(6)	800(40)
C(370)	-326(11)	2656(13)	12813(7)	1170(90)
C(371)	-200(30)	3142(18)	12798(19)	680(90)* 0.4
C(372)	-862(11)	3235(8)	13145(8)	860(40)*
La(1)	2882.4(3)	2629.4(6)	7871.6(2)	220.0(13)
N(41)	3004(5)	3760(4)	8357(4)	214(17)
C(42)	2497(6)	3842(5)	8844(5)	240(20)
C(43)	3096(7)	4102(6)	9436(5)	280(20)
C(44)	2944(7)	4244(6)	10068(5)	310(30)
C(45)	3701(8)	4463(5)	10527(6)	360(30)
C(46)	4577(8)	4533(6)	10380(6)	360(30)
C(47)	4702(8)	4395(6)	9747(5)	380(30)
C(48)	4001(6)	4149(7)	9301(5)	310(20)
C(49)	3881(6)	3959(4)	8605(5)	169(18)*
N(50)	4597(5)	3945(4)	8292(4)	270(20)

N(51)	3742(6)	3483(4)	7285(4)	247(18)
C(52)	4522(7)	3731(6)	7689(5)	280(20)
C(53)	5302(7)	3743(5)	7341(5)	270(20)
C(54)	6190(7)	3934(5)	7510(6)	300(20)
C(55)	6738(7)	3876(6)	7069(6)	410(30)
C(56)	6449(7)	3612(6)	6476(6)	390(30)
C(57)	5529(7)	3408(6)	6276(5)	320(30)
C(58)	4961(6)	3469(5)	6726(5)	240(20)
C(59)	3983(7)	3319(5)	6703(5)	280(20)
N(60)	3453(5)	3070(4)	6169(4)	270(19)
N(61)	2073(5)	3037(4)	6621(4)	269(19)
C(62)	2553(7)	2942(5)	6134(5)	250(20)
C(63)	1947(6)	2697(6)	5550(5)	250(20)
C(64)	2104(7)	2544(6)	4931(5)	340(30)
C(65)	1353(8)	2331(7)	4463(6)	450(30)
C(66)	488(8)	2255(7)	4617(5)	430(30)
C(67)	305(6)	2413(5)	5234(5)	340(30)
C(68)	1096(6)	2618(6)	5709(4)	207(17)
C(69)	1162(7)	2855(5)	6376(5)	310(20)
N(70)	457(5)	2851(4)	6681(4)	242(18)
N(71)	1301(5)	3306(4)	7710(4)	260(20)
C(72)	527(6)	3061(5)	7310(5)	220(20)
C(73)	-221(6)	3064(5)	7636(5)	240(20)
C(74)	-1162(7)	2847(6)	7438(5)	340(30)
C(75)	-1737(7)	2917(6)	7898(6)	380(30)
C(76)	-1370(8)	3181(6)	8552(6)	380(30)
C(77)	-490(7)	3385(6)	8727(6)	320(20)
C(78)	99(7)	3314(6)	8273(5)	280(20)
C(79)	1053(6)	3458(5)	8301(4)	220(20)
N(80)	1620(5)	3713(4)	8825(4)	221(17)
La(2)	2171.6(3)	4159.5(2)	712.1(2)	221(1)
N(81)	2180(4)	5067(3)	7789(3)	230(13)
C(82)	1521(6)	5169(4)	8172(4)	272(17)
C(83)	1957(6)	5530(4)	8747(4)	297(18)
C(84)	2836(5)	5633(4)	8682(4)	307(18)
C(85)	2959(6)	5349(3)	8080(4)	290(17)
C(86)	3805(5)	5373(3)	7850(4)	267(16)
C(181)	4624(6)	5684(4)	8279(4)	306(18)
C(182)	4617(6)	6268(4)	8379(5)	400(20)
C(183)	5417(8)	6549(5)	8784(5)	520(30)

C(184) 6137(7) 6212(5) 9059(5) 460(20)
C(185) 6169(6) 5621(5) 8947(5) 450(20)
C(186) 5415(5) 5337(4) 8564(4) 337(19)
N(91) 3269(4) 4872(3) 6770(3) 258(13)
C(92) 3914(6) 5150(4) 7226(4) 308(18)
C(93) 4745(6) 5225(4) 6970(4) 313(18)
C(94) 4562(6) 4991(4) 6351(4) 343(19)
C(95) 3630(6) 4772(3) 6204(4) 245(16)
C(96) 3160(5) 4508(3) 5612(4) 251(16)
C(191) 3700(5) 4432(4) 5070(3) 241(16)
C(192) 3972(7) 4911(4) 4767(4) 360(20)
C(193) 4512(6) 4846(4) 4275(4) 354(19)
C(194) 4689(7) 4304(5) 4070(4) 410(20)
C(195) 4372(6) 3790(4) 4373(4) 360(20)
C(196) 3909(5) 3877(4) 4871(4) 276(17)
O(197) 5167(5) 4165(3) 3588(3) 481(16)
C(198) 5563(8) 4686(7) 3281(5) 630(40)
C(199) 6051(7) 4398(9) 2785(5) 900(60)
C(200) 5409(8) 4029(7) 2216(5) 700(40)
C(201) 5908(19) 3500(15) 1860(8) 1690(140)
C(202) 6202(17) 2917(16) 2298(9) 1740(180)
N(101) 1622(4) 4326(3) 5909(3) 252(13)
C(102) 2218(5) 4336(4) 5479(3) 246(16)
C(103) 1732(5) 4124(4) 4823(4) 254(16)
C(104) 840(5) 4009(4) 4878(3) 254(16)
C(105) 762(6) 4155(4) 5540(4) 339(18)
C(106) -50(5) 4139(4) 5782(4) 285(16)
C(141) -929(6) 3971(4) 5319(4) 347(19)
C(142) -1309(7) 4312(5) 4786(5) 480(30)
C(143) -2139(7) 4163(7) 4353(5) 610(30)
C(144) -2587(8) 3668(8) 4481(5) 760(40)
C(145) -2202(8) 3305(6) 4991(5) 580(30)
C(146) -1402(7) 3468(5) 5431(5) 480(20)
N(111) 552(4) 4523(3) 6917(3) 243(13)
C(112) -166(6) 4319(4) 6427(4) 305(18)
C(113) -1009(6) 4337(4) 6645(4) 291(17)
C(114) -841(6) 4549(4) 7279(4) 313(18)
C(115) 152(5) 4692(4) 7460(3) 250(16)
C(116) 608(6) 4976(4) 8051(3) 272(17)
C(121) 60(6) 5113(4) 8564(4) 284(17)

C(122) -765(6) 5427(4) 8412(4) 360(20)
C(123) -1309(6) 5534(5) 8864(5) 430(20)
C(124) -1053(7) 5285(5) 9482(5) 470(20)
C(125) -212(7) 4926(4) 9655(5) 420(20)
C(126) 293(6) 4871(4) 9190(4) 370(20)
O(127) -1655(6) 5364(4) 9918(4) 650(20)
C(128) -1201(14) 5291(17) 10677(12) 1180(120) 0.7
C(129) -1411(12) 4772(7) 10948(7) 500(40) 0.7
C(130) -1190(20) 4785(17) 11771(14) 1830(170)
C(131) -1250(20) 4304(16) 11906(10) 1690(160)
C(132) -870(20) 4075(9) 12518(15) 2700(300)
C(133) -1225(12) 3655(10) 12784(9) 920(70)
C(138) -1637(9) 5029(6) 10454(6) 290(30)* 0.7
C(139) -828(15) 5304(10) 11032(9) 800(70) 0.7

O(701) 7975(7) 8997(11) 6919(5) 1370(90)
O(702) 8425(9) 9999(7) 7272(7) 1200(60)
O(703) 8493(9) 9228(7) 8388(6) 960(40)
O(704) 7208(15) 9839(13) 7603(11) 1370(80)*
O(705) 7597(11) 8812(8) 8164(4) 1230(70)
C(711) 7070(12) 7170(8) 8066(9) 840(50)*
C(712) 6479(7) 6733(5) 7648(5) 370(20)
C(713) 6925(7) 7848(7) 8059(5) 510(40)
C(714) 7800(11) 6915(6) 7380(8) 490(40)
C(715) 6406(7) 7583(6) 6563(6) 440(30)
O(716) 7449(8) 8057(6) 6839(4) 730(40)
C(717) 8178(9) 7104(11) 7356(6) 620(60)
C(718) 7767(11) 7628(9) 7589(7) 870(50)
C(719) 6990(20) 6994(9) 6980(20) 1930(180)
C(721) 6805(7) 9562(7) 7634(7) 400(30)
C(722) 6803(15) 9963(8) 7725(6) 630(50)

C(904) 5902(10) 5954(8) 1354(8) 630(40)
Cl(81) 5499(8) 6049(3) 475(2) 1880(40)
Cl(82) 4875(3) 5755(2) 1653(2) 739(12)
Cl(83) 6751(4) 5510(2) 1566(4) 1320(30)

C(901) 781(13) 5798(8) 6343(8) 880(60)
Cl(91) -131(2) 6045(2) 6676.0(18) 619(10)
Cl(92) 1790(2) 6322.7(19) 6648(2) 694(10)

Cl(93) 668(4) 5766(2) 5520(2) 911(14)

C(902) 2362(7) 6352(5) 921(5) 410(25)
Cl(94) 2091(2) 6296(2) 1700(2) 611(9)
Cl(95) 1506(4) 6753(3) 354(3) 1390(30)
Cl(96) 2434(5) 5687(2) 549.4(19) 1560(30)

C(903) 2664(10) 401(14) 4200(16) 2210(200)
Cl(97) 2851(3) 486(2) 3302(2) 640(10)
Cl(98) 3356(3) -42(3) 4564(3) 952(15)
Cl(99) 2480(3) 1116(3) 4445(3) 1003(14)*

- site occupancy, if different from 1.

* - U(iso) ($Å^2$ x 10^4)

Table 2. Molecular dimensions. Bond lengths are in Ångstroms, angles in degrees. E.s.ds are in parentheses.

N(1)-La(1)	2.493(6)	N(41)-La(2)	2.729(7)
N(11)-La(1)	2.503(7)	N(51)-La(2)	2.740(8)
N(21)-La(1)	2.498(7)	N(61)-La(2)	2.756(9)
N(31)-La(1)	2.445(6)	N(71)-La(2)	2.752(9)
La(1)-N(41)	2.763(9)	La(2)-N(81)	2.487(6)
La(1)-N(51)	2.742(8)	La(2)-N(91)	2.506(7)
La(1)-N(61)	2.753(9)	La(2)-N(101)	2.477(6)
La(1)-N(71)	2.754(8)	La(2)-N(111)	2.474(6)
La(1)-La(2)	3.8755(5)		

N(31)-La(1)-N(1)	71.3(2)	N(61)-La(1)-N(41)	90.1(3)
N(31)-La(1)-N(21)	73.6(2)	N(71)-La(1)-N(41)	60.4(2)
N(1)-La(1)-N(21)	113.0(2)	N(31)-La(1)-La(2)	124.63(16)
N(31)-La(1)-N(11)	112.5(2)	N(1)-La(1)-La(2)	123.07(17)
N(1)-La(1)-N(11)	73.1(2)	N(21)-La(1)-La(2)	123.89(15)
N(21)-La(1)-N(11)	70.6(2)	N(11)-La(1)-La(2)	122.88(16)
N(31)-La(1)-N(51)	167.79(18)	N(51)-La(1)-La(2)	45.00(18)
N(1)-La(1)-N(51)	118.77(18)	N(61)-La(1)-La(2)	45.33(19)
N(21)-La(1)-N(51)	106.21(17)	N(71)-La(1)-La(2)	45.24(19)
N(11)-La(1)-N(51)	78.30(18)	N(41)-La(1)-La(2)	44.77(15)
N(31)-La(1)-N(61)	108.74(18)	N(111)-La(2)-N(101)	71.5(2)
N(1)-La(1)-N(61)	166.65(18)	N(111)-La(2)-N(81)	72.8(2)
N(21)-La(1)-N(61)	79.14(19)	N(101)-La(2)-N(81)	112.9(2)
N(11)-La(1)-N(61)	117.75(16)	N(111)-La(2)-N(91)	113.0(2)
N(51)-La(1)-N(61)	59.8(3)	N(101)-La(2)-N(91)	72.7(2)
N(31)-La(1)-N(71)	79.76(19)	N(81)-La(2)-N(91)	71.9(2)
N(1)-La(1)-N(71)	106.75(17)	N(111)-La(2)-N(41)	119.60(16)
N(21)-La(1)-N(71)	120.56(19)	N(101)-La(2)-N(41)	166.28(19)
N(11)-La(1)-N(71)	166.3(2)	N(81)-La(2)-N(41)	79.48(19)
N(51)-La(1)-N(71)	90.2(3)	N(91)-La(2)-N(41)	107.27(16)
N(61)-La(1)-N(71)	60.8(2)	N(111)-La(2)-N(51)	165.18(18)
N(31)-La(1)-N(41)	119.66(16)	N(101)-La(2)-N(51)	107.18(18)
N(1)-La(1)-N(41)	78.82(17)	N(81)-La(2)-N(51)	119.90(18)
N(21)-La(1)-N(41)	165.41(15)	N(91)-La(2)-N(51)	79.82(17)
N(11)-La(1)-N(41)	106.74(15)	N(41)-La(2)-N(51)	59.9(2)
N(51)-La(1)-N(41)	59.5(2)	N(111)-La(2)-N(71)	77.88(16)

N(101)-La(2)-N(71) 117.92(17)
N(81)-La(2)-N(71) 107.28(19)
N(91)-La(2)-N(71) 167.57(16)
N(41)-La(2)-N(71) 60.8(2)
N(51)-La(2)-N(71) 90.3(3)
N(111)-La(2)-N(61) 106.11(17)
N(101)-La(2)-N(61) 77.81(19)
N(81)-La(2)-N(61) 167.52(18)
N(91)-La(2)-N(61) 118.90(16)
N(41)-La(2)-N(61) 90.7(3)
N(51)-La(2)-N(61) 59.7(2)
N(71)-La(2)-N(61) 60.8(3)
N(111)-La(2)-La(1) 122.57(15)
N(101)-La(2)-La(1) 122.76(15)
N(81)-La(2)-La(1) 124.37(14)
N(91)-La(2)-La(1) 124.44(15)
N(41)-La(2)-La(1) 45.47(19)
N(51)-La(2)-La(1) 45.04(17)
N(71)-La(2)-La(1) 45.29(17)
N(61)-La(2)-La(1) 45.27(19)

N(1)-C(2) 1.366(11)
N(1)-C(5) 1.372(10)
C(2)-C(36) 1.422(11)
C(2)-C(3) 1.440(11)
C(3)-C(4) 1.325(12)
C(4)-C(5) 1.459(11)
C(5)-C(6) 1.417(10)
C(6)-C(12) 1.394(11)
C(6)-C(661) 1.498(11)
C(661)-C(666) 1.400(14)
C(661)-C(662) 1.417(14)
C(662)-C(663) 1.390(14)
C(663)-C(664) 1.38(2)
C(664)-C(665) 1.43(2)
C(665)-C(666) 1.419(12)
N(11)-C(15) 1.360(11)
N(11)-C(12) 1.379(10)
C(12)-C(13) 1.469(11)
C(13)-C(14) 1.343(11)
C(14)-C(15) 1.398(11)
C(15)-C(16) 1.408(11)
C(16)-C(22) 1.443(11)
C(16)-C(161) 1.486(11)
C(161)-C(162) 1.406(13)
C(161)-C(166) 1.407(12)
C(162)-C(163) 1.436(12)
C(163)-C(164) 1.324(14)
C(164)-O(167) 1.334(11)
C(164)-C(165) 1.409(13)
C(165)-C(166) 1.379(12)
O(167)-C(168) 1.83(5)
C(168)-C(169) 1.28(5)
C(169)-C(170) 1.87(2)
C(170)-C(171) 1.48(2)
C(171)-C(172) 1.57(3)
C(172)-C(202) 1.23(3)
N(21)-C(22) 1.333(10)
N(21)-C(25) 1.422(9)
C(22)-C(23) 1.432(12)
C(23)-C(24) 1.316(13)
C(24)-C(25) 1.460(11)
C(25)-C(26) 1.380(11)
C(26)-C(32) 1.398(11)
C(26)-C(261) 1.498(10)
C(261)-C(262) 1.337(12)
C(261)-C(266) 1.429(12)
C(262)-C(263) 1.417(12)
C(263)-C(264) 1.387(14)
C(264)-C(265) 1.422(15)
C(265)-C(266) 1.336(13)
N(31)-C(35) 1.362(10)
N(31)-C(32) 1.428(10)
C(32)-C(33) 1.447(11)
C(33)-C(34) 1.357(12)
C(34)-C(35) 1.448(11)
C(35)-C(36) 1.412(12)
C(36)-C(361) 1.469(12)
C(361)-C(362) 1.421(13)

C(361)-C(366)	1.442(13)	N(61)-C(69)	1.391(13)
C(362)-C(363)	1.398(13)	C(62)-C(63)	1.446(15)
C(363)-C(364)	1.316(15)	C(63)-C(68)	1.373(12)
C(364)-O(367)	1.367(10)	C(63)-C(64)	1.385(13)
C(364)-C(365)	1.421(15)	C(64)-C(65)	1.389(16)
C(365)-C(366)	1.356(13)	C(65)-C(66)	1.387(15)
O(367)-C(368)	1.317(13)	C(66)-C(67)	1.398(16)
C(368)-C(369)	1.540(16)	C(67)-C(68)	1.428(12)
C(369)-C(370)	1.480(19)	C(68)-C(69)	1.459(13)
C(370)-C(371)	1.13(4)	C(69)-N(70)	1.322(13)
C(370)-C(372)	1.75(3)	N(70)-C(72)	1.362(13)
C(371)-C(372)	1.34(4)	N(71)-C(72)	1.373(12)
C(371)-C(133)	1.90(4)	N(71)-C(79)	1.387(12)
C(372)-C(133)	1.26(3)	C(72)-C(73)	1.407(13)
N(41)-C(49)	1.361(11)	C(73)-C(78)	1.412(14)
N(41)-C(42)	1.384(12)	C(73)-C(74)	1.444(14)
C(42)-N(80)	1.316(12)	C(74)-C(75)	1.406(14)
C(42)-C(43)	1.467(13)	C(75)-C(76)	1.467(16)
C(43)-C(44)	1.401(13)	C(76)-C(77)	1.349(16)
C(43)-C(48)	1.420(13)	C(77)-C(78)	1.414(14)
C(44)-C(45)	1.390(15)	C(78)-C(79)	1.430(13)
C(45)-C(46)	1.395(15)	C(79)-N(80)	1.345(12)
C(46)-C(47)	1.388(15)	N(81)-C(85)	1.339(11)
C(47)-C(48)	1.347(16)	N(81)-C(82)	1.394(10)
C(48)-C(49)	1.469(13)	C(82)-C(116)	1.385(12)
C(49)-N(50)	1.348(11)	C(82)-C(83)	1.471(10)
N(50)-C(52)	1.314(14)	C(83)-C(84)	1.348(11)
N(51)-C(59)	1.371(13)	C(84)-C(85)	1.444(11)
N(51)-C(52)	1.386(14)	C(85)-C(86)	1.423(12)
C(52)-C(53)	1.478(13)	C(86)-C(92)	1.421(12)
C(53)-C(54)	1.350(14)	C(86)-C(181)	1.510(11)
C(53)-C(58)	1.402(15)	C(181)-C(182)	1.351(14)
C(54)-C(55)	1.343(16)	C(181)-C(186)	1.428(11)
C(55)-C(56)	1.344(17)	C(182)-C(183)	1.439(12)
C(56)-C(57)	1.408(15)	C(183)-C(184)	1.334(15)
C(57)-C(58)	1.380(14)	C(184)-C(185)	1.374(16)
C(58)-C(59)	1.470(13)	C(185)-C(186)	1.378(13)
C(59)-N(60)	1.330(14)	N(91)-C(92)	1.342(11)
N(60)-C(62)	1.343(13)	N(91)-C(95)	1.396(10)
N(61)-C(62)	1.361(12)	C(92)-C(93)	1.443(12)

C(93)-C(94)	1.352(12)	C(144)-C(145)	1.364(19)
C(94)-C(95)	1.431(12)	C(145)-C(146)	1.374(14)
C(95)-C(96)	1.401(11)	N(111)-C(112)	1.374(10)
C(96)-C(102)	1.411(11)	N(111)-C(115)	1.422(9)
C(96)-C(191)	1.509(10)	C(112)-C(113)	1.407(12)
C(191)-C(192)	1.363(12)	C(113)-C(114)	1.363(11)
C(191)-C(196)	1.387(12)	C(114)-C(115)	1.464(11)
C(192)-C(193)	1.421(13)	C(115)-C(116)	1.414(10)
C(193)-C(194)	1.353(14)	C(116)-C(121)	1.491(11)
C(194)-O(197)	1.369(11)	C(121)-C(126)	1.373(12)
C(194)-C(195)	1.453(12)	C(121)-C(122)	1.387(12)
C(195)-C(196)	1.358(11)	C(122)-C(123)	1.373(12)
O(197)-C(198)	1.522(14)	C(123)-C(124)	1.367(15)
C(198)-C(199)	1.517(18)	C(124)-O(127)	1.401(11)
C(199)-C(200)	1.581(18)	C(124)-C(125)	1.464(15)
C(200)-C(201)	1.66(3)	C(125)-C(126)	1.336(13)
C(201)-C(202)	1.61(4)	O(127)-C(138)	1.336(15)
N(101)-C(102)	1.373(10)	O(127)-C(128)	1.57(3)
N(101)-C(105)	1.384(11)	C(128)-C(139)	0.81(2)
C(102)-C(103)	1.467(10)	C(128)-C(138)	0.92(3)
C(103)-C(104)	1.368(11)	C(128)-C(129)	1.37(4)
C(104)-C(105)	1.429(11)	C(129)-C(138)	1.16(2)
C(105)-C(106)	1.390(12)	C(129)-C(139)	1.48(3)
C(106)-C(112)	1.433(11)	C(129)-C(130)	1.65(3)
C(106)-C(141)	1.484(11)	C(130)-C(131)	1.14(4)
C(141)-C(142)	1.363(14)	C(131)-C(132)	1.37(3)
C(141)-C(146)	1.388(15)	C(132)-C(133)	1.27(4)
C(142)-C(143)	1.390(15)	C(138)-C(139)	1.62(2)
C(143)-C(144)	1.36(2)		

C(2)-N(1)-C(5)	107.3(6)	C(6)-C(5)-C(4)	124.6(6)
C(2)-N(1)-La(1)	122.5(5)	C(12)-C(6)-C(5)	125.4(7)
C(5)-N(1)-La(1)	121.8(5)	C(12)-C(6)-C(661)	117.9(7)
N(1)-C(2)-C(36)	124.2(8)	C(5)-C(6)-C(661)	116.7(7)
N(1)-C(2)-C(3)	108.7(7)	C(666)-C(661)-C(662)	120.9(8)
C(36)-C(2)-C(3)	126.8(8)	C(666)-C(661)-C(6)	120.2(8)
C(4)-C(3)-C(2)	108.5(7)	C(662)-C(661)-C(6)	118.7(9)
C(3)-C(4)-C(5)	106.9(7)	C(663)-C(662)-C(661)	118.2(11)
N(1)-C(5)-C(6)	126.7(6)	C(664)-C(663)-C(662)	123.1(12)
N(1)-C(5)-C(4)	108.6(6)	C(663)-C(664)-C(665)	118.6(9)

C(666)-C(665)-C(664) 119.5(11)
C(661)-C(666)-C(665) 119.5(11)
C(15)-N(11)-C(12) 106.8(7)
C(15)-N(11)-La(1) 123.2(5)
C(12)-N(11)-La(1) 120.3(5)
N(11)-C(12)-C(6) 127.9(7)
N(11)-C(12)-C(13) 108.2(7)
C(6)-C(12)-C(13) 123.9(7)
C(14)-C(13)-C(12) 105.7(7)
C(13)-C(14)-C(15) 109.1(7)
N(11)-C(15)-C(14) 110.2(7)
N(11)-C(15)-C(16) 123.4(7)
C(14)-C(15)-C(16) 126.1(8)
C(15)-C(16)-C(22) 126.5(7)
C(15)-C(16)-C(161) 115.1(7)
C(22)-C(16)-C(161) 118.3(7)
C(162)-C(161)-C(166) 117.9(8)
C(162)-C(161)-C(16) 120.1(8)
C(166)-C(161)-C(16) 121.7(8)
C(161)-C(162)-C(163) 118.4(8)
C(164)-C(163)-C(162) 123.2(8)
C(163)-C(164)-O(167) 128.0(9)
C(163)-C(164)-C(165) 117.7(8)
O(167)-C(164)-C(165) 114.1(8)
C(166)-C(165)-C(164) 121.7(8)
C(165)-C(166)-C(161) 120.4(8)
C(164)-O(167)-C(168) 111.7(17)
C(168)-C(169)-C(170) 88(3)
C(171)-C(170)-C(169) 106.7(10)
C(170)-C(171)-C(172) 109.0(11)
C(202)-C(172)-C(171) 115.5(18)
C(22)-N(21)-C(25) 107.0(6)
C(22)-N(21)-La(1) 124.9(5)
C(25)-N(21)-La(1) 121.1(5)
N(21)-C(22)-C(23) 110.1(7)
N(21)-C(22)-C(16) 124.5(7)
C(23)-C(22)-C(16) 125.2(7)
C(24)-C(23)-C(22) 108.6(8)
C(23)-C(24)-C(25) 107.6(8)
C(26)-C(25)-N(21) 125.2(7)
C(26)-C(25)-C(24) 128.1(7)
N(21)-C(25)-C(24) 106.6(7)
C(25)-C(26)-C(32) 129.2(7)
C(25)-C(26)-C(261) 117.2(7)
C(32)-C(26)-C(261) 113.5(7)
C(262)-C(261)-C(266) 116.7(8)
C(262)-C(261)-C(26) 123.6(8)
C(266)-C(261)-C(26) 119.7(8)
C(261)-C(262)-C(263) 123.8(9)
C(264)-C(263)-C(262) 119.6(9)
C(263)-C(264)-C(265) 115.6(9)
C(266)-C(265)-C(264) 123.9(10)
C(265)-C(266)-C(261) 120.3(9)
C(35)-N(31)-C(32) 105.1(6)
C(35)-N(31)-La(1) 123.2(5)
C(32)-N(31)-La(1) 122.0(5)
C(26)-C(32)-N(31) 123.8(7)
C(26)-C(32)-C(33) 127.3(7)
N(31)-C(32)-C(33) 108.8(6)
C(34)-C(33)-C(32) 107.8(7)
C(33)-C(34)-C(35) 106.7(7)
N(31)-C(35)-C(36) 124.8(7)
N(31)-C(35)-C(34) 111.5(7)
C(36)-C(35)-C(34) 123.6(7)
C(35)-C(36)-C(2) 126.0(7)
C(35)-C(36)-C(361) 118.8(7)
C(2)-C(36)-C(361) 115.2(8)
C(362)-C(361)-C(366) 115.8(8)
C(362)-C(361)-C(36) 121.1(8)
C(366)-C(361)-C(36) 123.0(8)
C(363)-C(362)-C(361) 119.0(9)
C(364)-C(363)-C(362) 125.1(10)
C(363)-C(364)-O(367) 120.2(10)
C(363)-C(364)-C(365) 117.0(8)
O(367)-C(364)-C(365) 122.6(9)
C(366)-C(365)-C(364) 121.4(9)
C(365)-C(366)-C(361) 121.3(9)
C(368)-O(367)-C(364) 122.1(9)
O(367)-C(368)-C(369) 108.3(11)
C(370)-C(369)-C(368) 111.7(12)

C(371)-C(370)-C(369) 112(3)
C(369)-C(370)-C(372) 107.6(15)
C(370)-C(371)-C(372) 90(3)
C(370)-C(371)-C(133) 119(3)
C(133)-C(372)-C(371) 94(2)
C(133)-C(372)-C(370) 121.1(13)
C(49)-N(41)-C(42) 107.3(8)
C(49)-N(41)-La(2) 116.0(6)
C(42)-N(41)-La(2) 115.1(6)
C(49)-N(41)-La(1) 115.6(6)
C(42)-N(41)-La(1) 112.6(6)
La(2)-N(41)-La(1) 89.8(2)
N(80)-C(42)-N(41) 128.7(9)
N(80)-C(42)-C(43) 121.8(8)
N(41)-C(42)-C(43) 109.5(8)
C(44)-C(43)-C(48) 120.4(9)
C(44)-C(43)-C(42) 132.4(9)
C(48)-C(43)-C(42) 106.9(8)
C(45)-C(44)-C(43) 116.6(9)
C(44)-C(45)-C(46) 122.5(10)
C(47)-C(46)-C(45) 119.4(10)
C(48)-C(47)-C(46) 119.8(11)
C(47)-C(48)-C(43) 120.8(9)
C(47)-C(48)-C(49) 134.5(9)
C(43)-C(48)-C(49) 104.2(8)
N(50)-C(49)-N(41) 126.0(9)
N(50)-C(49)-C(48) 122.0(8)
N(41)-C(49)-C(48) 111.8(7)
C(52)-N(50)-C(49) 122.9(9)
C(59)-N(51)-C(52) 107.4(8)
C(59)-N(51)-La(2) 114.7(6)
C(52)-N(51)-La(2) 114.3(7)
C(59)-N(51)-La(1) 114.7(7)
C(52)-N(51)-La(1) 115.3(6)
La(2)-N(51)-La(1) 90.0(2)
N(50)-C(52)-N(51) 127.5(9)
N(50)-C(52)-C(53) 122.2(10)
N(51)-C(52)-C(53) 110.3(9)
C(54)-C(53)-C(58) 121.1(9)
C(54)-C(53)-C(52) 133.7(10)
C(58)-C(53)-C(52) 105.2(9)
C(55)-C(54)-C(53) 118.9(11)
C(54)-C(55)-C(56) 122.5(10)
C(55)-C(56)-C(57) 120.7(10)
C(58)-C(57)-C(56) 117.0(10)
C(57)-C(58)-C(53) 119.8(9)
C(57)-C(58)-C(59) 133.1(10)
C(53)-C(58)-C(59) 107.0(9)
N(60)-C(59)-N(51) 128.4(9)
N(60)-C(59)-C(58) 121.6(9)
N(51)-C(59)-C(58) 110.0(9)
C(59)-N(60)-C(62) 122.3(9)
C(62)-N(61)-C(69) 107.3(9)
C(62)-N(61)-La(1) 116.4(6)
C(69)-N(61)-La(1) 115.3(6)
C(62)-N(61)-La(2) 115.4(7)
C(69)-N(61)-La(2) 112.6(7)
La(1)-N(61)-La(2) 89.4(2)
N(60)-C(62)-N(61) 125.9(10)
N(60)-C(62)-C(63) 123.7(9)
N(61)-C(62)-C(63) 110.4(8)
C(68)-C(63)-C(64) 121.7(9)
C(68)-C(63)-C(62) 106.6(8)
C(64)-C(63)-C(62) 131.7(8)
C(63)-C(64)-C(65) 117.4(9)
C(66)-C(65)-C(64) 121.2(10)
C(65)-C(66)-C(67) 122.6(10)
C(66)-C(67)-C(68) 114.7(9)
C(63)-C(68)-C(67) 122.1(8)
C(63)-C(68)-C(69) 107.1(8)
C(67)-C(68)-C(69) 130.2(9)
N(70)-C(69)-N(61) 128.6(9)
N(70)-C(69)-C(68) 122.8(9)
N(61)-C(69)-C(68) 108.5(8)
C(69)-N(70)-C(72) 122.6(8)
C(72)-N(71)-C(79) 106.6(7)
C(72)-N(71)-La(2) 115.5(6)
C(79)-N(71)-La(2) 116.3(7)
C(72)-N(71)-La(1) 114.5(7)
C(79)-N(71)-La(1) 114.1(6)

La(2)-N(71)-La(1) 89.5(2)
N(70)-C(72)-N(71) 126.6(8)
N(70)-C(72)-C(73) 123.1(8)
N(71)-C(72)-C(73) 110.2(8)
C(72)-C(73)-C(78) 107.7(8)
C(72)-C(73)-C(74) 131.6(9)
C(78)-C(73)-C(74) 120.6(9)
C(75)-C(74)-C(73) 116.7(10)
C(74)-C(75)-C(76) 120.4(10)
C(77)-C(76)-C(75) 122.0(10)
C(76)-C(77)-C(78) 118.2(11)
C(73)-C(78)-C(77) 121.9(10)
C(73)-C(78)-C(79) 105.1(8)
C(77)-C(78)-C(79) 133.0(10)
N(80)-C(79)-N(71) 125.1(8)
N(80)-C(79)-C(78) 124.6(8)
N(71)-C(79)-C(78) 110.3(8)
C(42)-N(80)-C(79) 123.9(8)
C(85)-N(81)-C(82) 107.5(6)
C(85)-N(81)-La(2) 123.4(5)
C(82)-N(81)-La(2) 121.9(5)
C(116)-C(82)-N(81) 127.7(7)
C(116)-C(82)-C(83) 124.2(7)
N(81)-C(82)-C(83) 108.1(7)
C(84)-C(83)-C(82) 106.4(7)
C(83)-C(84)-C(85) 107.8(7)
N(81)-C(85)-C(86) 126.6(7)
N(81)-C(85)-C(84) 110.2(7)
C(86)-C(85)-C(84) 123.2(8)
C(92)-C(86)-C(85) 124.1(8)
C(92)-C(86)-C(181) 117.7(7)
C(85)-C(86)-C(181) 118.1(7)
C(182)-C(181)-C(186) 121.3(8)
C(182)-C(181)-C(86) 121.6(7)
C(186)-C(181)-C(86) 117.1(8)
C(181)-C(182)-C(183) 119.8(9)
C(184)-C(183)-C(182) 117.7(9)
C(183)-C(184)-C(185) 123.3(8)
C(184)-C(185)-C(186) 120.5(9)
C(185)-C(186)-C(181) 117.2(9)
C(92)-N(91)-C(95) 108.8(6)
C(92)-N(91)-La(2) 120.6(5)
C(95)-N(91)-La(2) 121.1(5)
N(91)-C(92)-C(86) 127.0(7)
N(91)-C(92)-C(93) 109.2(7)
C(86)-C(92)-C(93) 123.7(8)
C(94)-C(93)-C(92) 106.4(8)
C(93)-C(94)-C(95) 109.1(8)
N(91)-C(95)-C(96) 126.1(7)
N(91)-C(95)-C(94) 106.6(7)
C(96)-C(95)-C(94) 127.3(7)
C(95)-C(96)-C(102) 124.7(7)
C(95)-C(96)-C(191) 116.8(7)
C(102)-C(96)-C(191) 118.4(6)
C(192)-C(191)-C(196) 119.6(7)
C(192)-C(191)-C(96) 119.8(8)
C(196)-C(191)-C(96) 120.7(7)
C(191)-C(192)-C(193) 120.4(8)
C(194)-C(193)-C(192) 119.5(9)
C(193)-C(194)-O(197) 126.9(8)
C(193)-C(194)-C(195) 120.4(8)
O(197)-C(194)-C(195) 112.7(9)
C(196)-C(195)-C(194) 117.6(8)
C(195)-C(196)-C(191) 122.4(8)
C(194)-O(197)-C(198) 114.9(8)
C(199)-C(198)-O(197) 102.6(12)
C(198)-C(199)-C(200) 115.8(9)
C(199)-C(200)-C(201) 117.6(12)
C(202)-C(201)-C(200) 116.5(12)
C(172)-C(202)-C(201) 121.6(16)
C(102)-N(101)-C(105) 106.6(6)
C(102)-N(101)-La(2) 122.3(5)
C(105)-N(101)-La(2) 124.8(5)
N(101)-C(102)-C(96) 128.1(7)
N(101)-C(102)-C(103) 109.5(6)
C(96)-C(102)-C(103) 122.3(6)
C(104)-C(103)-C(102) 105.9(6)
C(103)-C(104)-C(105) 107.9(7)
N(101)-C(105)-C(106) 124.4(8)
N(101)-C(105)-C(104) 109.8(7)

C(106)-C(105)-C(104) 125.8(8)
C(105)-C(106)-C(112) 127.3(7)
C(105)-C(106)-C(141) 118.4(7)
C(112)-C(106)-C(141) 114.1(7)
C(142)-C(141)-C(146) 118.2(9)
C(142)-C(141)-C(106) 121.2(9)
C(146)-C(141)-C(106) 120.5(9)
C(141)-C(142)-C(143) 121.8(11)
C(144)-C(143)-C(142) 118.4(11)
C(143)-C(144)-C(145) 121.1(10)
C(144)-C(145)-C(146) 119.8(12)
C(145)-C(146)-C(141) 120.3(11)
C(112)-N(111)-C(115) 106.5(6)
C(112)-N(111)-La(2) 124.9(5)
C(115)-N(111)-La(2) 120.3(5)
N(111)-C(112)-C(113) 110.4(7)
N(111)-C(112)-C(106) 123.4(7)
C(113)-C(112)-C(106) 126.2(7)
C(114)-C(113)-C(112) 108.8(7)
C(113)-C(114)-C(115) 106.8(7)
C(116)-C(115)-N(111) 126.8(7)
C(116)-C(115)-C(114) 125.8(7)
N(111)-C(115)-C(114) 107.4(6)
C(82)-C(116)-C(115) 124.4(7)
C(82)-C(116)-C(121) 117.2(7)
C(115)-C(116)-C(121) 118.3(7)
C(126)-C(121)-C(122) 116.7(7)
C(126)-C(121)-C(116) 120.9(8)
C(122)-C(121)-C(116) 121.9(7)
C(123)-C(122)-C(121) 123.2(9)
C(124)-C(123)-C(122) 118.1(9)
C(123)-C(124)-O(127) 117.0(10)
C(123)-C(124)-C(125) 120.6(8)
O(127)-C(124)-C(125) 122.3(10)
C(126)-C(125)-C(124) 116.7(9)
C(125)-C(126)-C(121) 124.5(9)
C(138)-O(127)-C(124) 123.4(10)
C(138)-O(127)-C(128) 36.0(12)
C(124)-O(127)-C(128) 115.5(11)
C(139)-C(128)-C(138) 137(4)
C(129)-C(128)-O(127) 114(2)
C(128)-C(129)-C(130) 113.0(19)
C(131)-C(130)-C(129) 103(3)
C(130)-C(131)-C(132) 124(3)
C(133)-C(132)-C(131) 124(3)
C(372)-C(133)-C(132) 132(2)
C(132)-C(133)-C(371) 94(2)
C(129)-C(138)-O(127) 164.6(16)
O(127)-C(138)-C(139) 105.4(13)

O(703)-O(705) 1.61(2)
O(704)-C(722) 0.75(3)
O(704)-C(721) 0.88(3)
C(711)-C(712) 1.47(2)
C(711)-C(713) 1.57(2)
C(711)-C(718) 1.88(2)
C(711)-C(714) 2.03(3)
C(712)-C(719) 1.81(3)
C(713)-C(718) 1.797(19)
C(714)-C(717) 0.716(16)
C(714)-C(719) 1.31(4)
C(714)-C(718) 1.69(3)
C(715)-C(719) 1.73(4)
C(715)-O(716) 1.864(18)
O(716)-C(718) 1.803(18)
C(717)-C(718) 1.47(3)
C(717)-C(719) 1.77(4)
C(721)-C(722) 0.94(2)

C(712)-C(711)-C(713) 127.1(14)
C(712)-C(711)-C(718) 113.1(12)
C(713)-C(711)-C(714) 111.6(11)
C(711)-C(712)-C(719) 86.0(14)
C(717)-C(714)-C(719) 119(2)
C(719)-C(714)-C(718) 87.5(14)
C(717)-C(714)-C(711) 114(3)
C(719)-C(715)-O(716) 90.7(12)

C(718)-O(716)-C(715)	89.4(9)	O(716)-C(718)-C(711)	132.7(11)
C(714)-C(717)-C(718)	95(2)	C(714)-C(719)-C(715)	135.3(18)
C(714)-C(718)-C(713)	117.9(13)	C(715)-C(719)-C(717)	116.5(14)
C(717)-C(718)-O(716)	102.4(11)	C(714)-C(719)-C(712)	87(3)
C(714)-C(718)-O(716)	108.9(12)	C(715)-C(719)-C(712)	112.9(13)
C(713)-C(718)-O(716)	103.0(10)	C(717)-C(719)-C(712)	104(2)
C(717)-C(718)-C(711)	91.4(13)		

C(904)-Cl(83)	1.597(16)	Cl(83)-C(904)-Cl(81)	115.0(10)
C(904)-Cl(81)	1.791(16)	Cl(83)-C(904)-Cl(82)	114.2(10)
C(904)-Cl(82)	1.808(15)	Cl(81)-C(904)-Cl(82)	104.7(8)
C(901)-Cl(93)	1.665(17)	Cl(93)-C(901)-Cl(91)	120.0(11)
C(901)-Cl(91)	1.726(15)	Cl(93)-C(901)-Cl(92)	105.2(8)
C(901)-Cl(92)	1.91(2)	Cl(91)-C(901)-Cl(92)	106.3(10)
C(902)-Cl(96)	1.717(13)	Cl(96)-C(902)-Cl(94)	113.1(7)
C(902)-Cl(94)	1.736(10)	Cl(96)-C(902)-Cl(95)	105.6(6)
C(902)-Cl(95)	1.775(10)	Cl(94)-C(902)-Cl(95)	111.9(6)
C(903)-Cl(98)	1.52(3)	Cl(98)-C(903)-Cl(99)	127.7(14)
C(903)-Cl(99)	1.75(2)	Cl(98)-C(903)-Cl(97)	108.8(9)
C(903)-Cl(97)	1.93(3)	Cl(99)-C(903)-Cl(97)	104(2)

Table 3. Anisotropic displacement parameters ($Å^2$ x 10^4) for the expression:

$\exp\{-2\pi^2(h^2a^{*2}U_{11} + ... + 2hka^*b^*U_{12})\}$

E.s.ds are in parentheses.

	U_{11}	U_{22}	U_{33}	U_{23}	U_{13}	U_{12}
N(1)	410(40)	320(40)	200(30)	90(30)	130(30)	30(30)
C(2)	320(40)	140(40)	420(50)	30(30)	-30(30)	50(30)
C(3)	450(50)	340(50)	150(30)	-20(30)	30(30)	30(40)
C(4)	350(40)	270(40)	310(40)	-60(30)	-10(30)	80(30)
C(5)	230(30)	360(40)	60(30)	-30(30)	-70(20)	-80(30)
C(6)	260(40)	300(40)	240(40)	70(30)	20(30)	30(30)
C(661)	230(40)	640(60)	210(40)	-160(40)	30(30)	-60(40)
C(662)	360(50)	750(80)	200(40)	-80(40)	-90(40)	90(50)
C(663)	380(50)	1300(120)	200(40)	-110(60)	-80(40)	80(70)
C(664)	280(50)	1100(110)	540(70)	-450(70)	100(50)	-130(60)
C(665)	190(40)	930(90)	660(70)	-460(70)	70(50)	-160(50)
C(666)	330(40)	470(60)	410(50)	-220(40)	-10(40)	-90(40)
N(11)	370(40)	230(30)	230(30)	-30(30)	0(30)	-30(30)
C(12)	320(40)	170(40)	230(40)	70(30)	50(30)	20(30)
C(13)	310(40)	320(50)	330(40)	-20(30)	80(30)	-10(30)
C(14)	260(40)	380(50)	190(40)	30(30)	60(30)	10(30)
C(15)	390(40)	80(30)	300(40)	20(30)	-10(30)	0(30)
C(16)	210(40)	260(40)	390(40)	10(30)	100(30)	-90(30)
C(161)	260(40)	280(40)	360(40)	-110(30)	60(30)	-90(30)
C(162)	550(50)	220(40)	290(40)	-120(30)	30(40)	30(40)
C(163)	560(60)	520(60)	210(40)	50(40)	180(40)	100(50)
C(164)	490(50)	370(50)	380(50)	0(40)	190(40)	-30(40)
C(165)	400(50)	380(50)	240(40)	-70(40)	50(30)	20(40)
C(166)	250(40)	300(50)	430(50)	60(40)	70(30)	0(30)
O(167)	560(40)	630(50)	460(40)	180(40)	270(30)	140(40)
C(169)	1050(110)	430(80)	2000(200)	-670(100)	910(130)	-370(80)
C(170)	580(70)	490(70)	510(60)	-80(50)	30(50)	-30(50)
C(171)	520(70)	1730(180)	1080(120)	-1190(130)	-380(80)	530(100)
C(172)	2400(300)	440(90)	2800(300)	-10(130)	2200(300)	150(120)
N(21)	260(30)	390(40)	160(30)	0(30)	10(30)	-110(30)

C(22) 270(40) 300(40) 230(40) 20(30) -50(30) 100(30)
C(23) 310(40) 400(50) 310(40) 90(40) 0(30) 110(40)
C(24) 550(50) 290(40) 130(30) -40(30) 30(30) 0(40)
C(25) 180(30) 410(50) 240(40) -60(30) 0(30) -90(30)
C(26) 370(40) 230(40) 210(40) -60(30) 10(30) -120(30)
C(261) 320(40) 290(40) 260(40) -100(30) 100(30) -140(30)
C(262) 330(40) 340(50) 290(40) -10(40) 60(30) -60(40)
C(263) 400(50) 430(50) 260(40) 20(40) -10(40) -40(40)
C(264) 320(50) 560(60) 460(50) -160(50) 70(40) -90(40)
C(265) 430(50) 440(60) 530(60) -70(50) 40(40) -80(40)
C(266) 420(50) 250(50) 440(50) -10(40) -10(40) 30(40)
N(31) 250(30) 290(40) 210(30) 10(30) 50(30) -80(30)
C(32) 290(40) 210(40) 220(40) 40(30) -10(30) -50(30)
C(33) 290(40) 350(50) 240(40) 50(30) 60(30) -60(30)
C(34) 230(40) 440(50) 290(40) 0(40) 70(30) -100(30)
C(35) 300(40) 340(50) 240(40) 40(30) 30(30) -50(30)
C(36) 340(40) 250(40) 290(40) 110(30) 110(30) -30(30)
C(361) 410(50) 270(40) 320(40) 40(30) 70(40) 30(30)
C(362) 400(50) 410(50) 360(50) 30(40) 50(40) 40(40)
C(363) 420(50) 490(60) 330(50) -60(40) 30(40) 40(40)
C(364) 340(40) 670(70) 160(40) -70(40) 90(30) 90(40)
C(365) 520(60) 550(60) 330(50) 220(50) 140(40) -90(50)
C(366) 470(50) 460(60) 320(50) -80(40) 220(40) -140(40)
O(367) 490(40) 850(60) 330(30) 60(40) 180(30) 60(40)
C(368) 500(60) 660(70) 390(50) -50(50) 140(40) -170(50)
C(369) 1000(100) 1010(120) 470(70) -60(70) 340(70) -90(90)
C(370) 720(90) 2500(300) 380(70) -470(110) 170(60) -440(130)
La(1) 260(2) 221(3) 166(3) 10(2) 18(2) -11(2)
N(41) 230(40) 260(50) 120(40) 70(30) -30(30) -40(30)
C(42) 320(50) 200(60) 160(50) -60(40) -10(40) -20(40)
C(43) 500(50) 160(60) 150(40) -60(50) -20(40) -20(50)
C(44) 340(50) 350(80) 250(50) 70(50) 110(40) -20(50)
C(45) 530(60) 300(70) 220(50) -80(50) 30(50) -120(50)
C(46) 420(60) 350(70) 280(60) -60(50) 30(50) -100(50)
C(47) 630(70) 350(70) 160(50) -140(40) 80(50) 80(50)
C(48) 330(40) 310(60) 300(50) -70(60) 80(40) 40(50)
N(50) 350(40) 320(50) 150(40) -20(40) 60(30) 0(30)
N(51) 380(40) 120(40) 250(40) -30(40) 90(40) -70(30)
C(52) 300(50) 280(60) 270(50) 40(50) 80(40) -10(40)
C(53) 360(50) 290(60) 200(50) 90(40) 120(40) 50(40)

C(54) 290(50) 190(50) 390(60) -30(40) -10(40) -50(40)
C(55) 230(50) 500(80) 450(70) 80(60) -20(50) -40(50)
C(56) 250(50) 440(80) 520(70) -130(60) 150(50) -50(50)
C(57) 330(50) 390(70) 240(50) -60(50) 70(40) -40(50)
C(58) 230(40) 130(50) 330(60) 20(40) -20(40) -40(40)
C(59) 350(50) 200(60) 290(60) 70(50) 100(40) 100(40)
N(60) 210(40) 290(50) 300(50) 0(40) 50(30) -30(30)
N(61) 280(40) 270(50) 270(50) -80(40) 80(30) -20(30)
C(62) 340(50) 230(60) 200(50) 90(40) 80(40) 70(40)
C(63) 220(40) 300(70) 220(50) 60(50) 40(30) 0(40)
C(64) 450(50) 390(80) 140(40) -90(50) 20(40) -100(50)
C(65) 480(60) 710(100) 170(50) -50(60) 110(50) -50(60)
C(66) 430(60) 630(100) 190(50) -90(60) -60(40) -190(60)
C(67) 230(40) 420(70) 300(60) 120(50) -70(40) -200(40)
C(68) 320(40) 180(50) 80(40) 30(40) -70(30) -80(40)
C(69) 460(50) 290(50) 150(40) -20(30) -40(30) -20(40)
N(70) 250(40) 200(50) 230(40) 30(30) -40(30) -40(30)
N(71) 190(40) 380(60) 160(40) 30(40) -20(30) 30(30)
C(72) 230(40) 200(60) 220(50) -20(40) -10(40) -50(40)
C(73) 220(40) 190(50) 270(50) -50(40) 0(40) -40(40)
C(74) 350(50) 470(80) 210(50) -40(50) 90(40) -60(50)
C(75) 370(60) 440(70) 380(60) -130(60) 190(50) -80(50)
C(76) 420(60) 450(80) 270(60) 30(50) 80(40) -70(50)
C(77) 370(50) 310(70) 290(60) 0(50) 100(50) 10(50)
C(78) 310(50) 350(70) 200(50) 30(50) 120(40) 30(40)
C(79) 290(50) 240(60) 110(40) 10(40) -10(40) -60(40)
N(80) 340(40) 160(40) 140(40) 0(30) 0(30) -10(30)
La(2) 269(2) 216(2) 163(2) 1(2) 14(2) -11(2)
N(81) 310(30) 120(30) 260(30) -10(20) 70(30) 50(20)
C(82) 360(40) 270(40) 200(40) -20(30) 90(30) -30(30)
C(83) 430(50) 280(40) 190(40) -160(30) 90(30) -100(30)
C(84) 220(40) 320(50) 360(40) -80(40) 30(30) -60(30)
C(85) 510(50) 120(40) 220(40) 30(30) 40(30) 40(30)
C(86) 210(40) 230(40) 360(40) 100(30) 60(30) 40(30)
C(181) 310(40) 380(50) 200(40) 50(30) -10(30) 0(30)
C(182) 310(40) 460(60) 380(50) -140(40) 0(40) -100(40)
C(183) 640(70) 360(60) 480(60) -200(50) -20(50) -220(50)
C(184) 470(50) 480(60) 320(50) -70(40) -180(40) -160(50)
C(185) 240(40) 670(70) 440(50) 10(50) 80(40) -130(40)
C(186) 250(40) 390(50) 360(50) 60(40) 50(30) 40(30)

N(91) 280(30) 250(40) 230(30) 30(30) 30(30) 10(30)
C(92) 410(50) 240(40) 270(40) -30(30) 80(30) 0(30)
C(93) 330(40) 250(40) 350(40) -10(30) 50(30) 10(30)
C(94) 420(50) 260(40) 340(40) 60(40) 60(40) 20(40)
C(95) 400(40) 150(40) 220(40) 60(30) 140(30) 20(30)
C(96) 350(40) 200(40) 180(30) 40(30) 20(30) 70(30)
C(191) 260(40) 370(50) 90(30) 40(30) 50(30) -20(30)
C(192) 540(50) 270(50) 210(40) 80(30) -60(40) 60(40)
C(193) 400(50) 460(60) 210(40) 0(40) 70(30) -40(40)
C(194) 470(50) 490(60) 270(40) 130(40) 70(40) -130(40)
C(195) 540(50) 270(50) 290(40) 50(30) 150(40) 130(40)
C(196) 310(40) 330(50) 210(40) 30(30) 80(30) -20(30)
O(197) 650(40) 560(40) 290(30) -40(30) 220(30) -40(40)
C(198) 570(60) 1160(110) 180(40) 150(50) 120(40) -180(70)
C(199) 310(50) 2170(190) 230(50) -70(80) 70(40) -230(80)
C(200) 640(70) 1230(120) 180(40) 130(60) 20(40) 320(70)
C(201) 2000(200) 2800(400) 380(80) -640(150) 420(120) -1200(200)
C(202) 1600(200) 3300(500) 460(90) 280(160) 470(110) 1700(300)
N(101) 240(30) 230(30) 250(30) -30(30) -40(30) 10(20)
C(102) 360(40) 290(40) 100(30) 30(30) 90(30) 10(30)
C(103) 280(40) 270(40) 210(40) 60(30) 40(30) 90(30)
C(104) 340(40) 300(40) 110(30) 30(30) 20(30) -20(30)
C(105) 440(40) 240(40) 360(40) 90(40) 120(40) 140(40)
C(106) 310(40) 300(40) 200(40) -60(30) -30(30) 20(30)
C(141) 370(40) 390(50) 270(40) -100(40) 30(30) 40(40)
C(142) 400(50) 730(80) 330(50) 40(50) 140(40) 70(50)
C(143) 430(60) 980(100) 370(60) 30(60) 0(40) 110(60)
C(144) 430(60) 1410(140) 330(60) -250(70) -160(50) -80(70)
C(145) 670(70) 630(80) 430(60) -250(50) 90(50) -230(60)
C(146) 420(50) 600(70) 410(50) -170(50) 60(40) -60(50)
N(111) 270(30) 290(40) 180(30) -10(30) 80(20) 60(30)
C(112) 340(40) 300(50) 240(40) -70(30) 10(30) -40(30)
C(113) 310(40) 330(50) 210(40) -40(30) 20(30) -90(30)
C(114) 340(40) 260(40) 340(40) -80(30) 70(30) -30(30)
C(115) 210(30) 430(50) 130(30) 10(30) 80(30) -10(30)
C(116) 410(40) 260(40) 120(30) -40(30) -10(30) 120(30)
C(121) 350(40) 300(40) 200(40) -20(30) 60(30) -40(30)
C(122) 400(50) 460(50) 190(40) -160(40) 0(30) -10(40)
C(123) 220(40) 570(60) 510(60) -110(50) 110(40) -30(40)
C(124) 490(60) 460(60) 550(60) -190(50) 340(50) -100(40)

C(125) 530(60) 340(50) 440(50) -30(40) 200(40) -40(40)
C(126) 320(40) 450(50) 390(50) 70(40) 160(40) 60(40)
O(127) 700(50) 850(60) 560(50) -150(40) 470(40) -60(40)
C(128) 380(100) 2600(400) 610(130) 360(190) 280(100) -260(160)
C(129) 680(100) 480(90) 360(70) -80(70) 150(70) 20(70)
C(130) 1600(200) 2500(400) 1300(200) 200(200) -80(180) -1500(300)
C(131) 1500(200) 2800(400) 630(110) -130(170) -30(120) 1500(300)
C(132) 3500(400) 540(110) 2400(300) 380(150) -2700(300) -520(180)
C(133) 960(120) 1270(170) 640(110) -540(110) 390(90) -410(120)
C(139) 830(140) 910(150) 410(90) -80(100) -460(100) 90(110)

O(701) 460(50) 3400(300) 250(50) 60(90) 150(40) -90(100)
O(702) 1260(100) 1310(120) 1450(110) 750(100) 1250(100) 470(90)
O(703) 1140(90) 1080(110) 710(70) 680(80) 300(70) 380(80)
O(705) 1730(130) 1740(150) 80(40) -40(60) -110(60) 1360(120)
C(712) 350(50) 420(60) 300(50) 100(40) 20(40) -190(40)
C(713) 330(50) 1030(110) 280(50) 130(60) 280(40) -50(60)
C(714) 300(70) 320(60) 680(90) 30(60) -280(60) -150(50)
C(715) 400(50) 340(60) 460(60) -10(50) -150(40) -20(50)
O(716) 930(70) 1140(100) 160(40) 250(50) 200(40) 470(70)
C(717) 220(60) 1470(190) 120(50) 310(80) -100(50) -150(90)
C(718) 730(90) 1280(150) 590(80) 210(90) 140(70) 60(100)
C(719) 2300(300) 570(120) 3600(500) -300(200) 2200(400) -220(160)
C(721) 230(50) 500(80) 500(70) 100(60) 130(50) 20(50)
C(722) 1200(150) 450(90) 180(50) 100(50) 40(70) 10(80)

C(904) 620(80) 540(100) 690(90) 40(70) 70(70) -10(70)
Cl(81) 4670(130) 540(30) 610(30) -240(20) 980(50) -820(50)
Cl(82) 680(20) 690(30) 880(30) -350(20) 230(20) -141(19)
Cl(83) 1200(40) 780(30) 2380(70) -730(40) 1290(40) -400(30)

C(901) 1440(150) 570(110) 840(110) 530(90) 720(110) 540(100)
Cl(91) 601(18) 680(30) 580(20) 250(20) 141(15) 53(17)
Cl(92) 664(19) 610(20) 840(20) -97(19) 218(17) -166(17)
Cl(93) 1350(30) 710(30) 600(20) -20(20) 50(20) 330(30)

C(902) 460(60) 480(60) 260(40) 50(40) 10(40) 150(50)
Cl(94) 583(18) 630(30) 610(20) -50(19) 118(15) 50(17)
Cl(95) 1440(40) 1730(60) 1300(40) 990(40) 1000(40) 1140(50)
Cl(96) 3160(80) 760(30) 374(16) -412(17) -460(30) 870(40)

C(903) 290(70) 2800(300) 3500(400) -2800(300) 270(130) -80(120)

Cl(97) 629(19) 710(30) 610(20) -200(20) 181(16) -148(18)

Cl(98) 990(30) 970(40) 970(30) 460(30) 370(20) 270(30)

Table 4. Hydrogen coordinates (x 10^4) and isotropic displacement parameters ($Å^2$ x 10^3). All hydrogen atoms were included in idealised positions with U(iso)'s set at 1.2*U(eq) or, for the methyl group hydrogen atoms, 1.5*U(eq) of the parent carbon atoms.

	x	y	z	U(iso)
H(3)	3096	2739	10546	38
H(4)	4706	2913	10459	38
H(662)	6058	2105	10286	55
H(663)	7455	2375	10993	78
H(664)	8226	3231	10843	77
H(665)	7626	3829	9890	71
H(666)	6147	3605	9209	50
H(13)	6667	2594	8575	38
H(14)	6305	2197	7432	33
H(162)	4213	2167	5697	44
H(163)	5126	1968	4900	50
H(165)	6903	1027	6227	41
H(166)	5978	1129	7000	39
H(16A)	6194	2257	4420	337
H(16B)	7129	1976	4217	337
H(16C)	5678	1290	4414	129
H(16D)	6457	1142	3979	129
H(17A)	5030	1710	3107	65
H(17B)	5096	2241	3628	65
H(17C)	6469	1928	2903	143
H(17D)	6678	2387	3508	143
H(17E)	5136	2572	2391	195
H(17F)	5562	3049	2939	195
H(23)	3409	1107	5932	42
H(24)	1796	931	5981	39
H(262)	-343	1842	6535	39
H(263)	-1637	1418	5828	45
H(264)	-1706	387	5695	54
H(265)	-330	-143	6158	57
H(266)	943	286	6784	46

H(33)	-239	1350	7830	35
H(34)	71	1832	8939	38
H(362)	1399	3260	9949	47
H(363)	512	3344	10750	51
H(365)	457	1618	10977	55
H(366)	1117	1481	10076	47
H(36A)	6	1902	11922	61
H(36B)	-925	1965	11353	61
H(36C)	-1384	2772	12005	96
H(36D)	-1398	2142	12345	96
H(44)	2353	4192	10176	37
H(45)	3618	4570	10957	43
H(46)	5084	4673	10710	43
H(47)	5280	4473	9629	46
H(54)	6422	4106	7933	36
H(55)	7353	4027	7180	49
H(56)	6870	3563	6188	47
H(57)	5308	3236	5851	39
H(64)	2702	2583	4831	40
H(65)	1433	2236	4029	54
H(66)	0	2089	4290	52
H(67)	-297	2386	5329	40
H(74)	-1381	2666	7018	41
H(75)	-2367	2792	7784	46
H(76)	-1763	3210	8861	46
H(77)	-273	3570	9145	38
H(83)	1676	5664	9094	36
H(84)	3292	5853	8981	37
H(182)	4085	6493	8183	47
H(183)	5431	6960	8854	62
H(184)	6655	6390	9347	56
H(185)	6716	5407	9134	54
H(186)	5422	4926	8493	40
H(93)	5310	5405	7191	38
H(94)	4985	4975	6061	41
H(192)	3801	5291	4886	43
H(193)	4747	5181	4092	43
H(195)	4484	3407	4229	43
H(196)	3723	3547	5090	33
H(19A)	5062	4952	3055	75

H(19B)	6007	4909	3621	75
H(19C)	6543	4138	3032	108
H(19D)	6360	4707	2573	108
H(20A)	5108	4303	1862	83
H(20B)	4908	3851	2404	83
H(20C)	5475	3385	1442	203
H(20D)	6472	3663	1738	203
H(20E)	6268	2601	1982	209
H(20F)	6830	2989	2575	209
H(103)	1986	4076	4438	31
H(104)	357	3858	4537	31
H(142)	-999	4661	4708	57
H(143)	-2387	4400	3977	73
H(144)	-3177	3576	4209	91
H(145)	-2487	2940	5043	70
H(146)	-1170	3235	5814	57
H(113)	-1599	4221	6391	35
H(114)	-1282	4596	7552	38
H(122)	-963	5576	7972	43
H(123)	-1847	5773	8752	51
H(125)	-33	4742	10077	51
H(126)	851	4650	9299	45
H(13A)	-564	4939	11957	220
H(13B)	-1658	5026	11934	220
H(13C)	-993	4076	11578	203
H(13D)	-1924	4212	11821	203
H(13E)	-231	3951	12499	319
H(13F)	-801	4405	12837	319
H(13G)	-1627	3850	13049	111
H(13H)	-1657	3466	12407	111

H(904)	6114	6345	1548	76
H(901)	967	5402	6532	105
H(902)	2973	6558	970	49
H(903)	2045	205	4147	265

Table 5. Torsion angles, in degrees. E.s.ds are in parentheses.

C(5)-N(1)-C(2)-C(36)	-174.5(8)	C(6)-C(661)-C(662)-C(663)	175.8(9)
La(1)-N(1)-C(2)-C(36)	36.9(10)	C(661)-C(662)-C(663)-C(664)	-0.6(16)
C(5)-N(1)-C(2)-C(3)	0.1(9)	C(662)-C(663)-C(664)-C(665)	-1.9(16)
La(1)-N(1)-C(2)-C(3)	-148.4(6)	C(663)-C(664)-C(665)-C(666)	4.4(15)
N(1)-C(2)-C(3)-C(4)	0.1(10)	C(662)-C(661)-C(666)-C(665)	2.2(13)
C(36)-C(2)-C(3)-C(4)	174.6(8)	C(6)-C(661)-C(666)-C(665)	-173.1(8)
C(2)-C(3)-C(4)-C(5)	-0.3(10)	C(664)-C(665)-C(666)-C(661)	-4.6(14)
C(2)-N(1)-C(5)-C(6)	176.3(8)	C(15)-N(11)-C(12)-C(6)	-176.2(8)
La(1)-N(1)-C(5)-C(6)	-34.9(11)	La(1)-N(11)-C(12)-C(6)	36.7(10)
C(2)-N(1)-C(5)-C(4)	-0.3(9)	C(15)-N(11)-C(12)-C(13)	1.3(8)
La(1)-N(1)-C(5)-C(4)	148.5(5)	La(1)-N(11)-C(12)-C(13)	-145.8(5)
C(3)-C(4)-C(5)-N(1)	0.4(10)	C(5)-C(6)-C(12)-N(11)	-0.9(13)
C(3)-C(4)-C(5)-C(6)	-176.3(8)	C(661)-C(6)-C(12)-N(11)	176.4(8)
N(1)-C(5)-C(6)-C(12)	-0.5(14)	C(5)-C(6)-C(12)-C(13)	-178.0(8)
C(4)-C(5)-C(6)-C(12)	175.6(8)	C(661)-C(6)-C(12)-C(13)	-0.7(12)
N(1)-C(5)-C(6)-C(661)	-177.9(8)	N(11)-C(12)-C(13)-C(14)	-0.2(9)
C(4)-C(5)-C(6)-C(661)	-1.7(12)	C(6)-C(12)-C(13)-C(14)	177.4(8)
C(12)-C(6)-C(661)-C(666)	68.0(11)	C(12)-C(13)-C(14)-C(15)	-0.9(9)
C(5)-C(6)-C(661)-C(666)	-114.5(9)	C(12)-N(11)-C(15)-C(14)	-1.8(9)
C(12)-C(6)-C(661)-C(662)	-107.4(9)	La(1)-N(11)-C(15)-C(14)	144.0(6)
C(5)-C(6)-C(661)-C(662)	70.2(11)	C(12)-N(11)-C(15)-C(16)	173.3(7)
C(666)-C(661)-C(662)-C(663)	0.4(14)	La(1)-N(11)-C(15)-C(16)	-40.8(10)

C(13)-C(14)-C(15)-N(11)	1.8(10)
C(13)-C(14)-C(15)-C(16)	-173.2(8)
N(11)-C(15)-C(16)-C(22)	0.2(13)
C(14)-C(15)-C(16)-C(22)	174.5(8)
N(11)-C(15)-C(16)-C(161)	178.5(7)
C(14)-C(15)-C(16)-C(161)	-7.2(12)
C(15)-C(16)-C(161)-C(162)	-120.7(8)
C(22)-C(16)-C(161)-C(162)	57.8(11)
C(15)-C(16)-C(161)-C(166)	66.3(10)
C(22)-C(16)-C(161)-C(166)	-115.3(9)
C(166)-C(161)-C(162)-C(163)	-5.4(12)
C(16)-C(161)-C(162)-C(163)	-178.7(8)
C(161)-C(162)-C(163)-C(164)	-1.3(15)
C(162)-C(163)-C(164)-O(167)	-179.6(10)
C(162)-C(163)-C(164)-C(165)	4.9(15)
C(163)-C(164)-C(165)-C(166)	-1.8(14)
O(167)-C(164)-C(165)-C(166)	-177.9(9)
C(164)-C(165)-C(166)-C(161)	-5.0(14)
C(162)-C(161)-C(166)-C(165)	8.5(12)
C(16)-C(161)-C(166)-C(165)	-178.3(8)
C(163)-C(164)-O(167)-C(168)	23(2)
C(165)-C(164)-O(167)-C(168)	-161.7(18)
C(164)-O(167)-C(168)-C(169)	-100(2)
O(167)-C(168)-C(169)-C(170)	160.0(13)
C(168)-C(169)-C(170)-C(171)	55(3)
C(169)-C(170)-C(171)-C(172)	-169.5(12)
C(170)-C(171)-C(172)-C(202)	-166.9(17)
C(25)-N(21)-C(22)-C(23)	-0.3(9)
La(1)-N(21)-C(22)-C(23)	-151.1(5)
C(25)-N(21)-C(22)-C(16)	-176.4(8)
La(1)-N(21)-C(22)-C(16)	32.9(11)
C(15)-C(16)-C(22)-N(21)	4.4(14)
C(161)-C(16)-C(22)-N(21)	-173.8(8)
C(15)-C(16)-C(22)-C(23)	-171.0(8)
C(161)-C(16)-C(22)-C(23)	10.7(13)
N(21)-C(22)-C(23)-C(24)	1.8(10)
C(16)-C(22)-C(23)-C(24)	177.8(8)
C(22)-C(23)-C(24)-C(25)	-2.3(10)
C(22)-N(21)-C(25)-C(26)	175.7(8)
La(1)-N(21)-C(25)-C(26)	-32.2(11)
C(22)-N(21)-C(25)-C(24)	-1.0(9)
La(1)-N(21)-C(25)-C(24)	151.0(5)
C(23)-C(24)-C(25)-C(26)	-174.5(9)
C(23)-C(24)-C(25)-N(21)	2.1(10)
N(21)-C(25)-C(26)-C(32)	-3.4(15)
C(24)-C(25)-C(26)-C(32)	172.6(8)
N(21)-C(25)-C(26)-C(261)	173.5(8)
C(24)-C(25)-C(26)-C(261)	-10.5(14)
C(25)-C(26)-C(261)-C(262)	-110.2(10)
C(32)-C(26)-C(261)-C(262)	67.2(10)

C(25)-C(26)-C(261)-C(266)	69.5(11)
C(32)-C(26)-C(261)-C(266)	-113.0(9)
C(266)-C(261)-C(262)-C(263)	-1.2(12)
C(26)-C(261)-C(262)-C(263)	178.6(8)
C(261)-C(262)-C(263)-C(264)	4.3(14)
C(262)-C(263)-C(264)-C(265)	-4.9(13)
C(263)-C(264)-C(265)-C(266)	2.9(15)
C(264)-C(265)-C(266)-C(261)	0.1(16)
C(262)-C(261)-C(266)-C(265)	-1.0(13)
C(26)-C(261)-C(266)-C(265)	179.2(9)
C(25)-C(26)-C(32)-N(31)	1.4(14)
C(261)-C(26)-C(32)-N(31)	-175.6(7)
C(25)-C(26)-C(32)-C(33)	-175.0(9)
C(261)-C(26)-C(32)-C(33)	8.0(12)
C(35)-N(31)-C(32)-C(26)	-175.8(8)
La(1)-N(31)-C(32)-C(26)	37.3(10)
C(35)-N(31)-C(32)-C(33)	1.2(9)
La(1)-N(31)-C(32)-C(33)	-145.8(5)
C(26)-C(32)-C(33)-C(34)	177.2(8)
N(31)-C(32)-C(33)-C(34)	0.4(9)
C(32)-C(33)-C(34)-C(35)	-1.7(10)
C(32)-N(31)-C(35)-C(36)	174.7(8)
La(1)-N(31)-C(35)-C(36)	-38.9(11)
C(32)-N(31)-C(35)-C(34)	-2.3(9)
La(1)-N(31)-C(35)-C(34)	144.1(6)
C(33)-C(34)-C(35)-N(31)	2.6(10)
C(33)-C(34)-C(35)-C(36)	-174.4(8)
N(31)-C(35)-C(36)-C(2)	-0.7(14)
C(34)-C(35)-C(36)-C(2)	175.9(8)
N(31)-C(35)-C(36)-C(361)	-179.7(8)
C(34)-C(35)-C(36)-C(361)	-3.0(13)
N(1)-C(2)-C(36)-C(35)	1.0(13)
C(3)-C(2)-C(36)-C(35)	-172.6(8)
N(1)-C(2)-C(36)-C(361)	-179.9(7)
C(3)-C(2)-C(36)-C(361)	6.4(12)
C(35)-C(36)-C(361)-C(362)	-115.4(10)
C(2)-C(36)-C(361)-C(362)	65.5(11)
C(35)-C(36)-C(361)-C(366)	63.6(12)
C(2)-C(36)-C(361)-C(366)	-115.5(10)
C(366)-C(361)-C(362)-C(363)	-1.6(13)
C(36)-C(361)-C(362)-C(363)	177.5(8)
C(361)-C(362)-C(363)-C(364)	3.1(15)
C(362)-C(363)-C(364)-O(367)	176.5(8)
C(362)-C(363)-C(364)-C(365)	0.8(14)
C(363)-C(364)-C(365)-C(366)	-6.3(14)
O(367)-C(364)-C(365)-C(366)	178.1(9)
C(364)-C(365)-C(366)-C(361)	7.9(15)
C(362)-C(361)-C(366)-C(365)	-3.7(14)
C(36)-C(361)-C(366)-C(365)	177.2(9)
C(363)-C(364)-O(367)-C(368)	173.5(9)

C(365)-C(364)-O(367)-C(368)	-11.0(14)
C(364)-O(367)-C(368)-C(369)	-176.5(9)
O(367)-C(368)-C(369)-C(370)	-72.0(18)
C(368)-C(369)-C(370)-C(371)	98(3)
C(368)-C(369)-C(370)-C(372)	151.1(13)
C(369)-C(370)-C(371)-C(372)	95(2)
C(369)-C(370)-C(371)-C(133)	63(3)
C(372)-C(370)-C(371)-C(133)	-31.5(15)
C(370)-C(371)-C(372)-C(133)	-136(2)
C(133)-C(371)-C(372)-C(370)	136(2)
C(371)-C(370)-C(372)-C(133)	54(3)
C(369)-C(370)-C(372)-C(133)	-51(2)
C(369)-C(370)-C(372)-C(371)	-105(3)
C(49)-N(41)-C(42)-N(80)	-179.8(11)
La(2)-N(41)-C(42)-N(80)	49.5(14)
La(1)-N(41)-C(42)-N(80)	-51.5(13)
C(49)-N(41)-C(42)-C(43)	-0.7(12)
La(2)-N(41)-C(42)-C(43)	-131.4(8)
La(1)-N(41)-C(42)-C(43)	127.6(8)
N(80)-C(42)-C(43)-C(44)	3(2)
N(41)-C(42)-C(43)-C(44)	-176.3(13)
N(80)-C(42)-C(43)-C(48)	176.4(11)
N(41)-C(42)-C(43)-C(48)	-2.7(13)
C(48)-C(43)-C(44)-C(45)	4.0(19)
C(42)-C(43)-C(44)-C(45)	176.9(13)
C(43)-C(44)-C(45)-C(46)	-1.1(19)
C(44)-C(45)-C(46)-C(47)	2(2)
C(45)-C(46)-C(47)-C(48)	-6(2)
C(46)-C(47)-C(48)-C(43)	9(2)
C(46)-C(47)-C(48)-C(49)	178.9(14)
C(44)-C(43)-C(48)-C(47)	-8(2)
C(42)-C(43)-C(48)-C(47)	177.5(13)
C(44)-C(43)-C(48)-C(49)	179.2(12)
C(42)-C(43)-C(48)-C(49)	4.7(14)
C(42)-N(41)-C(49)-N(50)	178.3(10)
La(2)-N(41)-C(49)-N(50)	-51.4(12)
La(1)-N(41)-C(49)-N(50)	51.7(12)
C(42)-N(41)-C(49)-C(48)	3.8(12)
La(2)-N(41)-C(49)-C(48)	134.1(8)
La(1)-N(41)-C(49)-C(48)	-122.7(8)
C(47)-C(48)-C(49)-N(50)	8(2)
C(43)-C(48)-C(49)-N(50)	179.8(10)
C(47)-C(48)-C(49)-N(41)	-176.8(15)
C(43)-C(48)-C(49)-N(41)	-5.4(14)
N(41)-C(49)-N(50)-C(52)	0.2(17)
C(48)-C(49)-N(50)-C(52)	174.2(12)
C(49)-N(50)-C(52)-N(51)	-1.1(19)
C(49)-N(50)-C(52)-C(53)	177.2(10)
C(59)-N(51)-C(52)-N(50)	-179.8(12)
La(2)-N(51)-C(52)-N(50)	51.8(14)

La(1)-N(51)-C(52)-N(50)	-50.5(15)	C(57)-C(58)-C(59)-N(60)	0(2)
C(59)-N(51)-C(52)-C(53)	1.8(12)	C(53)-C(58)-C(59)-N(60)	177.6(10)
La(2)-N(51)-C(52)-C(53)	-126.6(8)	C(57)-C(58)-C(59)-N(51)	-178.7(12)
La(1)-N(51)-C(52)-C(53)	131.1(8)	C(53)-C(58)-C(59)-N(51)	-1.2(12)
N(50)-C(52)-C(53)-C(54)	1(2)	N(51)-C(59)-N(60)-C(62)	0.1(19)
N(51)-C(52)-C(53)-C(54)	179.9(12)	C(58)-C(59)-N(60)-C(62)	-178.5(10)
N(50)-C(52)-C(53)-C(58)	178.9(11)	C(59)-N(60)-C(62)-N(61)	-0.9(18)
N(51)-C(52)-C(53)-C(58)	-2.5(12)	C(59)-N(60)-C(62)-C(63)	177.1(11)
C(58)-C(53)-C(54)-C(55)	2.3(17)	C(69)-N(61)-C(62)-N(60)	178.8(11)
C(52)-C(53)-C(54)-C(55)	179.5(12)	La(1)-N(61)-C(62)-N(60)	-50.5(14)
C(53)-C(54)-C(55)-C(56)	-3(2)	La(2)-N(61)-C(62)-N(60)	52.4(13)
C(54)-C(55)-C(56)-C(57)	3(2)	C(69)-N(61)-C(62)-C(63)	0.6(13)
C(55)-C(56)-C(57)-C(58)	-3(2)	La(1)-N(61)-C(62)-C(63)	131.4(8)
C(56)-C(57)-C(58)-C(53)	2.2(17)	La(2)-N(61)-C(62)-C(63)	-125.8(8)
C(56)-C(57)-C(58)-C(59)	179.4(12)	N(60)-C(62)-C(63)-C(68)	178.8(11)
C(54)-C(53)-C(58)-C(57)	-2.0(17)	N(61)-C(62)-C(63)-C(68)	-3.0(13)
C(52)-C(53)-C(58)-C(57)	-180.0(10)	N(60)-C(62)-C(63)-C(64)	0(2)
C(54)-C(53)-C(58)-C(59)	-179.9(10)	N(61)-C(62)-C(63)-C(64)	177.9(14)
C(52)-C(53)-C(58)-C(59)	2.2(12)	C(68)-C(63)-C(64)-C(65)	3(2)
C(52)-N(51)-C(59)-N(60)	-179.1(12)	C(62)-C(63)-C(64)-C(65)	-178.1(13)
La(2)-N(51)-C(59)-N(60)	-50.9(14)	C(63)-C(64)-C(65)-C(66)	-2(2)
La(1)-N(51)-C(59)-N(60)	51.3(14)	C(64)-C(65)-C(66)-C(67)	3(2)
C(52)-N(51)-C(59)-C(58)	-0.4(12)	C(65)-C(66)-C(67)-C(68)	-4(2)
La(2)-N(51)-C(59)-C(58)	127.8(7)	C(64)-C(63)-C(68)-C(67)	-5(2)
La(1)-N(51)-C(59)-C(58)	-130.0(7)	C(62)-C(63)-C(68)-C(67)	176.2(11)

C(64)-C(63)-C(68)-C(69)	-176.8(12)	N(71)-C(72)-C(73)-C(78)	-0.8(13)
C(62)-C(63)-C(68)-C(69)	4.0(13)	N(70)-C(72)-C(73)-C(74)	2.8(19)
C(66)-C(67)-C(68)-C(63)	5.1(18)	N(71)-C(72)-C(73)-C(74)	-178.3(12)
C(66)-C(67)-C(68)-C(69)	175.3(13)	C(72)-C(73)-C(74)-C(75)	179.3(12)
C(62)-N(61)-C(69)-N(70)	178.2(11)	C(78)-C(73)-C(74)-C(75)	2.1(18)
La(1)-N(61)-C(69)-N(70)	46.8(15)	C(73)-C(74)-C(75)-C(76)	-2.0(19)
La(2)-N(61)-C(69)-N(70)	-53.8(14)	C(74)-C(75)-C(76)-C(77)	2(2)
C(62)-N(61)-C(69)-C(68)	1.9(13)	C(75)-C(76)-C(77)-C(78)	-3(2)
La(1)-N(61)-C(69)-C(68)	-129.5(8)	C(72)-C(73)-C(78)-C(77)	179.5(11)
La(2)-N(61)-C(69)-C(68)	129.9(8)	C(74)-C(73)-C(78)-C(77)	-2.7(18)
C(63)-C(68)-C(69)-N(70)	179.7(11)	C(72)-C(73)-C(78)-C(79)	0.3(13)
C(67)-C(68)-C(69)-N(70)	8(2)	C(74)-C(73)-C(78)-C(79)	178.1(11)
C(63)-C(68)-C(69)-N(61)	-3.8(13)	C(76)-C(77)-C(78)-C(73)	3.0(19)
C(67)-C(68)-C(69)-N(61)	-175.2(12)	C(76)-C(77)-C(78)-C(79)	-178.0(13)
N(61)-C(69)-N(70)-C(72)	2.9(18)	C(72)-N(71)-C(79)-N(80)	-179.7(11)
C(68)-C(69)-N(70)-C(72)	178.6(11)	La(2)-N(71)-C(79)-N(80)	-49.3(13)
C(69)-N(70)-C(72)-N(71)	0.7(17)	La(1)-N(71)-C(79)-N(80)	52.9(13)
C(69)-N(70)-C(72)-C(73)	179.4(11)	C(72)-N(71)-C(79)-C(78)	-0.9(12)
C(79)-N(71)-C(72)-N(70)	179.9(11)	La(2)-N(71)-C(79)-C(78)	129.6(8)
La(2)-N(71)-C(72)-N(70)	49.0(13)	La(1)-N(71)-C(79)-C(78)	-128.3(8)
La(1)-N(71)-C(72)-N(70)	-52.9(13)	C(73)-C(78)-C(79)-N(80)	179.2(10)
C(79)-N(71)-C(72)-C(73)	1.0(12)	C(77)-C(78)-C(79)-N(80)	0(2)
La(2)-N(71)-C(72)-C(73)	-129.9(7)	C(73)-C(78)-C(79)-N(71)	0.4(13)
La(1)-N(71)-C(72)-C(73)	128.2(8)	C(77)-C(78)-C(79)-N(71)	-178.8(13)
N(70)-C(72)-C(73)-C(78)	-179.7(10)	N(41)-C(42)-N(80)-C(79)	1.2(18)

C(43)-C(42)-N(80)-C(79)	-177.8(11)
N(71)-C(79)-N(80)-C(42)	-1.3(17)
C(78)-C(79)-N(80)-C(42)	179.9(11)
C(85)-N(81)-C(82)-C(116)	178.2(8)
La(2)-N(81)-C(82)-C(116)	-30.5(11)
C(85)-N(81)-C(82)-C(83)	-1.5(9)
La(2)-N(81)-C(82)-C(83)	149.8(5)
C(116)-C(82)-C(83)-C(84)	-179.1(8)
N(81)-C(82)-C(83)-C(84)	0.7(9)
C(82)-C(83)-C(84)-C(85)	0.4(10)
C(82)-N(81)-C(85)-C(86)	-178.9(7)
La(2)-N(81)-C(85)-C(86)	30.4(10)
C(82)-N(81)-C(85)-C(84)	1.8(9)
La(2)-N(81)-C(85)-C(84)	-149.0(5)
C(83)-C(84)-C(85)-N(81)	-1.4(10)
C(83)-C(84)-C(85)-C(86)	179.2(8)
N(81)-C(85)-C(86)-C(92)	7.5(13)
C(84)-C(85)-C(86)-C(92)	-173.2(8)
N(81)-C(85)-C(86)-C(181)	-176.1(7)
C(84)-C(85)-C(86)-C(181)	3.2(11)
C(92)-C(86)-C(181)-C(182)	109.8(10)
C(85)-C(86)-C(181)-C(182)	-66.8(11)
C(92)-C(86)-C(181)-C(186)	-69.1(10)
C(85)-C(86)-C(181)-C(186)	114.2(8)
C(186)-C(181)-C(182)-C(183)	-0.3(14)
C(86)-C(181)-C(182)-C(183)	-179.2(8)
C(181)-C(182)-C(183)-C(184)	-1.4(15)
C(182)-C(183)-C(184)-C(185)	3.4(17)
C(183)-C(184)-C(185)-C(186)	-3.8(16)
C(184)-C(185)-C(186)-C(181)	1.8(13)
C(182)-C(181)-C(186)-C(185)	0.1(13)
C(86)-C(181)-C(186)-C(185)	179.1(8)
C(95)-N(91)-C(92)-C(86)	174.7(8)
La(2)-N(91)-C(92)-C(86)	-38.7(11)
C(95)-N(91)-C(92)-C(93)	-1.7(9)
La(2)-N(91)-C(92)-C(93)	144.9(5)
C(85)-C(86)-C(92)-N(91)	-2.1(13)
C(181)-C(86)-C(92)-N(91)	-178.5(8)
C(85)-C(86)-C(92)-C(93)	173.7(8)
C(181)-C(86)-C(92)-C(93)	-2.7(12)
N(91)-C(92)-C(93)-C(94)	0.7(10)
C(86)-C(92)-C(93)-C(94)	-175.8(8)
C(92)-C(93)-C(94)-C(95)	0.6(9)
C(92)-N(91)-C(95)-C(96)	-178.1(7)
La(2)-N(91)-C(95)-C(96)	35.6(10)
C(92)-N(91)-C(95)-C(94)	2.0(9)
La(2)-N(91)-C(95)-C(94)	-144.4(5)
C(93)-C(94)-C(95)-N(91)	-1.5(9)
C(93)-C(94)-C(95)-C(96)	178.5(8)
N(91)-C(95)-C(96)-C(102)	4.6(12)

C(94)-C(95)-C(96)-C(102)	-175.5(8)
N(91)-C(95)-C(96)-C(191)	-178.4(7)
C(94)-C(95)-C(96)-C(191)	1.5(12)
C(95)-C(96)-C(191)-C(192)	-66.2(10)
C(102)-C(96)-C(191)-C(192)	110.9(9)
C(95)-C(96)-C(191)-C(196)	114.7(8)
C(102)-C(96)-C(191)-C(196)	-68.1(10)
C(196)-C(191)-C(192)-C(193)	-3.4(12)
C(96)-C(191)-C(192)-C(193)	177.5(7)
C(191)-C(192)-C(193)-C(194)	5.4(13)
C(192)-C(193)-C(194)-O(197)	177.7(8)
C(192)-C(193)-C(194)-C(195)	-3.2(13)
C(193)-C(194)-C(195)-C(196)	-0.9(14)
O(197)-C(194)-C(195)-C(196)	178.3(8)
C(194)-C(195)-C(196)-C(191)	3.0(13)
C(192)-C(191)-C(196)-C(195)	-0.8(12)
C(96)-C(191)-C(196)-C(195)	178.2(8)
C(193)-C(194)-O(197)-C(198)	2.5(13)
C(195)-C(194)-O(197)-C(198)	-176.7(8)
C(194)-O(197)-C(198)-C(199)	179.3(8)
O(197)-C(198)-C(199)-C(200)	60.9(14)
C(198)-C(199)-C(200)-C(201)	-155.5(15)
C(199)-C(200)-C(201)-C(202)	74(2)
C(171)-C(172)-C(202)-C(201)	-169.7(17)
C(200)-C(201)-C(202)-C(172)	37(4)
C(105)-N(101)-C(102)-C(96)	176.9(8)
La(2)-N(101)-C(102)-C(96)	-29.8(11)
C(105)-N(101)-C(102)-C(103)	-4.1(9)
La(2)-N(101)-C(102)-C(103)	149.2(5)
C(95)-C(96)-C(102)-N(101)	-8.3(13)
C(191)-C(96)-C(102)-N(101)	174.7(7)
C(95)-C(96)-C(102)-C(103)	172.8(7)
C(191)-C(96)-C(102)-C(103)	-4.1(11)
N(101)-C(102)-C(103)-C(104)	1.8(9)
C(96)-C(102)-C(103)-C(104)	-179.2(7)
C(102)-C(103)-C(104)-C(105)	1.2(9)
C(102)-N(101)-C(105)-C(106)	-174.3(8)
La(2)-N(101)-C(105)-C(106)	33.3(11)
C(102)-N(101)-C(105)-C(104)	4.9(9)
La(2)-N(101)-C(105)-C(104)	-147.6(5)
C(103)-C(104)-C(105)-N(101)	-3.9(9)
C(103)-C(104)-C(105)-C(106)	175.3(8)
N(101)-C(105)-C(106)-C(112)	3.5(14)
C(104)-C(105)-C(106)-C(112)	-175.6(8)
N(101)-C(105)-C(106)-C(141)	177.4(8)
C(104)-C(105)-C(106)-C(141)	-1.6(13)
C(105)-C(106)-C(141)-C(142)	-65.4(12)
C(112)-C(106)-C(141)-C(142)	109.3(10)
C(105)-C(106)-C(141)-C(146)	116.6(10)
C(112)-C(106)-C(141)-C(146)	-68.7(11)

C(146)-C(141)-C(142)-C(143)	-1.1(14)
C(106)-C(141)-C(142)-C(143)	-179.1(9)
C(141)-C(142)-C(143)-C(144)	1.5(17)
C(142)-C(143)-C(144)-C(145)	-4.6(19)
C(143)-C(144)-C(145)-C(146)	7.3(19)
C(144)-C(145)-C(146)-C(141)	-6.7(16)
C(142)-C(141)-C(146)-C(145)	3.7(14)
C(106)-C(141)-C(146)-C(145)	-178.3(9)
C(115)-N(111)-C(112)-C(113)	-1.6(9)
La(2)-N(111)-C(112)-C(113)	146.4(6)
C(115)-N(111)-C(112)-C(106)	176.2(8)
La(2)-N(111)-C(112)-C(106)	-35.9(11)
C(105)-C(106)-C(112)-N(111)	-2.2(14)
C(141)-C(106)-C(112)-N(111)	-176.3(8)
C(105)-C(106)-C(112)-C(113)	175.2(9)
C(141)-C(106)-C(112)-C(113)	1.0(13)
N(111)-C(112)-C(113)-C(114)	-0.4(10)
C(106)-C(112)-C(113)-C(114)	-178.1(8)
C(112)-C(113)-C(114)-C(115)	2.2(10)
C(112)-N(111)-C(115)-C(116)	-173.8(8)
La(2)-N(111)-C(115)-C(116)	36.5(11)
C(112)-N(111)-C(115)-C(114)	2.8(9)
La(2)-N(111)-C(115)-C(114)	-146.9(5)
C(113)-C(114)-C(115)-C(116)	173.5(8)
C(113)-C(114)-C(115)-N(111)	-3.1(10)
N(81)-C(82)-C(116)-C(115)	-7.9(14)
C(83)-C(82)-C(116)-C(115)	171.8(8)
N(81)-C(82)-C(116)-C(121)	176.1(7)
C(83)-C(82)-C(116)-C(121)	-4.2(12)
N(111)-C(115)-C(116)-C(82)	4.3(13)
C(114)-C(115)-C(116)-C(82)	-171.7(8)
N(111)-C(115)-C(116)-C(121)	-179.6(7)
C(114)-C(115)-C(116)-C(121)	4.4(13)
C(82)-C(116)-C(121)-C(126)	-65.8(11)
C(115)-C(116)-C(121)-C(126)	117.9(9)
C(82)-C(116)-C(121)-C(122)	122.1(9)
C(115)-C(116)-C(121)-C(122)	-54.2(12)
C(126)-C(121)-C(122)-C(123)	4.2(14)
C(116)-C(121)-C(122)-C(123)	176.6(9)
C(121)-C(122)-C(123)-C(124)	-4.3(15)
C(122)-C(123)-C(124)-O(127)	-175.4(9)
C(122)-C(123)-C(124)-C(125)	1.2(14)
C(123)-C(124)-C(125)-C(126)	1.8(14)
O(127)-C(124)-C(125)-C(126)	178.2(9)
C(124)-C(125)-C(126)-C(121)	-1.9(15)
C(122)-C(121)-C(126)-C(125)	-0.9(14)
C(116)-C(121)-C(126)-C(125)	-173.3(9)
C(123)-C(124)-O(127)-C(138)	161.5(11)
C(125)-C(124)-O(127)-C(138)	-15.1(16)
C(123)-C(124)-O(127)-C(128)	-157.9(17)

C(125)-C(124)-O(127)-C(128)	25(2)
C(138)-O(127)-C(128)-C(139)	149(16)
C(124)-O(127)-C(128)-C(139)	37(15)
C(124)-O(127)-C(128)-C(138)	-112.4(16)
C(138)-O(127)-C(128)-C(129)	8.3(12)
C(124)-O(127)-C(128)-C(129)	-104.1(16)
C(139)-C(128)-C(129)-C(138)	-177(4)
O(127)-C(128)-C(129)-C(138)	-8.4(13)
C(138)-C(128)-C(129)-C(139)	177(4)
O(127)-C(128)-C(129)-C(139)	168(4)
C(139)-C(128)-C(129)-C(130)	28(3)
C(138)-C(128)-C(129)-C(130)	-155(2)
O(127)-C(128)-C(129)-C(130)	-163(2)
C(138)-C(129)-C(130)-C(131)	160(3)
C(128)-C(129)-C(130)-C(131)	-168(3)
C(139)-C(129)-C(130)-C(131)	-153(3)
C(129)-C(130)-C(131)-C(132)	160(3)
C(130)-C(131)-C(132)-C(133)	147(4)
C(371)-C(372)-C(133)-C(132)	-40(3)
C(370)-C(372)-C(133)-C(132)	-71(3)
C(370)-C(372)-C(133)-C(371)	-31.5(18)
C(131)-C(132)-C(133)-C(372)	144(3)
C(131)-C(132)-C(133)-C(371)	117(4)
C(139)-C(128)-C(138)-C(129)	4(5)
O(127)-C(128)-C(138)-C(129)	170.9(13)
C(139)-C(128)-C(138)-O(127)	-166(5)
C(129)-C(128)-C(138)-O(127)	-170.9(13)
C(129)-C(128)-C(138)-C(139)	-4(5)
O(127)-C(128)-C(138)-C(139)	166(5)
C(139)-C(129)-C(138)-C(128)	-2(2)
C(130)-C(129)-C(138)-C(128)	47(4)
C(128)-C(129)-C(138)-O(127)	36(5)
C(139)-C(129)-C(138)-O(127)	35(5)
C(130)-C(129)-C(138)-O(127)	84(6)
C(128)-C(129)-C(138)-C(139)	2(2)
C(130)-C(129)-C(138)-C(139)	49(3)
C(124)-O(127)-C(138)-C(128)	88(2)
C(124)-O(127)-C(138)-C(129)	52(6)
C(128)-O(127)-C(138)-C(129)	-36(5)
C(124)-O(127)-C(138)-C(139)	83.5(14)
C(128)-O(127)-C(138)-C(139)	-5(2)
C(138)-C(128)-C(139)-C(129)	-4(4)
O(127)-C(128)-C(139)-C(129)	-145(14)
C(129)-C(128)-C(139)-C(138)	4(4)
O(127)-C(128)-C(139)-C(138)	-141(18)
C(138)-C(129)-C(139)-C(128)	2(3)
C(130)-C(129)-C(139)-C(128)	-154(3)
C(128)-C(129)-C(139)-C(138)	-2(3)
C(130)-C(129)-C(139)-C(138)	-156(2)
C(129)-C(138)-C(139)-C(128)	-175(6)

O(127)-C(138)-C(139)-C(128)	14(6)	O(127)-C(138)-C(139)-C(129)	-171.0(15)
C(128)-C(138)-C(139)-C(129)	175(6)		

Crystal structure analysis of the La_2-triple-decked-phthal-porph-phthal complex with two O-$(CH_2)_{10}$-O bridges

Crystal data: $C_{140}\ H_{108}\ La_2\ N_{16}\ O_4$, 4($CHCl_3$) plus *ca* 16 C/O of unresolved solvent molecules, M = 3056.1. Monoclinic, space group $P2_1$ (no. 4), a = 14.71543(11), b = 22.86186(19), c = 20.55253(17) Å, V = 6753.66(10) $Å^3$. Z = 2, Dc = 1.503 g cm^{-3}, F(000) = 3090, T = 100(2) K, μ(Cu-Kα) = 75.6 cm^{-1}, λ(Cu-Kα) = 1.54184 Å.

The crystal was a dark blue cuboid. From a sample under oil, one, *ca* 0.17 x 0.03 x 0.03 mm, was mounted on a small loop and fixed in the cold nitrogen stream on a Rigaku Oxford Diffraction XtaLAB Synergy diffractometer, equipped with Cu-Kα radiation, HyPix detector and mirror monochromator. Intensity data were measured by thin-slice ω-scans. Total no. of reflections recorded, to θ_{max} = 70.0°, was 50,191 of which 22,236 were unique (Rint = 0.041); 20,702 were 'observed' with $I > 2\sigma_I$.

Data were processed using the CrysAlisPro-CCD and -RED (1) programs. The SHELXT (2A) program provided three possible space groups, $P2_1/n$, Pn and $P2_1$; the h0l reflections with h+l odd, in the first two of these space groups showed a good number of ‘weak’, rather than ‘unobserved’, reflections. The structure was determined for all three space groups by the intrinsic phasing routines in the SHELXT program (2A) and produced essentially identical structures of the La_2-triple-decked-phthal-porph-phthal complex with two O-$(CH_2)_{10}$-O bridges with accompanying chloroform and other, smaller, solvent molecules. Each of the three results was refined by full-matrix least-squares methods, on F^2's, in SHELXL (2B), and the all-round results for the $P2_1$ version showed the most likely structure. There are still regions of disorder, in the bridging link chains and amongst the solvent molecules. The non-hydrogen atoms of the La_2 complex and the chloroform molecules were refined with anisotropic thermal parameters. The hydrogen atoms of these moieties were included in idealised positions and their Uiso values were set to ride on the Ueq values of the parent carbon atoms. The remaining solvent molecules were not identified but were included as single oxygen or carbon atoms and refined isotropically. At the conclusion of the refinement, wR_2 = 0.132 and R_1 = 0.054 (2B) for all 22,236 reflections weighted $w = [\sigma^2(F_o^2) + (0.0641\ P)^2 + 16.629\ P]^{-1}$ with $P = (F_o^2 + 2F_c^2)/3$; for the 'observed' data only, R_1 = 0.050.

In the final difference map, the highest peak (*ca* 2.9 $eÅ^{-3}$) was near Cl(99).

Scattering factors for neutral atoms were taken from reference (3). Computer programs used in this analysis have been noted above, and were run through WinGX (4) on a Dell Optiplex 780 PC at the University of East Anglia.

References

(1) Programs CrysAlisPro, Rigaku Oxford Diffraction Ltd., Abingdon, UK (2018).

(2) G. M. Sheldrick, Programs for crystal structure determination (SHELXT), *Acta Cryst.* (2015) A**71**, 3-8, and refinement (SHELXL), *Acta Cryst.* (2008) A**64**, 112-122 and (2015) C**71**, 3-8.

(3) *'International Tables for X-ray Crystallography'*, Kluwer Academic Publishers, Dordrecht (1992). Vol. C, pp. 500, 219 and 193.

(4) L. J. Farrugia, *J. Appl. Cryst.* (2012) **45**, 849–854.

Legends for Figures

Figure 1. View of the La_2-triple-decked-phthal-porph-phthal complex with two O-$(CH_2)_{10}$-O bridges, indicating the atom numbering scheme. Thermal ellipsoids are drawn at the 50% probability level.

Figure 2. The La_2 complex viewed approximately along the La…La vector.

Notes on the structure

The core of this La-phthal-porph-phthal complex is very similar to those of previously reported structures, with a planar, central porphyrin ring, and the outer phthalocyanine rings tilted slightly towards an umbrella shape, Figure 1. The two O-$(CH_2)_{10}$-O bridging links are on opposite sides of the molecule and are related approximately by centrosymmetry; indeed, the whole molecule shows pseudo centrosymmetry, Figure 2..

As in isabf1405, the central N_4 groups of both phthalocyanines are capped by well-ordered chloroform molecules. There are several other molecules in the structure – further

chloroform molecules (some with disorder) and smaller molecules (probably MeOH, most of which are not fully defined and all with disorder).